Characterization and Consequences of Telomere Replication Gone Awry

Ofer Rog

Thesis submitted towards the degree of Doctor of Philosophy

UCL

Department of Biology

London, WC1E 6BT

The program of research was carried out

under the supervision of Dr. Julia Promisel Cooper

at Cancer Research UK, Telomere Biology Laboratory

44 Lincoln's Inn Fields, London, WC2A 3PX

October 2008

I, Ofer Rog, confirm that the work presented in this thesis is my own. Where information has been derived from other sources, I confirm that this has been indicated in the thesis.

Abstract

Telomeres, the ends of linear eukaryotic chromosomes, pose several unique challenges to genome stability. My thesis work is concerned with the difficulties the replication machinery encounters when attempting to replicate telomeres, and with possible consequences of defects in telomere replication.

The relevance of the DNA replication machinery precipitated while characterizing fission yeast cells lacking the telomeric binding protein Taz1 (a homologue of mammalian TRF1 & 2). In the absence of Taz1, replication forks stall when encountering telomeric sequences, leading to telomere breakage and loss. This unanticipated function of the telomeric complex suggests that telomeric sequences pose an obstacle to the replication machinery. Indeed, further experiments suggested that any repeated sequence has a propensity to cause replication fork stalling, suggesting that our findings may also be applicable to other parts of the genome.

Challenges to semi-conservative replication in cells lacking Taz1 are likely to be the underlying cause of another *taz1*Δ-specific phenomenon: telomere entanglement and loss of viability occurring specifically at cold temperatures. Screening for suppressors of this phenotype led to the identification of two additional factors involved in the etiology of dysfunctional telomeres: the post-translational modification SUMO, and the fission yeast member of the conserved RecQ helicase family, Rqh1. A novel sumoylation deficient allele of Rqh1 was able to suppress several *taz1*Δ-specific phenomena without dramatically affecting other genome-wide functions of Rqh1. Interestingly, genetic analysis revealed that this allele acts in a loss-of-function manner, suggesting that Rqh1 activity is detrimental for *taz1*Δ telomeres. Our findings underscore the significance of telomere-specific regulation, as Rqh1, and many other factors participating in telomere metabolism, are not exclusive to telomeres.

Table of Contents

List of Figures

Acknowledgments

First and foremost I would like to express the utmost of gratitude to Julie for giving me this great opportunity my PhD has been. My four years in her lab have been an incredible and exciting journey in so many ways. I never cease to be amazed by how much I am learning every day.

I cannot imagine my PhD without the great atmosphere in the lab, which would not be the same without the day-to-day contributions of all its members. It has been, and still is, a fantastic working environment, a place that is a pleasure to come into in the morning (and on week-ends), and continuous source of both intellectual stimulation and plain good time. Thank you to Chris, Miguel, Creighton, Kyle, Anna, Kazu, Thomas, Vitaliy, Luis, Devanshi, Jessica, Cécile, Pierre-Marie and Yuan. Many thanks to the other yeast groups at CRUK for help. Special thanks to Jessica for helping make this thesis readable. I also wish to thank Benoit Arcangioli, Johanne Murray, Jacob Seeler, Felicity Watts and Matthew Whitby for contribution of strains and reagents. I would like to acknowledge the contributions of my thesis committee members Axel Behrens and Gordon Peters. Of course, none of this work could have not taken place without the financial support of Cancer Research UK, Overseas Research Students Awards Scheme and B'nai B'rith Leo Baeck Lodge.

I would also like to thank my previous supervisors, Anat and Martin, for teaching me so much, and getting me excited on science. Sadly, Anat, with whom I started to work on yeast telomeres, is no longer with us. Yuval, for friendship and endless scientific discussions. My family, for bringing me up with such a sense of self worth and supporting me all along the way. Tal, for taking this academic journey with me, and despite geographical distance has always been there with me. And Chii Shyang, whose love exposed my life into a whole new dimension.

The work presented here is a summery of my work in Julie Cooper's lab in the last four years. Many of the experiments and ideas stems from the work of Kyle M. Miller, to whom I am greatly indebted – both for the great inheritance of my project and for teaching me so much. Much of this thesis has been published in a joint publication with Kyle (Miller et al., 2006), and some of the text and ideas in the introduction have been presented in a recent review (Rog and Cooper, 2008).

1 Chapter 1: Introduction

1.1 Telomeres

The telomere field was brought to life with the seminal observations of McClintock and Muller, who inferred the protective nature of telomeres from the consequences of (what we know now to be) telomere de-protection – the visually apparent chromosome breakage and rearrangement that follow telomere-telomere fusion and the consequent attempts of the cell to segregate dicentric chromosomes (McClintock, 1939; Muller, 1938). Later advances in our molecular understanding of DNA structure allowed definition of the 'end-replication problem', and the challenges of completing chromosome end replication became the major focus of interest. Substantial progress, greatly fueled by the discovery of telomerase (Greider and Blackburn, 1985), has since been made in understanding telomere maintenance. Nonetheless, the discovery of numerous components of the telomeric complex in a variety of model systems has allowed investigators to return to questions regarding telomere 'protection' – the ability of telomeres to prevent chromosome ends from being treated as damage-induced DNA double strand breaks (DSBs).

While my work touches both on telomere maintenance and protection, perhaps the most exciting aspect of it is the notion that the two functions of telomeres – chromosome end maintenance and protection - and thus the two 'sub-fields' within the telomere field, are intricately bound together, sharing many actors and molecular events. Cellular processes that were thought of mainly in the context of one or the other sub-field, namely semi-conservative DNA replication and the DNA damage response (DDR), each play active roles in both telomere maintenance and protection.

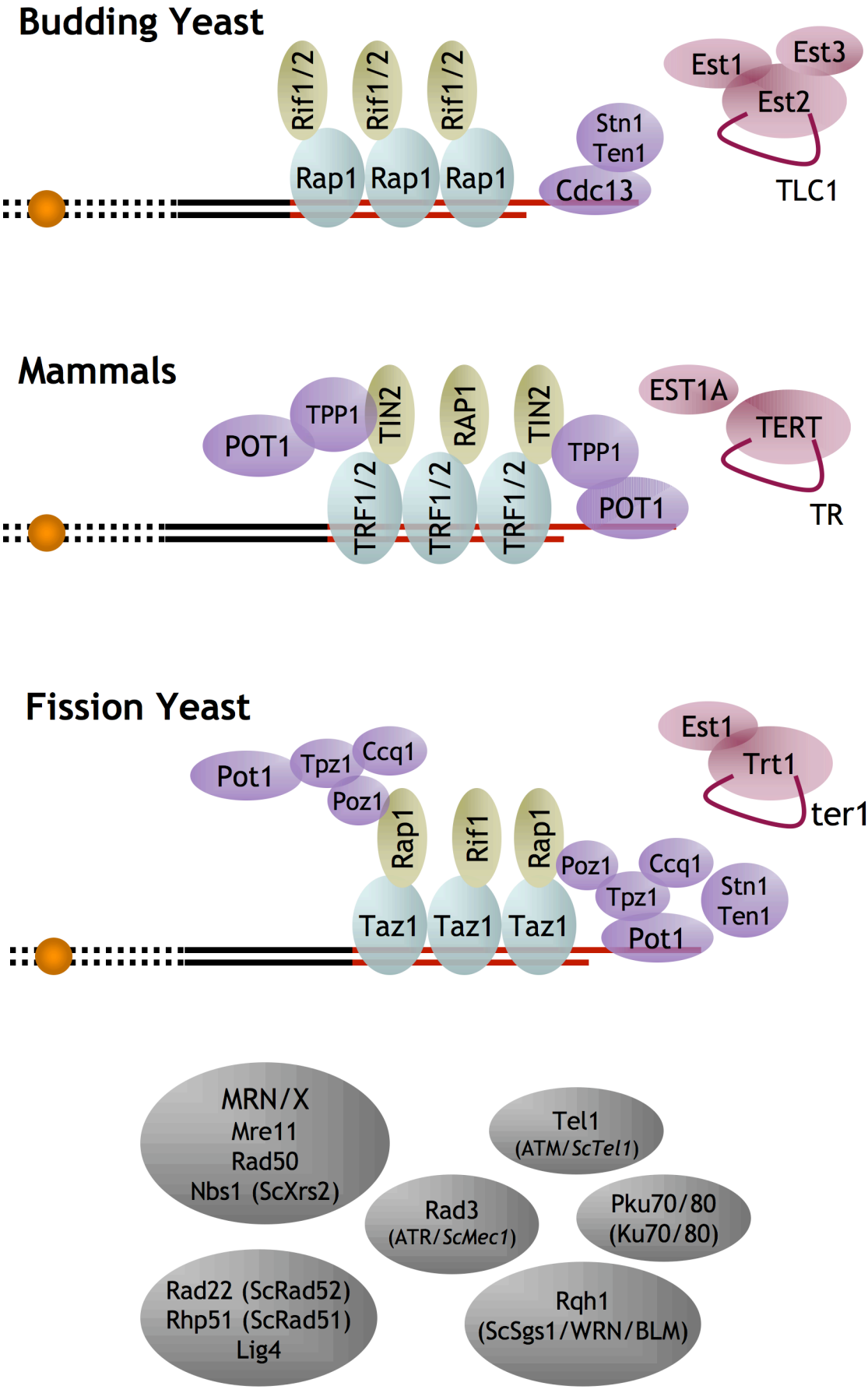
Budding Yeast
Rif1/2
Rif1/2
Rif1/2
Rap1
Rap1
Rap1
Stn1
Ten1
Cdc13
Est1
Est3
Est2
TLC1
Mammals
TPP1
TIN2
RAP1
TIN2
POT1
TRF1/2
TRF1/2
TRF1/2
TPP1
POT1
EST1A
TERT
TR
Fission Yeast
Pot1
Tpz1
Ccq1
Poz1
Rap1
Rif1
Rap1
Taz1
Taz1
Taz1
Poz1
Ccq1
Tpz1
Pot1
Stn1
Ten1
Est1
Trt1
ter1
MRN/X
Mre11
Rad50
Nbs1 (ScXrs2)
Tel1
(ATM/ScTel1)
Rad3
(ATR/ScMec1)
Pku70/80
(Ku70/80)
Rad22 (ScRad52)
Rhp51 (ScRad51)
Lig4
Rqh1
(ScSgs1/WRN/BLM)

Figure 1.1 Diagram highlighting core components of the telomeric complex in budding yeast, fission yeast and mammals

(previous page) Proteins are color-coded to reflect functional similarity, and not necessarily sequence or structural homology. Red lines mark the telomeric dsDNA and ssDNA overhang, and the small orange circles designate the centromeres. Telomeric dsDNA binding proteins are light blue, other accessory factors are colored olive. Telomeric ssDNA binding proteins and accessory factor are colored lilac. Telomerase and some of its accessory factors are colored in magenta. The mammalian telomere-specific protein complex is referred to as 'shelterin' (de Lange, 2005). Gray spheres at the bottom include some of the DDR and DNA repair factors involved in telomere metabolism in fission yeast, and their mammalian and budding yeast homologues.

In most eukaryotes, chromosomal DNA terminates with short, repetitive G-rich sequences. These telomeric repeats recruit dsDNA binding proteins (Figure 1.1), which in turn recruit a plethora of additional components (a subset of which are depicted in Figure 1.1). Telomeres end with a single stranded 3' overhang of the G-rich strand which recruits ssDNA binding proteins. Semi-conservative replication, thought to proceed from the telomeres' centromere proximal side, faces several challenges when attempting to generate two identical copies of telomeres. These challenges stem both from the inherent properties of the DNA replication machinery, which cannot fully replicate linear molecules (the so-called 'end-replication problem') (Olovnikov, 1973; Watson, 1972), and from telomere-specific processing events (Lingner et al., 1995). These problems cause telomere attrition, unless the telomeric repeats are replenished by a specialized reverse transcriptase, telomerase, that copies new telomere repeats onto the telomeric terminus from its own RNA template (Figure 1.1) (Greider and Blackburn, 1985). Alternatively, telomeres can be amplified through a recombination based mechanism, known as the **a**lternative **l**engthening of **t**elomeres ('ALT') (Bryan et al., 1997). Many of these issues are expanded on below.

1.2 Telomere dysfunction

Different genetic perturbations have been used throughout the years to expose different facets of telomere dysfunction, and to deduce the different

molecular activities carried out by specific telomeric proteins. It is a pertinent point that many times these deductions should be carried out vigilantly, as a perturbation in one component may affect the stoichiometry, stability or localization of other telomeric factors, thus complicating the identification of the actual molecular effectors of telomeric functions. In addition, a key question is which aspect of telomere protection decays as telomeres shorten in a physiological context.

1.2.1 End-to-end fusions

We can now define more precisely the questions stemming from the work of McClintock and Muller: how does the cell distinguish a DSB from a telomere as the two are structurally similar? This distinction is crucial, as failure to repair a DSB, or an inappropriate attempt to 'repair' a telomere by fusing it to another chromosome end, result in highly deleterious consequences. Naïve thinking about the role of telomeres in preventing DNA repair might predict that repair factors would be excluded from telomeres. However, genetic and physical data have proven otherwise: ATM, the MRN complex, Ku and many other repair factors are present at telomeres and play crucial roles in their protection and maintenance (for example Boulton and Jackson, 1998; Greenwell et al., 1995; Karlseder et al., 2004; Lustig and Petes, 1986; Zhu et al., 2000). The role telomeric proteins play in protection from DNA repair is thus likely to be found in the way they regulate DNA damage response and repair factors.

Once telomeres lose their protective structure, either through erosion of the telomeric tract or disruption of the telomeric protein complex, they elicit a DNA damage response. In mammals, this results in an ATM/ATR- and p53-dependent cessation of proliferation (Karlseder et al., 1999). The cytological manifestation of this response, termed TIFs (telomere dysfunction induced foci), mimics the cellular response to DSBs induced by gamma irradiation (IR) (d'Adda di Fagagna et al., 2003; Takai et al., 2003). It is characterized by the sequential recruitment of DNA damage response (DDR) proteins and chromatin modifications to distinct foci. The similarity between DSBs and unprotected telomeres extends also to the manner by which the two are repaired. Repair of DSBs is cell cycle regulated, such that they are repaired *via* nonhomologous

end-joining (NHEJ) in G1 and homologous recombination (HR) in G2 (Ferreira and Cooper, 2004) (See Section 1.2.2 below). Indeed, NHEJ occurs at unprotected telomeres in fission yeast, budding yeast and mammals, resulting in chromosome end-fusions; in both fission yeast *taz1Δ* cells and mouse TRF2$^{-/-}$ cells, this NHEJ is restricted to the G1 phase of the cell cycle (Celli and de Lange, 2005; Ferreira and Cooper, 2004). (Cell cycle dependency of NHEJ-mediated telomere fusions has not yet been reported in budding yeast.) Telomere fusions are observed in G2 only when mammalian TRF2 is displaced from telomeres using a dominant negative allele, and are thus not thought to represent a physiological response (Bailey et al., 2001; Smogorzewska et al., 2002).

The distinction of telomeres from DSBs is achieved through the combined efforts of the various components of the telomere complex, so that different experimental perturbations expose different facets of a DDR response. For example, while *taz1Δ* mutants exhibit de-protection from DNA repair reactions at telomeres (Ferreira and Cooper, 2001, 2004), they do not activate a checkpoint-mediated cell cycle arrest (MG Ferreira and JPC, unpublished). In contrast, TRF2 deletion results not only in aberrant telomeric 'repair' reactions but also in cell cycle arrest (Celli and de Lange, 2005; Karlseder et al., 1999). Consistent with these genetic data, human RAP1 and TRF2 were sufficient to provide protection from *in vitro* NHEJ reactions (Bae and Baumann, 2007). Mutations in telomeric ssDNA binding proteins result in robust checkpoint responses: fission yeast *pot1Δ* mutants and some mutations in budding yeast *CDC13* activate the DDR checkpoint concomitant with degradation and loss of the telomere tract (Baumann and Cech, 2001; Garvik et al., 1995); murine Pot1 proteins prevent ATR-mediated activation of DDR, even though their role in preventing end-fusion is relatively minor (Denchi and de Lange, 2007; Hockemeyer et al., 2006; Wu et al., 2006b).

1.2.2 Up-regulated homologous recombination

As mentioned above, a major function of the telomeric complex is to prevent DNA repair reactions from occurring at telomeres. If telomeres are fused through NHEJ-mediated repair, disastrous consequences ensue when the

cell enters mitosis. However, HR events at telomeres are potentially silent, as gene-conversions and crossing-over events between telomeres cause little or no sequence or structural changes due to the telomeres' polarity. However, despite being nearly genetically silent, they can be observed. A cytological method used to observe telomeric sister chromatid exchanges (T-SCE) on metaphase chromosome is CO-FISH (see explanation in Chapter 4) (Bailey et al., 2004; Cornforth and Eberle, 2001). Indeed, CO-FISH revealed that several genetic backgrounds, including cells lacking both TRF2 and Ku (Celli et al., 2006) and certain mutations in heterochromatin components (reviewed in Blasco, 2007), result in elevated levels of T-SCE. In yeast, while direct observation of exchanges is currently impossible, indirect consequences of exchanges are discernable, and can be observed mostly through exchanges between imperfect subtelomeric repeats. Instability of fission yeast subtelomeres has indeed been observed in cells lacking Ku (Baumann and Cech, 2000) or Taz1 (see Chapter 3). Subtelomeric instability is also a prominent feature of senescing cells lacking telomerase and of ALT cells (Lundblad and Blackburn, 1993; Nakamura et al., 1998; Subramanian et al., 2008; Varley et al., 2002). The functional importance of these recombination events and rearrangements is currently unclear, although they may contribute to telomere maintenance in the absence of telomerase (see section 1.3.2.1 below). In addition, it is important to remember that the intra-molecular strand invasion events that generate t-loops (see section 1.2.7 below), are structurally similar to the inter-sister and inter-chromosomal events resulting in T-SCE and other telomeric rearrangements.

1.2.3 Hyper-resection and deregulated telomeric ssDNA overhang

A conserved feature of telomeres is their termination with a 3' overhang composed of the G-rich strand. This overhang is thought to be crucial for maintaining telomere structure (for example, see t-loop in section 1.2.7 below), and is essential for telomere maintenance by serving as a substrate for reverse transcription reactions carried out by telomerase. In budding yeast, where careful analysis has been performed, wt telomeres were shown to harbour a short ssDNA overhang of 12-14bp throughout the cell-cycle, and longer

overhang of ~30bp in late S-phase (Larrivee et al., 2004; Wellinger et al., 1993). Other organisms, including humans, also show highly regulated overhangs, including defined starting and terminating nucleotides, supporting the idea that end processing is a thoroughly regulated event (Chai et al., 2006; Klobutcher et al., 1981; Raices et al., 2008; Sfeir et al., 2005).

Conceptually, telomeric 3' overhang formation can be a consequence of three processes: telomerase activity that is not accompanied by 'fill-in' synthesis of the C-rich strand; resection of the C-rich strand; and incomplete lagging-strand synthesis or aberrant Okazaki fragments processing. Indeed, perturbation of these processes can influence the telomeric overhang (Adams Martin et al., 2000; Carson and Hartwell, 1985; Tomita et al., 2004). Importantly, data from budding yeast and humans suggest that the two products of semi-conservative replication are not left unprocessed and that blunt-ended products of leading strand replication are likely not to exist (Chai et al., 2006; Wellinger et al., 1996).

Several techniques have been used to characterize the ssDNA overhang. One is native in-gel hybridization, which utilizes specific probes for detection of the G- and C-rich strands on non-denatured genomic DNA; this is followed by a denaturing step and re-probing to assess the total amount of telomeric DNA (Wellinger et al., 1993). Importantly, this technique allows assessment of the total ssDNA signal, but not the length or length distribution of the overhang. Other techniques, based on ligation and primer extension reactions, allow the measurement of single overhangs, and the assessment of the specific nucleotide at the beginning and end of the overhang (Forstemann et al., 2000; Sfeir et al., 2005). Crucially, all techniques must include a control demonstrating that the overhang signal is sensitive to digestion with a 3'-5' ssDNA exonuclease (i.e. ExoI).

De-regulated overhangs were readily observed in several genetic backgrounds. A temperature-sensitive mutation in *ScCDC13*, encoding the telomeric ssDNA binding protein in budding yeast, caused massive resection of telomeres upon shifting to the restrictive temperature, with ssDNA being identified as far as 30kb inside the chromosome (Garvik et al., 1995). This

abundant telomeric and non-telomeric ssDNA activates the DNA damage checkpoint, resulting in cell cycle arrest, accounting for the identification of *ScCDC13* in the original 'cdc' screen (Hartwell and Smith, 1985). Later, other genetic components modulating *cdc13*-related resection were identified, including Exo1, the KEOPS complex, and CDK activity (Downey et al., 2006; Frank et al., 2006; Maringele and Lydall, 2002; Vodenicharov and Wellinger, 2006). Ku is a conserved heterodimer that binds dsDNA ends and plays an essential role in NHEJ, in addition to its involvement in other DNA repair pathways. Somewhat surprisingly, mutations in Ku abolished the cell cycle regulation of the overhang, and resulted in overhang signal that was present throughout the cell cycle (Gravel et al., 1998; Kibe et al., 2003). Like mutations in Cdc13, Ku inactivation in budding yeast leads to excessive resection and activation of a DNA damage checkpoint when cells are grown at 37° (Gravel and Wellinger, 2002; Teo and Jackson, 2001).

Wild-type fission yeast also exhibit very weak overhang signal, which is intensified in S-phase (Kibe et al., 2003). Deletion of *pot1*$^{+}$, encoding the fission yeast telomeric ssDNA binding protein, results in rapid loss of all telomeric DNA and chromosome circularization (Baumann and Cech, 2001). Analysis of a temperature-sensitive mutant of *pot1*$^{+}$ confirmed that telomere loss is preceded by resection of the C-rich telomeric strand, and subsequently of the subtelomeres (C. Pitt and JPC, in preparation). Cells deleted for *taz1*$^{+}$ or *rap1*$^{+}$ exhibit dramatically stronger overhang signal compared with wt cells; presence of the overhang in *taz1*Δ is dependent on the MRN complex and the Dna2 nuclease (Miller et al., 2005; Tomita et al., 2004; Tomita et al., 2003). This massive amount of overhang in *taz1*Δ and *rap1*Δ cells does not elicit a cell cycle arrest, suggesting that presence of large amount of telomeric ssDNA does not inevitably activate the DDR. Pot1 binds telomeric ssDNA both in the presence and the absence of Taz1 or Rap1, consistent with a role for the Pot1 complex in protection from DDR.

1.2.4 Telomere entanglements and other chromosome segregation defects

Mutations in several telomeric factors result in chromosome segregation defects. In some cases, these segregation defects can be attributed to telomere end-to-end fusions, and are thus part of the Fusion-Bridge-Breakage cycle originally described by McClintock (McClintock, 1939). However, as described below, segregation defects were observed in the absence of discernable covalent end-fusions.

In fission yeast, cells lacking Taz1 exhibit no growth defect when grown at 32°; however, when shifted to 19-20°, the cells activate a DNA damage checkpoint, and exhibit chromosome mis-segregation, causing a reduction in viability (Miller and Cooper, 2003). These chromosome-chromosome associations, termed telomere entanglements, are not a consequence of covalent end-to-end fusions: first, entanglements are not suppressed by deleting Ku or Ligase IV, which are essential for NHEJ; second, analysis of terminal fragments from *taz1*Δ cells at 20° did not reveal end-to-end fusions, whereas fusions are readily observed in G1-arrested *taz1*Δ cells (Ferreira and Cooper, 2001; Miller and Cooper, 2003). Entanglements are thought to involve a topological link between chromosomes, as they restrict gel entry during whole-chromosome pulsed-field gel electrophoresis (PFGE) and are suppressed by a gain-of-function mutation in Topoisomerase II (T. Germe et al., in preparation and Miller and Cooper, 2003). Finally, entanglements are thought to originate during DNA replication, as cells experience segregation defects following passage through S-phase at cold temperatures (Miller and Cooper, 2003). The uniqueness of telomere entanglements is further exemplified by the fact that *rap1*Δ cells are not cold sensitive and do not exhibit chromosome mis-segragation (Miller et al., 2005). As *rap1*Δ telomeres resemble *taz1*Δ telomeres with respect to telomere length, extensive 3' overhang and de-protection from end-fusions in G1 (Chikashige and Hiraoka, 2001; Kanoh and Ishikawa, 2001; Miller et al., 2005), these are unlikely explanations for the chromosome segregation defect of *taz1*Δ cells at cold temperatures.

Much of the work discussed here has been done with the aim of understanding the aetiology of telomere entanglements: what structurally are entanglements? What are the genetic requirements for entanglements? And how are entanglements linked to other forms of telomere dysfunction?

1.2.5 Repression of transcription

Telomeres impose an epigenetic repression on RNA polymerase II transcription. This effect is not caused *via* sequence specific recruitment or exclusion of transcription factors, but through sequence-independent spreading *in cis* of a repressive chromatin state (Aparicio et al., 1991; Gottschling et al., 1990). This effect, termed telomere position effect (TPE), is mechanistically similar to much older observations of epigenetic regulation in flies (reviewed in Henikoff, 1992). While TPE has been studied extensively in yeast, evidence suggests TPE and heterochromatin are highly conserved features of telomeres (Baur et al., 2001; reviewed in Blasco, 2007).

De-repression of transcription at subtelomeres has been observed in mutants involved in heterochromatin formation (i.e. histone modifiers such as Clr4, Swi6 or ScSir2) (Aparicio et al., 1991; Ekwall et al., 1995; Lorentz et al., 1992; Thon et al., 1994; Thon and Klar, 1992), and mutations in telomeric proteins, such as deletion of *taz1*$^{+}$ or mutations in *ScRAP1* (Cooper et al., 1997; Kyrion et al., 1993). Interestingly, wt fission yeast cells exhibit a structure distinct from canonical nucleosome arrays, encompassing the terminal ~1-1.5kb of the chromosome; this poorly understood structure is abolished upon deletion of *taz1*$^{+}$, and its connection to TPE and to 'conventional' heterochromatin is currently unknown (JPC, unpublished observations).

The function of repressive telomeric heterochromatin is still unclear. Mutants in heterochromatic components do not exhibit gross telomere dysfunction, and in most cases, do not affect telomere length (Askree et al., 2004). However, the newly recognized RNA transcripts at telomeres (see section 1.2.7 below) might shed light on the functional importance of transcriptional regulation at telomeres.

1.2.6 Abrupt telomere loss

Telomeres of dividing cells undergo gradual shortening caused by the so-called 'end-replication problem': the inability of conventional DNA polymerases to replicate the very end of the chromosome, combined with DNA processing events (see section 1.3.1 below). However, in several instances, rapid loss of telomeres was observed. One such instance was described in budding yeast, where a single long telomere was introduced into an otherwise wt cell that maintains short telomere length. Unexpectedly, this long telomere does not gradually shorten until it reaches wt telomere length, but rather shortens rapidly and in discrete steps, in what had been termed 'telomere rapid deletion' (TRD) (Li and Lustig, 1996). While TRD is affected by mutations in the HR machinery and in telomeric heterochromatin, the exact mechanism by which telomere shortening occurs is still not clear; it was suggested that TRD occurs through an intra-telomeric recombination event, perhaps related to t-loop excision in mammalian cells (see section 1.2.7 below) (reviewed in Lustig, 2003; Wang et al., 2004).

Other instances where rapid telomere loss was observed are cells lacking WRN and cells overexpressing a truncated form of TRF2 ($TRF2^{\Delta B}$) (Crabbe et al., 2004; Wang et al., 2004). In both cases the initial puzzling observation was that telomeres were lost, as could be discerned by decline of telomeric hybridization signal and by FISH on metaphase chromosomes; however, telomere length did not decrease. It was later found that in both cases single sister telomeres are lost in a mechanism coupled to semi-conservative DNA replication (see further discussion in Section 4.2.1).

Finally, fission yeast cells lacking Taz1 exhibit a defect in telomere replication (see section 3.2) (Miller et al., 2006). This replication defect has led us to postulate that *taz1*Δ telomeres are synthesized *de novo* by telomerase in each cell cycle, and indeed, in the absence of telomerase, *taz1*Δ telomeres are lost within the first 10 generations – translating to loss of at least 300bp in each cell cycle (see section 3.3) (Miller et al., 2006). This loss is unlikely to be caused by the mere inability to semi-conservatively replicate telomeres, since mutations in the RecQ helicase Rqh1 rescue the abrupt telomere loss in *taz1*Δ cells

without assisting semi-conservative telomere replication (see chapter 5). Thus, telomere loss is likely to involve further processing, probably of stalled replication forks, by a mechanism involving Rqh1. However, the exact mechanism accounting for telomere loss, and to the way by which Taz1 acts to prevent it in wt cells, is currently under investigation.

1.2.7 Other structures at the end: TERRA and t-loops

Recent work has unearthed a new substance at human telomeres that may also obstruct their replication, telomeric RNA transcripts known as TERRA (Azzalin et al., 2007; Schoeftner and Blasco, 2008). TERRA localizes to telomeres and increases in local abundance in cells mutated for components of the nonsense-mediated mRNA decay pathway. Intriguingly, telomere length is reduced in these cells, suggesting that an excessive buildup of TERRA interferes with telomere maintenance. Further studies may reveal whether TERRA levels are altered through the cell cycle or when telomere proteins are lost, and whether TERRA provides a steric impediment to telomeric replication fork progression.

One of the exciting ideas to explain telomere protection is the t-loop, suggested to form when the 3' telomeric overhang invades a more internal section of the same telomere. The t-loop would prevent exposure of the 3' end, but not the exposure of a displaced G-rich single strand at the base of the t-loop. The existence of t-loops was revealed by the observation of circles and lasso-shaped molecules by electron microscopy in cross-linked DNA isolated from mammalian cells; t-loops can also be formed *in vitro* in the presence of TRF2 (Griffith et al., 1999). The biochemical activity that enables TRF2 to promote t-loop formation is unclear, although it was recently reported that TRF2 modifies the supercoiling of telomeric DNA, which may account for its ability to promote strand invasion and t-loop formation (Amiard et al., 2007). Importantly, it is still unclear whether indeed the t-loop is a protective structure, as it may represent an intermediate in (aberrant) telomere metabolism.

Conceptually, the t-loop presents a challenge for the cell since its base resembles a recombination intermediate. Aberrant processing of this structure can result in excision of the entire t-loop, resulting in telomere shortening. The

excised loops can be visualized cytologically as telomere-containing double minute chromosomes (TDM), or as circular telomeric forms (t-circles) discerned *via* neutral-neutral 2D gel electrophoresis. These structures have been isolated from cells mutated for the structure-specific endonuclease ERCC1/XPF (Zhu et al., 2003), and upon overexpression of a truncated form of TRF2 ($TRF2^{\Delta B}$) (Wang et al., 2004). The creation of t-circles requires the DNA repair factors XRCC3 and Nbs1 (part of the MRN complex) (Wang et al., 2004), suggesting that the base of the t-loop can indeed constitute a substrate for the DNA repair machinery.

The t-loop would also present a challenge to the semi-conservative replication machinery: the base of the t-loop might hinder replication fork progression, leading to the proposal that t-loop formation is cell cycle regulated, and that it is dismantled in S-phase. Several observations suggest a link between processing of t-loops and semi-conservative DNA replication. First, telomere loss in $TRF2^{\Delta B}$ was specifically observed at the sister chromatid that underwent leading strand replication, suggesting that t-loop excision is coupled to DNA replication (Wang et al., 2004). Second, ORC2, a component of the human origin recognition complex (ORC), interacts with TRF2 through the same domain missing in $TRF2^{\Delta B}$, and ORC2 depletion results in essentially the same telomeric phenotypes as $TRF2^{\Delta B}$ overexpression (Deng et al., 2007), suggesting that the role of TRF2 in preventing t-loop excision involves the origin recognition complex. Finally, the telomeric phenotypes conferred by $TRF2^{\Delta B}$ overexpression are dependent on the activity of WRN – a helicase involved in semi-conservative replication of telomeres (Crabbe et al., 2004; Li et al., 2008). Hence t-loops may present a specific challenge to DNA replication or processes coupled to it, such as origin firing, fork-reversal, fork-restart, or HR.

Alternatively, the observations linking t-loops to DNA replication may be interpreted to support the hypothesis that t-loops and/or t-circles are the products of aberrant attempts to restart stalled replication forks. Their presence would therefore be a manifestation of perturbed DNA replication. Consistent with this scenario is the fact that t-circles are abundant in ALT cells (Wang et al., 2004), which harbor unstable telomeres that may suffer fork-stalling.

1.2.8 Telomeres in cancer

Several concomitant telomere-related processes are postulated to take place during the progression of cancer (reviewed in Shay and Wright, 2006). First, cancers involve massive expansion of cells that are originally somatic and therefore do not express telomerase; during that expansion telomeres are eroded until cells enter a 'crisis' stage and proliferation is temporarily arrested. Cancers bypass that hurdle through inactivation of cellular checkpoints and activation of a telomere maintenance pathway – ~90% of known cancers activate telomerase, while the rest are thought to maintain telomeres through ALT. By adding an additional prerequisite for the formation of a full-fledged cancer, telomeres act as a cancer limiting mechanism ('tumour suppressor').

However, another hallmark of cancer is genomic instability, thought to promote cancer progression through its inherent mutagenicity. Telomere dysfunction can drive genome instability through all the mechanisms mentioned above; for example, Fusion-Bridge-Breakage cycles caused by telomere end-to-end fusions, telomere-telomere associations resulting in chromosome mis-segregation and aberrant anaphase, or abrupt telomere loss resulting in unprotected chromosome termini. An important unanswered question is whether the crisis evoked by the critically short telomeres, and the genome instability that ensues, are indeed major contributors to cancer progression *in vivo*; in that sense, telomeres, or perhaps imbalanced or critically short telomeres, can be thought of as 'oncogenes'. This is a particularly pertinent question, as telomerase inhibitors are constantly being developed and tested as specific anti-cancer drugs (reviewed in Harley, 2008). Such hypothetical telomerase inhibitors might be successful in driving cancer cells into crisis, thus limiting their short-term proliferation; but by achieving cellular crisis these drugs might inadvertently induce genomic instability that would allow the cancer to become more aggressive.

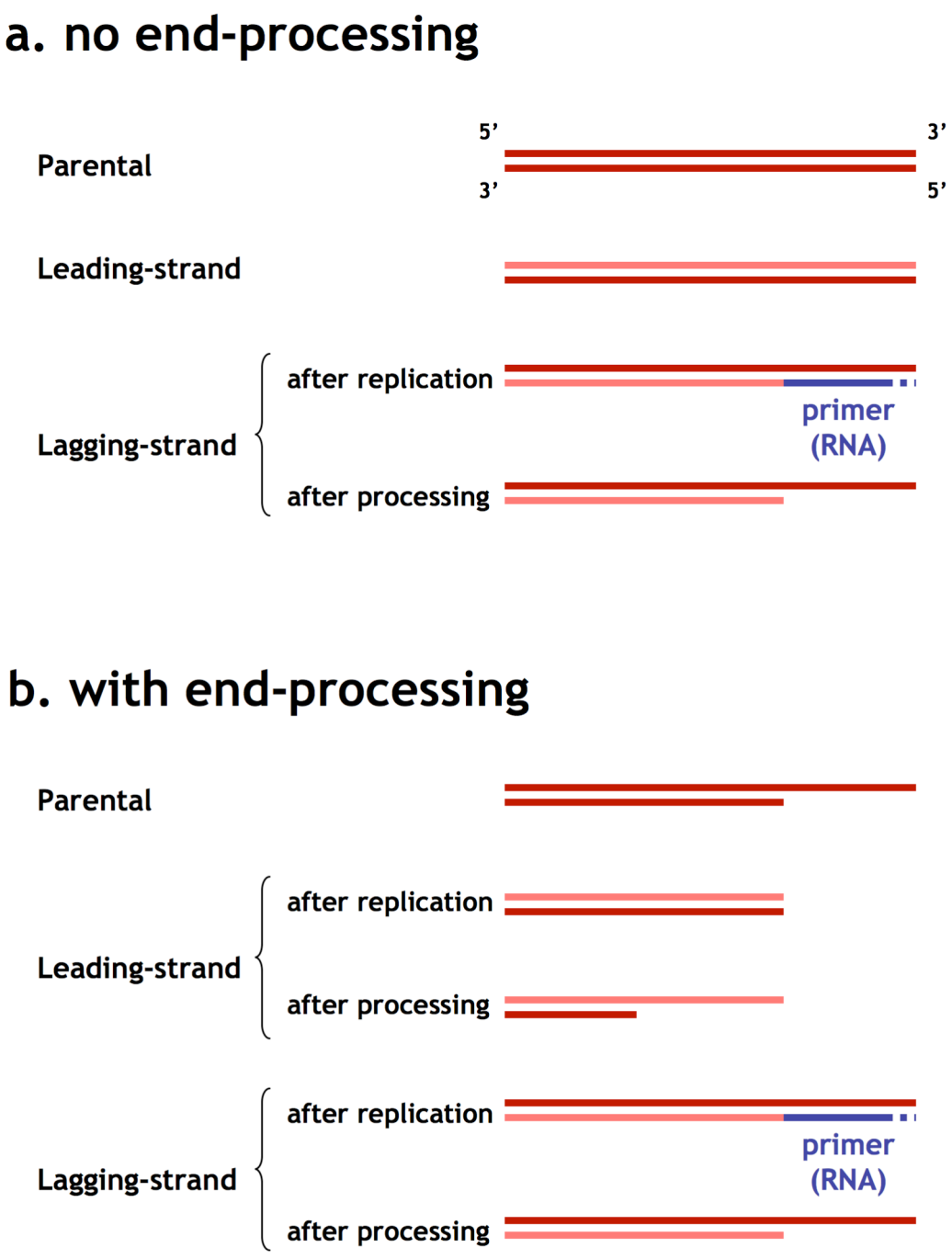

Figure 1.2 The end-replication problem

Red lines, the 'Watson' and 'Crick' strands of duplex DNA; top strand always runs 5' to 3'. Light red lines, nascent DNA strands. Blue line, RNA primer placed during lagging strand synthesis. (a) Original formulation of the end replication problem, assuming chromosomes terminate with a blunt end. (b) End replication problem assuming telomeres end with an overhang. See text for details.

1.3 Telomere replication

1.3.1 Semi-conservative telomere replication

Conventional semi-conservative DNA replication accounts for the bulk of telomere synthesis. However, early on, researchers realized that the conventional DNA replication machinery could not faithfully replicate linear molecules. The original formulation of the 'end-replication problem' (Olovnikov, 1973; Watson, 1972) assumed that leading strand replication can synthesize DNA virtually up to the very last nucleotide and that chromosomes terminate with a blunt end. Lagging strand replication cannot replicate past the end of the very last primer, thus leaving at least the size of a primer unreplicated (Figure 1.2a). However, careful analysis suggests blunt-ended products of leading strand replication are likely not to persist (see section 1.2.3) (Chai et al., 2006; Wellinger et al., 1996). Taking into account that telomeres end with an overhang, thinking about the end-replication problem was also revised (Lingner et al., 1995): lagging strand replication would thus recapitulate more or less the original template, assuming the size of the overhang is similar to the size left by the last primer. However, as the leading strand is templated by the shorter C-rich strand, the nascent G-rich strand will be shorter than the G-rich strand in the parental telomere. Following the resection events that recreate an overhang on the leading strand telomere, the end result is shorter than the parental telomere by exactly the size of the original overhang (Figure 1.2b). Under both interpretations, telomeres cannot be completely replicated by the semi-conservative replication machinery, and would undergo continuous attrition with cell divisions unless they can be extended by other mechanisms: telomerase or recombination (see below).

However, 'normal' semi-conservative replication has long been thought to be intimately related to telomerase-mediated telomere synthesis. Classic experiments in budding yeast demonstrated that telomerase activation requires passage of the replication fork through telomeres – linearized plasmids lacking an origin of replication (ARS) did not harbour overhangs, while similar constructs containing an ARS did (Dionne and Wellinger, 1998). A number of mechanisms are likely to contribute to this coupling between semi-conservative

and telomerase-based telomere replication. First, specific interactions between telomere proteins and components of the semi-conservative replication machinery are required for telomerase activity. This was hinted at by early studies showing telomere elongation in response to mutation of the DNA replication machinery (Carson and Hartwell, 1985). Subsequently, it was shown that the ability of telomerase to add telomere repeats to an induced DSB in mitotically arrested cells depends on the DNA polymerase α (Polα)/primase complex and Polδ (Diede and Gottschling, 1999); Polα was also found to interact with Cdc13 (Qi and Zakian, 2000). Likewise, components of the human origin recognition complex (ORC) appear to interact with hTRF2 (Deng et al., 2007). Furthermore, recent data demonstrate a striking structural similarity between the telomere-specific Cdc13/Stn1/Ten1 (CST) complex and the ubiquitous tri-subunit eukaryotic single strand DNA binding complex RPA, which plays integral roles in DNA replication, recombination and repair (Gao et al., 2007; Martin et al., 2007). The identification of CST as a 'telomere-specific RPA' prompts the notion that CST, which has a higher affinity for telomere sequences than RPA, displaces RPA as part of a choreographed hand-off between the conventional replication machinery and telomerase. Similarly, It has been proposed that a specialized replication factor C (RFC)-like complex containing Elg1 promotes polymerase processivity specifically at the telomere (Smolikov et al., 2004). Coupling between replication fork arrival and telomerase activity may conversely be enforced by a need for the former to strip telomeres of binding proteins to provide access for telomerase. Such stripping may also accompany telomere shortening itself if, for example, a threshold concentration of bound telomere proteins is necessary to confer a 'closed' telomeric configuration.

Surprisingly, interactions between telomere proteins and the replication machinery may be required not only for telomerase activity, but also to escort the semi-conservative replication fork through telomeres. This idea stems from work presented here, demonstrating that fission yeast telomeres lacking Taz1 accumulate paused replication forks (Miller et al., 2006). Telomere sequences themselves, perhaps because of their repetitiveness or the preponderance of G residues, appear to impede replication when 'naked', while replication proceeds

smoothly through telomeres bound by Taz1. Paused forks lead to several *taz1Δ* phenotypes, the most pertinent for this discussion being the abrupt loss of all telomeric repeats upon removal of telomerase (*trt1*$^{+}$ deletion) from *taz1Δ* cells. This telomere loss is particularly dramatic given that *taz1Δ* telomeres are unusually long (up to ~10 times wild type length (Cooper et al., 1997)), and indicates that these long telomeres must be synthesized virtually *de novo* in each S-phase. An extension of this reasoning suggests that the stalled *taz1Δ* telomeric replication forks are excellent substrates for telomerase. Finally, stalled forks at *taz1*Δ telomeres may also contribute to ALT-like survival by promoting recombination events at telomeres (see section 1.3.2.1).

It remains to be shown whether the facilitation of replication is a conserved function of telomere binding proteins. Fork stalling was observed at budding yeast subtelomeres and telomere sequences in wild type cells (Ivessa et al., 2002; Makovets et al., 2004). Hence, it appeared that replication forks would be impeded by telomere proteins; indeed, telomeric stalling in budding yeast was greatly enhanced in cells lacking the Rrm3 helicase, which is thought to assist fork progression through particularly stable protein-DNA complexes (Ivessa et al., 2003; Ivessa et al., 2002). However, the observation that replication forks stall at telomeres in *taz1*Δ cells predicts that the absence of Rap1 would exacerbate the accumulation of stalled forks in budding yeast telomeres, but this idea has not been tested. In mammals, the roles of Taz1 are generally shared by TRF1&2, and it is therefore possible that one of these, or a regulated ratio between them, is crucial for smooth telomeric replication. Intriguingly, replication of mammalian telomeres requires the RecQ helicase WRN, as cells lacking functional WRN exhibit telomere loss specifically from the sister chromatid copied by lagging strand synthesis (Crabbe et al., 2004) (see also section 4.2.1). As WRN interacts with TRF2 (Opresko et al., 2002), it may mediate a role for TRF2 in promoting telomere replication. Collectively, these data suggest that there are multiple causes of fork-stalling at telomeres, with both the repetitive telomere sequence itself and its associated heterochromatin presenting challenges to the replication machinery.

Further evidence suggesting that telomeres pose a challenge to replication forks, and particularly to collapsed replication forks, comes from analysis of mutants in the cohesin- and condensin-related Smc5/6 complex. When the activity of Smc5/6 is compromised, cells experience chromosome segregation defects that stem from problems in DNA replication of repetitive regions – the rDNA array and telomeres (Ampatzidou et al., 2006; Potts and Yu, 2007; Torres-Rosell et al., 2007; Torres-Rosell et al., 2005). This has led to the suggestion that Smc5/6 plays a crucial role in the repair of stalled/collapsed replication forks specifically in repetitive regions; alternatively, repetitive regions may be prone to fork collapse, rendering the activity of Smc5/6 essential particularly there. Finally, the apparent specificity of the Smc5/6 complex to rDNA and telomeres may be related to the fact that both these regions are replicated unidirectionally, rendering fork stalling or collapse a particularly destructive lesion as the unreplicated DNA in front of the fork cannot be replicated by an oncoming fork (Murray and Carr, 2008). Interestingly, the defects conferred by inactivation of Smc5/6 are somewhat analogous to the phenotypes conferred by *taz1*$^{+}$ deletion at cold temperatures: a defect in telomere replication and chromosome mis-segregation (Miller and Cooper, 2003; Miller et al., 2006).

1.3.2 Telomere maintenance: ALT and telomerase

Despite the challenges encountered by the semi-conservative replication machinery and the end-replication problem, telomeres are maintained at a relatively constant length, suggesting that the cells employ mechanisms that can counteract telomere attrition and loss. The mechanisms that operate to allow telomere elongation can be classified into two classes: recombination-based mechanisms and telomerase-mediated repeat addition.

1.3.2.1 Recombination-based telomere elongation

Recombination based mechanisms are thought to be the chief telomere elongation pathway only in a minority of the species studied so far, and in a fraction of cancers that failed to activate telomerase (so called ‘alternative lengthening of telomeres’ or ALT cells). While ‘perfect’ homologous recombination events would be silent and would not allow telomere elongation,

several other modes of homology-driven recombination may allow overall telomere elongation and maintenance:

1. **Unequal recombination**: unequal crossing-over events can lengthen one telomere at the expense of another, thus maintaining the total amount of telomeric DNA in the cell, and failing to account for telomere maintenance over time. However, when coupled to strong selection against cells harbouring short telomeres, it may allow overall gain of telomeric sequences in the population; for example, when considering a scenario where an unequal exchange of telomeric repeats between two sister telomeres is followed by senescence of the daughter cell that inherited the shortened telomere.
2. **Break-induced replication (BIR)**: in BIR, a telomere 3' end would invade another telomere, followed by extension of the invaded end by the DNA replication machinery until the terminus of the template telomere. Invasion of a telomere into an internal site at another telomere would result in telomere elongation and net gain of telomeric sequences. Indeed, the non-essential replication factor Pol32, which is essential for BIR, is also essential for survival of budding yeast cells lacking telomerase (Lydeard et al., 2007). Interestingly, a BIR invasion event of a telomere into itself, which generates a structure similar to a t-loop, would result in potentially never-ending elongation, similar to rolling circle amplification (see below).
3. **Rolling circle replication/amplification**: Researchers postulated that telomere elongation could be achieved by BIR events that include invasion into an extra-chromosomal circle of telomeric DNA. As circles lack a terminus, extension in this case is virtually limitless, which may explain observations of sudden and massive amplification of telomeric DNA in yeast. Although direct evidence for rolling circle amplification of telomeres is lacking, circumstantial evidence suggests that extra-chromosomal telomeric DNA circles can be found in various organisms and in ALT cells (Cohen and Mechali, 2002; Groff-Vindman et al., 2005; Wang et al., 2004). In addition, in the budding yeast *Kluyveromyces lactis,* telomere extension events that are consistent with rolling circle amplification were observed (Natarajan and McEachern, 2002).

4. **Subtelomeric amplification**: While all the above options were described for telomeric repeats, they might be applied to subtelomeric repeated elements, which are abundant in many organisms. In that case, the resulting end-structures would be composed of tandem non-telomeric repeats with interspersed telomeric sequences that provide docking sites for the telomeric complex, thus providing end protection (see further discussion in section 3.5).

1.3.2.2 Regulation of telomerase and the 'critically short telomere'

The more evolutionarily common mechanism to counteract telomere attrition caused by the end-replication problem, and possibly other assaults, is the action of the reverse transcriptase telomerase. Telomerase can copy telomeric repeats from its own template RNA onto the 3' end of the exposed telomeric G-rich overhang (Greider and Blackburn, 1985, 1987). Telomerase activity can be reconstituted *in vitro* using only the catalytic subunit of telomerase, telomerase RNA and a substrate containing telomeric 3' ssDNA (Weinrich et al., 1997). However, telomerase activity *in vivo* requires additional factors (see section 1.4).

It had long been observed that telomerase maintains telomere length within a constant range, specific to each organism, suggesting telomerase activity is tightly controlled. Elegant early studies demonstrated that this length control is exerted *in cis* – for example, when a linear plasmid harbouring a short telomere is introduced into the cell, that telomere is elongated without affecting other telomeres (see also Marcand et al., 1999; Shampay et al., 1984). Since then, a vast number of genes and regulatory pathways affecting telomere length have been described (for example Askree et al., 2004). It was demonstrated that Rap1 (and its functional orthologs Taz1 and TRF1) assesses the number of the telomeric repeats using a so-called 'counting mechanism'; once the 'appropriate' number of telomeric repeats is reached, the counting mechanism exerts negative regulation *in cis* on telomerase (Krauskopf and Blackburn, 1996; Levy and Blackburn, 2004; Marcand et al., 1997). However, the detailed molecular activities dictating how telomerase preferentially elongates the short telomeres remain unclear. A seminal paper established a system for inferring

the *in vivo* dynamics of telomerase activity by identifying those specific telomere sequences added to a marked telomere during a single cell cycle. This analysis revealed that telomerase acts only on a subset of telomeres (ca. 7%) in each cell cycle, these telomeres being the shortest in the cell (Teixeira et al., 2004). This mode of regulation can explain how each telomere's length is individually monitored to maintain overall telomere length homeostasis. A key question is thus how shorter telomeres are detected.

A handful of recent studies have provided insight into both the short-telomere preference of telomerase recruitment and its cell cycle dependency. While budding yeast telomerase acts in late S phase, its presence at telomeres appears to peak twice: at late S/G2 and, less so, at G1 (Taggart et al., 2002). Its cell cycle regulated activity was thus explained by the late S phase-specific presence of Est1, a regulatory subunit of telomerase (Evans and Lundblad, 1999). Furthermore, several recent studies confirmed that Est1 and telomerase are specifically recruited to short telomeres, thus explaining their differential susceptibility to elongation (Bianchi and Shore, 2007b; Sabourin et al., 2007). Two groups addressed the differential occupancy on short telomeres by creating a unique short telomere, using an inducible recombination system to excise telomere sequences flanked by recombinase sites. (Marcand et al., 1999; Marcand et al., 1997). This shortened telomere exhibited enhanced binding of telomerase components (including Est1), but not other telomeric factors such as the Ku complex, Cdc13 or Rif1 (Bianchi and Shore, 2007b; Sabourin et al., 2007).

In addition to the known telomere factors, preferential recruitment of Tel1 (the budding yeast ATM homolog) to short telomeres was observed (Bianchi and Shore, 2007b; Sabourin et al., 2007). Enhanced Tel1 binding is also seen at telomeres shortened either by growth in the absence of telomerase or by the telomere loss seen at high temperatures in strains lacking Ku (Hector et al., 2007). These results provide a framework for interpreting early observations that loss of both the ATM and ATR homologs in budding or fission yeast result in telomere loss (Naito et al., 1998; Ritchie et al., 1999), and that human TRF2 can directly bind and inhibit ATM (Karlseder et al., 2004). In additional support for a role for Tel1 in marking short telomeres, the bias of telomerase toward

shorter telomeres is lost in the absence of Tel1 (Arneric and Lingner, 2007). Intriguingly, the role of Tel1 is suggested to extend beyond dictating the short-telomere preference to influencing telomerase processivity as well. Analysis of the extension profiles of extremely short telomeres revealed that a single telomerase complex could act multiple times in one cell cycle on a single telomere. Such repeated activity requires Tel1 (Chang et al., 2007). Taken together, these works suggest a model whereby a short telomere is transiently recognized as a DSB, leading to Tel1 recruitment and consequently to telomerase recruitment and activation. By extension of this logic, activation of DDR at telomeres, for example by stalled replication forks, is likely to promote telomerase recruitment and activity. Furthermore, the short telomeres that activate DDR may be related to the 'critically short telomeres' that limit cellular survival and induce senescence upon telomere attrition in mammalian cells lacking telomerase (Hemann et al., 2001).

Crucially, it remains to be shown whether short telomeres locally activate a DDR (as opposed to just recruiting Tel1), and whether this mode of regulation is conserved. Insight into these questions comes from primary human cells, which are thought to harbor 'normal' telomeres. Careful cell cycle analysis in these cells revealed that telomeres locally activate the DDR response during G2, as assessed by foci of activated ATM and telomeric presence of ATM and MRN. Concomitant with this activation, 'exposed' ends (which can be extended by terminal transferase *in situ*) are observed, suggesting that these telomeres adopt a structure that indeed resembles a DSB (Verdun et al., 2005; Verdun and Karlseder, 2006). Altogether, these experiments suggest that engagement of the DDR is not limited to cells harboring mainly eroded or dysfunctional telomeres, but might be a general feature of the cell-cycle regulation of telomeres. However, a critical open question is whether local DDR activation is limited to the shorter telomeres in normal cells.

A comprehensive model for the events downstream of ATM/Tel1 activation at short telomeres must also include an explanation for the differences between a DSB and a telomere. Importantly, short telomeres do not elicit a global checkpoint response or cell cycle arrest, whereas a single, persistent DSB does (Bennett et al., 1993). In other words, where on the DDR cascade is the 'short

telomere response' differentiated from the DSB response? Telomere-specific factors are likely to mediate this attenuation of the DDR, and indeed, long telomere sequences have been shown to exert an 'anti-checkpoint' activity, inhibiting a persistent DDR from occurring at an adjacent induced DSB (Michelson et al., 2005). These data, along with the lack of checkpoint activation in *taz1Δ* cells (see above) raise the possibility that the telomeric ssDNA binding proteins Cdc13 and Pot1 mediate the 'anti-checkpoint' response.

The identity of the lesion that activates DDR and telomerase at short telomeres is still unknown. Several (not mutually exclusive) candidates have been suggested, including an extended 3' overhang and abolition of a t-loop structure. However, direct evidence for either idea is lacking. The work described herein provides evidence for an additional hypothesis: shortened telomeres may lead to stalled telomeric replication forks, which constitute a signal for activation of DDR and telomerase. In the absence of telomerase, these stalled forks may contribute to or constitute the signal causing senescence, and may also trigger the recombination events that constitute the ALT mode of telomere maintenance (Bryan et al., 1997).

Recently, an additional and unexpected feature of the 'critically short telomere' was described, suggesting a further link between semi-conservative telomere replication and telomerase activation (Bianchi and Shore, 2007a). Shore and colleagues used the inducible recombination system described above to create a genetically marked, critically short telomere. A chromatin immunoprecipitation (ChIP) assay was then employed to assess localization of the replication forks at normal *versus* foreshortened telomeres. Budding yeast telomeres generally replicate late in S-phase (Ferguson and Fangman, 1992), and while the subtelomeric regions contain ARS elements, these are usually kept dormant. However, telomeric excision has a surprising *cis* effect on the adjacent subtelomeric ARS: the curtailed telomeres replicated markedly earlier than normal telomeres. This early replication utilizes the adjacent, normally dormant subtelomeric ARS elements. These observations could be explained by chromatin structure; late replication timing, prevention of DDR, and restricted telomerase access may be consequences of a closed chromatin state, which is promoted by longer telomeres and lost as they decline in length. Whether

stalled telomeric replication forks could contribute to the broader peaks of replication fork occupancy seen at short telomeres remains to be addressed.

1.4 Fission yeast telomeres

Fission yeast provides a great model system to study chromosome biology as it combines ease of genetic manipulation with chromosome structure related to that of metazoans. Some of the conserved features of fission yeast chromosomes are complex centromeres and heterochromatin, RNAi machinery, and a telomeric complex that resembles that of mammals.

Fission yeast chromosomes end with ~300bp of degenerate sequence TTAC(A)(C)G_{2-8}. The six subtelomeres can be divided into two classes: chromosomes I and II end with >19kb of loosely conserved repeated region, divided into subtelomeric elements 1, 2 and 3 (STE1/2/3). Most of the difference between the subtelomeres can be explained by variable number of repeated elements; these include an ~86bp repeat in the telomere proximal STE1, and a ~1kb repeat in the more internal part of the subtelomere (Sugawara, 1988). The subtelomeres also include sequences homologous to the centromeric dh/dg repeats that are thought to function in RNAi (Cam et al., 2005; Kanoh et al., 2005), as well as four copies of a poorly understood RecQ-like helicase ORF (Mandell et al., 2005). Both sides of chromosome III contain the rDNA arrays, which are flanked by the telomeric sequences, and possibly also contain subtelomeric elements (Sugawara, 1988).

The telomeric proteins can be roughly divided into 4 groups: telomeric dsDNA complex, telomeric ssDNA complex, telomerase and its regulatory subunits and additional non-telomeric proteins that are present at telomeres, and mostly include DDR and DNA repair proteins (see Figure 1.1).

1. **Telomeric dsDNA complex**: The only telomeric dsDNA binding protein described so far is Taz1 (Cooper et al., 1997). Taz1 recruits Rap1 and Rif1 to the telomeres (Chikashige and Hiraoka, 2001; Kanoh and Ishikawa, 2001) (see section 4.1.3 for details). The telomeric dsDNA complex is involved in many telomeric processes, including protection from DNA repair reactions and telomerase regulation. However, in fission yeast, it is not strictly required for viability – *taz1*Δ and *rap1*Δ

cells, despite harbouring de-protected telomeres that are prone to undergo DNA repair reactions including NHEJ and HR, are viable and grow indistinguishably from wt cells at optimal growing conditions (Cooper et al., 1997). This initially surprising observation is reconciled by the fact that growing fission yeast cells spend most of the cell cycle in G2 and effectively lack a G1 phase, and it is only in G1 that the deleterious NHEJ reactions take place (Ferreira and Cooper, 2001, 2004). Therefore, *taz1*Δ and *rap1*Δ cells are able to escape NHEJ at telomeres and proliferate, allowing examination of other functions of the telomeric complex.

2. **Telomeric ssDNA complex**: The recently described telomeric ssDNA complex assembles around the telomeric ssDNA binding protein Pot1 (Baumann and Cech, 2001). In addition, it includes Tpz1, Poz1 and Ccq1 (Miyoshi et al., 2008). Pot1 and Tpz1 have homologues in mammals (POT1 and TPP1, respectively), and are structurally related to TEBPα and TEBPβ in ciliates (Baumann and Cech, 2001; Miyoshi et al., 2008; Wang et al., 2007; Xin et al., 2007). The telomeric ssDNA complex is also present at internally placed telomeric stretches, which lack an overhang, and is thought to be localized there through a protein-protein interaction between Rap1 and Poz1 (Miyoshi et al., 2008). Two other budding yeast homologues that are thought to act together with Pot1 are Stn1 and Ten1 (Martin et al., 2007). The absence of Pot1, Tpz1, Stn1 or Ten1 prompts immediate loss of all telomeres, suggesting that the telomeric ssDNA-binding complex is essential for maintenance of telomeric 'identity' (Baumann and Cech, 2001; Martin et al., 2007; Miyoshi et al., 2008).

3. **Telomerase**: The two essential subunits required for telomerase reverse-transcription activity *in vitro* are the catalytic subunit Trt1 (Nakamura et al., 1998) and the recently identified RNA subunit *ter1* (Leonardi et al., 2008; Webb and Zakian, 2008). In addition, several additional gene deletions result in gradual telomere shortening typical of telomerase-null cells – termed 'ever shorter telomeres' (EST) phenotype: *est1*$^+$ (Beernink et al., 2003), *ccq1*$^+$ (K. Tomita and JPC,

submitted) and the combined deletion of the ATM and ATR homologues *tel1*$^{+}$ and *rad3*$^{+}$ (Naito et al., 1998). Although thorough screening for additional telomerase regulatory subunits in fission yeast has not been carried out, by analogy with other systems it is likely to reveal numerous other factors involved in modulating telomerase activity. In the absence of telomerase activity, telomeres gradually shorten with cell divisions until the cells reach a crisis stage, where most cells cease to proliferate. Rare survivors can be readily observed, and fall into three main categories, the latter two unique to fission yeast: linear survivors that maintain telomeres through a recombination-based mechanism, similar to ALT cancer cells and type I & II survivors in budding yeast; so called 'circular' survivors, where the three chromosomes have undergone intra-molecular fusions to form three circles lacking telomeric sequences (Nakamura et al., 1998); and the newly identified linear survivors that lack telomeric sequences, but have amplified heterochromatic regions such as the rDNA array or the subtelomeres (D. Jain *et al.*, in preparation).

4. **DDR, DNA repair and heterochromatin factors**: Many other factors, which are not specific to telomeres, are also present or acting at telomeres, both in fission yeast and in other studied systems. These factors include the Ku heterodimer (Pku70/80) (Baumann and Cech, 2000), the MRN/X complex (Mre11, Rad50 and Nbs1) (Manolis et al., 2001), the ATM and ATR homologues (Tel1 and Rad3, respectively) (Naito et al., 1998), the 9-1-1 complex (Rad9, Rad1 and Hus1) (Dahlen et al., 1998), and the RecQ helicase Rqh1 (Kibe et al., 2007).

During interphase, the 6-12 telomeres are clustered into 1-4 (most commonly 1-2) foci at the nuclear periphery, which can be discerned *via* FISH against telomeric and subtelomeric sequences, indirect immunofluorescence (IF) against telomeric proteins, or using fluorescently tagged telomeric proteins. Deletions of several RNAi-related genes (*ago1*$^{+}$, *dcr1*$^{+}$, or *rpd1*$^{+}$) are the only mutations reported to confer telomere de-clustering (Hall et al., 2003); so far no mutations have been reported to de-localize interphase telomeres from the

nuclear periphery, and thus the importance of peripheral localization has not been studied. In meiotic prophase, telomeres exchange places with the centromeres, which are usually located at the spindle pole body (SPB; yeast centrosome equivalent), and are all clustered at the SPB in the so-called 'meiotic bouquet' (Chikashige et al., 1994; Chikashige et al., 1997). This clustering is mediated by protein-protein interactions involving Taz1, Rap1, Bqt1 & 2 and the SPB component Sad1 (Chikashige et al., 2006). This highly conserved telomere congregation is then followed by dynamic back and forth movements of the prophase nucleus which is led by the SPB, known as the 'horsetail movement' (Chikashige et al., 1994; Chikashige et al., 1997). While the meiotic bouquet likely contributes to chromosome pairing, its crucial role is controlling the SPB to ensure proper function of the spindle in later meiotic divisions (Tomita and Cooper, 2007).

1.5 List of Abbreviations

2DGE	neutral-neutral 2-dimensional gel electrophoresis
5-FOA	5-Fluoroorotic acid
ALT	alternative lengthening of telomeres
ARS	autonomously replicating sequence (yeast origin of replication)
ATM	Ataxia Telangiectasia mutated (Tel1 in yeast)
ATR	ATM and Rad3 related (SpRad3/ScMec1)
BIR	break-induced replication
ChIP	chromatin immunoprecipitation
CO-FISH	chromosome-orientation FISH
CST	Cdc13/Stn1/Ten1
D-loop	displacement loop
DDR	DNA damage response
DSB	double strand break
FEN1	flap endonuclease 1
FISH	fluorescent *in situ* hybridization
HR	homologous recombination
IF	indirect immunofluorescence
HJ	Holliday junction
IP	immunoprecipitation
IR	ionizing (gamma) radiation
MCS	multiple cloning site
MMS	methylmethane sulfonate
MRN	MRE11/RAD50/NBS1
NHEJ	nonhomologous end-joining
ORC	origin recognition complex

PCNA	proliferating cell nuclear antigen
Polα	DNA polymerase α
PFGE	pulsed-field gel electrophoresis
RFC	replication factor C
RNAi	RNA interference
RPA	replication protein A (eukaryotic SSB)
SCE	sister-chromatid exchanges
SPB	spindle pole body (yeast centrosome equivalent)
STE1/2/3	subtelomeric elements 1/2/3
STL	sister telomere loss
t-loop	telomere loop
T-SCE	telomeric sister chromatid exchange
TDM	telomere-containing double minute chromosome
TERRA	telomeric repeat-containing RNA
TIFs	telomere dysfunction induced foci
TPE	telomere position effect
TRD	telomere rapid deletion

2 Chapter 2: Materials and Methods

2.1 Fission yeast strains and techniques

Standard media and growth conditions were used. Gene replacements with antibiotic and auxotrophic markers and C-terminal tagging were performed by the one-step PCR technique (Bahler et al., 1998; Sato et al., 2005). *trt1*$^{+}$ was deleted by transformation with a *trt1::his3* PCR fragment (Nakamura et al., 1998). Standard genetic techniques were used to construct strains harboring multiple mutations. Five-fold dilution assays were performed with starting concentration of $1x10^{7}$ cells/mL (1 O.D per mL). Recombination was measured as previously described (Ahn et al., 2005). A list of strains used is included in section 2.13.

2.1.1 G1 arrest

Cells were inoculated so that they would to be logarithmically growing overnight at 32° in minimal media with 1/3 of the normal amount of supplements (75mg/L uracil, adenine, histidine and leucine). In the following day, cells were washed 3 times with minimal media lacking supplements or nitrogen and supplemented with 1% glucose. Cells were then diluted to 0.1-0.2 O.D. and incubated shaking for 24hr at 25°. G1 arrested cells were scored by FACS (see below). Generally, 30-50% G1 cells were obtained using strains with auxotrophies, while prototrophs yielded 70-80% G1 arrest.

2.1.2 *trt1*Δ loss experiments

Heterozygous diploids were placed on sporulation media (malt extract, ME) and incubated at 25° for 2-3 days; the resulting asci were digested with Helix Pomatia Juice (4hr at 32°, or overnight at RT). No differences in telomere length were observed between spores of *rap1*$^{\Delta/\Delta}$*trt1*$^{\Delta/+}$ and *taz1*$^{\Delta/\Delta}$*trt1*$^{\Delta/+}$ strains (see Figure 3.6). Spores were germinated and propagated on YES media, re-streaking every 3 days. *En masse* sporulation was performed by germinating ~10^{6} spores in EMM media lacking histidine, growing the cells to logarithmic phase and harvesting every 24h.

2.1.3 Construction of internal telomere strains and related constructs

The internal telomere cassette (*ura4::ScLEU2*) was constructed by cloning a 250bp telomere fragment (from the plasmid pNSU70 (Sugawara, 1988)) upstream of the *ScLEU2* gene in plasmid pIRT2. The synthetic telomeres and other repetitive inserts were created by tandemly ligating annealed 49 bp oligonucleotides and cloning them into pIRT2 (see section 2.3 below). *ura4::insert* constructs (see Chapter 4) were constructed by cloning fragment of *ura4*$^+$ into pBlueScript; subsequently a multiple cloning site (MCS) disrupting *ura4*$^+$ was introduced into the *Nsi*I-*Stu*I sites, followed by sub-cloning the different inserts into the MCS. The MCS contained stop codon and *Sma*I, *Xba*I and *Sph*I sites, and abolished the flanking *Nsi*I and *Stu*I sites. All internal constructs were integrated into the genomic *ura4*$^+$ locus (Figure 3.4) by transformation and selection for 5-Fluoroorotic Acid (5-FOA) resistant clones, and verification by sequencing. 'Random GC-rich' sequence of 500bp with GC-content of 55% was ordered from Integrated DNA technologies (IDT) and was subcloned into the abovementioned constructs.

2.1.4 Construction of *rqh1*$^+$ mutants

A fragment containing bp 1288-3009 of *rqh1*$^+$ was cloned into the *Xho*I-*Not*I sites in pBlueScript, and point mutations were introduced using the QuikChange® Multi site-directed mutagenesis kit (Stratagene). The mutated *rqh1*$^+$ fragments (*Xho*I & *Not*I digest) were used to transform a *rqh1::ura4*$^+$ strain in which *ura4*$^+$ was inserted between positions 1549-2772 in *rqh1*$^+$. Transformants were selected on medium containing 5-FOA, and were verified by PCR and sequencing. C-terminally Myc-tagged Rqh1 was constructed by integration of 13xMyc cassette into the genomic *rqh1*$^+$ loci (or the different *rqh1* mutants) (Bahler et al., 1998). Myc-tagged Rqh1 conferred mild sensitivity to HU, but unlike Rqh1-hd, Rqh1-Myc conferred neither a growth defect nor abolished *taz1Δ* cold sensitivity (data not shown).

2.2 Genomic DNA 'smash-preps'

1. Grow 3-10mL of culture to saturation.

2. Spin down the cells and wash once with 10mL water.
3. Spin down the cells, and transfer to a 1.5mL tube.
4. Add 200μL of glass beads, 400μL phenol mixture (25:24:1 phenol:cloroform:isoamyl alcohol), and 400μL smash-prep buffer.
5. Break down the cells using vortexing (45'' @ 4.5 in a Fast-prep machine, or ~10min on a vortex).
6. Spin down 10min @ 13,000 rpm (preferably @ 4°C).
7. Transfer top (clear) fraction to a new tube, and add 2x volumes of 100% ethanol. Mix well by vortexing.
8. Keep at -20°C for 1hr (or more).
9. Spin down 10min @ 13,000 rpm (preferably @ 4°C).
10. Wash pellet with 70% ethanol. Discard ethanol, spin down again and aspirate all liquid.
11. Air-dry (or @ ~40-50°C).
12. Add 50μL TE (with RNase A, 5μl in 50mL TE). Re-suspend pellet (possibly by incubating @ ~40-50°C).
13. Use 5-15μL for digestion for Southern Blot, or 0.5-1μL for PCR.

Smash-prep Buffer (for 500mL):

2% Triton X-100 (10mL)

1% SDS (25ml of 20% stock)

100mM NaCl (10mL of 5M stock)

10mM Tris-HCl pH=8 (5mL of a 1M stock)

1mM EDTA (1mL of 0.5M stock)

2.3 Construction of synthetic telomeres

1. Phosphorylate the two complimentary oligonucleotides at their 5' end using T4 Polynucleotide Kinase (NEB) and ATP to allow ligation. (Phosphorylation of only one of the oligonucleotides is sufficient as well). Clean oligonucleotides using Qiagen columns.
2. Anneal the two complementary oligonucleotides using a PCR machine (5' @ 95°, followed by a slow gradient to 25°, 1° per minute).

3. Incubate the duplex DNA was with T4 DNA Ligase (NEB). A non-phosphorylated duplex could be included as a control. Clean reactions using Qiagen columns.
4. When running the samples on high-percentage agarose gel, a ladder of bands appears, which is dependent on phosphorylation, ligase and ATP.
5. To allow cloning, blunting of the ends should be performed. This could be achieved using Klenow fragment of DNA Polymerase I (NEB) or Quick Blunting® Kit (NEB).
6. Required fragments could be purified by using Qiagen columns, or by cutting appropriately sized bands from an agarose gel, followed by purification.
7. The blunt ended fragments could now be cloned. Due the relatively low efficiency of cloning, it could be useful to use colony hybridization (see section 2.6 below) to screen for positive clones.

2.4 Southern blotting

1. Run DNA samples on agarose gels until required separation is achieved. For telomere length analysis we normally use 0.8% agarose in 1x TAE. Make sure RNase A had been added to the samples. Ethidium bromide can be added to the gel, at 1μL per 100mL.
2. Visualize gels under UV lamp.
3. Incubate the gel with 0.25N HCl (freshly diluted from a 1N stock) on a gently shaking platform for 15-20min at RT. The colour of bromophenol blue should change to yellow. The purpose of this step is to introduce nicks to DNA to allow efficient transfer to the membrane.
4. Replace with Blot I, and incubate for further 30min. The colour of bromophenol blue should change back to blue. The purpose of this step is to denature the DNA.
5. Replace with Blot II, and incubate for 30-60min.
6. Blot the gel on the following stack:
    i. 10-15cm of paper towels.
    ii. Two pieces of 3MM (Whatman) paper, roughly the size of the gel, soaked in Blot II.

iii. Nitrocellulose membrane (we used either Duralon UV or Amersham Hybond-N). Use pencil to label the membrane. Soak thoroughly with Blot II before placing on the stack.

iv. Place the gel carefully on top. Avoid any air bubbles, as these would interfere with the transfer.

v. Pour some Blot II on top of the gel.

vi. Cover with Saran Wrap, and place a flat piece of glass or plastic with a small weight on top to avoid further movement.

7. Leave overnight.
8. In the morning, separate the membrane and allow to air dry (~10min).
9. **Crosslink**: Crosslink DNA to membrane (120,000μJ on a Stratalinker machine; 'Auto Crosslink' setting). At this point the membrane could be kept indefinitely.
10. **Probe preparation**: random-primed probes are prepared with Prime-It II kit (Stratagene), using 5μL of $P^{32}\alpha$-dCTP and 10-20ng of template DNA. End-labelled probes are made using T4 polynucleotide kinase (PNK from NEB), using 3μL $P^{32}\gamma$-ATP, 4μL oligonucleotide at 50μM, 1μL PNK and 1μL PNK buffer in a 10μL reaction volume (Cooper et al., 1997).
11. **Pre-hybridization**: Incubate the membrane in Church-Gilbert (CG) Buffer at the appropriate hybridization temperature for at least 15min. We use 65° for random-primed probes and 45° for end-labelled probes.
12. **Hybridization**: Boil probe for 5min and immediately add to CG Buffer. Incubate at hybridization temperature overnight.
13. **Washing**: Discard the CG Buffer. Wash twice with Blot Wash. Discard, and add Blot Wash again, incubate at the hybridization temperature for at ~45min. Discard and wash once more with Blot Wash. Discard, place membrane on a Saran Wrap and aspirate liquid with a paper towel. Seal and expose using PhosphoImager for 1-2 days.
14. **Stripping:** If stripping is necessary, add boiling Stripping Buffer. Incubate for 15min at 65°, and discard liquid. Repeat if signal is still detectable with Geiger Counter (or by exposing the membrane in the PhosphoImager). Once signal is undetectable, repeat hybridization, starting with the Pre-hybridization step.

DNA Loading Buffer (10ml):

30% glycerol (3.7ml of 80% glycerol in H_2O)

6mM EDTA (120μL of 0.5M stock)

12mg bromophenol blue

12mg xylene cyanol

(for alkaline gels, the dyes should be replaced with 12mg bromcresol green)

6.1ml H_2O

Blot I (for 8L):

0.5M NaOH (160g NaOH pellets)

1.5M NaCl (700.8g NaCl)

Blot II (for 8L):

1M NH_4 Acetate (616g NH_4 Acetate)

20mM NaOH (6.4g NaOH pellets)

Church-Gilbert Buffer (for 4L):

1mM EDTA (8mL of 0.5M stock)

0.5M Phosphate Buffer (536g Na_2HPO_4-$7H_2O$, 16mL H_3PO_4 [concentrated phosphoric acid])

7% SDS (1.4L 20% SDS)

dissolve all the above reagents in ~3L of H_2O, and stir on a hot plate until all solids have dissolved

1% bovine serum albumin (40g BSA)

BSA should first be dissolved in H_2O (~500mL), and added to the buffer only once all the other reagents have dissolved

Blot Wash (for 1L):

2x SSC (100mL of 20x SSC stock)

0.1% SDS (5ml of 20% SDS stock)

Stripping Buffer (for 150mL):

1x SSC (7.5mL of 20x SSC stock)

0.1% SDS (750μL of 20% SDS stock)

Boil in microwave, and immediately pour on the membrane.

2.5 Southern blotting probes

Telomeres were detected using a random prime labelled 400-500bp synthetic telomeric fragment or a telomeric fragment from pNSU70 (Miller et al., 2006; Sugawara, 1988). STE1 was detected using the random prime labelled *Apa*I fragment of pNSU70 (Sugawara, 1988). LMIC bands were detected as previously described (Ferreira and Cooper, 2001). Random labelled *ScLEU2* digested from pIRT2 or PCR amplified *ura4*$^{+}$ were used for Southern blot analysis of internal telomere 2DGE. PCR amplified fragment of SPAC4A8.02c was used for internal loading control of *Apa*I and *Nsi*I digested genomic DNA. In-gel hybridization was performed as described (Tomita et al., 2004).

2.6 Colony hybridization (E. coli)

1. Plates with ~50-200 colonies could be used.
2. Prepare appropriately sized nitrocellulose membranes (about 1cm smaller in diameter than the plate). Label membranes with pencil, and cut non-symmetrical markers, so that later the membrane could be aligned with the plate and positive clones could be retrieved.
3. Place membranes on plates. Mark the plates for orientation, and gently lift membrane. The plates could be returned to 37° for a few hours to allow re-growth.
4. Place the membrane with the bacteria facing up on two 3MM (Whatman) papers soaked with 1% SDS. Leave for 3min. Transfer the membranes in the same way to two new 3MM papers soaked in the following solutions:
   i. Blot I (0.5M NaOH, 1.5M NaCl).
   ii. Blot II (1M NH_4 Acetate, 20mM NaOH).
   iii. Blot Wash (2x SSC, 0.1% SDS).
5. Place membrane between two 3MM paper, and bake for 30min at 80°.

6. Wash membrane briefly with 5x SSC, 0.5% SDS, 1mM EDTA (for 400ml: 100ml 20x SSC, 10ml 20% SDS, 800μL 0.5M EDTA).
7. Wash membrane briefly with 2x SSC (or Blot Wash).
8. Continue with standard Southern Blotting. As signal for positive clones is usually very strong, hybridization time could be shorter and ~4hr would generally yield a sufficient signal.

2.7 Preparation of genomic DNA in agarose plugs

1. Grow yeast to log phase ($O.D._{600}$=0.5-1.0). For a single 2DGE, use total of 200-300 O.D. of cells (approximately 2-3x10^9 cells). For single plugs, use ~15 O.D. cells per plug. Amounts are given for a single 2DGE sample, and could be scaled up or down accordingly.
2. (For 2DGE only) Add sodium azide (1/100 from a 10% stock in H_2O, kept @ 4ºC, Sigma S-8032). Stops ATP synthesis in the cell.
3. Add cold EDTA (1/10 from a 0.5M stock). Chill on ice or in ice water (~10min).
4. Filter or spin, and wash once with 25ml cold 25xTE.
5. Wash once with 10ml cold SP1.
6. Divide into two 2ml tubes, spin down and decant supernatant.
7. Add 1ml of SP1 + Zymolase-100T (1mg/ml, prepare fresh). Incubate 10-15min @ 37°C, until >99% of cell are spheroplasts (bursting upon addition of 20% SDS). For PFGE plugs a shorter digestion time is preferred.
8. During the Zymolase treatment, prepare 1.1% InCert agarose in SP1 (divide into 1.5ml tubes, boil for 5min, and keep @ 55ºC).
9. Spin down spheroplasts (gently, 5krpm, 1min), and discard all supernatant. From this stage on, no vortexing, and use only cut tips.
10. Add ~100μl of SP1 per tube.
11. Quickly, add 450μL melted agarose, pipette gently but thoroughly, and then pipette into 100μL plug moulds (Bio-Rad). You should have 16-20 plugs from a 300O.D. culture.
12. Keep 30min @ 4°C.
13. In the meanwhile, defrost DB @ 50ºC.

14. Release plugs into 50mL tubes, and add 10mL DB. Incubate ~30min @ 50ºC. (All following treatments and washing should be done in 50mL tubes).
15. Replace DB, and incubate for further 30min.
16. Replace DB, and incubate overnight.
17. Decant DB, and fill tube with 50xTE. Keep gently rocking at 4ºC for ~4hr.
18. Replace 50xTE, and keep rocking overnight. (Protocol could be paused at this stage; plugs can be kept indefinitely at 4° for use in PFGE, and normally there is no problem to keep the plugs a few days at 4° for 2DGE).
19. Wash once with 1xTE (30min – 1hr) at 4ºC.
20. Wash once with 2x digestion buffer (depending on enzyme), 30min at 4ºC.
21. Wash once with 1x digestion buffer (depending on enzyme), 30min at 4ºC.
22. Separate into 2ml tubes (4-5 plugs per tube). Add 1x NEB buffer, BSA (if necessary) and 200-300 units restriction enzyme. If not following with 2DGE, add also RNase A - 2μL of 30mg/mL. The *Apa*I isoschizomer *PspOM*I is used in place of *Apa*I. In addition, we have successfully used the following enzymes from NEB: *Not*I, *Nsi*I, *Eco*RV, *Spe*I and *Acl*I. Incubate over-night at appropriate temperature for the enzyme.
23. If used for PFGE, plugs should be washed once in the appropriate running buffer (normally 0.5xTBE), and kept ~30min at 4°, to allow further solidification of the agarose and easier handling. Once the plugs are inserted into the gel mould, gel should be run according to the manufacturer instructions, and the can then be processed by standard Southern Blotting. For visualization, gel should be incubated ~1hr with ethidium bromide, and then washed in water for 2-16hr, replacing the water a few times.

SP1

1.2M Sorbitol, 50mM Citrate Phosphate, 40mM EDTA

For 500ml (filter sterilize, and keep @ room-temperature):

300ml 2M Sorbitol

70ml 0.5M Na_2HPO_4

55ml 0.2M Citric Acid

40ml 0.5M EDTA

35ml H_2O

Digestion Buffer (DB)

1% Lauroyl Sarcosine, 1mg/ml Proteinase K, 25mM EDTA

For 500ml (divide into 50ml tubes, and keep @ -20°C):

5g N-Lauroyl sarcosine (Sigma L-5125)

500mg Proteinase K (Sigma)

25mL 0.5M EDTA

2.8 2DGE

(Based on protocol from B. Arcangioli)

2.8.1 DNA extraction from agarose plugs

1. Release from plugs:
    a. Incubate tubes 10min @ 70°C.
    b. Add:
        i. 2ul RNase A (Sigma, 30mg/ml)
        ii. 15ul β-Agarase (NEB, total of 15 Units)
        iii. β-Agarase Buffer for final x1 concentration
    c. 90-120min incubation @ 42°C.
    d. 10min @ 70°C.
    e. Centrifuge 1min @ 13,000rpm.
    f. Decant supernatant into a new tube. Supernatant should now include only digested DNA, preserving all structures. Handle very carefully from now on.
    g. Adjust NaCl concentration to 1M.

2. BND enrichment for ssDNA:
    a. Prepare BND (could be kept for few weeks @ 4°).
        i. Weigh 6g BND (Sigma B-6385) into a 50 ml tubes. Perform following washes (after each wash centrifuge 1 min @ 2krpm):
            a. 5x washes in 5M NaCl.
            b. 1 wash in H_20.
            c. 3x washes in NET (1M NaCl, TEx1).
    b. Prepare fresh NET + Caffeine (1.8% w/v) (dissolve in 50°C).
    c. Mix BND, and pour 7ml into a chromatography column (Bio-Rad 731-1550). After the BND settles down, there should be ~1ml of it.
    d. After all liquid goes down, wash once with 5ml NET.
    e. Carefully decant the DNA, collecting the flow-through into a tube.
    f. Wash with 5ml NET, collecting the flow-through into a tube.
    g. Sequentially elute the DNA into four 2ml Eppendorf tubes, using 1ml of NET + Caffeine for each tube.
    h. Check elution by running 15-20ul from each fraction (including original flow-through and NET wash) in a regular agarose gel. Most of the DNA should be in the flow-through fraction, and there should be a peak around the 2^{nd}-3^{rd} elution with Caffeine. You might also notice that in the elution fractions the DNA is more retarded in the gel (presumably due to its structured nature). The running of the loading dye might be somewhat disrupted due to the high salt concentration. This gel can also be blotted and hybridized to ensure proper digestion, and for future reference.
    i. Do not wait for the gel to run. Add 1ml isopropanol to each elution tube, mix by gently inverting the tube, and precipitate DNA for at least few hours at -20°C.
    j. This part is adapted from the Huberman Lab website, where other useful advices could also be found: http://asajj.roswellpark.org/huberman/2D_Gel_Docs_HTML.html

2.8.2 2DGE

2.8.2.1 1st Dimension

1. Prepare a gel: 0.4% agarose in TBE. 15x25cm gel (relatively thick, 250ml). No Ethidium Bromide.
2. Precipitate DNA (~15min @ 4°, 13000rpm). All following handling of DNA should be done very carefully, with cut tips to prevent shearing.
3. Pool together the fraction containing DNA (judged by the 1D gel or the pellet). Elute in 20ul of H_2O or 10mM Tris-HCl, pH 8.5 (EB buffer from Qiagen kits). (In case the DNA does not dissolve easily, put for 1 min @ 50°). Add 20ul of DNA loading buffer.
4. Load gel. Allow at least 2 empty wells between each sample. Also load Markers (I use one regular 10kb marker, and a *Hind*III digest of Lambda, for higher molecular weights).
5. Run for ~40hr @ 1V/cm (25V for the BioRad gel system) at RT. Adjust for separation of shorter or longer fragments. Preferably, cover with aluminium foil to avoid UV damage.

2.8.2.2 2nd dimension

1. Prepare agarose: ~450ml per tray, 1.1% agarose in TBE. 6ul Ethidium Bromide per 100ml (final concentration 0.6μg/ml).
2. Prepare tanks with 1xTBE in a cold-room (preferably the night before, so it would be cold).
3. Take the 1st dimension gel out of the buffer (careful - very slippery!), and leave standing for ~10-20 min (makes handling easier).
4. Carefully cut the slices (use a ruler and a new razor blade), so that there is one sample in the middle, surrounded by an empty lane from each side. The slice containing the markers should be stained with Ethidium bromide and visualized for reference.
5. Transfer slices with a 90° rotation into a 25x25cm tray (2 slices per tray: one on top and one in the middle).
6. Pour agarose between the slices.
7. After the gel solidifies, transfer to tanks (preferably allow to stand for ~15min to allow buffer to equilibrate, and gel to cool).

8. Cover the top with aluminium foil.
9. Run 4hr @ 185V (~5V/cm). Longer runs are possible for separation of especially large fragments.
10. At this point the gels should be visualized by UV light ('arc of linears' should be visible). Gels can be blotted as any other Southern.

2.9 IP with denatured extracts

(based on Johnson and Blobel, 1999; Zhao and Blobel, 2005)

1. Start with 30-100 $O.D._{600}$ of logarithmically growing cells. If treated with MMS, add 0.01% for ~3hr.
2. Spin down cells, and wash with 10-15mL of 20% freshly prepared TCA.
3. Transfer to screw cap 1.5mL tube (at this stage the TCA can be aspirated, and the pellets can be kept at -80°C).
4. Add 400uL 20% TCA, and ~200μL glass beads. Place on Ice.
5. Break cells (2x45sec @ 6.5 strength using the FastPrep machine). Put back on ice to cool samples down.
6. Puncture hole at he bottom of the tube, and spin briefly (30sec @ 3.0krpm @ RT) to transfer to a 2mL tube.
7. Wash glass beads twice with 200μL 5% TCA, and then keep spinning for 10min to precipitate proteins.
8. Carefully aspirate TCA (do not put on ice). (For standard protein preps start with a much less cells [~5O.D. is sufficient], and in the stage add gel loading [Laemmli] buffer, and load onto SDS-PAGE gel). Wash pellet with 800μL cold acetone using a pipette tip (at this stage a part of the pellet might not break, so you should break it using the pipette tip). Place on ice. Spin down for 2min @ 4krpm @ 4°C. Aspirate supernatant with a pipette carefully, so as to not lose the pellet – it is not necessary to get all the liquid out. Wash pellet 2x more times with acetone – it is not necessary to pipette up and down at this stage, just add the acetone and vortex.
9. Dry remaining acetone using speed-vac (~20min, medium heat). The dried pellet can be kept at -20°C.

10. Add Re-suspension Buffer (140μL per 10 O.D. cells). Vortex and incubate for 20min @ 65°C. Vortex every 5-10min. Spin down for 10min @ 13krpm, and transfer the supernatant to a fresh tube (it should be clear). Keep on ice. (This supernatant could be kept at -20°C).
11. (EZView Myc beads, Sigma) Dispense beads (50μL of Sigma EZview myc) to 15mL tubes, and wash once with 5mL RIPA. Spin down at 2krpm for 1min.
12. (IgG Pan Mouse 4.5μm Dynabeads, Invitrogen) Use 20μL beads per sample into one tube (i.e. 100μL beads for 5 samples). Wash 3x times with RIPA. Add ~800 μL RIPA, and 5μL antibodies per sample (9B11, Cell Signalling). Rotate ~1hr at RT. Wash three times with RIPA, and resuspend in the original volume. The beads could be kept @ 4°C for a few days.
13. Prepare IP buffer: RIPA + protease inhibitors (1 tablet per 10mL, Roche) + 50mM NEM (N-ethylmaleimide, Sigma, from a 1M stock in ethanol, kept at -20°C). Add up to 14mL buffer per IP reaction.
14. Add protein extract, 30μL per 1mL of buffer.
15. (IgG Beads) Add 20uL beads per sample.
16. Incubate for 2hr rotating at 4°C.
17. Washes are performed with RIPA + 0.2% SDS.
18. (EZView) After the first spin (2krpm for 1min), transfer the beads to a 1.5mL tubes. Do total of 8 washes, with three of them including 10min rotating @ 4°C. Spinning down for 20sec @ 10krpm @ 4°C (rotating the tube 180° midway can help produce a tighter pellet).
19. (IgG Beads) Use large magnets to collect beads to the side of the tube (wait 2-3 min). Discard the liquid carefully. Spin down (3krpm, 1min), and transfer the beads to a 1.5ml tubes. Do ~10 washes, with 3 of them at ~20min long (i.e. 3 short ones, and then a long one, and the 2-3 short ones, etc.)
20. After the last wash, spin down to collect any remaining buffer, and add 30μL (can be less for the IgG beads – ~15-20μL) of loading buffer (LDS buffer, Invitrogen, or Laemmli), supplemented with DTT (as it is important

to completely reduce the samples for the 2nd Ab, add 200mM, although 100mM is sufficient). Boil for 5min.

21. For Western Blotting, I have used αMyc (9B11, 1/1000) and αSUMO (J. Seeler, 1/10,000 (Xhemalce et al., 2004)), and TrueBlot Rabbit or Mouse (both 1/4,000). Antibodies could be kept in milk (use 5ml in a 50ml tube) at 4°C for a few days. If longer preservation is necessary, add 0.01% Thiomersal (Sigma, from a 1% stock in water). For stripping, add Stripping Buffer, and incubate at 70° for 15min, followed by blocking.

Re-suspension Buffer (for 100mL):

0.5M Tris-HCl pH=6.8 (50mL of 1M stock)

6.5% SDS (32.5mL of 20% stock)

12% Glycerol (12mL)

100mM DTT (add just prior to use, 1M stock in -20°C)

RIPA (for 500mL):

50mM Tris-HCl pH=7.5 (25mL of 1M stock)

150mM NaCl (15mL of 5M stock)

5mM EDTA (5mL of 0.5M stock)

1% Triton-X (5mL)

Stripping Buffer (for 500mL):

50mM Tris-HCl pH=7 (25mL of 1M stock)

2% SDS (50mL of 20% SDS stock)

50mM DTT (added fresh before use)

2.10 Fission yeast transformation

1. Start with logarithmically growing culture (<0.8 O.D.). The amount of cells depends on the number and kind of transformations – more cells are necessary for integrative transformations. Usually 50mL of culture are sufficient for 1-4 transformations.

2. Prepare 2mL tubes, one per transformation. Make sure to include a 'no DNA' control. Boil salmon sperm DNA (~10mg/mL) for 5min, and cool to RT.
3. Spin cells down (3min @ 3krpm, RT), and wash with 10mL of 1x LiAcetate Buffer (0.1M Lithium Acetate, 10mM Tris-HCl pH=8, 1mM EDTA). Spin again.
4. Discard supernatant, and resuspend the cells in sufficient amount of 1x LiAcetate Buffer to have 100μL per transformation.
5. To each 2mL tube add: 5μL of Salmon sperm DNA, 0.5-5μL DNA (0.5μL of plasmid DNA or ~5μL of linear fragments for integrative transformations), 100μL of cells. Mix and incubate 5min at RT.
6. Add 280μL of 50% PEG-4000 in LiAcetate Buffer (1x) (Filter sterilized). Mix and incubate 45-60min at 32°, or appropriate growing temperature for the strain.
7. Add 43μL of DMSO. Mix and place for 5min at 42°.
8. Centrifuge gently (5krpm for 1min). Discard supernatant and wash with 1mL YES (or water). If plating immediately, spin again, discard supernatant and resuspend in appropriate volume for plating.
9. **Plasmid transformation**: plate 10-50% of the cells on selective plates.
10. **Integrative transformation, option I**: plate 100% of the cells on YES plates and incubate for 24hr at 32° (or optimal growing temperature; if lower than 32°, longer incubation time may be necessary). Once a relatively thick lawn of cells has grown, replica-plate onto selective media.
11. **Integrative transformation, option II**: Add the cells to 10mL of YES, and place on shaking incubator for 4hr at 32° (or optimal growing temperature; if lower than 32°, longer incubation time may be necessary). Spin down the cells, and plate onto selective media.
12. For transformation on 5-FOA, and in rare cases on other media, an additional round of replica-plating after 2-3 days is necessary.

LiAcetate Buffer, 10x stock:

1M Lithium Acetate

10mM EDTA

100mM Tris-HCl pH=8

Filter Sterilize. Dilute 10x with sterilized water.

2.11 FACS

1. Start with ~0.5-1.0 O.D cells. Wash once with water. Re-suspend in 70% Ethanol. Keep indefinitely in 4°C.
2. Wash twice with 0.5M Sodium Citrate (pH 7.4).
3. Resuspend in 500μL 0.5M Sodium Citrate + 0.1mg/ml RNase A (from stock solution of 32mg/ml).
4. Incubate at least 2hr @ 37°C.
5. Add 500μL 0.5M Sodium Citrate + 10μg/ml (1:100) Propidium Iodide.
6. Sonicate: 10sec @ 10microamplicon.
7. Measure samples in FACS machine.

2.12 Indirect immunoflourescence

(Based on protocol from JPC)

1. Start with 10 ml culture of ~5X10^6 cells/ml (i.e. ~5O.D.).
2. Spin down cells and resuspend in 810μL PEM. Add 190μL para-formaldehyde (from freshly-opened ampule, stock solution 16%, to a final concentration of 3%), mix and incubate 10-15 minutes at room temperature.
3. All washes are performed @ 12krpm, 10sec, in a volume of ~1mL. In order to get a tighter pellet, it is possible to turn the tube 180° midway through the spin.
4. Wash cells 3x with PEM. Resuspend in PEMS (to ~5X10^7 cells/ml).
5. Add Zymolyase-100T to 1mg/ml. Incubate 90 minutes @ 37°C, mixing occasionally.
6. Wash 3X with PEMS, resuspend in PEMS + 1% Triton-X100. Wait 30 sec (or up to 5 minutes). Spin down and wash 3X with PEM.
7. Resuspend in PEMBAL + 0.2mg/ml RNase. Rotate fixed cells in PEMBAL @ room temp for 30min. (For complete RNA digestion, incubate at 37°C for 2 hours).

8. Spin down and resuspend in 40μL PEMBAL + antibody (1/400 αRqh1 (Caspari et al., 2002), 1/1000 αPK). Rotate O/N at room temp.
9. Wash 3X with PEMBAL. Rotate 30min in PEMBAL. Suspend in 200μL PEMBAL + secondary antibody (1/2000 αMouse or αRabbit conjugated to Alexa dyes).
10. Rotate @ room temp for 2 hours. Wash 3x in PEMBAL, store in PBS + 0.1% sodium azide (from 10% stock, filter sterilized and kept at 4°).

PEM (can make 2x stock, to dilute into PEMS and PEMBAL)

100mM PIPES, pH 6.9 (pH with 5N NaOH to dissolve)

1mM EGTA

1mM $MgSO_4$

PEMS

PEM + 1.2M Sorbitol

Autoclave

PEMBAL

PEM + 1% BSA

0.1% Sodium azide

100mM Lysine hydrochloride

Filter sterilize

2.13 List of Strains

Strain	Relevant Genotype	Source
JCF1	*wt*	
JCF28	*taz1::ura*	
JCF212	*h⁻ pmt3::ura4*	
JCF409	*rap1::kanMX*	
JCF495	*ura4::LEU2::telo*	
JCF496	*taz1::kanMX ura4::LEU2::telo*	
JCF1026	*h⁻ rap1::kanMX*	
JCF1531	*h⁺/⁻ diploids rap1::kanMX/rap1::kanMX trt1⁺/trt1::his*	
JCF1559	*h⁺/⁻ diploids trt1⁺/trt1::his*	
JCF1582	*h⁺/⁻ diploids taz1::kanMX/taz1::kanMX trt1⁺/trt1::his*	
JCF1639	*h⁺/⁻ diploids taz1⁺/taz1::ura*	
JCF1643	*ura4::LEU2::reverse-telo*	
JCF1650	*Pnmt1-taz1::kanMX*	
JCF1651	*Pnmt41-taz1::kanMX*	
JCF1657	*Pnmt1-taz1::kanMX rap1::kanMX*	
JCF1658	*Pnmt41-taz1::kanMX rap1::kanMX*	
JCF1662	*h⁺/⁻ diploids rap1⁺/rap1::ura*	
JCF1669	*ura4::LEU2::telo-reverse-200*	
JCF1670	*Pnmt1-taz1::kanMX rap1::kanMX ura4::LEU2::telo*	
JCF1673	*taz1::kanMX ura4::LEU2::reverse-telo*	
JCF1674	*taz1::kanMX ura4::LEU2::telo-reverse-200*	
JCF1675	*ura4::LEU2::telo-reverse-450*	
JCF1677	*taz1::kanMX ura4::LEU2::telo-reverse-450*	
JCF1684	*h⁺ taz1::kanMX rap1::kanMX*	
JCF1684	*taz1::kanMX rap1::kanMX*	
JCF1706	*ura4::LEU2::G-forming-400*	
JCF1716	*ura4::LEU2::scrambled-600*	
JCF1720	*taz1::hygMX ura4::LEU2::G-forming-400*	
JCF1722	*taz1::hygMX ura4::LEU2::scrambled-600*	
JCF1750	*ura4::telo-450*	
JCF1751	*taz1::hygMX ura4::telo-450*	
JCF1762	*h⁹⁰ pli1::kanMX*	B. Arcangioli
JCF1770	*h⁻ pli1::kanMX taz1::hygMX*	
JCF1773	*h⁻ pmt3::ura4 taz1::hygMX*	
JCF1779	*h⁻ Pnmt81-ulp1::kanMX taz1::ura4*	

JCF1786	*h+ ulp1::ura4 pmt3.GG::ura4*	F. Watts
JCF1787	*h- ulp2::kanMX*	F. Watts
JCF1793	*h- ulp2::kanMX taz1::hygMX*	
JCF1797	*h+ pmt3.GG::ura4 taz1::hygMX*	
JCF2209	*h? pmt3.GG::ura4*	
JCF2210	*h+ ulp1::ura4 pmt3.GG::ura4 taz1::hygMX*	
JCF2232	*ura4::random-G-rich*	
JCF2246	*h+/- diploids taz1+/taz1::hygMX slx8+/slx8::kanMX*	
JCF2254	*h- rqh1::kanMX*	
JCF2255	*h- rqh1::kanMX taz1::hygMX*	
JCF2268	*h- rqh1::ura4 (inserted in bp 1549-2772)*	
JCF2282	*h-*	
JCF2285	*h- rqh1-SM*	
JCF2287	*h- taz1::hygMX*	
JCF2288	*h- rqh1-SM taz1::hygMX*	
JCF2289	*h- rqh1-SM* taz1::hygMX*	
JCF2316	*h- rqh1-hd*	
JCF2318	*h- rqh1-hd taz1::hygMX*	
JCF2336	*h? taz1::kanMX ura4::telo-ScLEU2*	
JCF2338	*h? taz1::kanMX ura4::telo-ScLEU2 rqh1-SM*	
JCF2368	*h- rqh1-G8-myc::kanMX*	
JCF2371	*h- rqh1-G8-myc::kanMX taz1::hygMX*	
JCF2372	*h- rqh1-SM-G8-myc taz1::hygMX*	
JCF2391	*h- rad22::natMX fbh1::kanMX*	
JCF2393	*h? rad22::natMX fbh1::kanMX taz1::hygMX*	
JCF2394	*h? rad22::natMX fbh1::kanMX taz1::hygMX rqh1-SM*	
JCF2396	*h- taz1::hygMX rhp51::ura4*	
JCF2397	*h- taz1::hygMX rhp51::ura4 rqh1-SM*	
JCF2399	*h- rhp51::ura4*	
JCF6263	*h? ade6::RTSactive*	
JCF6264	*h? ade6::RTSactive rqh1-SM*	
JCF6265	*h? ade6::RTSactive rqh1::ura*	
JCF6266	*h? ade6::RTSinactive*	
JCF6267	*h? ade6::RTSinactive rqh1-SM*	
JCF6268	*h? ade6::RTSinactive rqh1::ura*	
JCF6733	*h- rqh1-SM (^{724}PRRD^{727}) taz1::hygMX*	
JCF6734	*h- rqh1-SM (^{921}IRQD^{924}) taz1::hygMX*	
JCF6736	*h+ nse2.CH::ura4*	F. Watts

JCF6737	*h+ nse2.SA::ura4*	F. Watts
JCF6738	*h+ nse2.CH::ura4 taz1::hygMX*	
JCF6739	*h+ nse2.SA::ura4 taz1::hygMX*	
JCF6758	*h? nse2.CH::ura4 rqh1-G8-myc::kanMX taz1::hygMX*	
JCF6759	*h? nse2.SA::ura4 rqh1-G8-myc::kanMX taz1::hygMX*	

3 Chapter 3: Taz1 is Required for Semi-conservative Telomere Replication

3.1 Introduction

Telomere replication is achieved through the combined action of conventional DNA replication machinery and the reverse transcriptase, telomerase. While telomere-binding proteins were known to have crucial roles in controlling telomerase activity, little was known about their role in controlling semi-conservative replication, which synthesizes the bulk of telomeric DNA (Teixeira et al., 2004). It is generally assumed that telomere-binding proteins impede replication fork progression. In this work we showed that, on the contrary, Taz1 is crucial for efficient replication fork progression through the telomere. As the human telomere proteins TRF1 and TRF2 are Taz1 orthologues, we predict that one or both of the human TRFs may orchestrate fork passage through human telomeres. Stalled forks at dysfunctional human telomeres are likely to accelerate the genomic instability that drives tumorigenesis.

3.2 Replication forks stall at telomeres in cells lacking Taz1

3.2.1 Aberrant replication patterns of *taz1*Δ telomeres

To analyse replication intermediates, we subjected genomic DNA to neutral-neutral two-dimensional gel electrophoresis (2DGE) (Brewer and Fangman, 1987). 2DGE separates DNA molecules according to molecular weight in the 1st dimension; gel slices are then turned 90° and run under conditions that separate molecules according to shape: high voltage and presence of Ethidium Bromide. The bulk of digested genomic dsDNA runs on the 'arc of linears' (Figure 3.1a), thus blotting for a unique fragment yields a spot depending on the size of the restriction fragment ('1N spot'). As a fragment is replicated, it is progressively retarded more in the 1st dimension; in the 2nd dimension, molecules that undergo unidirectional replication are initially retarded as complexity increases, but once the replication fork passes the centre of the molecule, further replication diminishes the structural complexity,

allowing easier passage through the gel, generating an arc shape ('Y-arc', Figure 3.1a).

*Nsi*I digestion released telomere-containing restriction fragments from five of the six wild-type chromosome ends in *S. pombe*, as seen by Southern blotting (Figure 3.1b, c). 2DGE revealed that all of these telomere-containing fragments are replicated as simple Y-arcs (Figure 3.1d), indicating that replication proceeds unidirectionally from a centromere-proximal origin. This result is consistent with previous work showing that fission yeast replication origins are all markedly AT-rich, in contrast to the GC-rich telomere repeats, and that regions 7–17 kb centromeric to the terminal *Nsi*I sites contain multiple replication origins (Segurado et al., 2003). Notably, some of the wild-type telomere-containing fragments showed replication pause sites in the subtelomeric region (red arrows in Figure 3.1d), as observed in budding yeast (see below).

Southern blot analysis of *taz1Δ* telomere-containing *Nsi*I-digested fragments revealed a heterogeneous smear of products, with most telomere probe hybridization between 5 kb and 7 kb (Figure 3.1c). We therefore expected that 2DGE of DNA from *taz1Δ* cells would yield an amalgamation of superimposed Y-arcs ranging from ≤5 kb for the smallest 1N spots (unreplicated DNA) to ≥14 kb for the largest 2N spots (almost completely replicated DNA), with the vast majority of signal appearing as a semicircle encompassed by arcs F3 and F5 (Figure 3.1d). Instead, the telomere signal intensified at the top of the superimposed Y-arcs and spread into higher molecular weight fragments, forming a plume that extended well beyond the predicted size for the replicating telomeres (Figure 3.1d). This plume of intermediates of higher molecular weight and complexity was not accompanied by corresponding intermediates descending towards the arc of linears. Thus, the lack of appreciable signal descending from the top of the arcs to the 2*N* region suggests that forks rarely progress to the ends of *taz1Δ* telomeres.

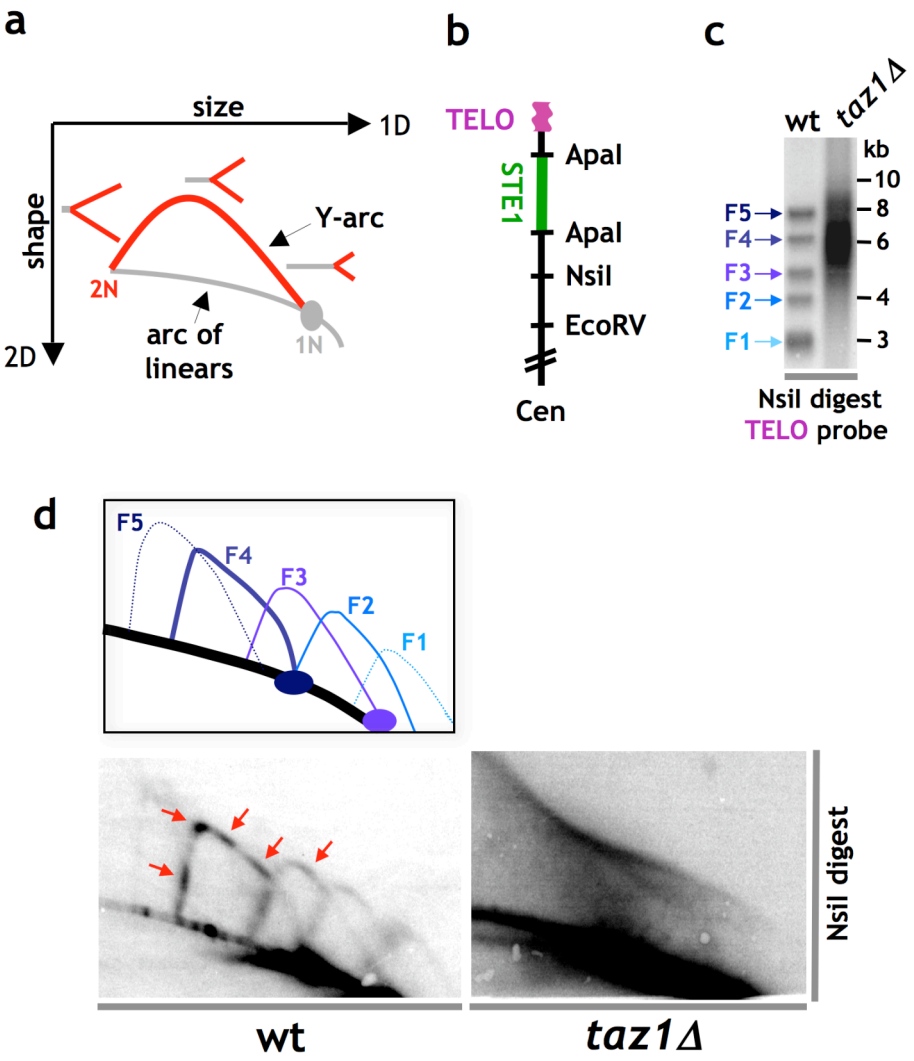

Figure 3.1 Anomalous replication patterns of *taz1*Δ cells

a, The Y-arc pattern seen by 2DE analysis. For each restriction fragment, the unreplicated form runs as the '1*N* spot'. The '2*N* spot' represents the theoretical duplication of that fragment. Unreplicated DNA fragments of all sizes run in the arc of linears. The Y-arc pattern is generated by unidirectional movement of a replication fork across a DNA fragment. Unreplicated DNA is shown in grey, replicated DNA in red. **b**, Relative positions of restriction sites in telomeric (TELO) and subtelomeric (STE1) regions of chromosomes I and II. Cen, centromere. **c**, Southern blot analysis of telomeric *NsiI*-digested fragments. **d**, 2DGE analysis of telomeric *NsiI* fragments. 'F' labels on the interpretive diagram indicate the corresponding unreplicated bands in **c**. Red arrows indicate subtelomeric pause sites.

This anomalous migration pattern is not due to an inability of our gel system to detect Y-arcs representing long DNA fragments, as an rDNA repeat fragment of >8kb produces Y-arcs. Likewise, it is not an artefact generated by

in vitro interactions between the extensive G-rich overhangs at *taz1Δ* telomeres, as no anomalous patterns were observed in G1 arrested *taz1*Δ cells, where overhangs are abundant (see below and Miller et al., 2006).

Rap1 binds to Taz1 and mediates a subset of its functions (Chikashige and Hiraoka, 2001; Kanoh and Ishikawa, 2001; Miller et al., 2005). Hence, telomeres of long and heterogeneous length, as well as increased telomeric 3′ overhang signals, are found in both *taz1Δ* and *rap1Δ* cells (Figure 3.2a and Chikashige and Hiraoka, 2001; Kanoh and Ishikawa, 2001; Miller et al., 2005). Strikingly, however, *rap1Δ* telomeres did not share the anomalous replication pattern of *taz1Δ* telomeres (Figure 3.2b). Rather, *rap1Δ* telomeres yielded discernable broad Y-arcs, with smears of hybridization descending from the top of the superimposed Y-arcs to the arc of linears, suggesting that replication forks proceed to the terminus of a substantial fraction of *rap1Δ* telomeres. The 2DGE pattern suggests that not all *rap1Δ* telomeres are fully replicated, consistent with the idea that cellular Taz1 levels are insufficient to bind the entire *rap1Δ* telomere, effectively leading to 'partially *taz1Δ*' telomeres (see also Chapter 4). Nevertheless, the clear difference between the *taz1Δ* and *rap1Δ* 2DGE patterns indicates that the *taz1Δ* pattern is not merely a consequence of increased telomere length, heterogeneity in length, extended 3' overhang or elevated NHEJ.

The observation that *rap1*Δ cells, which harbor the same extensive 3' overhang signals as do *taz1*Δ cells, show broad Y-arcs rather than the plume pattern indicates that the plume is not a necessary consequence of the 3' G-rich ssDNA. Nonetheless, to address a possible role of the telomeric ssDNA, and to understand better the structural nature of the plume, we checked the nuclease sensitivity of *taz1*Δ 2DGE patterns. Our initial experiments suggest that treatment with either S1 (ssDNA endonuclease) or ExoI (3'-5' ssDNA exonuclease) nuclease has no effect on the plume pattern, even though both treatments clearly diminish the 3' overhang signal as verified by nondenaturing gel electrophoresis followed by hybridization with a C-rich telomere probe (Figure 3.3). These results suggest that the anomalous replication intermediates in *taz1*Δ telomeres are composed largely of dsDNA; however, these results do

not rule out a role for telomeric ssDNA in the aetiology of these structures. In addition, it remains to be shown how the different nuclease treatments alter the relative abundance and migration of other well-characterized non-dsDNA structures – for example the replication intermediates that generate Y-arcs.

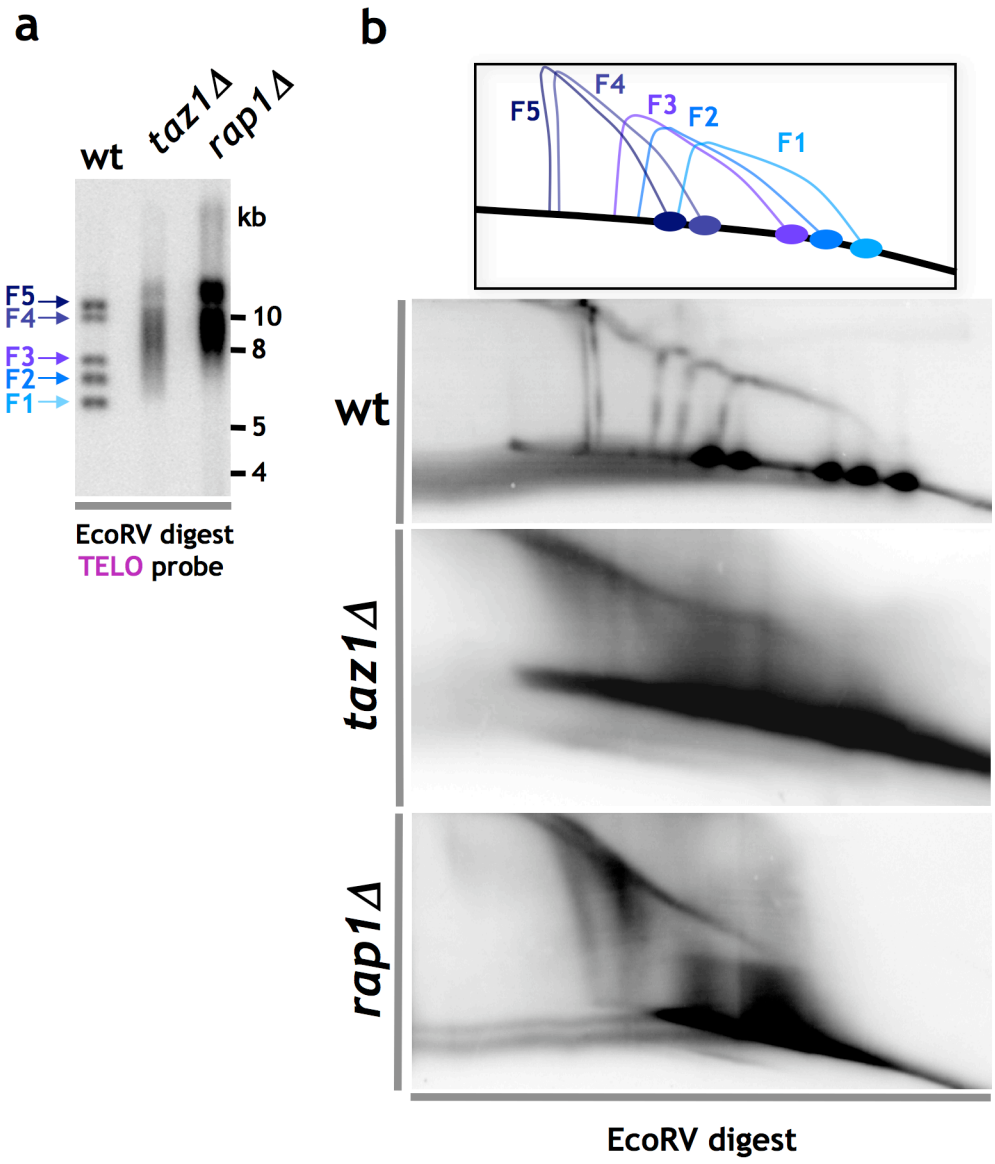

Figure 3.2 Efficient semi-conservative replication through telomeres requires Taz1 but not Rap1

a, Southern blot analysis of telomeric *Eco*RV-digested fragments. **b**, 2DGE of telomeric *Eco*RV-digested fragments. *taz1Δ* and *rap1Δ* cells show distinct patterns of telomere replication patterns.

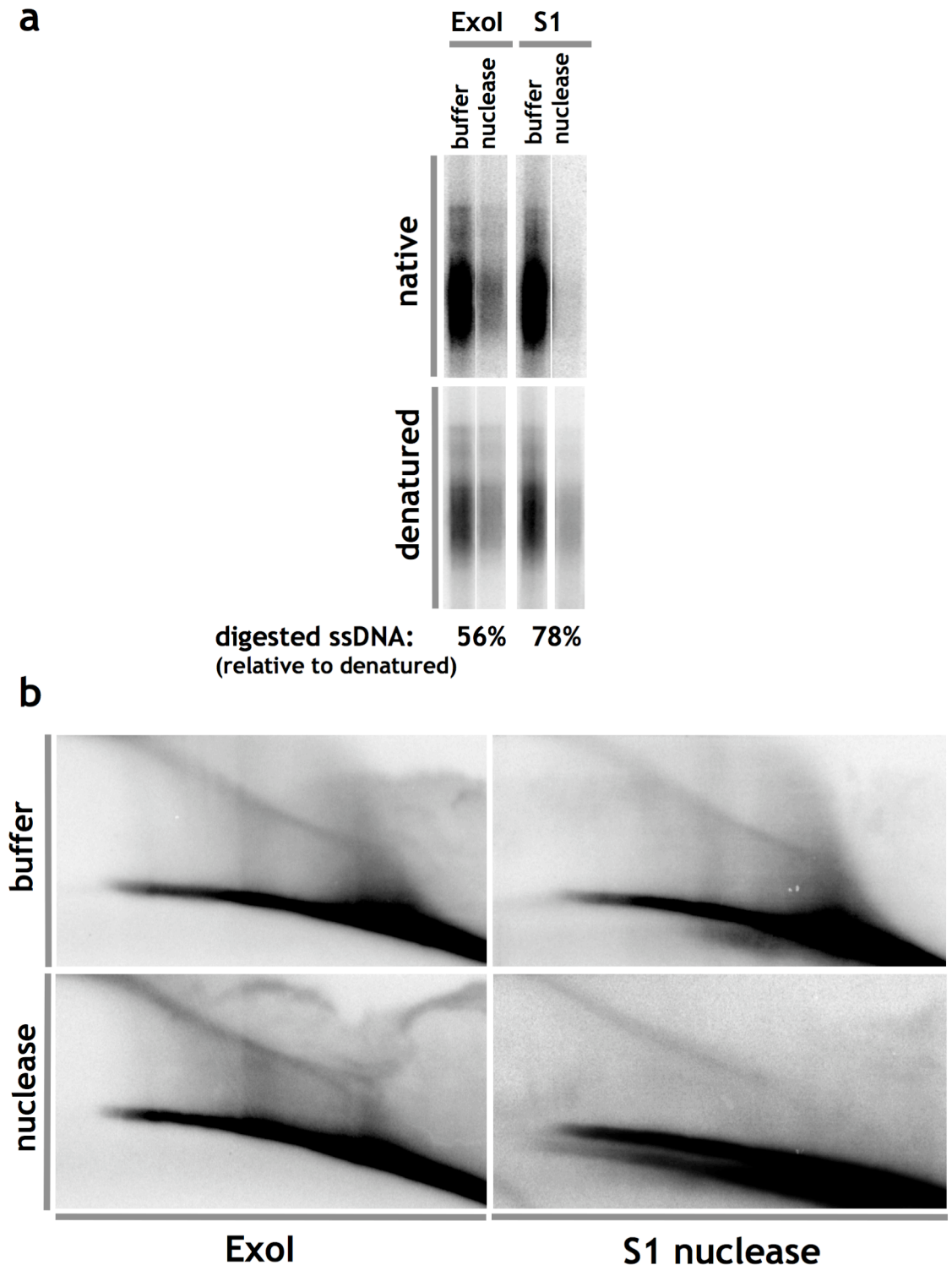

Figure 3.3 *taz1*Δ 'plume' 2DGE pattern is not sensitive to ssDNA nucleases.

a, In-gel hybridization with a C-rich telomeric probe of *Nsi*I digested *taz1*Δ genomic DNA, treated with ExoI or S1 nuclease, and respective buffer controls. Following hybridization to native DNA samples (top), the DNA was denatured and then re-probed to the same probe to assess the total amount of telomeric DNA (bottom). The amount of digested ssDNA was calculated by dividing 'native' by 'denatured' signal, and comparing the nuclease *versus* buffer samples. **b**, 2DGE analysis of the samples in **a**. *taz1*Δ telomeric hybridization pattern is unaffected by nuclease treatment.

3.2.2 Telomeric sequences impede replication in cells lacking Taz1

To assess replication of telomeric DNA without the complication of heterogeneous telomere size, we analysed an internally placed telomeric tract of 250 bp, inserted ~8 kb from a well-characterized cluster of replication origins on chromosome III (Figure 3.4a and (Dubey et al., 1994); this strain was originally constructed by A. Hebden). As expected, *Nsi*I digestion yielded a 3.5-kb internal telomere-repeat-containing fragment that was replicated as a simple Y-arc in wild-type cells. However, *taz1*$^{+}$ deletion resulted in fork stalling specifically through the region containing the telomere repeat stretch (Figure 3.4a). Digestion with *Acl*I generates a ~4.5 kb fragment in which the telomeric stretch is shifted slightly towards the origin-distal end (relative to its position in the *Nsi*I fragment), and generates a pause site that has correspondingly shifted to the left in the descending portion of the Y-arc (Figure 3.4b). Thus, telomeric DNA lacking Taz1 results in fork pausing, regardless of whether the telomere stretch terminates with a chromosome end. For further characterization and analysis of replication at the internally placed telomeric sequences, see Chapter 4.

Figure 3.4 Taz1 is required for efficient replication through internally placed telomere tracts.

(next page) **a,** Map showing the genomic region of chromosome III containing an ectopically inserted telomere tract of 200 bp. The ARS3002-4 cluster (ori) is located ~8 kb centromeric to *ura4* and has been shown to replicate this locus (Dubey et al., 1994). The telomere tract is 2.5 kb from the ori-proximal end of the 3.5-kb *Nsi*I fragment. In each illustration, the telomeric stretch is shown in purple, and the position of *ScLEU2* is shown in light blue. *Nsi*I-digested DNA was subjected to 2DGE and hybridized with an *ScLEU2* probe, generating a smooth arc in the presence of Taz1 but not in its absence. Top, insert is a cloned telomere of ~250bp; bottom, insert is a synthetic telomere of ~500bp (see Chapter 4 for details). **b,** Map is similar to **a**, except that *Acl*I sites are also shown (green). The telomere fragment (cloned ~250bp telomere) is located 3.4 kb from the ori-proximal end of the 4.5 kb *Acl*I fragment.

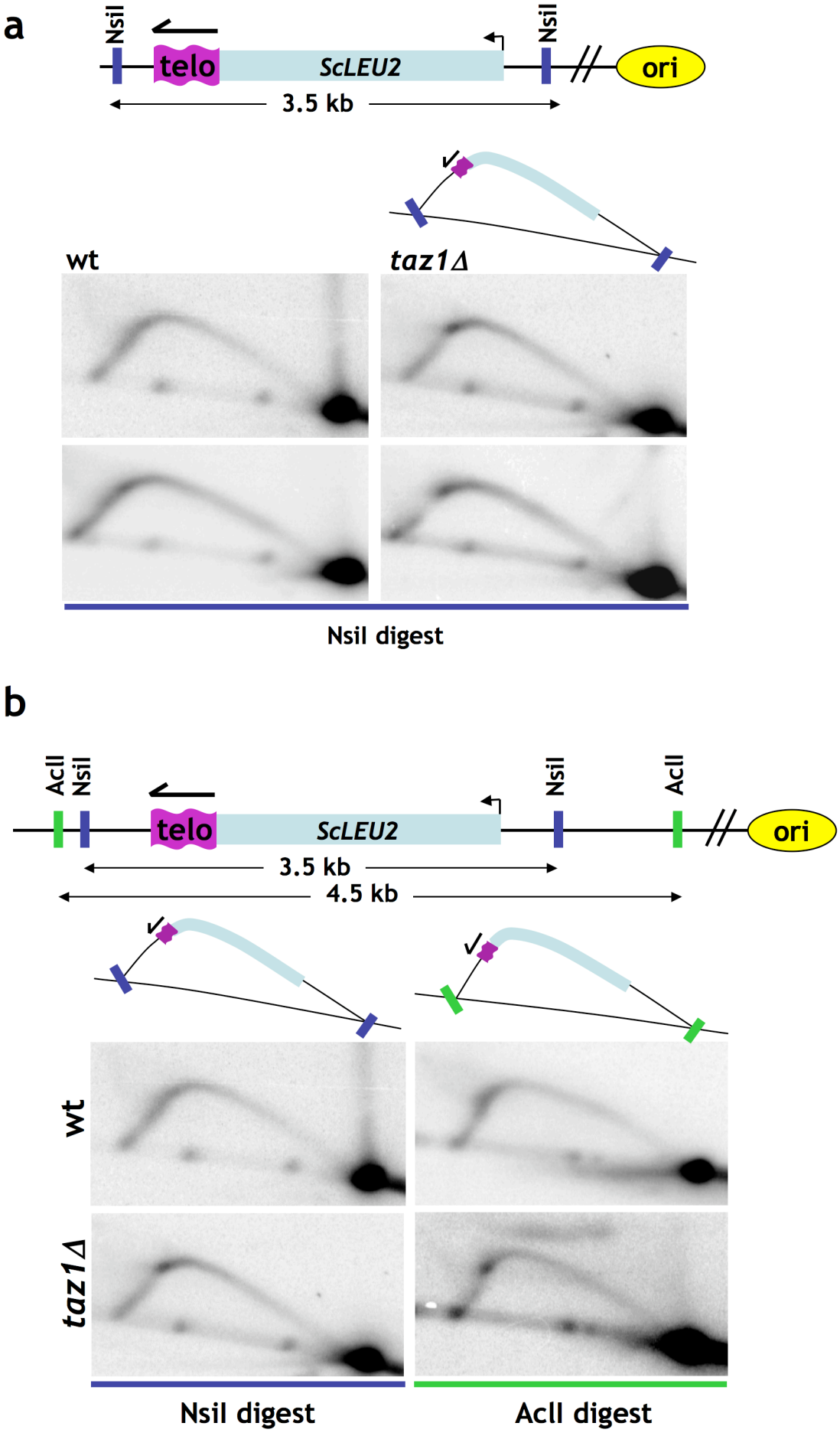
a
NsiI
telo
ScLEU2
NsiI
ori
3.5 kb
wt
taz1Δ
NsiI digest
b
AclI
NsiI
telo
ScLEU2
NsiI
AclI
ori
3.5 kb
4.5 kb
wt
taz1Δ
NsiI digest
AclI digest

A sizeable fraction of the molecules present in these Y-arcs complete replication, indicating that pausing at these internal telomeric sites is reversible or does not occur in all *taz1Δ* cells. These pause sites appear not to elicit a pronounced cell cycle arrest, as we did not observe a difference in the growth profiles of *taz1⁺ versus taz1Δ* strains carrying internal telomere stretches (data not shown), consistent with the observation that pausing at the replication fork barrier RTS1 fails to trigger measurable cell-cycle arrest (Lambert et al., 2005). Although the probability of pausing may be small over a 250bp internal telomere stretch, the chances of a fork progressing to the end of a 1-4kb *taz1Δ* telomere decrease exponentially with distance from the centromere. For example, a 20% chance of stalling over a 250bp telomeric stretch translates into <7% chance of traversing a 3kb telomeric tract without stalling. Accumulation of stalled forks along a *taz1Δ* telomere may underlie the anomalous replication patterns seen at *taz1Δ* chromosome ends (Figure 3.1 and 3.2; discussed below).

To explore the extent of anomalous replication of *taz1Δ* telomeres, replication in subtelomeric regions was examined. We also observed *taz1*Δ-specific accumulation of replication intermediates using *Apa*I, a restriction enzyme that cleaves in the subtelomere, 32bp from the subtelomere/telomere border and a subtelomeric probe (Sugawara, 1988). Stalling in the absence of Taz1 was limited to the distal end of the probed ApaI fragment (KM Miller and Miller et al., 2006). Therefore, Taz1 is required for efficient fork progression specifically through the telomeric end of subtelomeric regions. As unwinding activities associated with the replication fork may occur up to ~200 bp ahead of the fork itself (Gasser et al., 1996; Sogo et al., 2002), we speculate that in the absence of Taz1, these activities are obstructed as they encounter the telomere, leading to stalling at the telomere/subtelomere boundary. Notably, *rap1⁺* deletion did not elicit replication fork pausing at the distal end of subtelomeric regions (KM Miller and Miller et al., 2006). Thus, Taz1 binding is sufficient to prevent fork stalling at the subtelomere/telomere boundary, and this protection does not require Rap1.

3.3 Rapid telomere loss in the absence of Taz1 and telomerase

3.3.1 Telomere loss in the absence of telomerase

If conventional replication forks are unable to efficiently traverse *taz1Δ* telomeres, then most of the 1-4kb *taz1Δ* telomeres must be synthesized by telomerase in every cell cycle. If this were true, deletion of the gene encoding the telomerase reverse transcriptase (*trt1*$^{+}$) in a *taz1Δ* background would trigger a precipitous loss of telomere repeats, rather than the gradual telomere attrition seen upon *trt1*$^{+}$ deletion in wild-type cells. Previous results support this prediction, as loss of Taz1 in cells lacking telomerase has been shown to accelerate viability loss by 100 fold (Beernink et al., 2003; Nakamura et al., 1998) - an initially puzzling observation given that the elongated *taz1Δ* telomeres might be expected to postpone senescence. To address this further, we monitored the fates of long telomeres after *trt1*$^{+}$ deletion in *taz1Δ* and *rap1Δ* backgrounds by sporulating *taz1*$^{\Delta/\Delta}$ *trt1*$^{+/\Delta}$ and *rap1*$^{\Delta/\Delta}$ *trt1*$^{+/\Delta}$ diploids and following telomere length over time. Both parental diploid strains had highly elongated telomeres, as we expected (Figure 3.5a). However, a marked difference in *taz1Δ versus rap1Δ* telomeres was seen in spores lacking Trt1. When single colonies from *rap1Δ trt1Δ* spores were continuously cultured, their telomeres showed progressive length reduction, culminating in near-complete loss of telomere signal by ~150 generations (3-4 re-streaks) (Figure 3.5a). In contrast, *taz1Δ trt1Δ* colonies showed erratic telomere hybridization patterns, with an immediate loss of the bulk of the telomere signal followed by a variable level of signal maintenance. The difference between *rap1*Δ *trt1*Δ and *taz1*Δ *trt1*Δ can also be observed when comparing many colonies at the same time point – as soon as colonies were first formed from spores (Figure 3.5b). The difference between *taz*1Δ and *rap1*Δ is unlikely to be caused by the difference in starting telomere length, as the telomeres that remain in *rap1*Δ *trt1*Δ cells after the 1st restreak are markedly shorter than *taz1*Δ telomeres (~1kb *versus* >3kb) yet still require more than one restreak to be completely lost (Figure 3.5a).

Similar phenomena were observed when spores were germinated *en masse* under selection for the *trt1⁺* deletion, to allow for the isolation of sufficient quantities of DNA for Southern blot analysis at earlier time points - starting at ~10 generations. Telomere length declined progressively in *rap1Δ trt1Δ* populations but showed an abrupt decline followed by variable maintenance in *taz1Δ trt1Δ* populations (Figure 3.6a). It was our concern that *taz1Δ* telomeres might be lost during meiosis in the absence of Trt1, rather than being lost during the S-phases subsequent to germination. This is highly unlikely to be a problem since *rap1Δ* meiosis suffers the same defects as *taz1Δ* meiosis: telomere fusions in the G1 arrest phase that precedes meiosis along with an inability to cluster telomeres at the spindle pole body during meiotic prophase. Indeed, these meiotic defects are even more severe in *rap1Δ* than in *taz1Δ* cells (Tomita and Cooper, 2007). Nonetheless, we found identical telomere length distribution in spores of $taz1^{\Delta/\Delta}trt1^{\Delta/+}$ and $rap1^{\Delta/\Delta}trt1^{\Delta/+}$ meiosis (Figure 3.6b), demonstrating that the difference we observe does not reflect meiotic events. We note that spores in both strains exhibit telomere lengths that are more heterogeneous than the respective parental diploids, which might reflect telomere fusions, recombination and/or the different physiology of spores and dividing cells.

Figure 3.5 Differences in the kinetics of telomere attrition in *taz1Δ* versus *rap1Δ* cells after *trt1⁺* deletion.

(next page) **a**, Diploids homozygous for *taz1Δ* or *rap1Δ* and heterozygous for *trt1Δ* were sporulated. *trt1Δ* progeny were selected, serially re-streaked and subjected to Southern blot analysis of telomere length every 25–30 generations. **b**, Similar analysis to the one performed in **a**, but 16 independent *taz1*Δ *trt1*Δ and *rap1*Δ *trt1*Δ colonies were analyzed at the same time point, equivalent to the 1st resreak in **a**. While *rap1*Δ *trt1*Δ colonies still harbor ~1kb of telomeres, *taz1*Δ *trt1*Δ colonies already exhibit telomeric hybridization pattern characteristic of survivors.

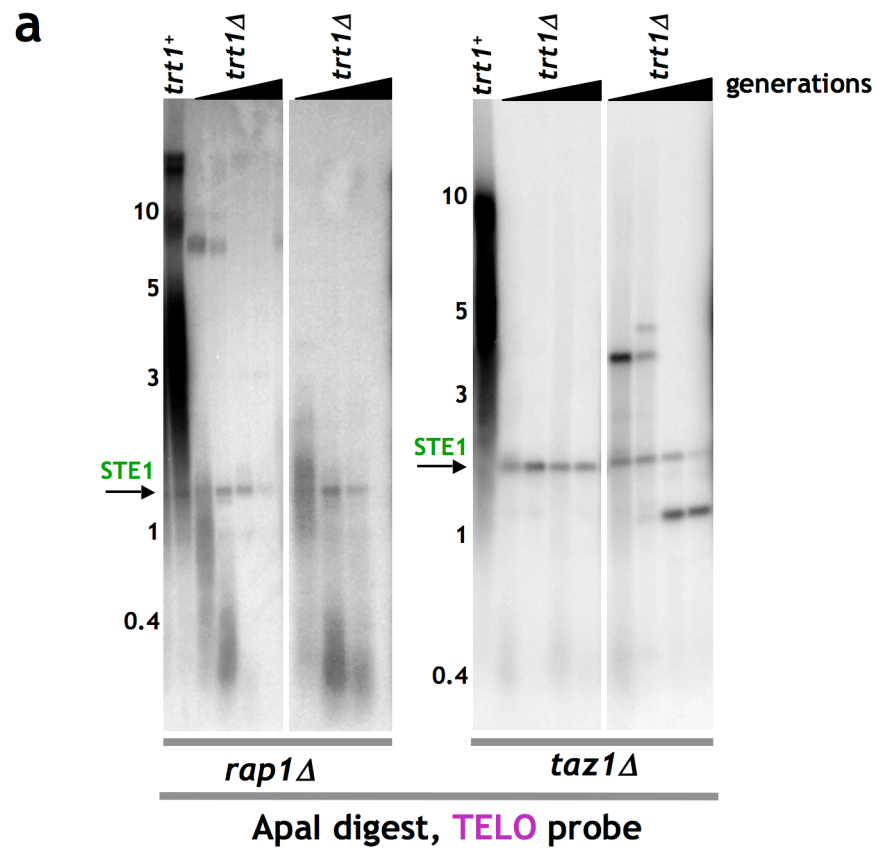
a
trt1+
trt1Δ
trt1Δ
trt1+
trt1Δ
trt1Δ
generations
10
5
3
STE1
1
0.4
10
5
3
STE1
1
0.4
rap1Δ
taz1Δ
ApaI digest, TELO probe

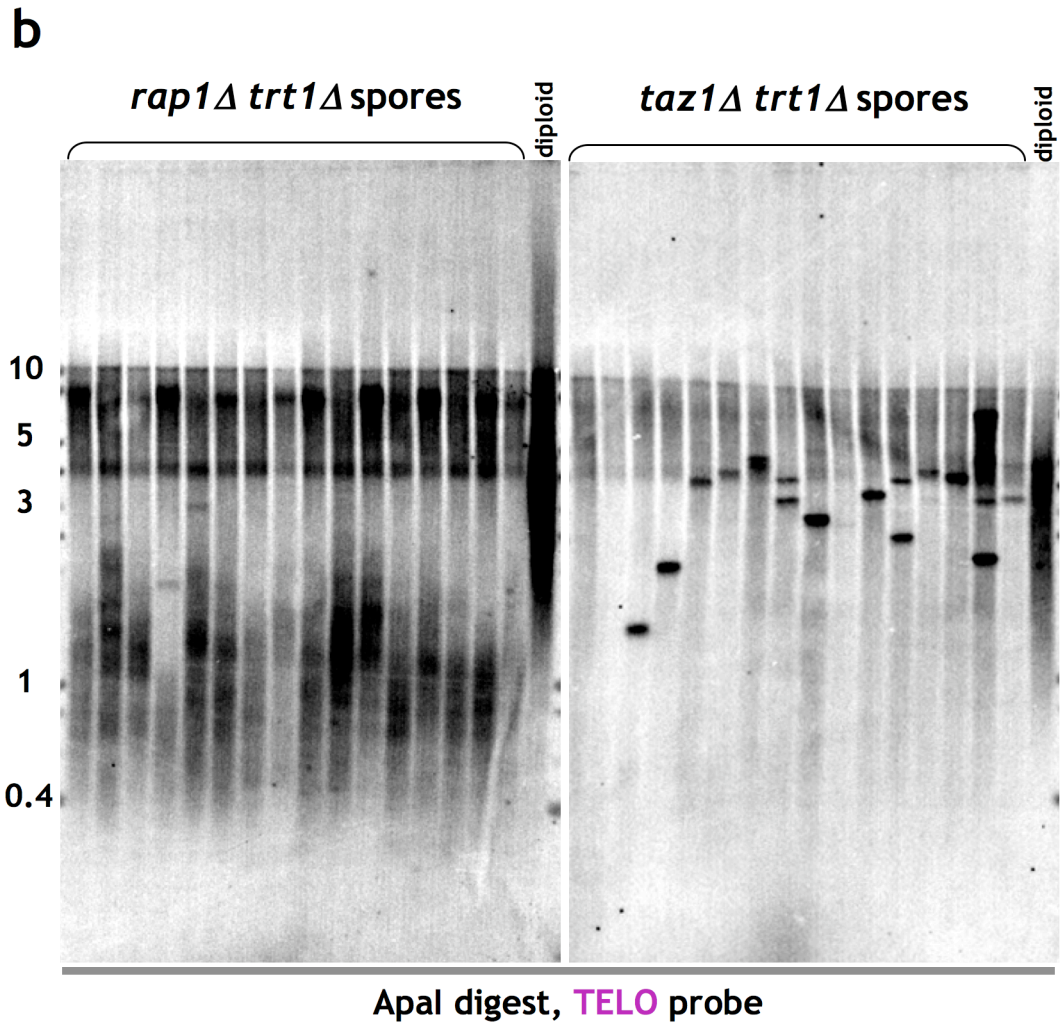
b
rap1Δ trt1Δ spores
diploid
taz1Δ trt1Δ spores
diploid
10
5
3
1
0.4
ApaI digest, TELO probe

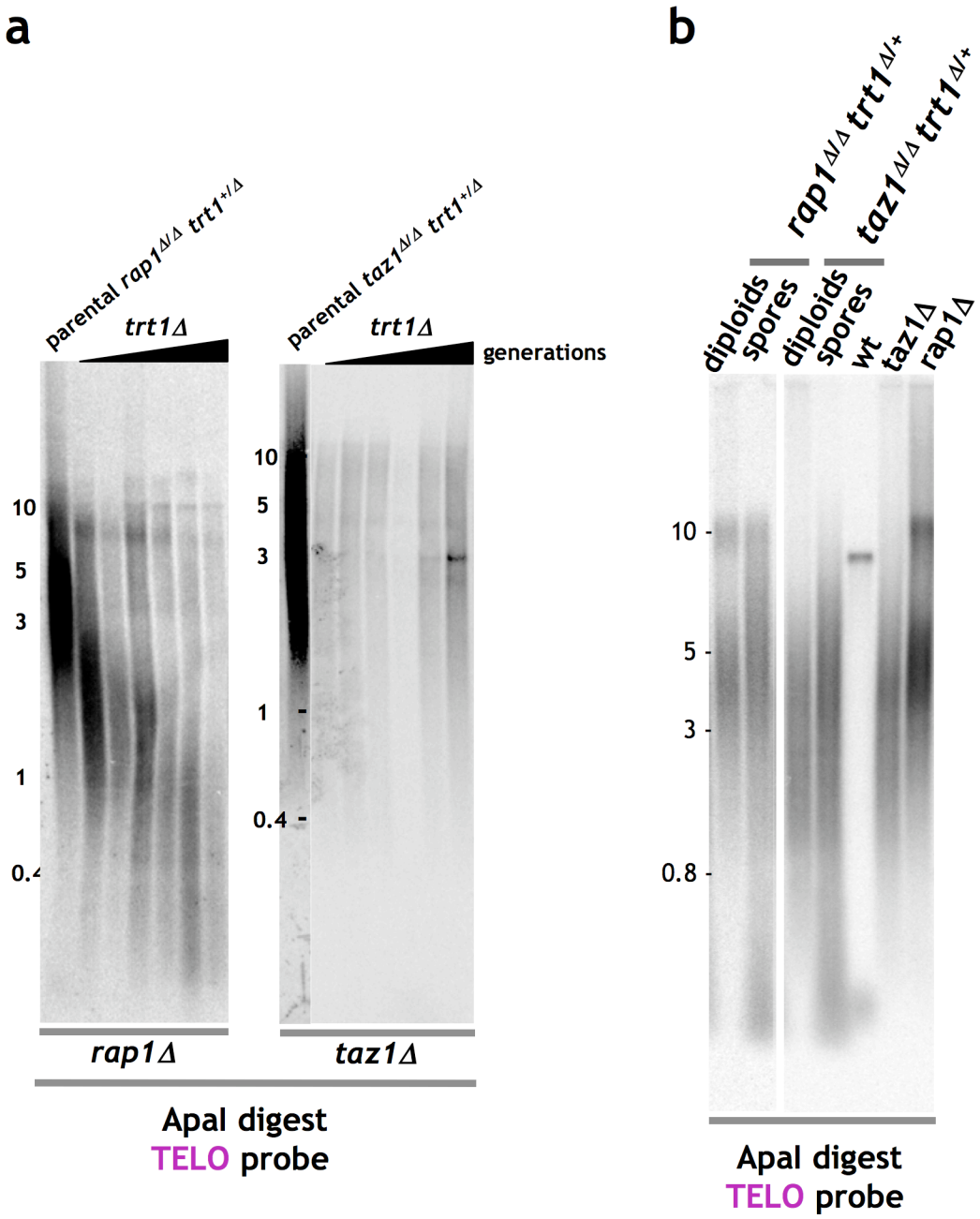

Figure 3.6 Differences in the kinetics of telomere attrition in *taz1Δ* versus *rap1Δ* cells after *trt1*$^{+}$ deletion

a, The diploids described in Figure 3.5 were sporulated and germinated *en masse*. Cultures were grown logarithmically under selection for *trt1Δ* and analyzed every 24 h (~5–10 generations). **b**, The telomere loss seen in *taz1Δ trt1Δ* progeny of *taz1*$^{Δ/Δ}$*trt1*$^{Δ/+}$ diploids occurs during the S-phases subsequent to germination, and not during meiosis. Telomere length in ungerminated spores of *taz1*$^{Δ/Δ}$*trt1*$^{Δ/+}$ and *rap1*$^{Δ/Δ}$*trt1*$^{Δ/+}$ meiosis was assessed by Southern blotting. Note that DNA isolated from spores always contains fragmented species, seen with probes to any region of the genome. Telomere length distribution in *rap1Δ* and *taz1Δ* spores is identical, despite their striking departure from identity after germination.

The abrupt telomere loss seen upon deletion of *trt1*$^{+}$ from *taz1Δ* cells is consistent with an inability to maintain *taz1Δ* telomeres through conventional replication. Likewise, the gradual telomere attrition seen in *rap1Δ trt1Δ* cells agrees with our observation that semi-conservative telomere replication is largely complete in the absence of Rap1. The notion that telomerase synthesizes a large fraction of the telomeres in each cell cycle is consistent with its ability to confer complete *taz1*Δ telomere elongation within ~10 generations (see Chapter 4 for further discussion).

3.4 Hyper-recombination at taz1Δ telomeres

3.4.1 Hyper-recombination at *taz1*Δ sub-telomeres

Replication fork pausing can trigger not only DNA breakage, but also DNA recombination pathways (Ahn et al., 2005; Cotta-Ramusino et al., 2005; Lambert et al., 2005). We thus wished to measure the levels of recombination at *taz1*Δ *versus rap1*Δ and wt telomeres.

Telomeric recombination can be assessed *via* the stability of the hybridization pattern in the subtelomeric regions (STE1) of chromosomes 1 and 2, which are similar but not identical between the four subtelomeres (Baumann and Cech, 2000; Sugawara, 1988). As expected, the STE1 restriction pattern remains stable in a wild-type strain upon serial passaging (Figure 3.7). However, *taz1Δ* subtelomeres display an erratic restriction pattern that changes from one restreak to the next (Figure 3.7). This instability is likely to reflect amplification of repeat tracts located between restriction sites (Sugawara, 1988), due to hyper-recombination in the region; indeed, rearrangements are dependent on the recombination protein Rhp51^{Rad51} (MG Ferreira, unpublished observations). This is specific for *taz1Δ* cells, as subtelomeric restriction patterns remain stable in *rap1Δ* cells (Figure 3.7). Thus, the stability of the subtelomeres is specifically disrupted in *taz1*Δ cells.

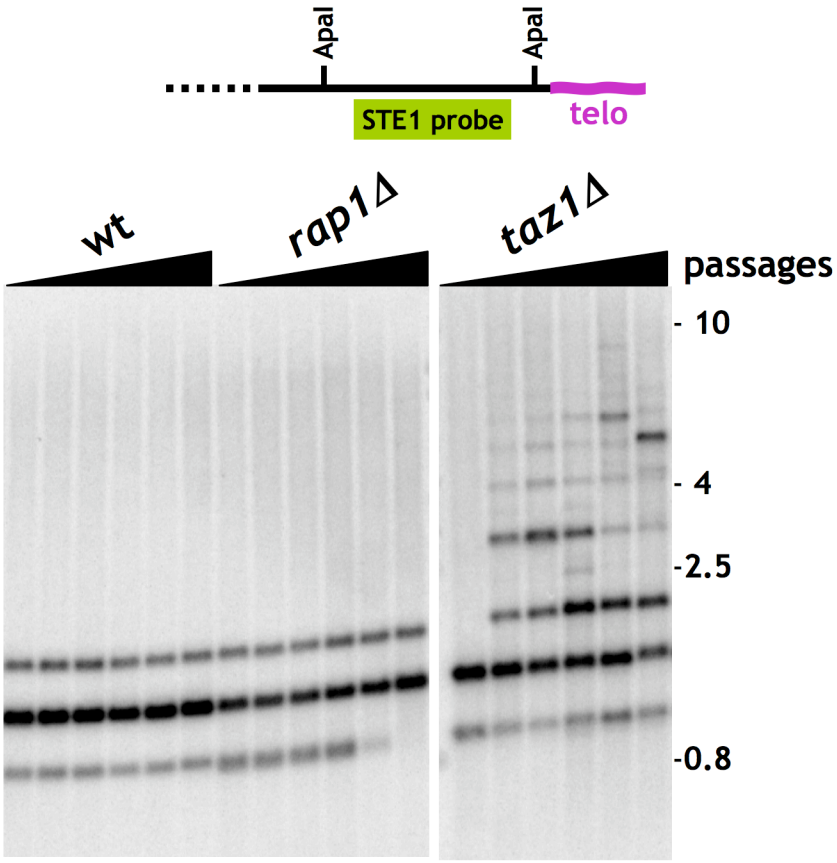

Figure 3.7 Subtelomeric re-arrangements in *taz1*Δ cells

Schematic diagram of fission yeast subtelomeres (top). Strains were re-streaked on rich medium plates (YES) every 2-3 days. A single colony from each re-streak was cultured, and sub-telomeres were analyzed by *Apa*I digestion of genomic DNA, followed by Southern blotting with an STE1 probe. Subtelomeres were stable in wt and *rap1*Δ background, but displayed erratic hybridization pattern in *taz1*Δ cells.

An alternative method to assess the stability of the subtelomere and thus, indirectly, recombination at the telomeres, is to monitor maintenance of a marker inserted at a subtelomere. This method was employed in the past in other yeasts, and relies on the availability of negative selection against strains expressing the *ScURA3*/*ura4*$^+$ gene (Louis and Haber, 1990). We used strains in which *his3*$^+$ and *ura4*$^+$ are inserted at the left subtelomeres of chromosomes I and II, respectively (Nimmo et al., 1998). As was previously reported, fission yeast exhibit telomere position effect (TPE, see Chapter 1). Hence, these telomere-adjacent genes are silenced in a wt background, but expressed upon mutation of heterochromatin factors, for example the histone methyltransferase

clr4$^+$ (Figure 3.8a) (Allshire et al., 1995; Ekwall and Ruusala, 1994). *taz1*$^+$ deletion substantially relieves TPE, and TPE is also relieved, although to a lesser extent, in *rap1*Δ cells (Figure 3.8a and Kanoh et al., 2005; Nimmo et al., 1998). In order to allow expression of *ura4*$^+$ and to exclude the effects of TPE, double mutants with *clr4*Δ were constructed. Interestingly, *clr4*$^+$ deletion, while conferring only a mild growth defect in the cold, dramatically exacerbated the cold-sensitivity of *taz1*Δ cells (Figure 3.8a,b), probably due to the role of Clr4 in centromere function (KM Miller and JPC, unpublished data and Miller and Cooper, 2003). As in *clr4*Δ cells, TPE was abolished in *rap1*Δ *clr4*Δ and *taz1*Δ *clr4*Δ cells, as *ura4*$^+$ expression allowed the cells to grow on plates lacking uracil. However, recombination events at the subtelomere may result in deletion of *ura4*$^+$, thus allowing growth on 5-FOA. In a *clr4*Δ background, 5-FOA resistant colonies grew at a rate of ~10^{-4}, which is likely to reflect a basal level of recombination at telomeres. Importantly, *taz1*$^+$ deletion increased the rate of growth on 5-FOA by ~10-fold, while no such increase was observed after *rap1*$^+$ deletion (Figure 3.8b,c).

These preliminary results require verification - Southern blotting of DNA derived from the 5-FOA resistant colonies should be used to verify that indeed *ura4*$^+$ was lost. In addition, other genetic backgrounds can be used to accentuate the difference between *taz1*Δ, *rap*Δ and wt cells, and to verify that *taz1*$^+$ deletion stimulates recombination in genetic backgrounds other than *clr4Δ*. Nonetheless, as this is a genetic assay, it may provide a useful alternative method for addressing the determinants of subtelomeric recombination.

Figure 3.8 Assaying subtelomeric rearrangements through the stability of a subtelomeric marker.

(next page) **a,b** 5-fold serial dilution of logarithmically growing cells harboring *ura4*$^+$ and *his3*$^+$ at telomeres 2L and 1L, respectively (Nimmo et al., 1998). Cells were plated on YES media, minimal media lacking uracil or histidine, or minimal media containing 5-FOA. Plates were incubated at 32° unless otherwise indicated. **c**, Cells were plated on the indicated plates, and incubated at 32° for 3-5 days until colonies appeared. *taz1*$^+$ deletion increased ~10 fold the rate of generating 5-FOA resistant colonies.

a

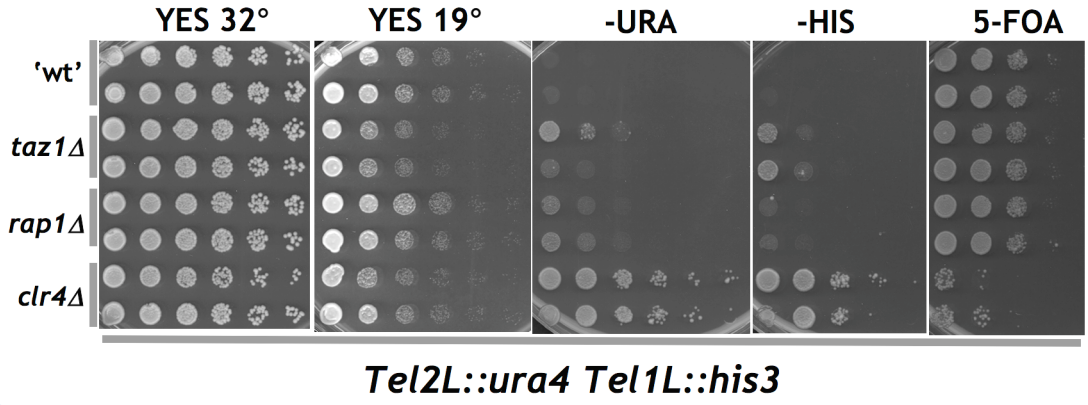
YES 32°
YES 19°
-URA
-HIS
5-FOA
'wt'
taz1Δ
rap1Δ
clr4Δ
Tel2L::ura4 Tel1L::his3

b

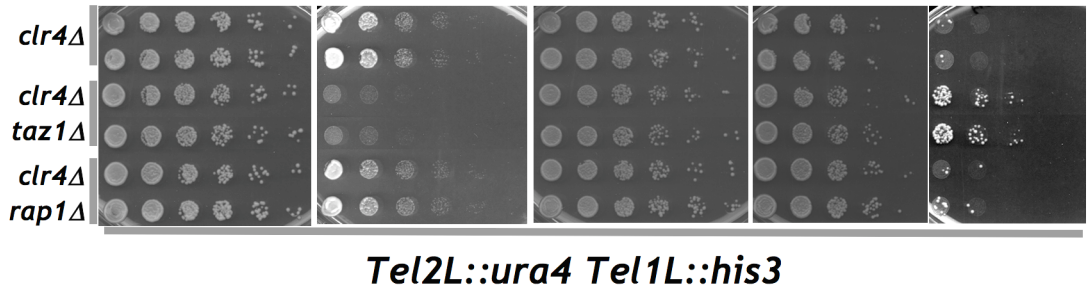
clr4Δ
clr4Δ taz1Δ
clr4Δ rap1Δ
Tel2L::ura4 Tel1L::his3

c

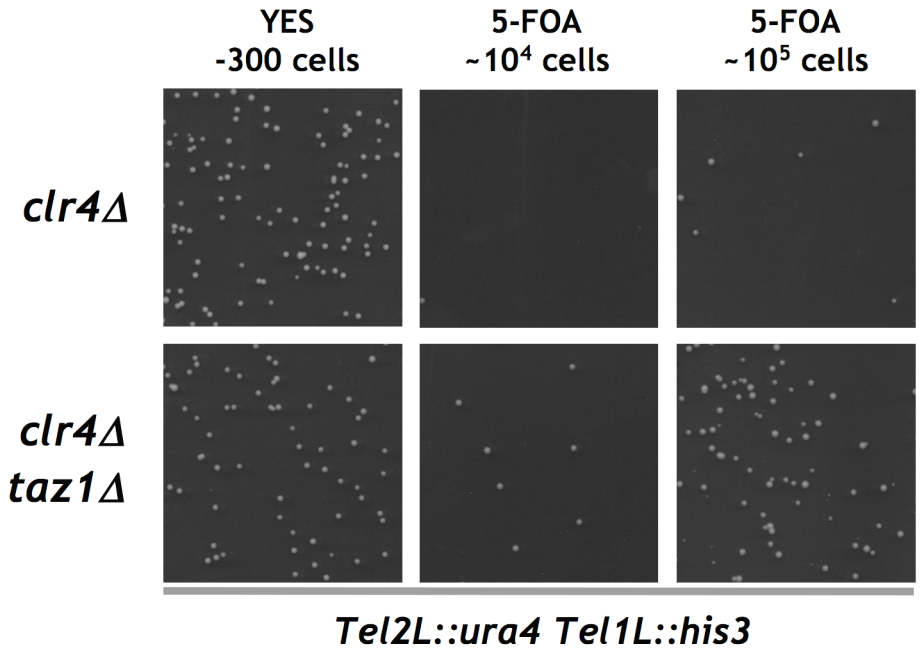
YES
-300 cells
5-FOA
~10⁴ cells
5-FOA
~10⁵ cells
clr4Δ
clr4Δ taz1Δ
Tel2L::ura4 Tel1L::his3

3.4.2 Survival mode of *taz1Δ trt1Δ* cells

Fission yeast cells lacking telomerase eventually lose all telomeric DNA and survive by sustaining intramolecular end-fusions that result in circularization of each of the three chromosomes (see diagram in Figure 3.9). More rare survivors, which are faster growing, can be selected by growing *trt1Δ* cells in liquid; these survivors bear linear chromosomes, presumably maintaining telomeres through a recombination based mechanism, reminiscent of ALT (Nakamura et al., 1998). The exact nature of the recombination events that promote linear survival mode is not yet delineated. Nonetheless, we wondered whether the prevalence of linear survivors may be used to assess recombination events at telomeres.

rap1Δ trt1Δ strains, like 'normal' *trt1Δ* strains, eventually lose all telomeric DNA and survive by circularizing their chromosomes when grown on plates (Figure 3.9). In contrast, under the same selection regime, *taz1Δ trt1Δ* survivors maintain linear chromosomes with variable amounts of telomeric DNA, presumably through recombination (Figure 3.9). A recently published study confirmed that this survival mode of *taz1Δ trt1Δ* cells relies on the recombination protein $Rad22^{Rad52}$ (see below and Subramanian et al., 2008). The uniqueness of this survival mode to *taz1Δ* but not *rap1Δ* cells supports the idea that it stems from stalled forks that elicit hyper-recombination.

While recombination at telomeres cannot be measured directly, our results, utilizing assays for different consequences of recombination at telomeres and subtelomeres, support the notion that recombination events are abundant at *taz1Δ* telomeres. The high level of recombination at *taz1Δ* subtelomeres and the distinct patterns of telomere attrition and survival following telomerase loss in *taz1Δ* and *rap1Δ* backgrounds are compatible with the idea that high levels of telomeric fork stalling that elicit hyper-recombination are unique to *taz1Δ* cells.

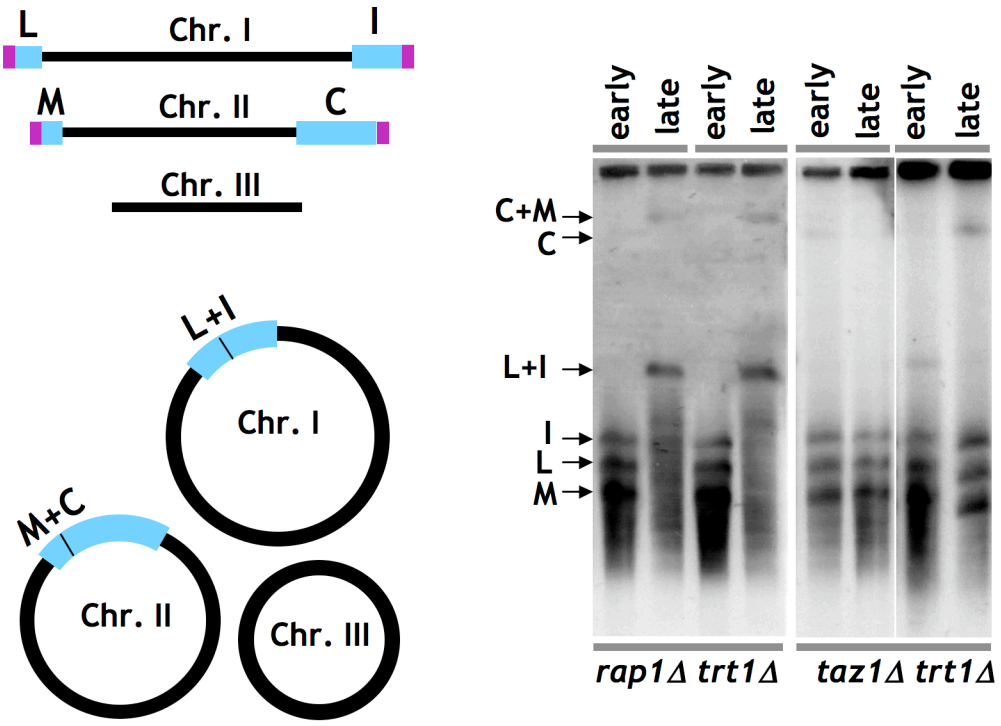

Figure 3.9 Survival mode of *taz1Δ versus rap1Δ* cells after *trt1*$^{+}$ deletion

DNA from 'early' (~50 generations after *trt1*$^{+}$ loss) and 'late' (~200 generations after *trt1* loss) cultures of *trt1Δ* survivors was digested with *Not*I, separated by pulsed-field gel electrophoresis, blotted and hybridized with probes against 'L', 'M', 'I' and 'C' (left panel) on chromosomes (Chr.) I and II. L, M, I and C bands indicate linear chromosomes; L+I and M+C fusion bands indicate circular chromosomes. 'Late' *rap1*Δ *trt1*Δ survivors are circular while *taz1*Δ *trt1*Δ survivors are linear.

3.5 Analysis of taz1Δ trt1Δ survivors

The erratic banding pattern of telomeric hybridization in *taz1*Δ *trt1*Δ survivors has intrigued us. On the one hand, we learned that the chromosomes of these survivors are linear (Section 3.4.2 above). On the other hand, the bands of telomeric hybridization appeared sharper than would be expected from heterogeneous 'wt' telomeres, suggesting that they are not terminal. For example, compare the F1 band in the wt sample in Figure 3.1c, which is diffuse due to heterogeneity in telomere length, to the 1kb band in the *taz1*Δ *trt1*Δ

sample in Figure 3.5a, which is much sharper in appearance despite containing much shorter DNA fragments.

To address the end structure of these survivors, we performed BAL-31 digestion of genomic DNA. BAL-31 is a dsDNA/ssDNA exo- and endo-nuclease, whose combined activities cause ssDNA digestion and attrition of linear dsDNA molecules from their ends. An internal linear control was added to the reactions in Figure 3.10 to assess the amount of digestion. Based on digestion of this control molecule, we can estimate that ~1kb was digested during the course of the experiment. Indeed, when wt or *taz1*Δ samples were incubated with BAL-31, the telomeric signal diminished in intensity and length, confirming that telomeres are terminal (Figure 3.10). However, when genomic DNA from a *taz1*Δ *trt1*Δ survivor was incubated under the same conditions, no change in migration of the sharp telomere repeat-containing bands was apparent; we note, however, the reduction in the faint low-molecular weight signal (Figure 3.10). Thus, most of the telomeric sequences in these survivors are not terminal.

To determine what might serve as an alternative end structure in *taz1*Δ *trt1*Δ survivors, we examined the subtelomeric sequences, using a probe for the sub-telomeric element adjacent to the telomere (STE1). When we re-probed genomic DNA from *taz1*Δ *trt1*Δ survivors which arose on plates with STE1, we observed rearranged and amplified STE1 in all clones; note the faint hybridization in the parental diploids, and the different patterns of rearrangements, for example, in clones 4, 5 and 6 (Figure 3.11a). While some of the telomeric bands co-localize with the STE1 bands (e.g. clone 4), many of them do not (e.g. clone 15). To assess the level of STE1 amplification, we performed Southern blot analysis on genomic DNA isolated from *taz1*Δ *trt1*Δ spores germinated and grown in liquid, which allowed monitoring of the early stages of survival. We observed that as the cells were propagated, STE1 sequences were amplified by >5-fold during the first 5 days, relative to an internal probe used as loading control (Figure 3.11b). Thus, survival of *taz1*Δ *trt1*Δ cells occurs concomitantly with amplification and rearrangements in the subtelomeric regions.

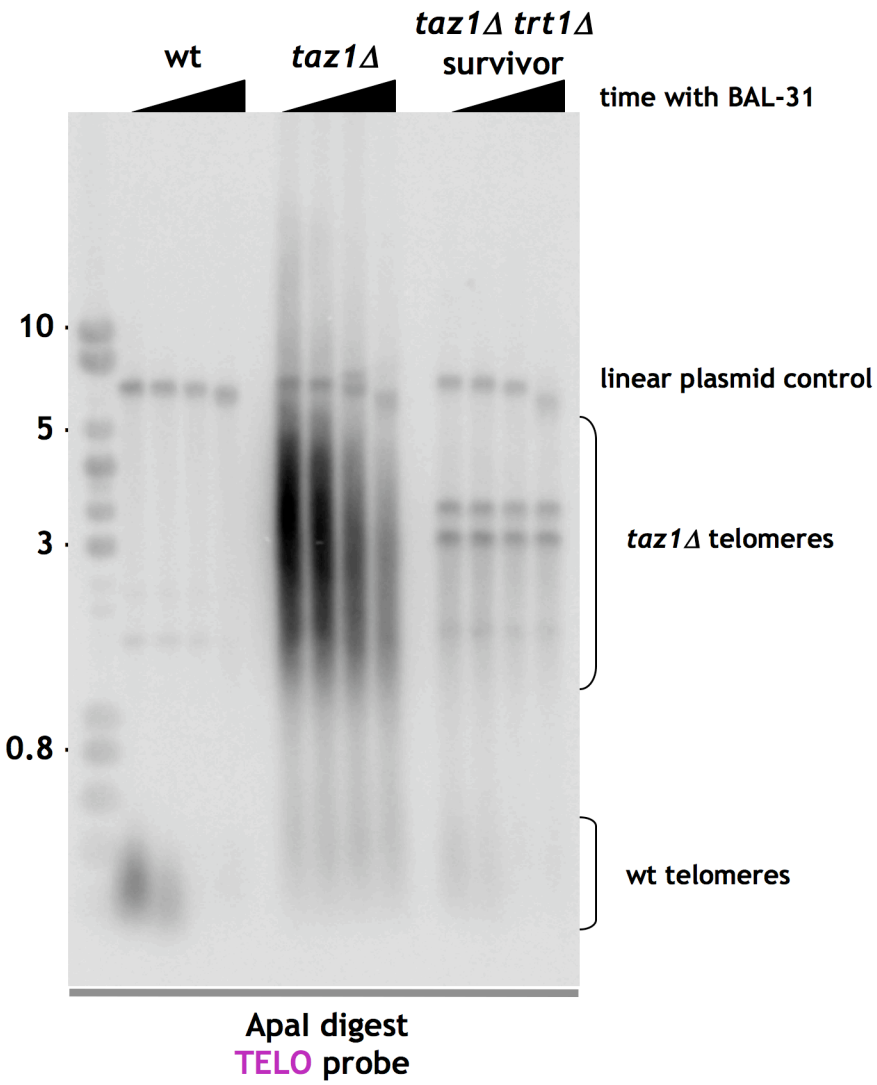

Figure 3.10 Telomere hybridization signal in *taz1*Δ *trt1*Δ survivors is mostly not terminal

Genomic DNA from wt and *taz1*Δ cells and from a *taz1*Δ *trt1*Δ survivor was treated with BAL-31 for increasing lengths of time (0, 10, 30 and 60 minutes). A linearized plasmid was added to each reaction to assess the amount of digestion. Following inactivation and removal of BAL-31, DNA was digested with *Apa*I. Southern Blot analysis was performed with a telomeric probe. While the telomere signal in wt and *taz1*Δ is progressively reduced in length and intensity, the banding pattern of *taz1*Δ *trt1*Δ is unaffected.

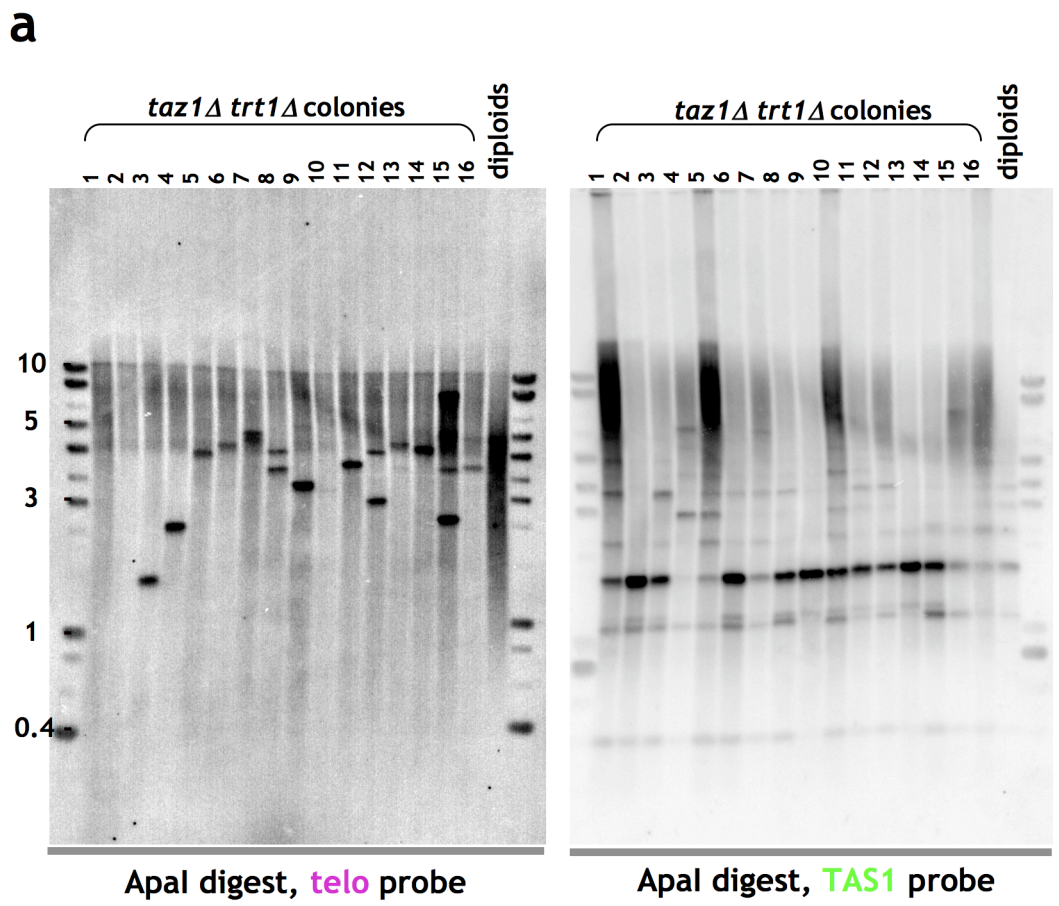
a
taz1Δ trt1Δ colonies
diploids
1 2 3 4 5 6 7 8 9 10 11 12 13 14 15 16
10
5
3
1
0.4
ApaI digest, telo probe
taz1Δ trt1Δ colonies
diploids
1 2 3 4 5 6 7 8 9 10 11 12 13 14 15 16
ApaI digest, TAS1 probe

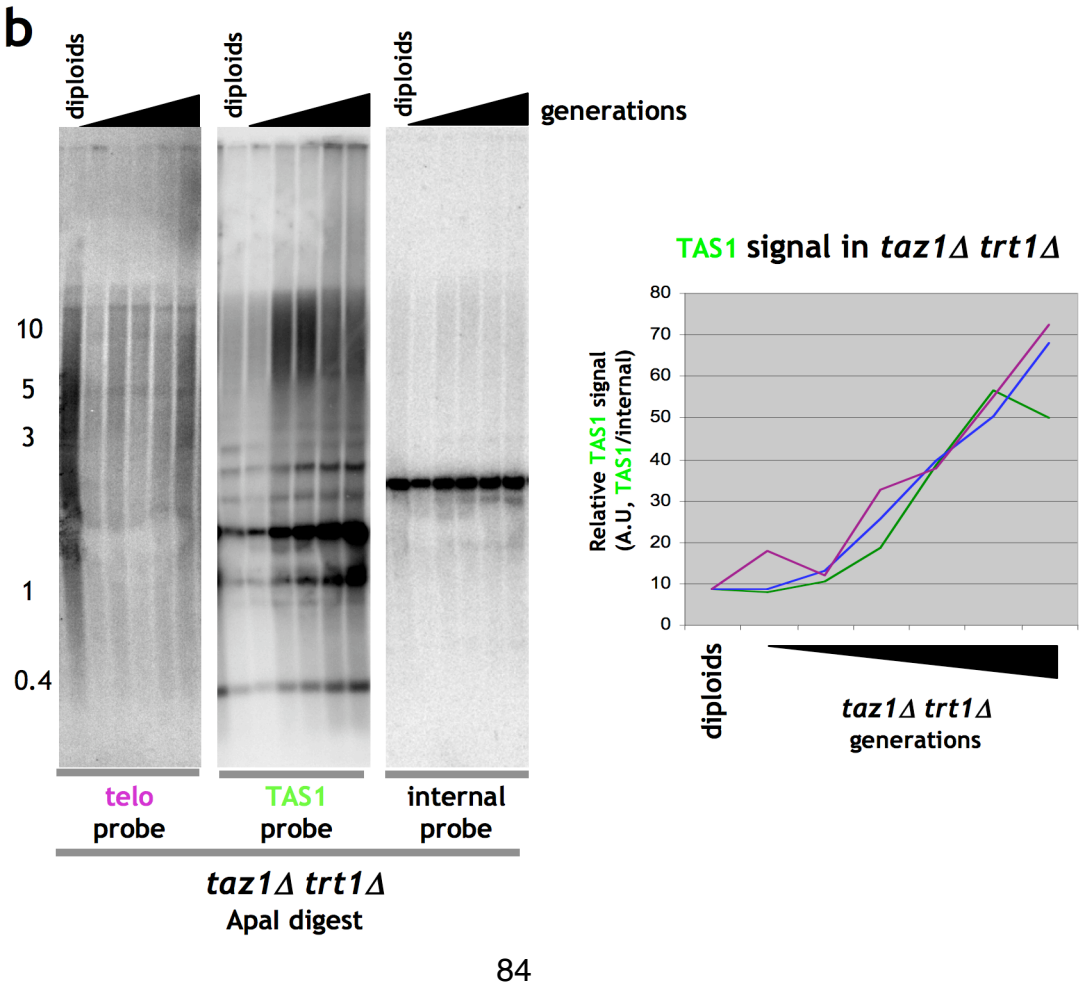
b
diploids
diploids
diploids
generations
10
5
3
1
0.4
telo probe
TAS1 probe
internal probe
taz1Δ trt1Δ
ApaI digest
TAS1 signal in taz1Δ trt1Δ
Relative TAS1 signal (A.U, TAS1/internal)
80
70
60
50
40
30
20
10
0
diploids
taz1Δ trt1Δ generations

Figure 3.11 STE1 sequences are amplified in *taz1*Δ *trt1*Δ survivors

(previous page) **a,** Genomic DNA from 16 independent *taz1*Δ *trt1*Δ survivors and the parental diploid (*taz1*$^{\Delta/\Delta}$ *trt1*$^{+/\Delta}$) was digested with *Apa*I. Southern blotting with telomeric and STE1 probes reveals rearrangements and amplification of the STE1 hybridization pattern. **b**, *taz1*$^{\Delta/\Delta}$ *trt1*$^{+/\Delta}$ diploids were sporulated and germinated *en masse*. Cultures were grown logarithmically under selection for *trt1Δ* and analyzed every 24 h (~5–10 generations). Southern Blots were performed with telomeric, STE1 and internal probes. Quantification (right) depicts 3 different experiments.

We speculate that *taz1*Δ *trt1*Δ survivors maintain telomeres by amplifying a subtelomeric fragment containing a short stretch of telomeric sequences, which are maintained at the chromosome terminus by unequal crossing-over or break-induced replication (BIR) events between subtelomeres (Figure 3.12). This is consistent with the BAL-31 results, as in this model most telomeric sequences are not terminal. The existence of the telomeric sequences provides telomeres with enough protection to maintain linear chromosomes, and prevents chromosome circularization. Telomeric sequences in the absence of Taz1 will promote fork-stalling, which may underlie the recombination events that help maintain these telomeres. Indeed, the absence of Taz1 promotes the maintenance, in addition to generation, of the linear mode of survival, as re-introduction of *taz1*$^{+}$ leads to chromosome circularization (Subramanian et al., 2008). The variability in restriction pattern between different *taz1*Δ *trt1*Δ clones may be due to different subtelomeric elements being amplified, or to variable preservation of the *Apa*I restriction site that was used during the analysis.

Following publication of most of these data, further analysis of *taz1*Δ *trt1*Δ cells was published by T. Nakamura's lab (Subramanian et al., 2008). They found that generation of linear *taz1*Δ *trt1*Δ survivors requires the recombination genes *rad22*$^{+}$, *tel1*$^{+}$ (ATM) and the MRN complex, consistent with a maintenance mechanism involving recombination events. Surprisingly, Trt1 by itself, independently of its reverse transcriptase activity, was also capable of suppressing recombination-based linear survival.

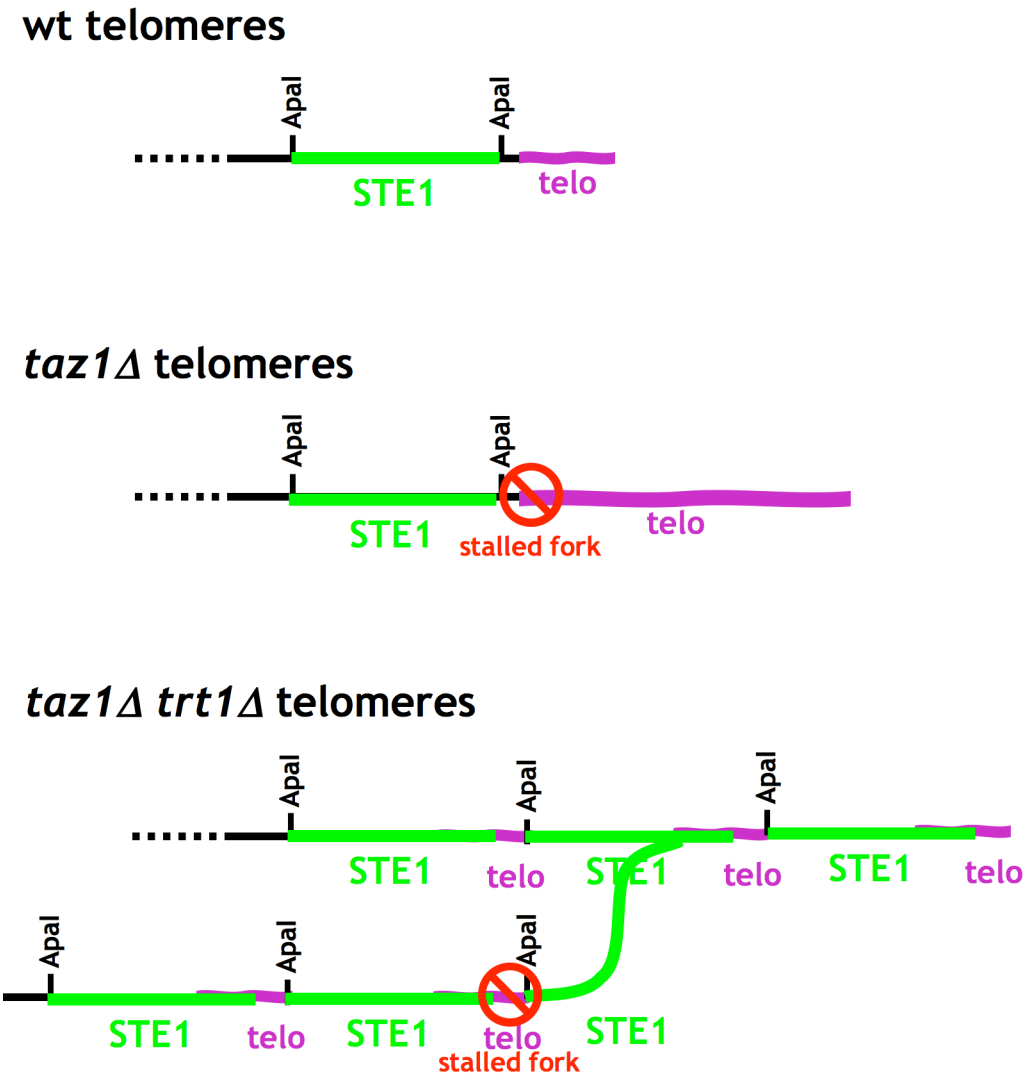

Figure 3.12 Model for telomere structure and maintenance in *taz1*Δ *trt1*Δ survivors

Chromosome termini are depicted, such that the centromere proximal side is to the left. Telomeres ('telo', magenta squiggle), STE1 (green), and *Apa*I restriction sites are shown. Invading STE1 fragment designates a BIR event resulting in elongation of the lower telomere. Telomeric sequences promote fork-stalling in the absence of Taz1 (red 'No' symbol). See text for further details.

Similar recombination-based modes of survival have been described in budding yeast following loss of telomerase. Two types of survivors were described: Type II survivors maintain short telomeres of variable length, presumably through unequal recombination events between the telomeric repeats. Type I survivors, which are perhaps more similar to *taz1*Δ *trt1*Δ

survivors, amplify subtelomeric elements (Y' elements) interspersed with very short stretches of telomeric sequences, which presumably help to maintain telomere identity. Interestingly, the two types of survivors have different genetic requirements. While both types of survivors require Rad52 and the BIR protein Pol32 (Lundblad and Blackburn, 1993; Lydeard et al., 2007), Type I uniquely requires genes of the *RAD51* epitasis group, and Type II uniquely requires *RAD50* (part of the MRN/X complex) and the RecQ helicase Sgs1 (Chen et al., 2001; Cohen and Sinclair, 2001; Huang et al., 2001; Johnson et al., 2001).

ALT cells, which also maintain telomeres in the absence of telomerase, are presumably doing so using a recombination-based pathway (Bryan et al., 1997). While some genes were implicated in ALT, thorough genetic analysis has not been performed, as technical difficulties hamper the creation of ALT cells *de novo* in the lab (reviewed in Cesare and Reddel, 2008). In addition, while rearrangements at telomeres and subtelomeres of ALT cells have been observed (Varley et al., 2002), the overall structure of ALT telomeres and subtelomeres, and the contribution of rearrangements to their generation and survival, is far from being well understood.

3.6 Implications for telomere dysfunction

The data presented here demonstrate an unexpected role for a telomeric dsDNA binding protein: promotion of semi-conservative replication through telomeres. In the absence of Taz1, replication forks stall at telomeres, and are likely to promote telomere breakage, loss, and recombination.

An important question is the nature of the aberrant replication patterns at *taz1*Δ telomere (the 'plume'), which include molecules of large molecular weight and structural complexity. Paused replication at *taz1Δ* telomeres may generate unwound, unreplicated strands of DNA that can invade other chromosomes. The G-rich nature of telomere repeats and/or long 3' single-strand overhangs in *taz1Δ* cells might facilitate such interactions between strands of DNA from distinct duplexes. Thus, the plumes of hybridization seen upon 2DGE of *taz1Δ* telomeres may represent branched structures generated from telomeric strand invasion reactions. Intriguingly, *taz1Δ* mutants accumulate entangled telomeres that fail to separate at mitosis if the preceding S-phase occurred at a cold

temperature (≤20 °C) (Miller and Cooper, 2003). Thus, we speculate that stalled replication forks at *taz1Δ* telomeres elicit telomeric entanglement, manifested by the plume pattern in 2DGE gels, and that resolution of these entangled telomeres is compromised in the cold. Like the precipitous telomere loss upon *trt1⁺* deletion, the *taz1Δ* chromosomal entanglement phenotype is absent from *rap1Δ* cells (Miller et al., 2005), supporting the idea that stalled telomeric replication forks are the originating defect.

How might Taz1 facilitate replication through telomere sequences? Taz1 may coordinate loosening, remodelling or removal of the telomere complex to allow replication fork progression. Alternatively, Taz1 may facilitate unwinding of the G-rich telomere repeats or prevent them from forming spurious intra- or interstrand G-rich quadruplex structures once unwound. Such challenges have been invoked to explain defective telomere replication in mammalian cells lacking the WRN or RTEL helicases (Crabbe et al., 2004; Ding et al., 2004). These studies, together with our results, raise the possibility that Taz1, and by analogy human TRF1 or TRF2, may promote unimpeded replication by recruiting such helicases to telomeres. Finally, it is possible that Taz1 binding to telomeric dsDNA prevents transient melting of the duplex or protect it from interactions with telomeric ssDNA, thus obstructing the formation of secondary structures or telomere-telomere associations.

Previous studies have suggested that telomere-binding proteins hinder, rather than facilitate, replication fork progression. Stalled forks have been observed at sites of steric hindrance by stable DNA–protein complexes, including ribosomal DNA and telomeric regions in budding yeast (Ivessa et al., 2003; Ivessa et al., 2002). Deletion of the Rap1 carboxy terminus had no effect on replication pausing through budding yeast telomeres, but shorter telomeres alleviated pausing (Makovets et al., 2004). These results led to the conclusion that the Rap1 amino terminus, which contains its DNA-binding domain, generates an obstacle to replication fork passage, with the larger number of bound Rap1 molecules at long telomeres exacerbating this effect (Makovets et al., 2004). However, loss of the N-terminal DNA-binding domain of Rap1 would be more equivalent to *taz1⁺* deletion, and might reveal a role for Rap1 in promoting, rather than impeding, fork passage. In an *in vitro* simian virus (SV40)

replication system, expression of human TRF1 and TRF2 creates a replication block at the telomeric termini of a linear plasmid (Ohki and Ishikawa, 2004). By analogy with Taz1, we suggest that physiological concentrations of human TRFs may facilitate, rather than hinder, passage of the replication fork *in vivo*.

Our results suggest that stalled forks may arise from an altered balance of telomere-binding proteins that accompanies telomere attrition in human telomerase-negative cells. Stalled replication forks may accelerate telomere attrition and/or trigger the recombination reactions that constitute the "alternative lengthening of telomeres (ALT)" (Londono-Vallejo et al., 2004) and "telomere rapid deletion (TRD)" (Lustig, 2003; Wang et al., 2004) pathways seen in telomerase-negative cancer cells. Hence, the 'end replication problem' begins before the replication fork reaches the chromosomal terminus, and requires telomere-binding proteins not only to recruit and control telomerase but also to ensure passage of the semi-conservative replication fork.

4 Chapter 4: Determinants of Replication Fork-stalling at Telomeres

4.1 Introduction

4.1.1 Properties of telomeric sequences rendering them prone to stalling

Our work has shown that semi-conservative telomere replication requires Taz1. In the absence of Taz1, replication forks stall when they encounter telomeric sequences. These stalled telomeric replication forks are liable to initiate processing events leading to telomere breakage and loss and to recombination events at telomeres. They are also likely to be good substrates for elongation by telomerase. Our finding that telomeres pose an impediment to semi-conservative replication forks raises the question: what specific characteristics of telomeres demand 'special attention' during replication?

Telomeric sequences ($G_{3\text{-}6}$TTAC(A)(C) in fission yeast) are GC-rich compared with the rest of the genome (55% *versus* 36%). Moreover, one of the strands is very G-rich ('strand bias'). The G-rich strand harbours stretches of guanines that can adopt very stable non-Watson-Crick secondary structures known as G-quartets. Although the existence of G-quartets *in vivo* is still contentious, their formation can potentially hinder passage of the replication fork. An additional characteristic of telomeric sequences is their repetitive nature; fission yeast telomeres are composed of degenerate ~7-11bp repeats, while vertebrate telomeres are composed of precise 6bp repeats. The repeated sequences may help to promote formation of secondary structures or cause polymerase slippage. Finally, sequence-specific factors that bear affinity to telomeric sequences could generate a stable complex that would hinder replication.

4.1.2 How does Taz1 assist telomere replication?

A different formulation of the question posed in the previous section is: how does Taz1 assist replication of telomeric sequences? The different causes of stalling outlined above entail different molecular activities Taz1 may engage

in to relieve stalling. First, Taz1 may relieve stalling simply by binding to telomeres. Under this model, DNA binding itself, in a manner that is perhaps analogous to 'ironing', may restrict the occurrence of inter- and intra-strand interactions or prevent formation of secondary structures. Such interactions are predicted to be specifically abundant and troublesome during DNA replication, concomitant with the unwinding of the double helix.

Alternatively, Taz1 binding may recruit or regulate other DNA processing enzymes that affect the replication fork. Candidates for such interactors are helicases, endonucleases, ssDNA binding proteins and other components of the replication fork. Many such factors were shown to interact with Taz1 orthologs or to modulate telomere replication: the RecQ helicases WRN and BLM, the nucleases FEN1, Apollo and Artemis, the MRN complex, the PI3-like kinases DNA-PK, ATM and ATR, and ORC components, to name just a few (reviewed in de Lange, 2005).

Finally, Taz1 binding may restrict binding of a yet unidentified telomere binding protein. This postulated protein would cause stalling when bound to telomeres. The only other known protein that binds telomere sequences, Tbf1, is not abundant at *taz1*Δ telomeres (C. Pitt and JPC, unpublished observations). Despite this observation, the existence of another telomere binding factor was not formally ruled out.

4.1.3 Telomere dysfunction in fission yeast telomeres: roles of Taz1 and Rap1

The first telomeric component identified in fission yeast was the telomeric dsDNA binding protein Taz1, an ortholog of mammalian TRF1 & 2 (Cooper et al., 1997). The telomeric complex was later extended to include homologs of two budding yeast and human proteins: Rap1 and Rif1 (Chikashige and Hiraoka, 2001; Kanoh and Ishikawa, 2001). The telomeric complex also includes a group of proteins assembled on the 3' ssDNA overhang: Pot1, Tpz1, Ccq1 and Poz1, which may provide a link to the telomeric dsDNA complex through an interaction with Rap1 (Baumann and Cech, 2001; Miyoshi et al., 2008)(see also section 1.4).

In budding yeast, where the telomeric complex has been studied in depth, Rap1 is a telomeric DNA binding protein, which recruits, through interactions with its C-terminus, the telomeric proteins Rif1 & 2, and the silencing factor Sir4 (Hardy et al., 1992; Moretti et al., 1994), and is responsible for many telomeric functions. However, in fission yeast and in mammals the situation is different, and only Taz1 or TRF1 & 2 bind telomeric dsDNA, and then recruit Rap1 to telomeres. In fission yeast, Rif1 localization to telomeres also depends on Taz1 (Chikashige and Hiraoka, 2001; Kanoh and Ishikawa, 2001).

Genetic analysis of telomere dysfunction in *taz1*Δ and *rap1*Δ cells revealed that both single deletions and the double mutant exhibit several similar phenotypes: long telomeres (although not identical in length), de-protection from end-to-end fusion in G1, extended 3' overhangs, relief of telomeric silencing (telomere position effect, TPE), and a meiotic defect (Chikashige and Hiraoka, 2001; Kanoh and Ishikawa, 2001; Kanoh et al., 2005; Miller et al., 2005; Tomita and Cooper, 2007). Rap1 absence from telomeres is the common feature of *taz1*Δ, *rap1*Δ and *taz1*Δ *rap1*Δ strains - all exhibiting telomere dysfunction. Thus, the simplest explanation was that Rap1 carries out the major effects of the telomeric complex *in cis*, while Taz1's main function is to recruit Rap1 to telomeres. This model received support from analysis of chimeric Rap1-Taz1^{Cter} (containing part of Taz1 including the Myb DNA binding domain). This chimeric protein was recruited to telomeres, and was able to partially suppress the meiotic phenotype of *taz1*Δ *rap1*Δ cells (Chikashige and Hiraoka, 2001).

The picture was complicated, however, by later observations. First, Rif1 cannot be detected at telomeres by ChIP in the absence of Taz1 (Kanoh and Ishikawa, 2001), yet it is required for the cold-sensitivity exhibited by *taz1*Δ cells (Miller et al., 2005). Similarly, deletion of *rap1*$^{+}$ exacerbates the cold-sensitivity of *taz1*Δ cells (Miller et al., 2005), and prevents recombination-based survival of *taz1*Δ *trt1*Δ cells (Subramanian et al., 2008). Again, in both cases Rap1 cannot be detected at telomeres by ChIP (Kanoh and Ishikawa, 2001; Subramanian et al., 2008). These results suggest that Rif1 and Rap1 may function also *in trans*, possibly affecting cell cycle, transcription or DDR related processes. However, residual recruitment of Rap1 to telomeres may still take place in *taz1*Δ cells, since during meiosis a fraction of the telomeres exhibits Rap1 localization

(Chikashige and Hiraoka, 2001). This observation raises the possibility that Taz1-independent mechanisms may recruit Rap1, perhaps involving heterochromatin (Kanoh et al., 2005) or the telomeric ssDNA-binding complex (Miyoshi et al., 2008).

In addition, several observations suggested that Rap1 might not be the only effector of Taz1. As mentioned above, Taz1 carries out its function in allowing replication fork passage through telomeres independently of Rap1 (Miller et al., 2006). Taz1, but not Rap1, also functions to suppress several additional phenotypes: telomere entanglements occurring at cold temperatures (Miller and Cooper, 2003; Miller et al., 2005); hyper-recombination at telomeres, occurring both in the presence of telomerase and during survival following loss of telomerase (Chapter 3); and positive regulation of telomere length (*taz1*Δ and *taz1*Δ *rap1*Δ telomeres are 5-10 fold longer compared with wt telomeres, but are still shorter than *rap1*Δ telomeres) (Kanoh and Ishikawa, 2001). A pertinent question relates to the interdependencies between these different phenotypes. Taz1 likely acts to prevent a single common lesion that underlie many of these *taz1*Δ-specific defects – possibly stalled telomeric replication forks.

4.2 Orientation of the telomeric sequence is not crucial for *taz1*Δ-specific stalling

4.2.1 Lagging strand replication of the G-rich strand: a potential impediment

Natural telomeres are polar, with the G-rich strand always running 5'-3' toward the terminus, and telomere replication is unidirectional, travelling from the centromere proximal side. The polarity and directionality of natural telomeres, while making it feasible to follow telomere replication (see below), also render it challenging to experimentally separate problems stemming from lagging strand replication from problems caused by replication of the G-rich strand.

Mammalian cells lend a unique opportunity to analyse telomere replication using CO-FISH (chromosome orientation fluorescence *in situ* hybridization) (Bailey et al., 2004; Bailey et al., 2001). CO-FISH allows identification of the two

products of semi-conservative DNA replication by relying on the unidirectional replication of telomeres. It utilises UV-sensitive nucleotide analogues that allow specific digestion of the newly synthesized strands of metaphase chromosomes *in situ*, followed by strand specific non-denatured FISH to detect the G- and C-rich strands. This allows detection of the two sister telomeres that templated lagging and leading strand synthesis. CO-FISH can also be used to detect crossing-over events between telomeres (termed T-SCE, telomere sister chromatid exchanges).

CO-FISH was found to be useful when studying several mutant backgrounds exhibiting telomere shortening or loss; CO-FISH revealed surprising bias for loss of either the leading or lagging telomeres, thus suggesting the mutated proteins have a role in events specific for replication of one of the telomere strands. Two of the better-studied perturbations are mutations in the RecQ helicase WRN, and overexpression of a truncated form of TRF2 (Crabbe et al., 2004; Wang et al., 2004).

The pathologies associated with mutations in WRN have long been associated with telomere dysfunction. In mice, which harbour very long telomeres, mutations in WRN manifest themselves in premature aging only when telomeres are short (due to prolonged propagation without telomerase) (Chang et al., 2004). Likewise, in human cells, manifestations of WRN inactivation are suppressed by expression of telomerase (Crabbe et al., 2007; Crabbe et al., 2004). Thus, it may not have been surprising that analysis of cells lacking functional WRN revealed cytological manifestation of telomere dysfunction (e.g. telomere breakage and ATM phosphorylation). Analysis of metaphase chromosomes by CO-FISH revealed that sister telomere loss (STL) occurred exclusively at the sister that underwent lagging strand replication (the sister that was templated by the G-rich strand) (Crabbe et al., 2004). This suggested that WRN is specifically required for lagging-strand telomere replication. It was hypothesized that the large amount of ssDNA exposed during lagging-strand replication, combined with the propensity of the G-rich strand to fold into G-quartets, would pose a problem for the replication machinery. G-quartets are excellent substrates for WRN *in vitro* (Mohaghegh et al., 2001), hinting at a possible mechanism for WRN activity during telomere replication.

Interestingly, it was recently reported that depletion of Flap Endonuclease 1 (FEN1), involved in lagging strand synthesis through its role in Okazaki Fragment maturation, also causes a lagging-strand-specific STL (Saharia et al., 2008). However, as mentioned above, it is unclear whether lagging-strand STL indeed requires both the G-rich strand and lagging-strand replication in order to occur, since there are no natural telomeres at which the G-rich strand is replicated by leading-strand replication. It remains to be tested whether lagging-strand replication of the C-strand or leading-strand replication of the G-strand poses a problem for the cell, or is differentially affected by WRN inactivation. Finally, while it has not been analyzed in such depth, inactivation of the RTEL helicase, suggested to specifically process G-quartets, also causes telomere dysfunction (Ding et al., 2004).

Another genetic manipulation resulting in strand-specific telomere loss is overexpression of a truncated form of TRF2 ($TRF2^{\Delta B}$) (Wang et al., 2004). Overexpression of $TRF2^{\Delta B}$ leads to telomere loss (but not telomere shortening), and to the appearance of excised loops that can be visualized cytologically as telomere-containing double minute chromosomes (TDM), or as circular telomeric forms (t-circles) discerned *via* 2DGE. CO-FISH revealed that telomere loss in $TRF2^{\Delta B}$ was specifically observed at the sister chromatid that underwent leading strand replication, suggesting that t-circle excision is coupled to DNA replication (Wang et al., 2004) (for further discussion see Chapter 5). These results are consistent with a role for ds telomeric DNA binding proteins in regulating semi-conservative replication, and suggest that strand-specific processing events may be taking place during semi-conservative telomere replication.

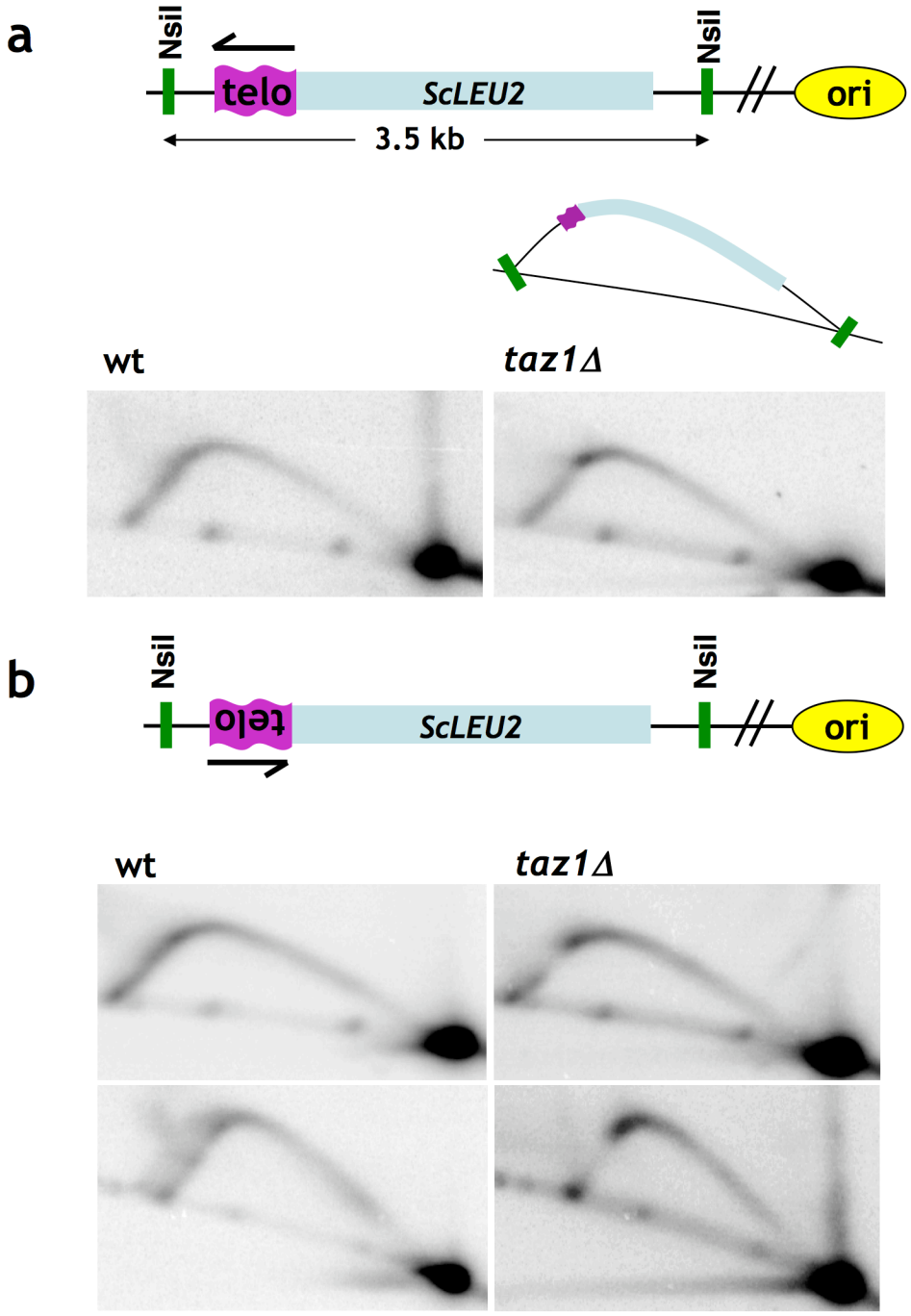

Figure 4.1 Taz1 is required for efficient replication through internally placed telomere tracts

Maps show the genomic region of Chr III containing an ectopically inserted telomere tract. The ARS3002-4 cluster (ori) is located ~8 kb centromeric to *ura4* and has been shown to replicate this locus (Dubey et al., 1994). The telomere tract is 2.5 kb from the ori-proximal end of the 3.5 kb *Nsi*I fragment. In each illustration, the purple wavy line represents the location of the telomeric stretch, and the light-blue curve represents the position of *ScLEU2*. **a**, telomeric constructs were placed in the same orientation relative to the direction of replication as wt telomeres (G-strand replicated by lagging strand synthesis). *Nsi*I-digested DNA was subjected to 2DGE and hybridized with *ScLEU2* probe. (Same gel appears in Figure 3.4a, and is shown here for comparison). **b,** Synthetic telomere constructs of 200 (top) and 450 (bottom) bp were inserted at the *ura4* locus as in **a** but in the opposite orientation, with the 3' end of the telomeric G-strand oriented towards ori.

4.2.2 Fork stalling in the absence of Taz1 is independent of orientation

As mentioned above, natural telomeres are oriented such that the G-rich telomeric strand always serves as the template for lagging-strand synthesis, and the internal telomere sequence used in Chapter 3 and Figure 4.1a shares this polarity. To determine whether the telomeric replication fork pausing seen in the absence of Taz1 is linked specifically to lagging-strand replication of the G-rich strand, we oriented the internal telomere stretch in reverse to natural telomeres, such that the G-rich strand is copied by leading-strand replication (Figure 4.1b). Deletion of *taz1*$^{+}$ from this strain again resulted in the accumulation of stalled replication forks in the telomeric stretch. Therefore, Taz1 is required for efficient replication of telomeric repeats regardless of their orientation with respect to the direction of replication.

Assuming that similar determinants for fork-stalling exist at internal and natural telomeres, the result described above suggests that it is not the specific exposure of the G-rich strand during lagging strand replication that causes fork stalling. Thus, if one assumes that WRN assists telomere semi-conservative replication by acting on G-quartets in the exposed ssDNA of the lagging strand, this orientation independent stalling would argue against a common mechanism underlying *taz1*Δ-fork-stalling and WRN-associated STL. Consistent with this notion, we did not observe an effect of Rqh1 inactivation on telomeric stalling (data not shown, and see also Chapter 5). However, until the molecular cause for stalling is delineated, and the relevant *in vivo* substrate for WRN is identified, a possible connection between the two phenomena cannot be ruled out.

4.3 Repetitive nature of telomeres causes stalling in the absence of Taz1

4.3.1 Other repetitive sequence also stall replication forks

In order to address the sequence requirement for replication fork stalling we created synthetic sequences, inserted them into the chromosome and analyzed their replication using 2DGE. As these sequences depart from the telomeric consensus sequence, they are not predicted to bind Taz1, and

therefore their replication is unlikely to be affected by Taz1 absence. The synthetic telomeres used in Chapter 3 were created by ligating 49bp oligonucleotides duplex ending with a non-palindromic overhang to allow directional ligation ('synthetic-telo', Figure 4.2a). These tandem arrays were then cloned, and integrated into chromosome III at the *ura4*$^{+}$ locus with an adjacent *ScLEU2* gene. Arrays composed of 49bp repeats of telomeric sequences exhibited similar properties to cloned telomeres – both allowed smooth replication in the presence of Taz1, and stalled replication forks in its absence (Figure 4.2b and Chapter 3).

The same method was then employed to create two other kinds of sequences (Figure 4.2a). The first kept the stretches of guanines, but scrambled the other nucleotides, keeping the overall nucleotide composition and strand bias ('G-forming'). This sequence is expected to no longer bind Taz1 (or any other sequence specific binding protein), but still has the propensity to fold into G-quartets. The second sequence includes a scrambled telomeric sequence ('scrambled'). This sequence is not predicted to bind any sequence specific factors or to fold into G-quartets. However, this sequence still retains the GC-richness and the strand bias of telomeres. Importantly, both sequences, while not containing the typical ~7-11bp telomeric repeats, include 6-8 49bp repeats that were used for their construction.

Surprisingly, when analyzed using 2DGE, both sequences caused stalling, regardless of their polarity (Figure 4.2b and data not shown). The 2DGE patterns resembled the stalling caused by telomeric sequences, but, as expected, were independent of Taz1 absence. Assuming that these sequences cause stalling by a similar mechanism to the one causing telomeric stalling, this result argues against several possibilities outlined above. As the 'scrambled' sequence lacks the propensity to fold into G-quartets, they are an unlikely cause of the stalling. Moreover, as both sequences lack any sequence similarity to telomeres, this result argues against a sequence specific factor as the reason for stalling. Two remaining possibilities are the base composition and the repetitive nature of the sequence.

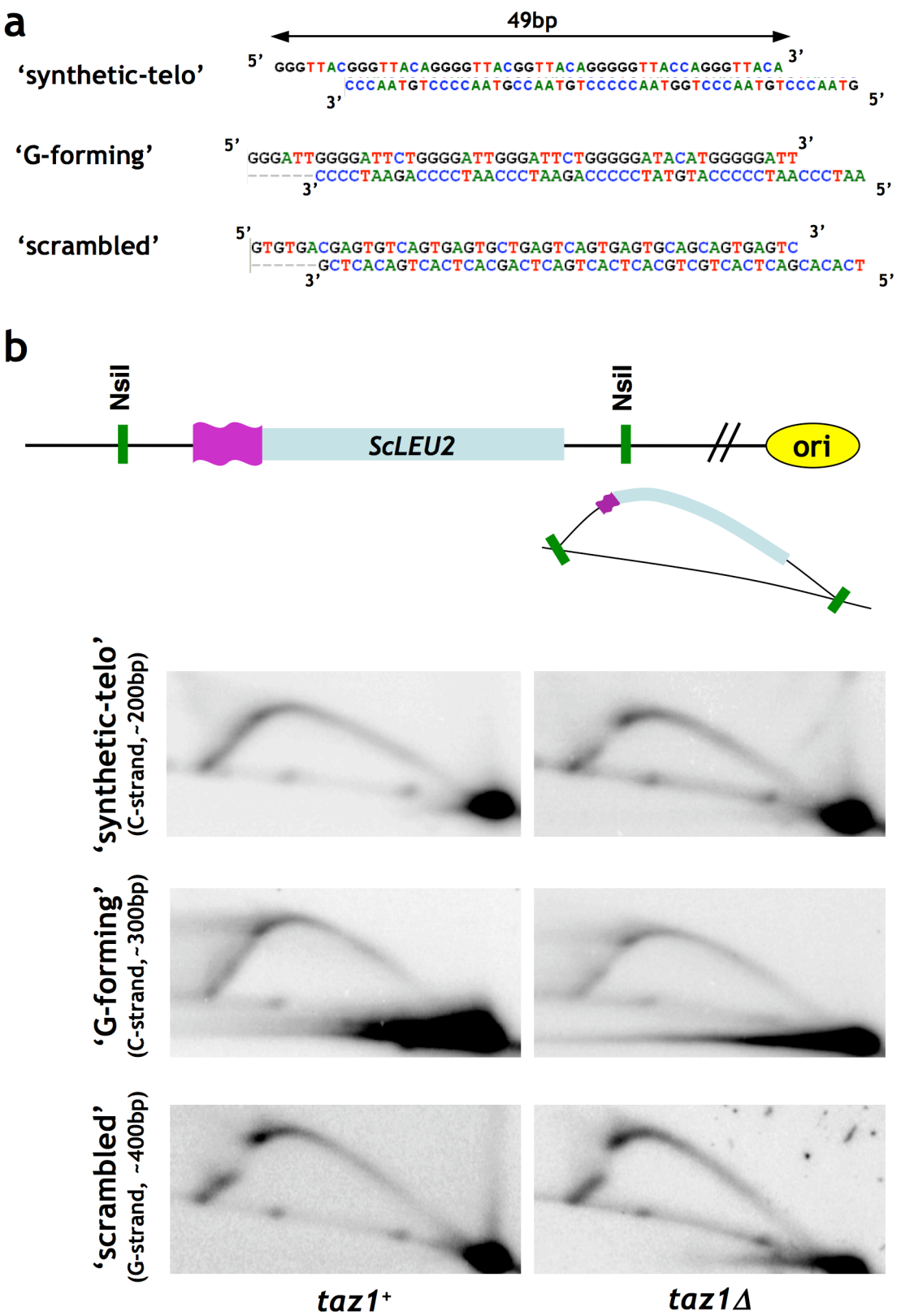
a
49bp
'synthetic-telo'
5' GGGTTACGGGTTACAGGGGTTACGGTTACAGGGGGTTACCAGGGTTACA 3'
3' CCCAATGTCCCCAATGCCAATGTCCCCCCAATGGTCCCAATGTCCCAATG 5'
'G-forming'
5' GGGATTGGGGATTCTGGGGATTGGGATTCTGGGGGGATACATGGGGGATT 3'
3' CCCCTAAGACCCCTAACCCTAAGACCCCCTATGTACCCCCTAACCCTAA 5'
'scrambled'
5' GTGTGACGAGTGTCAGTGAGTGCTGAGTCAGTGAGTGCAGCAGTGAGTC 3'
3' GCTCACAGTCACTCACGACTCAGTCACTCACGTCGTCACTCAGCACACT 5'
b
NsiI
NsiI
ScLEU2
ori
'synthetic-telo'
(C-strand,~200bp)
'G-forming'
(C-strand,~300bp)
'scrambled'
(G-strand, ~400bp)
taz1+
taz1Δ

Figure 4.2 Scrambled arrays also stall replication forks

(previous page) **a,** The different sequences used to construct repeated arrays. **b**, (top) Maps show the genomic region of Chr III containing an ectopically inserted arrays (see legend in Figure 4.1). (bottom) *NsiI*-digested DNA was subjected to 2DGE and hybridized with *ScLEU2* probe. Telomeric tract causes stalling only in the absence of Taz1. Non-telomeric arrays cause stalling in the presence and absence of Taz1. 'Synthetic-telo' images are identical to the ones in Figure 4.1b, and are included for comparison).

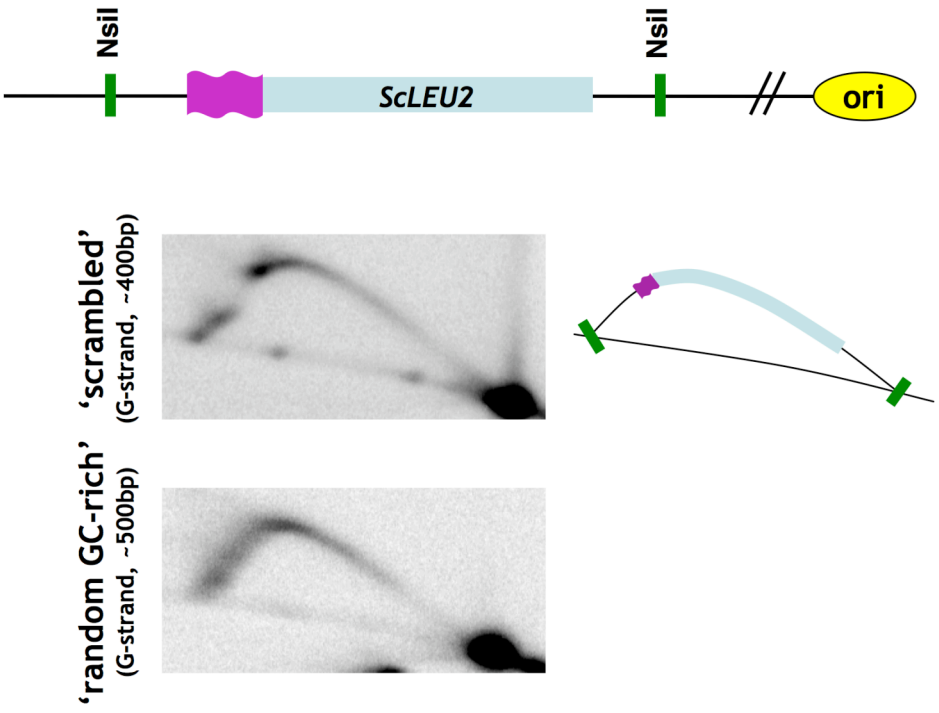

Figure 4.3 GC-rich sequences do not stall replication forks

(top) Map showing the genomic region of Chr III containing an ectopically inserted arrays (see legend in Figure 2.1). The purple swivel designates the inserts. (bottom) *NsiI*-digested DNA was subjected to 2DGE and hybridized with a *ScLEU2* probe. 'G-forming' repetitive array causes stalling, while non-repetitive array of the same base composition does not cause stalling.

4.3.2 GC-rich sequences do not cause stalling

Two kinds of sequences were constructed to address the role of the base composition in fork stalling. First, a tandem array of scrambled sequences was created where the GC-richness was reduced to 48% (genome-wide GC content is 36%). This sequence caused stalling, which was, as before, independent of Taz1 absence (data not shown). This sequence had a substantially lower GC-richness compared with the original sequences used (section 4.3.1), thus arguing against GC-base composition as a reason for stalling. However, in order to rule out GC-base composition as a cause for stalling using this strategy, repeated sequences with GC content closer to 36% would have to be tested.

In a separate experiment, a non-repetitive 500bp sequence was constructed, with similar GC-richness to fission yeast telomeres (55%, 'random GC-rich'; see Chapter 2 for construction details). This sequence did not exhibit stalling (Figure 4.3). Taken together, these results point to the repetitive nature of telomeres as the underlying reason for replication fork stalling, and suggest that any repetitive sequence would cause stalling. It remains to be tested what is the minimum repeat number that would elicit stalling, and to what extent stalling depends on the length of the repeated unit: so far we observed stalling for exact 49bp repeats, and also at telomeres composed of degenerate ~7-11bp repeats.

4.3.3 Implications for telomere replication, Taz1 function at replication forks and genome stability

Our finding that any repetitive sequences can result in replication fork stalling may hint at the mechanism of Taz1 activity at telomeres. It argues against a mechanism involving exclusion of other telomere binding factors since stalling is not sequence specific, and was observed using a wide array of constructs. However, it does not rule out exclusion of a yet unknown 'repeats' binding factor, capable of recognizing, binding and stalling any repeated region in the genome. Such a mechanism may be involving or related to RNAi, which uses processed transcribed RNA to affect chromatin of homologous sequences,

but is not sequence specific. Under this scenario, Taz1 prevents stalling by excluding such a factor from telomeres.

Our results also argue against a mechanism involving G-quartets. This of course, does not argue against G-quartet existence *in vivo* or address their function during telomere replication. Our results also argue against a mechanism involving the telomeric ssDNA complex (Pot1/Tpz1/Ccq1/Poz1), as its localization to telomeres is sequence specific, and it is not likely to be recruited to the non-telomeric repeated sequences used here. However, as before, it is possible that stalling involves interactions between ssDNA exposed during replication (or the telomeric 3' overhang) and the homologous repeats that precede the replication fork: the exposed ssDNA undergoing lagging strand replication would anneal to the template of the leading strand. Such interactions would be caused by repeats, but are sequence independent, and would generate bias toward one of the strands when the lesion is processed, thus accounting for the mammalian data regarding WRN and $TRF^{\Delta B}$. Under this model, the function of Taz1 would be to prevent such interactions at telomeres, perhaps by protecting the telomeric dsDNA repeats from invasion by exposed ssDNA.

Expansion of repeats in the human genome causes a variety of disorders, many of which could be genetically anticipated by a phenotypically silent prior expansion of naturally occurring repeats (reviewed in Pearson et al., 2005). While the most abundant and well-studied repeats are trinucleutide repeats (TNRs), longer repeats, up to several kbp long, have also been reported and were associated with disease. The mechanism of repeat expansion is not completely clear, but there is evidence for the involvement DNA replication and DNA repair processes. Some of the specific mechanisms suggested include slippage of the polymerase during replication or formation of secondary structures of exposed ssDNA. Lagging-strand-specific exposed ssDNA may also be involved: some TNRs cause replication fork-stalling in a length- and orientation-dependent manner, leading to the hypothesis that strand-specific secondary structures formed by certain sequences may cause fork-stalling. However, to our knowledge, extensive analysis of replication patterns of non-TNR repeats was not performed. In addition, while we cannot rule out

secondary structures formed by the sequences we used here, the fact that stalling was observed in various sequences argues against a highly specific secondary structure that causes stalling.

Our results suggest that any repetitive region of the genome may pose a barrier to replication. These regions are abundant even in the relatively streamlined fission yeast genome, and much more so in mammalian genomes. In fission yeast, for example, it would be intriguing to examine the sequences at the centromeric region. It is also tempting to speculate that these sequences are associated with functional homologues of Taz1 – DNA binding proteins whose function is to relieve stalling. Interestingly, a common feature of repetitive regions is their heterochromatic nature. Telomeric chromatin in fission yeast, in addition to displaying many hallmarks of 'classic' heterochromatin (i.e. specific histone modifications and repression of transcription), are also composed of a structure distinct from canonical nucleosome arrays, which is disrupted in the absence of Taz1 (JPC, unpublished observations). It remains to be tested whether the synthetic repeats introduced in this chapter affect the local chromatin structure. Genetic analysis of mutants involved in heterochromatin did not reveal obvious telomeric phenotypes apart from an effect on TPE, suggesting that they cannot solely account for the stalling; however, the contribution of heterochromatin and telomeric chromatin to fork stalling has not been directly tested.

4.4 Analysis of stalling using alternative constructs

During the course of our work, we tried to construct controls for non-telomeric, non-repetitive sequences inserted into the genome in the same locus and using the same construct as the abovementioned sequences. However, when we inserted a non-telomeric coding sequence ('null') or no sequence at all into the *ura4::ScLEU2* construct, we observed mild stalling (Figure 4.4). This stalling was distinct from the telomeric or repetitive stalling, both in its extent and its pattern; unlike 'repetitive stalling', the pattern conferred by these alternative sequences lacked the empty region of the arc that appears following the accumulation of hybridization signal (compare to 'synthetic-telo' or 'G-forming' stalling, top). Importantly, this mild stalling was independent of the

presence of Taz1. Although the reason for this stalling is currently unclear, it is likely caused by a sequence located upstream of the inserts relative to the direction of replication (i.e. inside *ScLEU2*), as the 'spot' moved up when a short, unrelated sequence was inserted (compare 'null' to no insert, Figure 4.4). It is also unclear what prevented this '*ScLEU2'* stalling in *taz1*$^{+}$ cells with a telomeric insert (Figure 4.4, *taz1*$^{+}$ 'synthetic-telo', and see also Chapter 3). Our preliminary attempts to observe stalling in constructs lacking *ScLEU2* confirmed that the source of the unspecific stalling lies within *ScLEU2*, and have so far recapitulated the results obtained with the abovementioned constructs (data not shown).

Figure 4.4 Minor stalling at the *ura4::ScLEU2* construct regardless of the insert

(next page) (top) Map showing the genomic region of Chr III containing ectopically inserted arrays (see legend in Figure 2.1). Presumed point of stalling denoted by red asterisk. (bottom) *Nsi*I-digested DNA was subjected to 2DGE and hybridized with *ScLEU2* probe. Stalling caused by the telomeric tract and by the 'G-forming' array shown for comparison. Mild stalling is apparent with no insert, and with insert of a short cloned sequence. Stalling is independent of Taz1 absence.

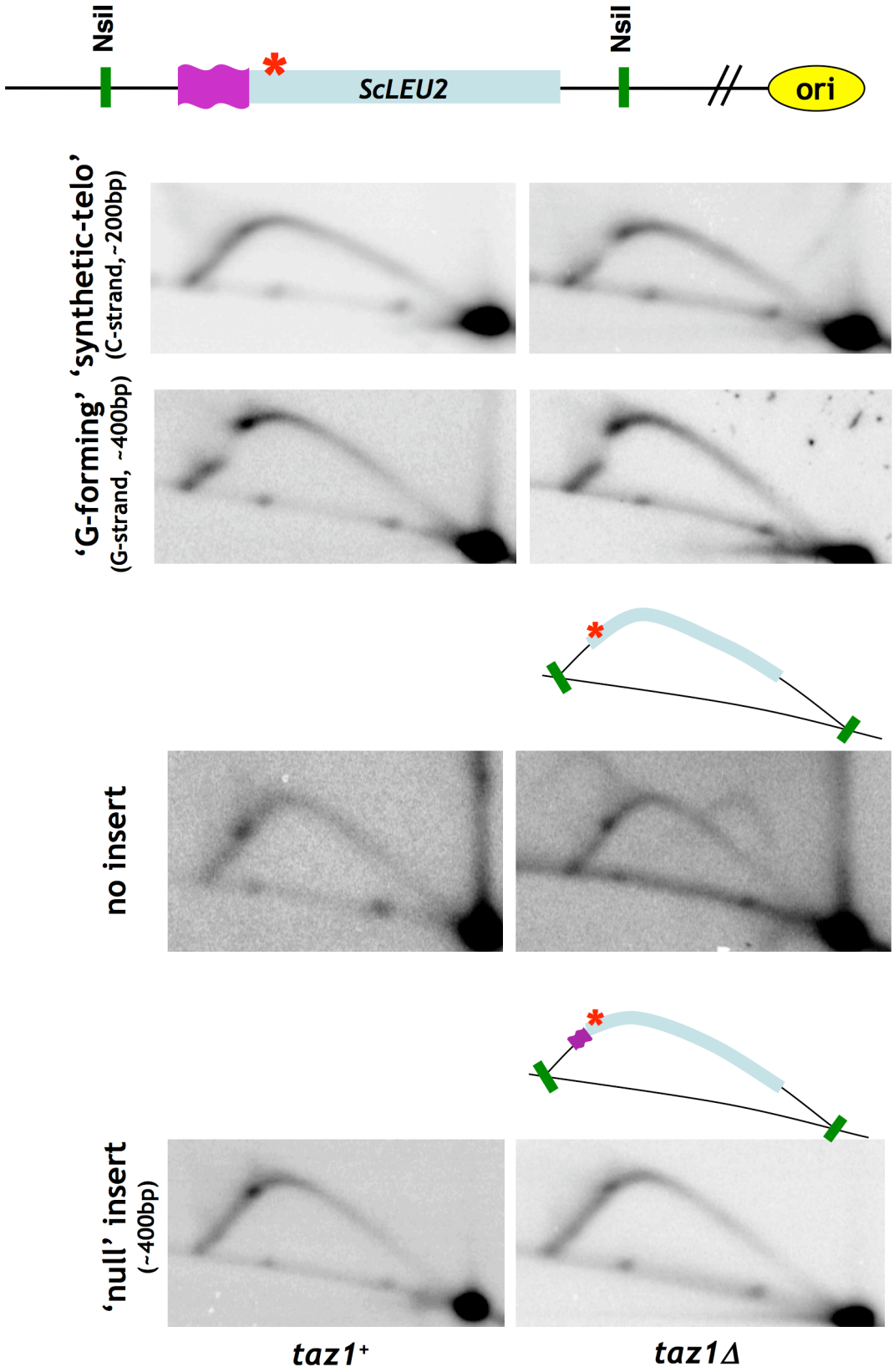
NsiI
NsiI
ScLEU2
ori
'G-forming' 'synthetic-telo'
(G-strand, ~400bp) (C-strand, ~200bp)
no insert
'null' insert
(~400bp)
taz1+
taz1Δ

4.5 Taz1 occupancy at telomeres regulates replication fork stalling

4.5.1 *rap1*Δ cells exhibit an intermediate telomeric stalling phenotype

As shown in Chapter 3, *rap1*Δ cells exhibited dramatically different telomeric fork-stalling phenotypes compared with *taz1*Δ cells. This was exemplified in the improved migration patterns of telomere replication (Figure 3.2), in the suppression of stalling in the telomere/subtelomere border (Miller et al., 2006), and in the gradual telomere loss in the absence of telomerase (Figures 3.5 and 3.6). Importantly, however, while *rap1*Δ cells did resemble wt cells, substantial differences were still observed. Replication patterns of telomeres were still slightly different from those expected of long 'wt' telomeres (see Chapter 3). Furthermore, telomere loss in the absence of telomerase was still accelerated compared with wt cells. This was suggested by the difference in the amount of loss in the 1st (~3kb) *versus* the 2nd and 3rd restreaks (<500bp) (Figure 3.5). In addition, *rap1*Δ cells senesce after similar number of divisions following loss of the telomerase compared with wt cells, despite starting with telomeres that are more than 10-fold longer (data not shown). Finally, we did observe fork stalling at an internally placed telomeric sequence in cells lacking Rap1 (KM Miller and JPC, unpublished observations, and see below).

A hypothesis that may explain these observations is that Taz1 occupancy at telomeres is a decisive factor in determining the extent of stalling, and that in *rap1*Δ cells the very long telomeres titrate Taz1 and lower its occupancy, thus resulting in a mild stalling phenotype. This model also provides an explanation for the pattern of telomere loss in *rap1*Δ *trt1*Δ cells: initially Taz1 level is limiting, and thus telomeres are lost at a fast rate, resembling *taz1*Δ *trt1*Δ cells; however, as telomeres get shorter Taz1 occupancy increases, and so the loss rate resembles that of the wt. We were thus interested in testing this hypothesis by examining the effects of Taz1 overexpression in *rap1*Δ background.

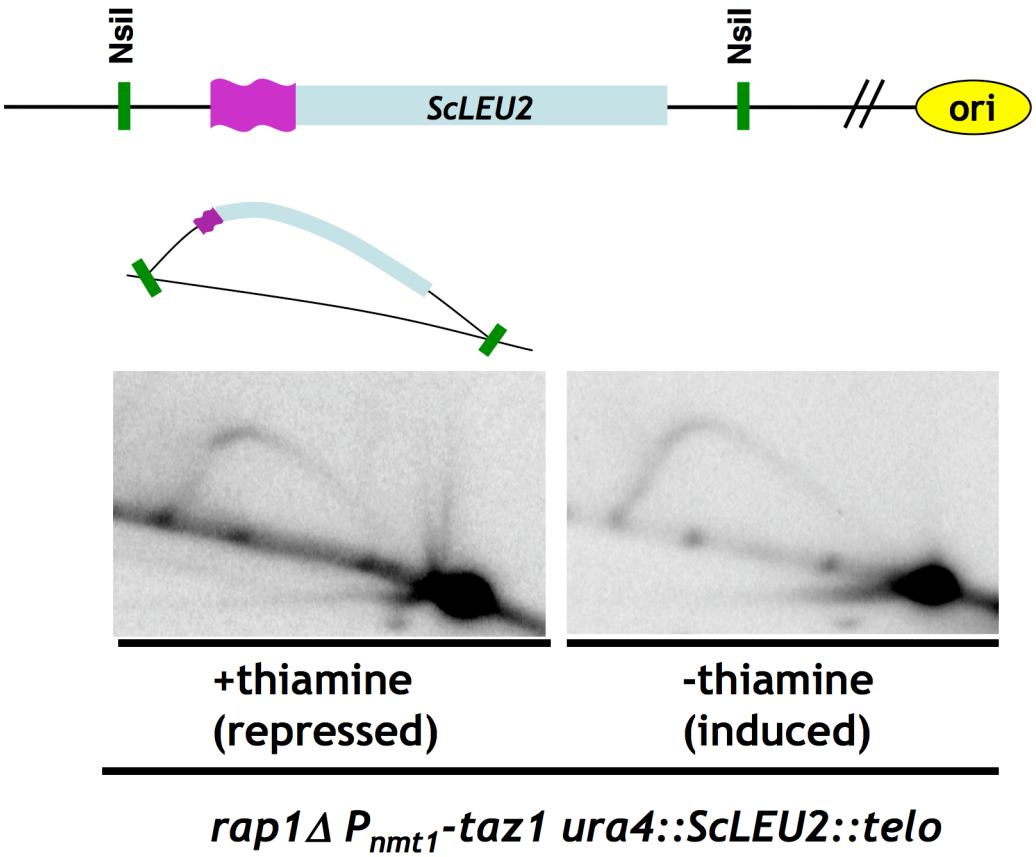

Figure 4.5 Taz1 overexpression suppresses fork-stalling at internal telomeric sequences in *rap1*Δ cells

(top) Map showing genomic region of Chr III containing an ectopically inserted telomeric tract (purple swivel). (bottom) *Nsi*I digested genomic DNA from cells grown in minimal media in the presence or absence of thiamine was subjected to 2DGE and probed with a *ScLEU2* probe. Stalling is not observed in the absence of thiamine when Taz1 is overexpressed.

4.5.2 *rap1*Δ fork-stalling at internal sequences is rescued by overexpression of *taz1*$^+$

We constructed strains where *taz1*$^+$ was placed under the control of the inducible *nmt1*$^+$ promoter (P_{nmt1}, later named '*taz1-OE*'). While stalling was observed when cells were grown in media containing thiamine (repressed promoter), replication proceeded smoothly when *taz1*$^+$ was overexpressed (absence of thiamine) (Figure 4.5). This result supports our hypothesis that

Taz1 occupancy is a decisive factor in the stalling caused by telomeric sequences, and confirms our previous conclusion that Taz1 is sufficient to prevent stalling at telomeric sequences in a manner that is independent of Rap1.

4.5.3 *taz1*$^{+}$ overexpression suppresses many *rap1*Δ phenotypes

While using the abovementioned construct we noticed that, unexpectedly, overexpression of Taz1 dramatically shortens *rap1*Δ telomeres (Figure 4.6a). Similar shortening was also observed when *taz1*$^{+}$ expression was driven by the weaker P_{nmt41} promoter (Figure 4.6a), or the even weaker P_{nmt81} promoter placed on a multicopy pREP episome (pREP81-taz1) (Figure 4.6b). In all cases, telomere shortening was dependent on the absence of thiamine.

A possible mechanism to explain these results involves a competition between Rap1 and Rif1 for Taz1 binding, postulating that a major function of Rap1 is to prevent Rif1 from binding to Taz1. In the absence of Rap1, Rif1 is aberrantly recruited to telomeres, but when Taz1 is overexpressed it titrates out Rif1. However, Rif1 was not essential for this suppression (data not shown), arguing against such a mechanism.

Telomere shortening and lengthening occurred rapidly: the bulk of the telomeres was lost or gained within 20 generations of Taz1 expression or repression, respectively (this includes ~5 generations necessary to induce P_{nmt1} after withdrawal of thiamine) (Figure 4.6c). The rapid lengthening is in line with our observations suggesting telomerase is capable of synthesizing a large fraction of the *taz1*Δ telomere in a single cell cycle (Chapter 3); the rapid shortening suggests that constant loss of telomeres, resembling the *taz1*Δ situation, occurs to a certain extent also at long *rap1*Δ telomeres. These results suggest that Taz1, at least when overexpressed, is capable of exerting negative regulation on telomerase independently of Rap1.

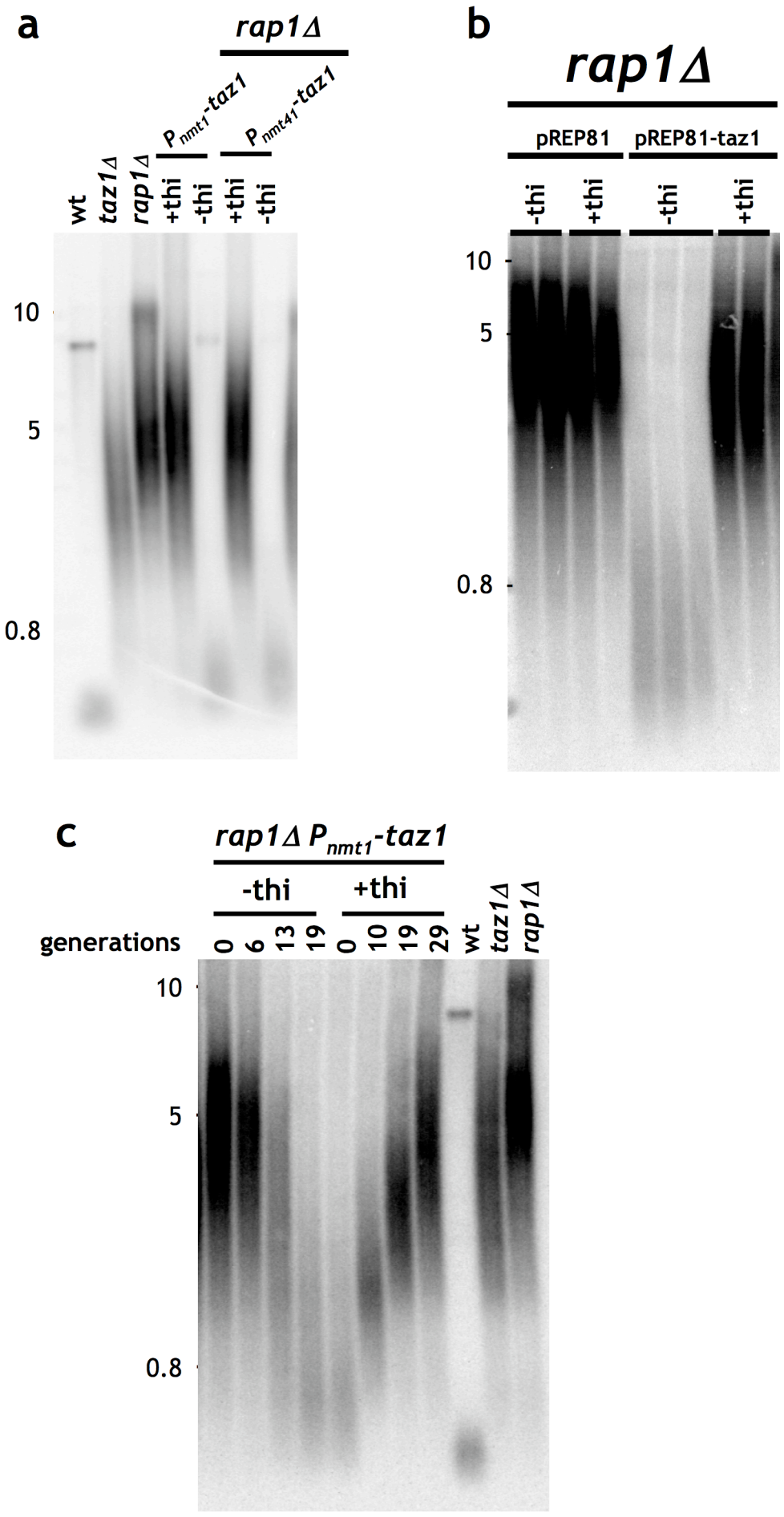
a
rap1Δ
P nmt1-taz1
P nmt41-taz1
wt
taz1Δ
rap1Δ
+thi
-thi
+thi
-thi
10
5
0.8
b
rap1Δ
pREP81
pREP81-taz1
-thi
+thi
-thi
+thi
10
5
0.8
c
rap1Δ P nmt1-taz1
-thi
+thi
generations
0
6
13
19
0
10
19
29
wt
taz1Δ
rap1Δ
10
5
0.8

Figure 4.6 Taz1 overexpression suppresses telomere elongation in *rap1*Δ cells

(previous page) Southern Blot analysis of *Apa*I digested genomic DNA probed with a telomeric probe. Wt, *taz1*Δ and *rap1*Δ samples are shown for comparison. **a**, Taz1 overexpression, driven by P_{nmt1} or the weaker P_{nmt41}, shortens telomeres in a *rap1*Δ background. Cells were grown for at least one restreak in the appropriate media (lacking or containing thiamine) before DNA was extracted. **b**, Taz1 overexpression, driven from the multi-copy episome pREP81, also shortens *rap1*Δ telomeres. Cells were grown for at least one restreak in the appropriate media (lacking or containing thiamine) before DNA was extracted. **c**, Dynamics of telomere length after addition or withdrawal of thiamine. Cells were grown in media lacking thiamine for at least 3 days prior to shifting to a media containing thiamine, and *vice versa*. Number of cell divisions was estimated based on average generation time.

Figure 4.7 Taz1 overexpression suppresses telomere NHEJ defect but not telomere clustering in *rap1*Δ cells

(next page) **a**, *Not*I digested genomic DNA prepared in agarose plugs was subjected to PFGE and blotted with and 'LMIC' probe. 'log', logarithmically growing cells (mostly in G2); '-N', cells arrested in media lacking nitrogen (mostly in G1). Telomere fusions are apparent in G1 arrested *rap1*Δ cell and *rap1*Δ cells where Taz1 expression is repressed, but not in G1 arrested *rap1*Δ cells where Taz1 is overexpressed. **b**, h^{90} *rap1*Δ cells overexpressing Taz1 underwent meiosis and were observed under fluorescent microscope, to reveal that telomeres are not clustered at the SPB. Cells expressed C-terminally tagged Pot1-GFP (localized at telomeres) and Sid4-mRFP (an SPB component).

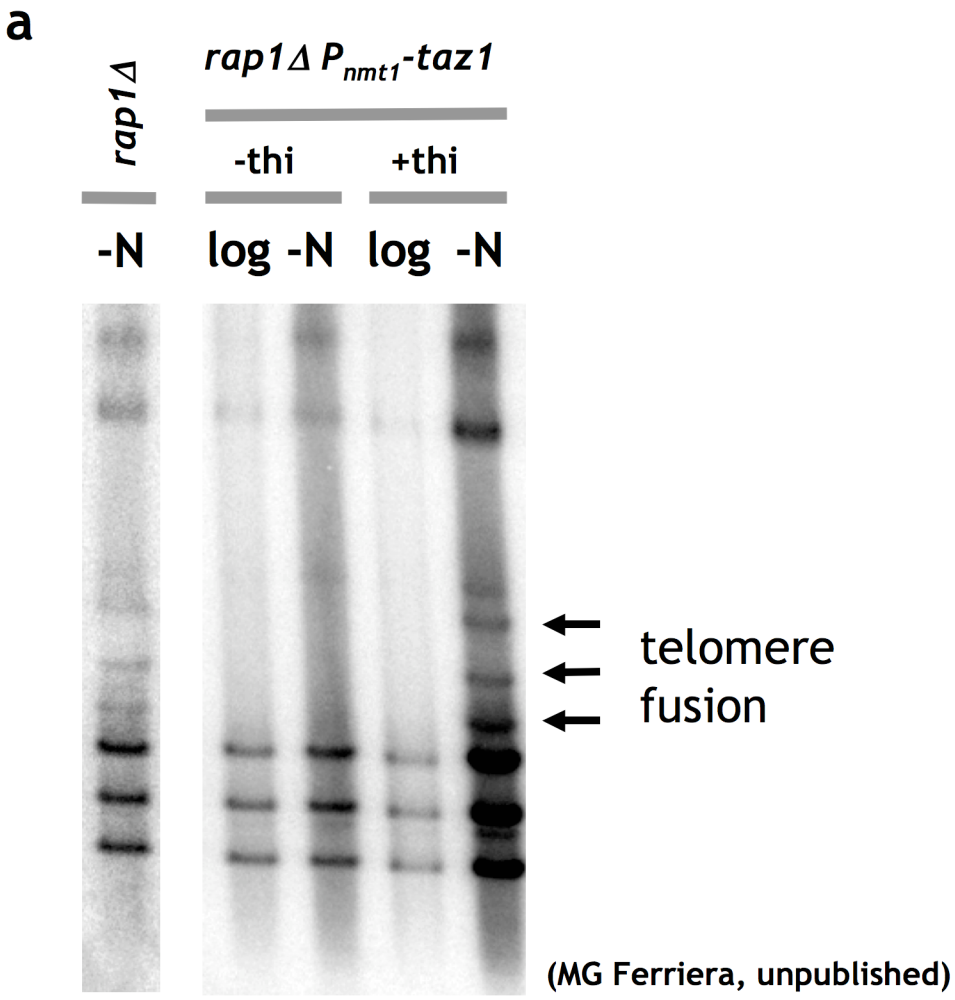
a
rap1Δ
rap1Δ Pnmt1-taz1
-thi
+thi
-N
log -N
log -N
telomere
fusion
(MG Ferriera, unpublished)

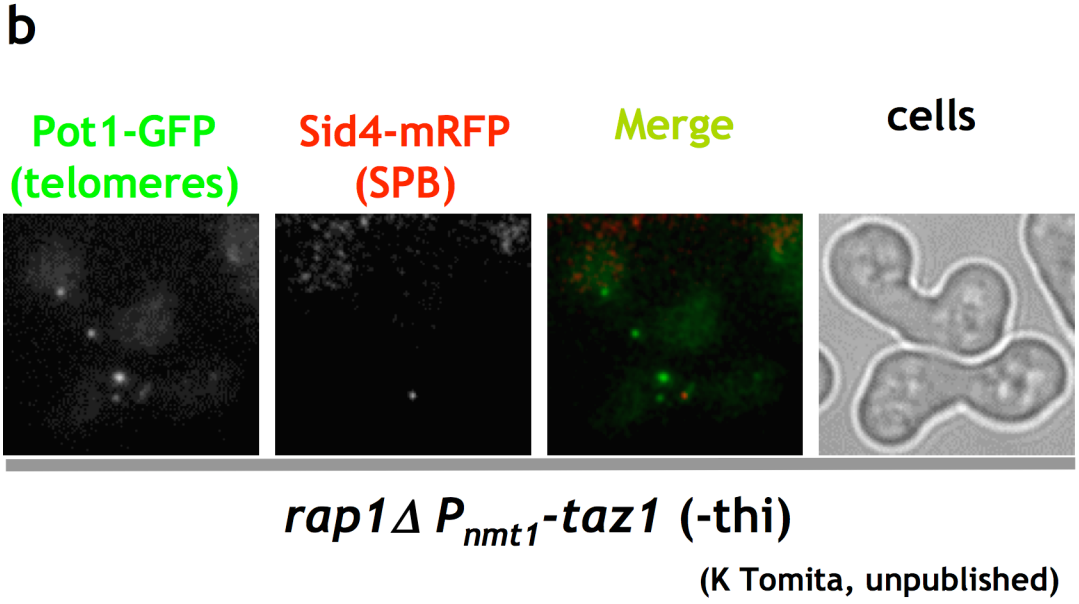
b
Pot1-GFP
(telomeres)
Sid4-mRFP
(SPB)
Merge
cells
rap1Δ Pnmt1-taz1 (-thi)
(K Tomita, unpublished)

Next, we examined several other hallmarks of telomere dysfunction shared between *taz1*Δ and *rap1*Δ cells. *taz1*Δ and *rap1*Δ cells, once arrested in G1 phase of the cell cycle (e.g. during nitrogen starvation), exhibit telomere end-to-end fusions due to elevated non-homologous end-joining (NHEJ) (Ferreira and Cooper, 2001; Miller et al., 2005). These fusion bands are readily observed using *Not*I-digested PFGE, probed for the terminal fragments of chromosomes I and II ('LMIC' probe). Fusion bands were observed in G1 arrested *rap1*Δ cells, and in G1 arrested *rap1*Δ P_{nmt1}-*taz1* cells grown with thiamine. However, no fusions were visible when *rap1*Δ P_{nmt1}-*taz1* cells were grown without thiamine (MG Ferreira, Figure 4.7a). Thus, when overexpressed, Taz1 can protect telomeres from NHEJ, obviating the need to recruit Rap1.

Finally, we examined the ability of overexpressed Taz1 to suppress the meiotic defect of bouquet deficient cells. In *taz1*Δ, *rap1*Δ and *bqt1/2*Δ cells, telomeres fail to cluster at the spindle pole-body (SPB) during meiotic prophase, resulting in SPB and spindle defects, and consequently failed chromosome segregation (Tomita and Cooper, 2007). The recruitment of the telomeres to the SPB is thought to be mediated by a series of interactions: telomeres→Taz1→Rap1→Bqt1/2→Sad1→SPB (Chikashige et al., 2006). Overexpression of Taz1 in the absence of Rap1 failed to suppress the defect in meiotic telomere clustering; telomeric foci do not co-localize with the SPB (K. Tomita, Figure 4.7b). The inability of Taz1 overexpression to compensate for Rap1 absence supports a role for specific protein-protein interactions between Rap1 and Bqt1/2 that mediate clustering. In addition, it supports other data suggesting that the meiotic defect is separate from the cause of telomere length de-regulation and de-protection from NHEJ - namely, that *bqt1/2*Δ cells exhibit a meiotic defect but no other discernable telomeric defects (Chikashige et al., 2006; Tomita and Cooper, 2007). It remains to be tested whether other hallmarks of telomere dysfunction common to *rap1*Δ and *taz1*Δ cells can be suppressed by Taz1 overexpression; mainly, de-repression of TPE and extensive, deregulated 3' overhang.

4.5.4 Dynamics of telomere addition

Our data demonstrate non-linear dynamics for telomere loss in *rap1*Δ *trt1*Δ cells: initially a fast rate of telomere loss, followed presumably by increased Taz1 occupancy and thus a slower loss rate. It is conceivable that the reverse process could be observed as well. Closely following the dynamics of cells recently deleted for *rap1*$^{+}$ may reveal two stages of telomere lengthening: initial slow telomere lengthening that is followed by rapid lengthening ('run-away' telomeres), until a steady-state length is achieved.

First, we attempted to characterize the dynamics of *taz1*Δ spores that were generated from heterozygous diploids harbouring short telomeres (*taz1*$^{+/\Delta}$). Spores were germinated *en masse* while selecting for *taz1*$^{+}$ deletion. No elongation of telomeres was observed during the first 2-3 cell divisions (8hr) (data not shown); *taz1*Δ telomeres were, however, completely elongated within ~19 generations, with most lengthening during divisions 4-14 (Figure 4.8a). This result suggests that fission yeast telomerase is capable of synthesizing ~10% of *taz1*Δ telomeres in each cell cycle (i.e. ~300bp, the length of wt telomeres). This may be an underestimate, as the elongating *taz1*Δ telomeres are likely to undergo constant breakage and loss events. The ability of telomerase to synthesize a large fraction of the telomere in each cell cycle is consistent with our analysis of the immediate telomere loss in *taz1*Δ *trt1*Δ spores (Figures 3.5 and 3.6), suggesting telomerase synthesizes a large fraction of *taz1*Δ telomeres in each cell cycle.

When we compared *taz1*Δ and *rap1*Δ spores generated in a similar way, we noticed that *rap1*Δ spores, while reaching a longer steady-state length (Figure 4.8b), took longer to reach that state. The initial rate of telomere lengthening was slower in *rap1*Δ *versus taz1*Δ cells (e.g. compare the 5 generations time-point), consistent with a role for Taz1 levels in regulating telomerase activity. However, extensive experiments would be required to verify the significance of this result, and to allow better resolution that would enable exact measurement of telomere length dynamics.

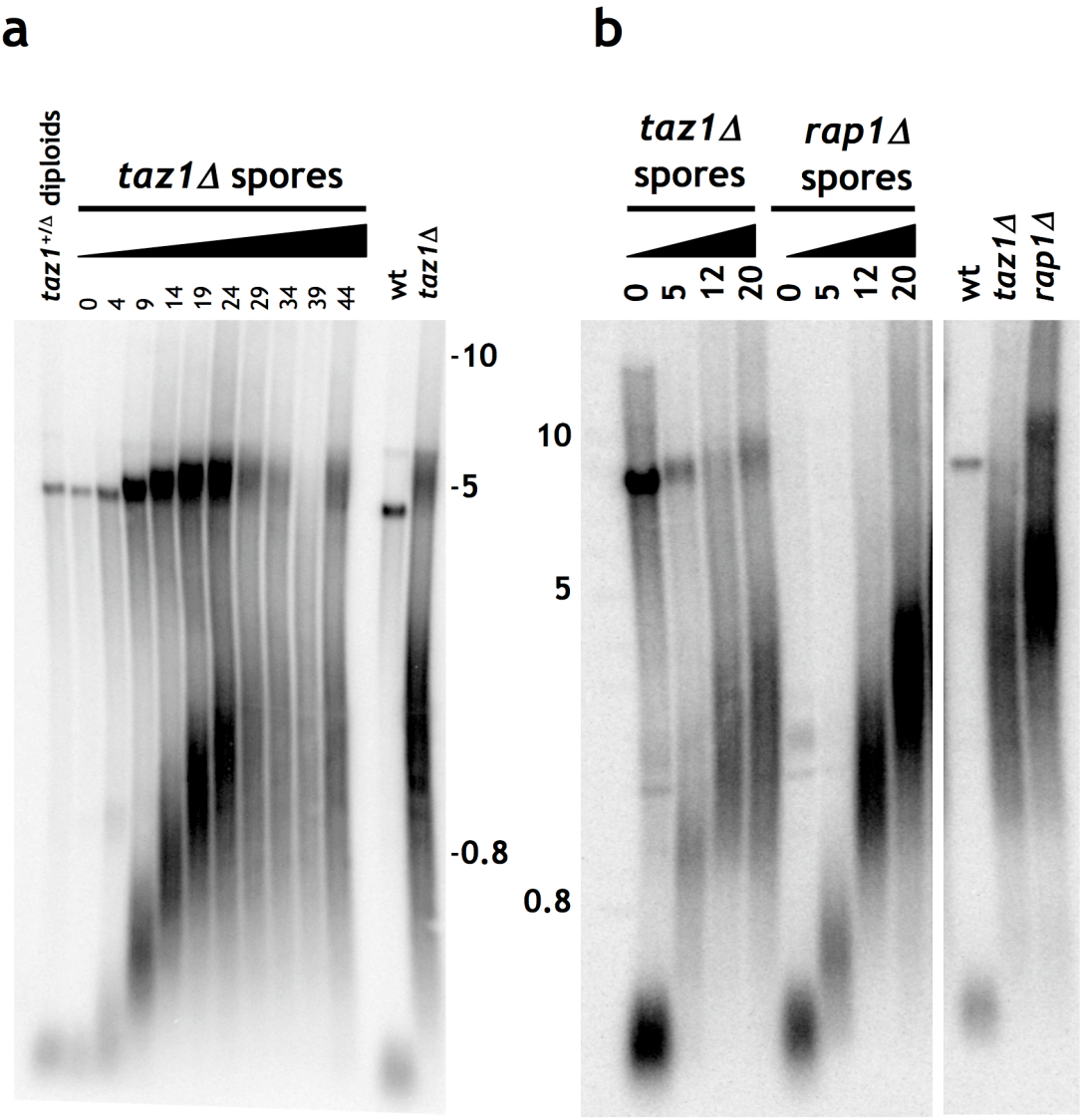

Figure 4.8 Dynamics of telomere addition in cells lacking *taz1*$^{+}$ or *rap1*$^{+}$

Southern Blot analysis of *Apa*I digested genomic DNA probed with a telomere probe. Number of cell divisions was estimated based on average generation time. Wt, *taz1*Δ and *rap1*Δ samples are shown for comparison. **a**, Spores from *taz1*$^{+/\Delta}$ diploids (harbouring short telomeres) were grown in media selecting for *taz1*Δ spores. Majority of *taz1*Δ telomere length was gained between division 4 and 14. **b**, Spores from *taz1*$^{+/\Delta}$ and *rap1*$^{+/\Delta}$ diploids (harbouring short telomeres) were grown in media selecting for *taz1*Δ and *rap1*Δ spores, respectively. Telomeres are gained at a faster rate in *taz1*Δ *versus rap1*Δ spores.

In wt budding yeast cells, telomerase only adds telomeric sequences to 7% of telomeres in one cell cycle, with average addition of 44bp, amounting to ~1% of a wt telomere per cell cycle (Teixeira et al., 2004). This is compared with our observed rates of ~100% of a wt telomere length per telomere per cell cycle in *taz1*Δ cells. Telomere length regulation is thought to act through *in cis* regulation of the susceptibility of each telomere to elongation by telomerase (Marcand et al., 1999; Teixeira et al., 2004). However, in most organisms, telomerase levels were found to be limiting - interfering with telomerase RNA or protein levels substantially affects telomere length (Armanios et al., 2005; Cristofari and Lingner, 2006; Hathcock et al., 2002; Mozdy and Cech, 2006). Assuming telomerase levels are limiting in fission yeast as well, it remains to be explained how can telomerase activity be increased ~100 fold in cells that recently lost Taz1. In other words, even if all *taz1*Δ telomeres are susceptible to elongation in each cell cycle, it is expected that limiting telomerase levels would prevent such a rapid telomere elongation. Furthermore, even extension of all telomeres by the average addition observed in budding yeast (44bp) would not account for the observed telomere lengthening. To reconcile these observations, we hypothesize that Taz1's role in telomere length regulation extends beyond limiting the telomeres' accessibility to elongation. Such additional regulation could be exerted through modulation of telomerase processivity (Chang et al., 2007) or by limiting the cell cycle phase in which telomerase can act (Marcand et al., 2000).

4.5.5 Roles of Taz1 and Rap1 in preventing telomere dysfunction

Early genetic data favoured a model where Rap1 is the major effector of the telomeric dsDNA complex, placing it at the heart of many telomeric functions. Several specific protein-protein interactions supported these genetic data. The interaction of Rap1 with Bqt1/2 recruits telomeres to the SPB in meiosis (Chikashige et al., 2006), and an interaction of Rap1 with Poz1, a component of the telomeric ssDNA/Pot1 complex, was suggested to regulate telomere length by conveying the 'sum' of the so-called 'counting-mechanism' to telomerase's substrate – the telomeric overhang (Miyoshi et al., 2008). Interactors of Rap1 that contribute to regulation of 5' degradation and to protection from NHEJ are still unidentified.

Several mechanisms may explain our observation that Rap1 and Taz1, which lack any significant homology beyond the DNA binding Myb domains (itself non-functional in Rap1), are interchangeable for several telomeric functions. It is possible that Rap1 is required for a modification that enhances Taz1's functionality – a requirement that is bypassed by Taz1 overexpression. Alternatively, it is possible that Taz1 and Rap1 cooperatively bind a third protein that acts as effector of various telomeric functions.

Finally, it is conceivable that Rap1's function is limited to telomere length regulation and meiotic telomere clustering, while other telomeric functions are actually carried out by Taz1. This model predicts that Rap1 has a role in regulating telomere lengths that are roughly similar to wt telomeres. Loss of Rap1 would lead to telomerase de-regulation, but not 'general' telomere dysfunction. Telomerase dysfunction, leading to further telomere lengthening (see below), is thus a result of Taz1 titration (Figure 4.9). It is still unknown what is the minimum occupancy of Taz1 at telomeres needed to prevent telomere dysfunction. In addition, it remains unexplained why telomeres in *rap1*Δ *taz1-OE* cells are very close in size to wt telomeres – our model would predict *rap1*Δ *taz1-OE* telomeres to be substantially longer than wt telomeres due to the inactivation of the 'counting mechanism'. *rap1*Δ *taz1-OE* telomeres are much shorter than *rif1*Δ telomeres, for example, and in the scenario of *rif1*Δ telomeres, Taz1 is yet to be titrated out. However, complex genetic interactions may reconcile these observations: for example, Rif1 may promote telomere dysfunction, consistent with the suppression of the cold-sensitivity of *taz1*Δ cells by *rif1*$^{+}$ deletion (Miller et al., 2005).

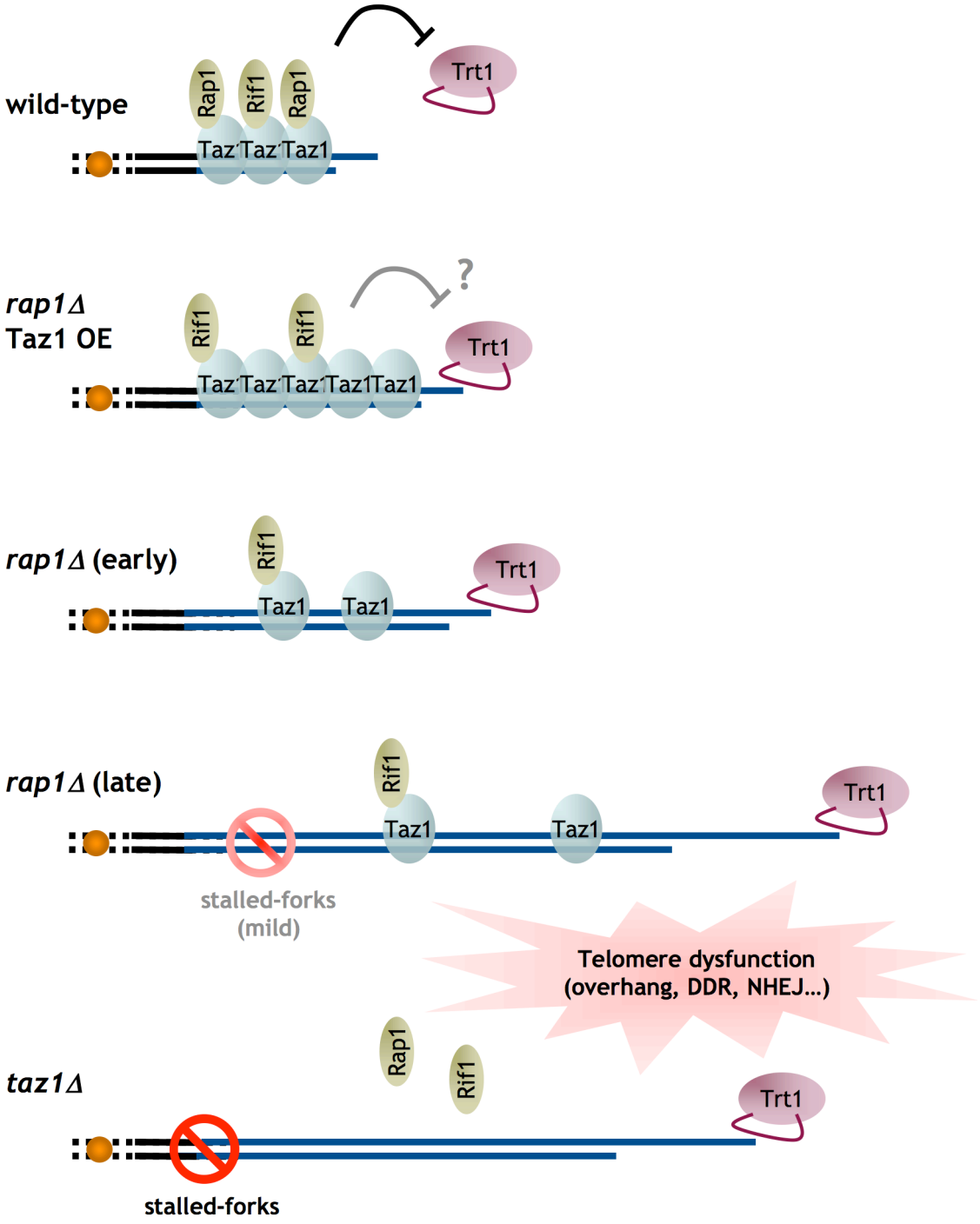

Figure 4.9 Model for the interplay between Taz1 and Rap1 at telomeres

See text for details. Blue lines mark the telomeric dsDNA and ssDNA overhang, and the small orange circle designates the centromere. Taz1 is light blue, Rap1 and Rif1 are colored olive. Telomerase (its catalytic subunit Trt1) and telomerase RNA (*ter1*) are colored in magenta. Red stop sign denotes stalled telomeric replication forks.

Our work suggests that while Rap1 may contribute to telomere length regulation and protection from NHEJ *in vivo*, these functions may be carried out by Taz1. This may hint that the molecular mechanism underlying these activities does not involve specific protein-protein interactions, but rather a common lesion that is prevented by Taz1. Taking into account Taz1's functions in the prevention of telomeric fork-stalling, telomere breakage and loss in the absence of telomerase, and telomeric hyper-recombination, a possible common lesion becomes evident. Stalled replication forks at telomeres may account for many of the DNA repair related phenotypes, and may also provide excellent substrates for telomerase, accounting for the de-regulated telomere length.

Conceivably, stalled telomeric replication forks could represent a key trigger for elements of the DDR at telomeres, and may even constitute the essential difference between 'critically short' and 'not critically short' telomeres. Stalled forks are interesting candidate triggers for telomere DDR for several reasons. Unlike DSBs, stalled forks can elicit DNA repair processes without activation of checkpoint-mediated cell cycle arrest, thus mimicking a property of both dysfunctional telomeres and unperturbed telomeres during the transient ATM activation that occurs in each cell cycle (Verdun et al., 2005). Second, the role for Taz1 in promoting fork progression could provide a component of a 'counting mechanism' – once telomere attrition confers sufficient loss of Taz1 binding sites, fork stalling may commence and trigger telomerase activity (Miller et al., 2006). Third, the hyperrecombination that results from stalled forks represents a feasible initiating stimulus for ALT, which again would allow telomere elongation following telomere repeat attrition/telomere protein attrition. Indeed, telomerase-null mouse cells are more likely to engage in ALT when they lack WRN, and therefore experience perturbed telomere replication (Laud et al., 2005). Finally, close analysis of apoptosis in telomerase-null mice shows that passage through S-phase is required for eroding telomeres to trigger cell death (Rajaraman et al., 2007). Consistent with this notion, replication of telomeres, as assayed by BrdU incorporation, indeed correlates with presence of DDR factors at telomeres (Verdun and Karlseder, 2006).

4.6 Future Work

Our finding that any repetitive sequence causes replication fork stalling opens up an opportunity to directly study the function of Taz1 in relieving stalling. An array could be created that includes the recognition sequence of a well-characterized DNA binding factor (such as ScGal4 or LacI). Our data predicts an array of such sequences would cause stalling. Next, we can ask whether ectopically recruiting Taz1, or parts of it, to the site of stalling is capable of relieving it. Of course, it is conceivable that no chimeric protein would be functional in repressing stalling, or that stalling would be affected by the expression of the transcription factor itself. Nonetheless, establishing such a system would open up a window into molecular dissection of Taz1 function in promoting semi-conservative replication. Our system of detecting stalling at telomeric and non-telomeric sequences may also be used to determine the genetic determinants of this stalling. For example, whether stalling is affected by the activity of certain helicases or by factors that modulate chromatin (e.g. the RNAi pathway).

Our work following the effects of Taz1 overexpression could be continued in several ways. First, we should extend our analysis of *rap1Δ taz1-OE* cells to examine other hallmarks of telomere dysfunction. These include relief of silencing of a telomeric marker (TPE), existence of large amount of overhang throughout the cell cycle, and loss of telomeric chromatin structure (which is lost in *taz1*Δ cells [JPC, unpublished observations]). Differential regulation of one of these pathways may indicate that different mechanisms or interacting factors are involved. In addition, quantitative methods could be used to confirm that overexpressing Taz1 indeed affects Taz1 protein levels, and that *rap1*$^{+}$ deletion does not affect Taz1 levels. Quantitative ChIP may be utilized to directly assess Taz1 occupancy at telomeric sequences, and confirms it is indeed influenced by *taz1*$^{+}$ expression levels.

A related question that may shed light on the mechanism of Taz1 and Rap1 function is the interplay between the telomeric dsDNA complex (Taz1, Rap1 and Rif1) and the telomeric ssDNA complex (Pot1, Tpz1, Ccq1 and Poz1). In both human cells and fission yeast, the ssDNA-binding complex was also found to localize to the dsDNA part of the telomere and to internally placed

telomeric sequences, presumably through protein-protein interactions (Loayza and De Lange, 2003; Miyoshi et al., 2008). Poz1, which interacts with Rap1 but not with Taz1, was postulated to provide a link between the two complexes. The elongated telomeres of *poz1*Δ cells (which are epistatic with *taz1*$^{+}$ and *rap1*$^{+}$ deletions) support the notion of a functional interaction (Miyoshi et al., 2008). However, our results with Taz1 overexpression suggest that either this interaction is not essential, or that additional interactions exist. Measuring the relative amount of the ssDNA complex at telomeres and at internally placed telomeric sequences may provide an answer to these questions. In addition, it is intriguing to ask whether the long telomeres observed in *poz1*Δ cells are indeed related to the long telomeres of *rap1*Δ cells, and whether likewise they can be suppressed by Taz1 overexpression.

5 Chapter 5: Sumoylation of the Fission Yeast RecQ Helicase Regulates Telomere Dysfunction

5.1 Introduction

5.1.1 RecQ helicases

Mutations in the human RecQ homolog WRN cause premature aging accompanied by genome instability and high incidence of cancer. The WRN phenotypes are caused, at least in part, by telomere loss, as they are rescued by expression of telomerase (Chang et al., 2004; Crabbe et al., 2007; Wyllie et al., 2000). In yeast, loss of RecQ function results in a cornucopia of phenotypes relating to DNA replication, damage sensing and repair, chromosome segregation, and maintenance of the repetitive DNA regions (reviewed in Mankouri and Hickson, 2004; Sharma et al., 2006). The large variation in null phenotype suggests that RecQ homologs act at multiple steps of replication and recombination, but the precise molecular activities that underlie these phenotypes have not been delineated.

RecQ helicases are ATP-dependent DNA helicases, translocating 3'->5' along an ssDNA strand (Karow et al., 1997). While perfect duplex dsDNA is a poor substrate for RecQ helicases, forked structures with either ss- or dsDNA branches are unwound with high efficiency (Mohaghegh et al., 2001). Some of the intermediates in DNA replication and repair that were found to be good substrates *in vitro* include synthetic replication forks, where RecQ helicases were found to unwind the duplex in the direction of replication; 'flap' structures that are generated during Okazaki fragment maturation; and D-loops (displacement loops), where an ssDNA partially anneals to one strand of DNA and displaces the other strand (Brosh et al., 2002). Finally, while typical helicases unwind B-form DNA, RecQ helicases are unique in their ability to also unwind other forms of DNA, including triple-helices and G-quadruplexes (Brosh et al., 2001; Sun et al., 1998). These activities were indeed mapped to the conserved RQC domain (Figure 5.4a), which is distinctive to RecQ helicases (Huber et al., 2006).

Several other biochemical activities reported for RecQ helicases include strand annealing of complementary ssDNA molecules (Machwe et al., 2005), branch migration of Holliday junctions (HJ) (Constantinou et al., 2000; Karow et al., 2000), dismantling of Rad51 filaments from ssDNA (Bugreev et al., 2007; Hu et al., 2007) and, through a conserved complex with Top3 (TopIIIα) and Rmi1 (BLAP75), dissolution of topological linkage between DNA strands (Ira et al., 2003; Wu et al., 2006a; Wu and Hickson, 2003). An important regulator of RecQ helicases is the ssDNA binding protein RPA (replication protein A), which can greatly facilitate the unwinding activity of RecQ helicases, both through binding to the ssDNA product and through direct stimulation of the helicase activity (Shen et al., 1998). Conversely, RPA plays an inhibitory role in the regulation of the strand-annealing activity of RecQ helicases (Garcia et al., 2004). Finally, RecQ helicases play multiple roles in the DNA replication checkpoint - the cellular response to replication stress. These roles include helicase-dependent roles in stabilization of stalled replication forks and allowing replication restart (Frei and Gasser, 2000), as well as helicase-independent roles in mediating the checkpoint response (Bjergbaek et al., 2005).

Even this partial list of the various activities RecQ helicases play in DNA metabolism demonstrates how RecQ helicases can affect DNA replication and repair in multiple, and occasionally opposing, ways. While not required for bulk DNA replication, RecQ helicases are likely to play a role in fork progression through certain regions of the genome, and in response to and recovery from replication stress. In addition, mutations in RecQ helicases usually confer a defect in HR together with higher levels of 'illegitimate' recombination, leading researchers to unravel several pathways by which RecQ helicases can suppress recombination. Some of the ways by which RecQ activity would prevent recombination are (1) suppression of replication fork collapse through stabilisation of fork components and prevention of fork-regression, (2) prevention of crossing-over by dissolution of recombination and replication intermediates, (3) dismantling of Rad51 filaments and D-loops, both of which are early intermediates in HR, and (4) unwinding of stable non-B-form DNA thus removing potential obstacles to DNA replication. However, RecQ helicases could also bring about pro-recombinogenic outcomes. Several such activities

may be promotion of strand annealing and facilitation of D-loop extension by DNA polymerase. In addition, it was recently reported that in budding yeast Sgs1, together with the nucleases Exo1 and Dna2, facilitate much of the 5'-end resection occurring around a DSB, thus promoting HR (Mimitou and Symington, 2008; Zhu et al., 2008).

5.1.2 SUMO

Sumoylation is a conserved multi-step process, which, like ubiquitylation, utilizes specialized E1-activating, E2-conjugating and E3-ligase factors to create an iso-peptide bond between SUMO (the **s**mall **u**biquitin-like **mo**difier; fission yeast Pmt3) and a lysine on a target protein (Geiss-Friedlander and Melchior, 2007). Ulp1 and Ulp2 are specialized iso-peptidases that de-conjugate SUMO from target proteins (Geiss-Friedlander and Melchior, 2007; Kosoy et al., 2007; Taylor et al., 2002). While many proteins have been shown to be sumoylated *in vitro* or *in vivo*, the function of sumoylation is well understood only in a handful of cases. The general rule that has emerged is that SUMO modifies protein function by altering cellular localization or protein-protein interactions (Geiss-Friedlander and Melchior, 2007).

5.1.3 Telomere entanglements

Fission yeast cells lacking Taz1 grow indistinguishably from wild-type cells at optimal growing temperatures; however, in cells grown at cold temperatures (19°-20°), *taz1Δ* telomeres fail to separate properly during mitosis, causing DNA breaks, chromosome missegregation and loss of viability (Miller and Cooper, 2003) (See also Chapter 1). Several lines of evidence suggest that the entanglement of *taz1Δ* telomeres stems from stalled replication forks. First, the promotion of fork movement through telomeres, the prevention of immediate telomere loss upon *trt1*$^{+}$ deletion, and the prevention of telomere entanglements at cold temperatures are Taz1-specfic functions not shared by other components of the telomeric complex, such as the Taz1-interacting factor Rap1. This contrasts with the shared roles of Taz1 and Rap1 in controlling telomerase, telomeric NHEJ-mediated fusions, 3' overhang formation and other telomeric events (Chikashige and Hiraoka, 2001; Kanoh and Ishikawa, 2001; Miller et al.,

2005; Miller et al., 2006). Furthermore, cell-cycle analysis has shown that the originating defect causing telomere entanglements occurs in S-phase (Miller and Cooper, 2003). Hence, our data suggest that stalled telomeric replication forks result in aberrant associations between *taz1Δ* telomeres that cannot be resolved at cold temperatures.

In order to understand the nature and genesis of telomeric entanglements, we set out to uncover factors involved in instigating or resolving them. Here we show that the entanglement, breakage and loss of *taz1Δ* telomeres are promoted by the activity of the fission yeast RecQ helicase Rqh1. These observations implicate Rqh1 activity in the aberrant processing of stalled telomeric replication forks. In addition, analysis of a novel SUMO-deficient allele indicates that sumoylation promotes Rqh1 activity at dysfunctional telomeres.

5.2 Results

5.2.1 Screening for suppressors of *taz1*Δ cold sensitivity

With the aim of understanding the mechanism underlying entanglement of *taz1Δ* telomeres at cold temperatures, we carried out a screen for high-copy suppressors of *taz1Δ* cold sensitivity. A *taz1Δ rap1Δ* strain, which is more cold sensitive than *taz1Δ* (Miller et al., 2005), was transformed with an *S. pombe* cDNA library where expression is driven by the inducible *nmt1*$^+$ promoter and *ura4*$^+$ is used for selection (Fersht et al., 2007). Identification of suppressors of cold sensitivity was attempted using three methods (Figure 5.1a):

I. Following transformation, cells were plated on selective media, and incubated at 32° until colonies appeared. Single transformants were patched onto new selective plates, grown for ~16hr at 32° and then replica-plated and incubated at 19°. ~3,000 clones were screened using this method, isolating two clones. An example of a plate with a positive candidate is shown in Figure 5.1b.

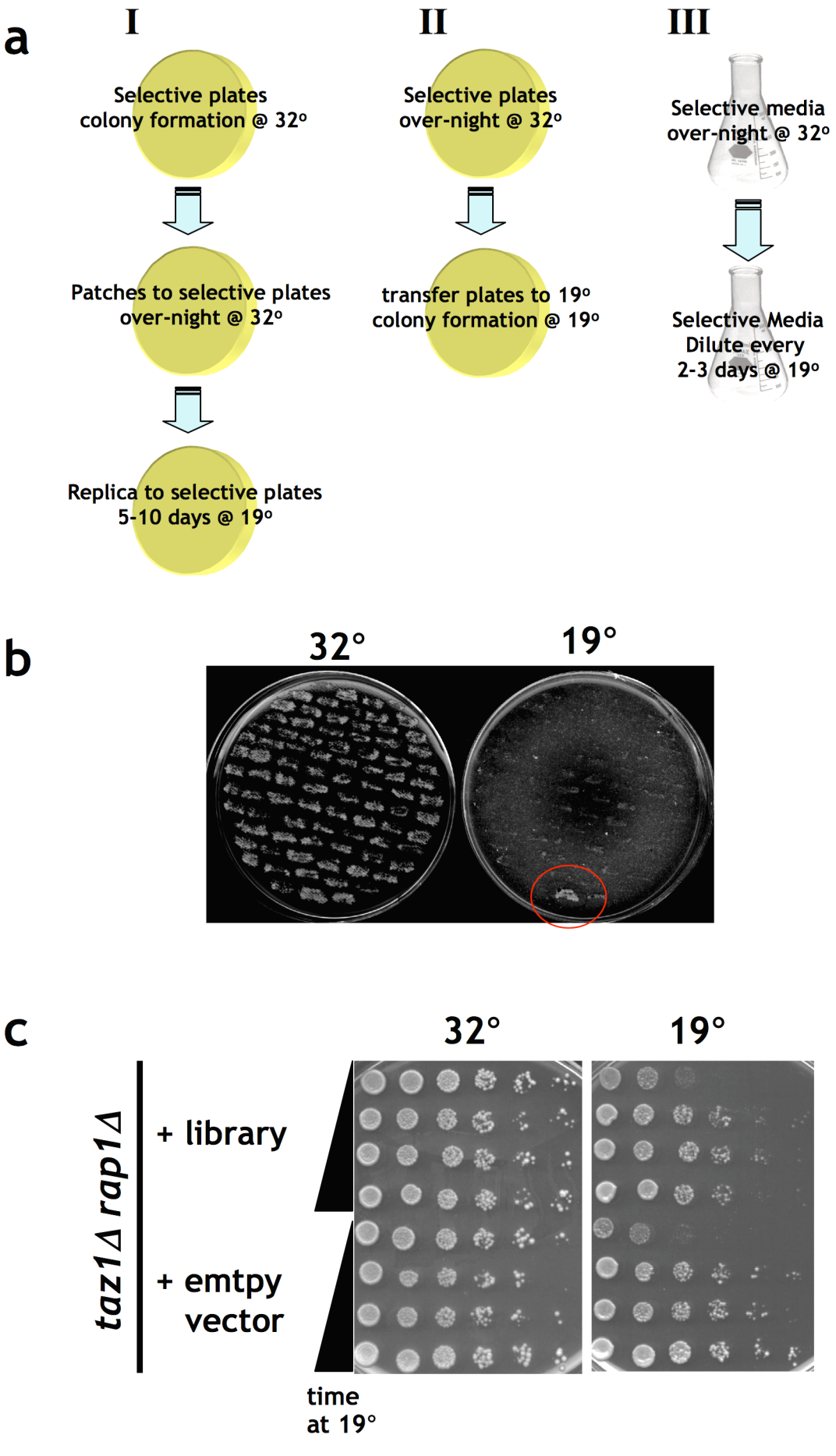
a
I
Selective plates
colony formation @ 32°
Patches to selective plates
over-night @ 32°
Replica to selective plates
5-10 days @ 19°
II
Selective plates
over-night @ 32°
transfer plates to 19°
colony formation @ 19°
III
Selective media
over-night @ 32°
Selective Media
Dilute every
2-3 days @ 19°
b
32°
19°
c
32°
19°
taz1Δ rap1Δ
+ library
+ emtpy
vector
time
at 19°

Figure 5.1 Screening for suppressors of *taz1*Δ *rap1*Δ cold-sensitivity

(previous page) (a) Three strategies used to isolate suppressors of *taz1*Δ *rap1*Δ cold-sensitivity (see text for details). (b) Sample plate from strategy I. Patches were replica-plated onto selective medium (EMM lacking uracil), and were incubated at 32° or 19°. Red circle, candidate positive clone. (c) Strategy III failed to enrich for positive clones. Five-fold serial dilutions of log-phase *taz1Δ rap1Δ* cultures that were transformed with an empty vector or with a cDNA library. Following transformation and recovery, cultures were grown at 19° to enrich for fast-growing clones. In each time point, cells were spotted onto selective medium (EMM lacking uracil), and were incubated at 32° or 19°.

II. Immediately following transformation, cells were plated onto selective media. Plates were incubated for ~16hr at 32° allowing for the transformants to recover, and were then transferred to 19°. Clones that grew faster at 19° were picked. Parallel transformations with an empty plasmid and with a plasmid containing *taz1*$^{+}$ were carried out as controls, and demonstrated that an increased growth could be readily observed when complementing a *taz1*$^{+}$ deletion (data not shown). ~25,000 clones were screened, isolating 5 clones. While this method allows for easier screening of more clones compared with method I, many more of the clones that are initially picked are 'false-positive'. Most false-positives fail to exhibit a growth advantage at 19° when re-tested using a dilution assay. In addition, many clones exhibit improved growth at 19° even after loss of the plasmid on 5-FOA media, suggesting they harbour extragenic suppressors unrelated to the plasmid (data not shown; see also method III).

III. In order to assist screening, we attempted to enrich for positive clones using competitive growth in liquid media. Immediately following transformation, cells were diluted into selective liquid media and grown for ~16hr at 32° to allow for recovery and selection for the plasmids. The cells were then transferred to 19°, and continuously diluted every 2-3 days to maintain competitive growing conditions. Parallel transformation with an empty plasmid was carried out as a control. When samples were examined using a dilution assay,

increased growth was apparent when comparing the cells immediately following transfer to 19° and cells in the 2nd time-point (Figure 5.1c). However, this improved growth was not dependent on the library and was observed also with the empty vector (Figure 5.1c), suggesting that extragenic suppressors are easily obtained, and rendering enrichment for positive clones ineffective.

The seven verified clones harboured plasmids with the following inserts: *taz1*$^+$ (twice), *ulp1*$^+$ (4 times) and *cdc10*$^+$ (once). Suppression was not dependent on the presence or absence of thiamine, although induction did cause general reduction in viability in a manner that was independent of *taz1*$^+$ deletion (data not shown). All three suppressors also suppress the cold sensitivity of a *taz1Δ* single mutant (Figure 5.2a). Integrating the strong *nmt1*$^+$ promoter upstream of endogenous *ulp1*$^+$ or *cdc10*$^+$ also suppressed the cold sensitivity of *taz1Δ* strains (data not shown), demonstrating that suppression does not depend on the plasmids themselves.

Cdc10 (*ScSWI6*) is a transcription factor that controls transcription of a number of S-phase specific genes including *ulp1*$^+$ (Rustici et al., 2004). However, the direct experiment checking whether *ulp1*$^+$ is required for the suppression conferred by *cdc10*$^+$ is not possible, since *ulp1*$^+$ deletion is already epistatic with *taz1*$^+$ deletion (see below). Nonetheless, the suppressions conferred by *ulp1*$^+$ and *cdc10*$^+$ overexpression share the same genetic requirements: suppression by *cdc10*$^+$ requires SUMO, and suppression by either *ulp1*$^+$ or *cdc10*$^+$ requires Rqh1 (Figure 5.3b and data not shown). Thus, we speculate that *cdc10*$^+$ overexpression alleviates *taz1Δ* cold sensitivity by increasing *ulp1*$^+$ expression.

5.2.2 SUMO pathway modulates *taz1Δ* cold-sensitivity

Ulp1 is a SUMO-specific iso-peptidase that removes SUMO from target proteins. It also acts in the SUMO maturation process, in which the C-terminus of the nascent SUMO peptide is truncated to expose the conserved glycine that participates in iso-peptide bond formation (Li and Hochstrasser, 1999). To determine which Ulp1 function, SUMO maturation or SUMO de-conjugation, underlies suppression by *ulp1*$^+$ overexpression, we utilized a strain carrying a

truncated allele of SUMO (*pmt3.GG*) that confers no overt growth defects, but obviates the need for processing of nascent SUMO by Ulp1 (Taylor et al., 2002). This strain was rendered cold sensitive by *taz1*$^{+}$ deletion (Figure 5.2b), suggesting that the relevant activity of Ulp1 for suppression of cold sensitivity is not SUMO processing, but rather SUMO de-conjugation.

In order to verify that the suppression achieved by *ulp1*$^{+}$ overexpression is not an artifact caused by protein overexpression but rather a consequence of *bona fide* modulation of the SUMO pathway, we investigated genetic interactions between components of the SUMO pathway and *taz1*$^{+}$. *ulp1Δ* cells are moderately sick at all temperatures, despite harbouring the *pmt3.GG* truncation that improves their viability (Taylor et al., 2002). However, *taz1*$^{+}$ deletion confers no further loss of viability in the cold; hence, *ulp1*$^{+}$ deletion is epistatic with *taz1Δ* cold sensitivity (Figure 5.2b). Furthermore, deletion of the gene encoding the second fission yeast SUMO de-conjugating enzyme, Ulp2, also suppressed the cold-specific loss of viability of *taz1Δ* cells (Figure 5.2b). The seemingly paradoxical observation that both deletion and overexpression of *ulp1*$^{+}$ have similar effects is not without precedent in the SUMO field (Palancade et al., 2007). As free SUMO may be limiting in the cell, the absence of Ulp1 may result in reduced SUMO availability, thus mimicking *ulp1*$^{+}$ overexpression; indeed, deletion of either *ulp1*$^{+}$ or *ulp2*$^{+}$ reduces the overall level of sumoylated proteins in the cell (data not shown). Alternatively, some processes may require switches between sumoylated and desumoylated states. In either case, our results unambiguously implicate the balance of protein sumoylation in the survival of *taz1Δ* cells at cold temperatures.

SUMO has previously been implicated in fission yeast telomere length regulation. In the absence of either SUMO or the SUMO E3-ligase Pli1 (orthologous to budding yeast *SIZ1/2*), telomeres are elongated (Tanaka et al., 1999; Xhemalce et al., 2004). However, *pli1*$^{+}$ deletion fails to suppress *taz1Δ* cold sensitivity (Figure 5.16a and Xhemalce et al., 2007), suggesting that sumoylation regulates different processes/proteins in the case of telomere length regulation *versus taz1Δ* cold sensitivity.

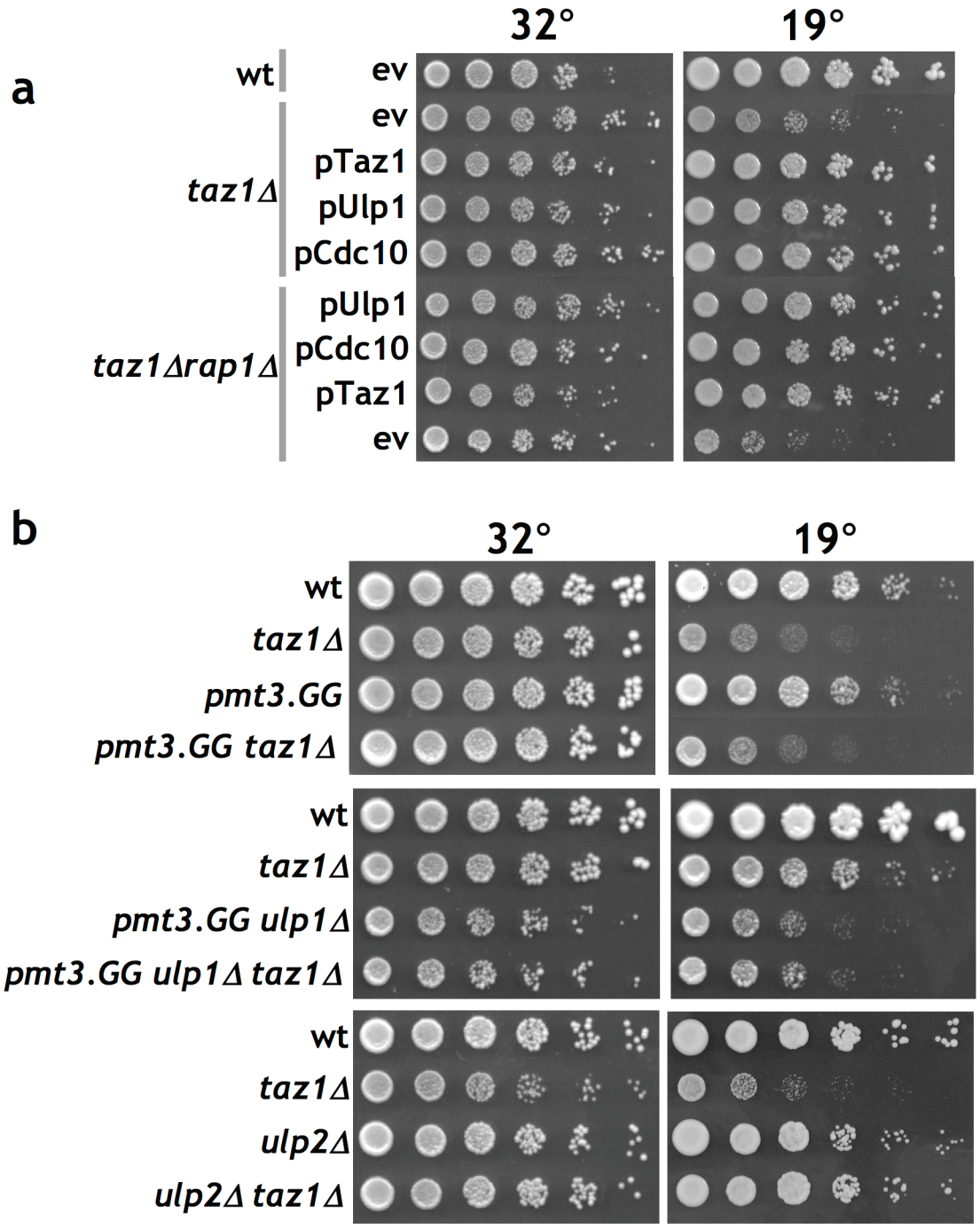

Figure 5.2 Suppressors of *taz1Δ* cold-sensitivity

(a) Five-fold serial dilutions of log-phase wt, *taz1Δ* or *taz1Δ rap1Δ* cultures harboring an empty vector (ev) or a vector containing the indicated genes were spotted onto selective medium (EMM lacking uracil). (b) Five-fold serial dilutions of log-phase cultures were spotted onto rich medium (YES) and incubated at 32º or 19º. Note that *ulp1Δ* cells also harbor the *pmt3.GG* truncation that improves their viability (Taylor et al., 2002).

The sumoylation of the replication fork processivity clamp PCNA (proliferation cell nuclear antigen) is thought to regulate DNA repair through recruitment of the Srs2 helicase, which in turn suppresses illicit Rad51^{rhp51}-mediated HR (Papouli et al., 2005; Pfander et al., 2005). PCNA sumoylation was characterized in budding yeast, and it is currently unclear how conserved this mode of regulation is, as PCNA sumoylation was not readily observed in response to DNA damage in fission yeast (Frampton et al., 2006). Nonetheless, we entertained the possibility that telomere entanglement is regulated through sumoylation of PCNA. However, genetic data argue against such involvement. First, in budding yeast, PCNA sumoylation is mediated by the SUMO E3 ligases Siz1 & 2, but as previously mentioned, disruption of *pli1*$^{+}$ did not have any effect on cold sensitivity of *taz1*Δ cells (Figure 5.16a and Xhemalce et al., 2007). Secondly, deletion of *srs2*$^{+}$ did not modify the cold sensitivity of *taz1*Δ cells (data not shown). Finally, we tested the possible involvement of the F-box helicase Fbh1, which was proposed as a functional homologue of Srs2 in fission yeast and mammals (Chiolo et al., 2007; Watts, 2006). However, deletion of *fbh1*$^{+}$ did not suppress the cold sensitivity of *taz1*Δ cells (data not shown). However, as *fbh1*$^{+}$ deletion conferred viability loss at all temperatures (Morishita et al., 2005; Osman et al., 2005), it was impossible to rule out a possible genetic interaction with *taz1*$^{+}$. Altogether, these results argue against PCNA being the relevant SUMO target for *taz1*Δ cold-sensitivity.

5.2.3 Sumoylation mutant of *rqh1*$^{+}$ suppress phenotypes associated with stalled telomeric replication forks

In considering potential SUMO targets that might modulate *taz1Δ* cold sensitivity, the fission yeast RecQ helicase Rqh1 emerged as an intriguing candidate for several reasons. First, RecQ helicases in yeast and mammals are specifically involved in telomere metabolism (Cohen and Sinclair, 2001; Crabbe et al., 2004; Huang et al., 2001; Johnson et al., 2001). Second, the RecQ helicases BLM (in human) and Sgs1 (in budding yeast) have been shown to be sumoylated *in vivo* (Branzei et al., 2006; Eladad et al., 2005), although the sites and functions of this sumoylation remain unknown. Finally, Rqh1 is necessary for suppression of *taz1Δ* cold sensitivity by *ulp1*$^{+}$ and *cdc10*$^{+}$ (Figure 5.3).

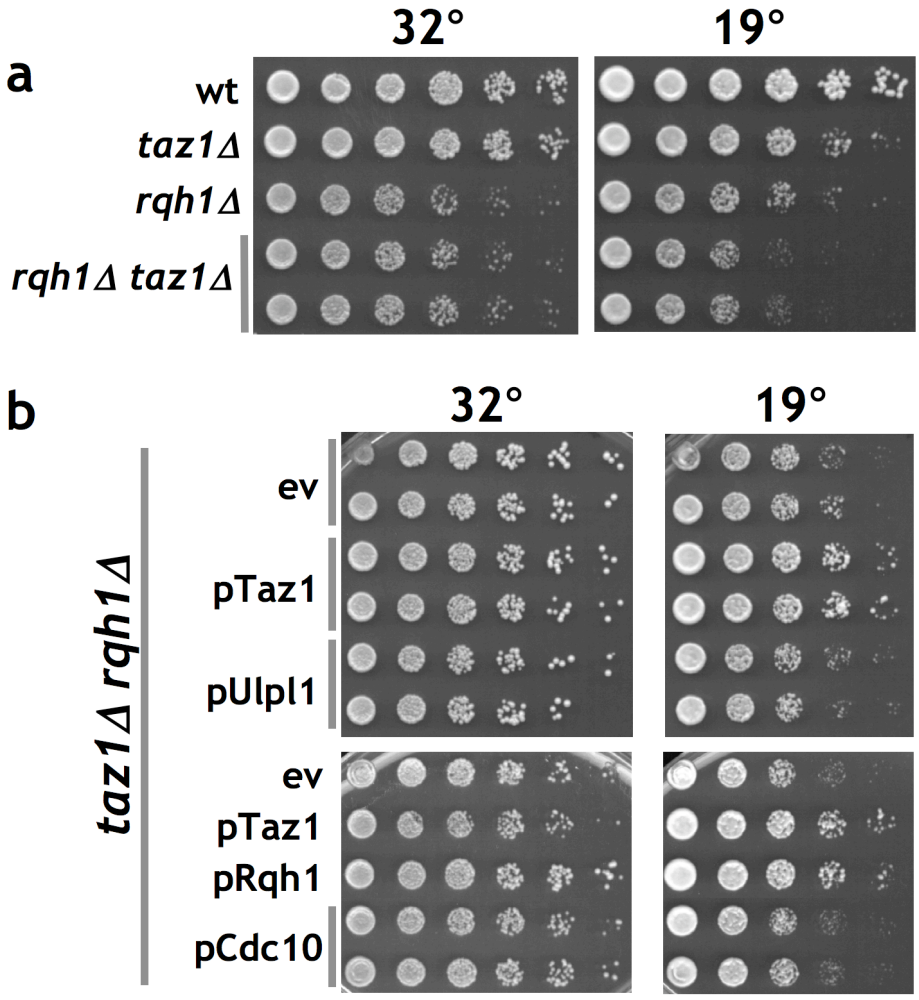

Figure 5.3 Rqh1 is necessary for *ulp1*$^{+}$- and *cdc10*$^{+}$-mediated suppression

(a) Five-fold serial dilutions of log-phase cultures were spotted onto rich medium and incubated at 32º or 19º. (b) Five-fold serial dilutions of log-phase *taz1Δ rqh1Δ* cultures harboring an empty vector (ev), or a vector containing the indicated genes were spotted onto selective medium (EMM lacking uracil) and incubated at 32º or 19º.

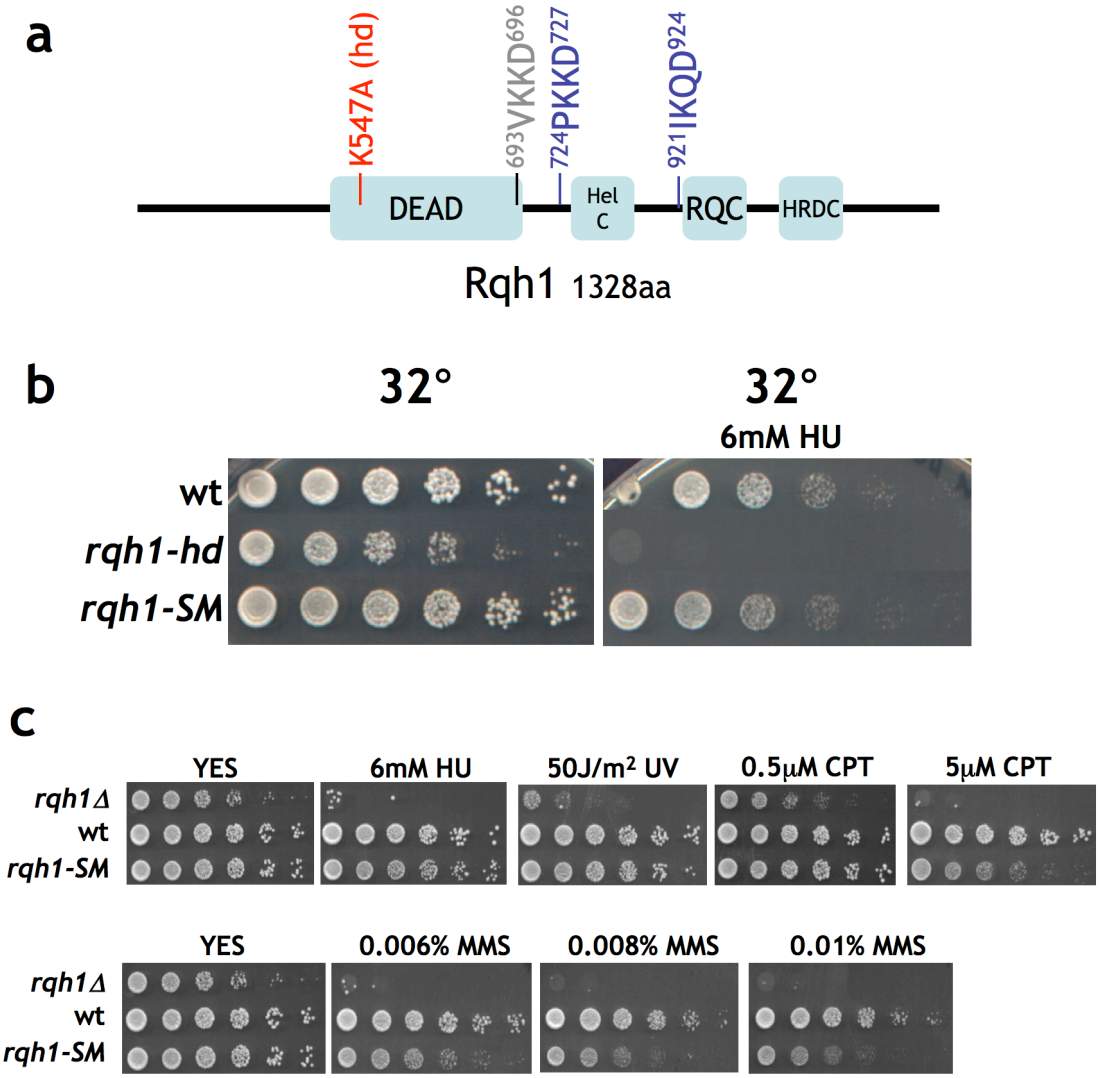

Figure 5.4 Generating sumoylation mutants of Rqh1

(a) Schematic map depicting the conserved domains in Rqh1. The *rqh1-hd* K547A mutation is marked with red. The two mutated SUMO sites in *rqh1-SM* are colored blue. In grey is a third predicted sumoylation site not included in *rqh1-SM* (see text for details). (b-c) *rqh1-SM* is mildly sensitivity to various genotoxins. Five-fold serial dilutions of log-phase cultures were spotted onto rich medium (YES), including the indicated genotoxins and incubated at 32º. UV-irradiation was performed immediately after spotting the cells onto the plates.

To address the function of Rqh1 sumoylation, we sought to construct a SUMO-deficient allele of *rqh1⁺*. We scanned the Rqh1 sequence using the SUMOplot™ Prediction program, and mutated lysine to arginine at two of the three most likely sumoylation sites (^{724}PKKD^{727} and ^{921}IKQD^{924}), thus creating *rqh1-SM* (for **S**UMO **m**utated) (Figure 5.4a). These two sites lie outside the conserved helicase domain, and therefore were not expected to abolish Rqh1 helicase activity. Indeed, re-integration of *rqh1-SM* into the *rqh1⁺* locus conferred no apparent growth phenotype and only very mild sensitivity to hydroxyurea (HU), ultra-violet (UV) light, methylmethane sulfonate (MMS) and camptothecin (Figure 5.4b-c). This contrasts with the slow growth and HU hypersensitivity caused by deletion of *rqh1⁺* or its replacement with a helicase-dead allele (*rqh1-hd*) (Figure 5.4b-c and Murray et al., 1997; Stewart et al., 1997). In addition, Western blots suggest that Rqh1 stability is unaffected by the *SM* mutations (data not shown).

In addition to the two sumoylation sites included in *rqh1-SM* (^{724}PKKD^{727} and ^{921}IKQD^{924}), we also mutated the second most likely sumoylation site, ^{693}VKKD^{696}, which is positioned on the edge of the conserved DEAD helicase domain (Figure 5.4a). Mutations in this site, when combined with *rqh1-SM* (denoted *rqh1-SM**), rendered the cells hypersensitive to HU and other genotoxins, and, when combined with a *taz1⁺* deletion, resulted in essentially the same telomeric phenotypes described for *rqh1-SM* (Figure 5.12a and data not shown). As the mutant including ^{693}VKKD^{696} is a more pleiotropic hypomorph of Rqh1, we limited our discussion to the telomere-specific *rqh1-SM* allele.

To explore the role of Rqh1 sumoylation in *taz1Δ* cold sensitivity, we investigated the effects of *rqh1-SM* at telomeres. Strikingly, the *rqh1-SM* allele substantially suppressed the growth defect of *taz1Δ* cells at cold temperatures (Figure 5.5a-b). *rqh1-SM* also suppressed the cell elongation and anaphase bridges exhibited by *taz1Δ* cells at cold temperatures (Figure 5.6a-d). Analysis of mutations at a single sumoylation site revealed that mutating ^{724}PKKD^{727} suppresses *taz1Δ* cold sensitivity to the same extant as *rqh1-SM* (Figure 5.5c), suggesting ^{724}PKKD^{727} is solely responsible for the various *rqh1-SM* phenotypes (see below).

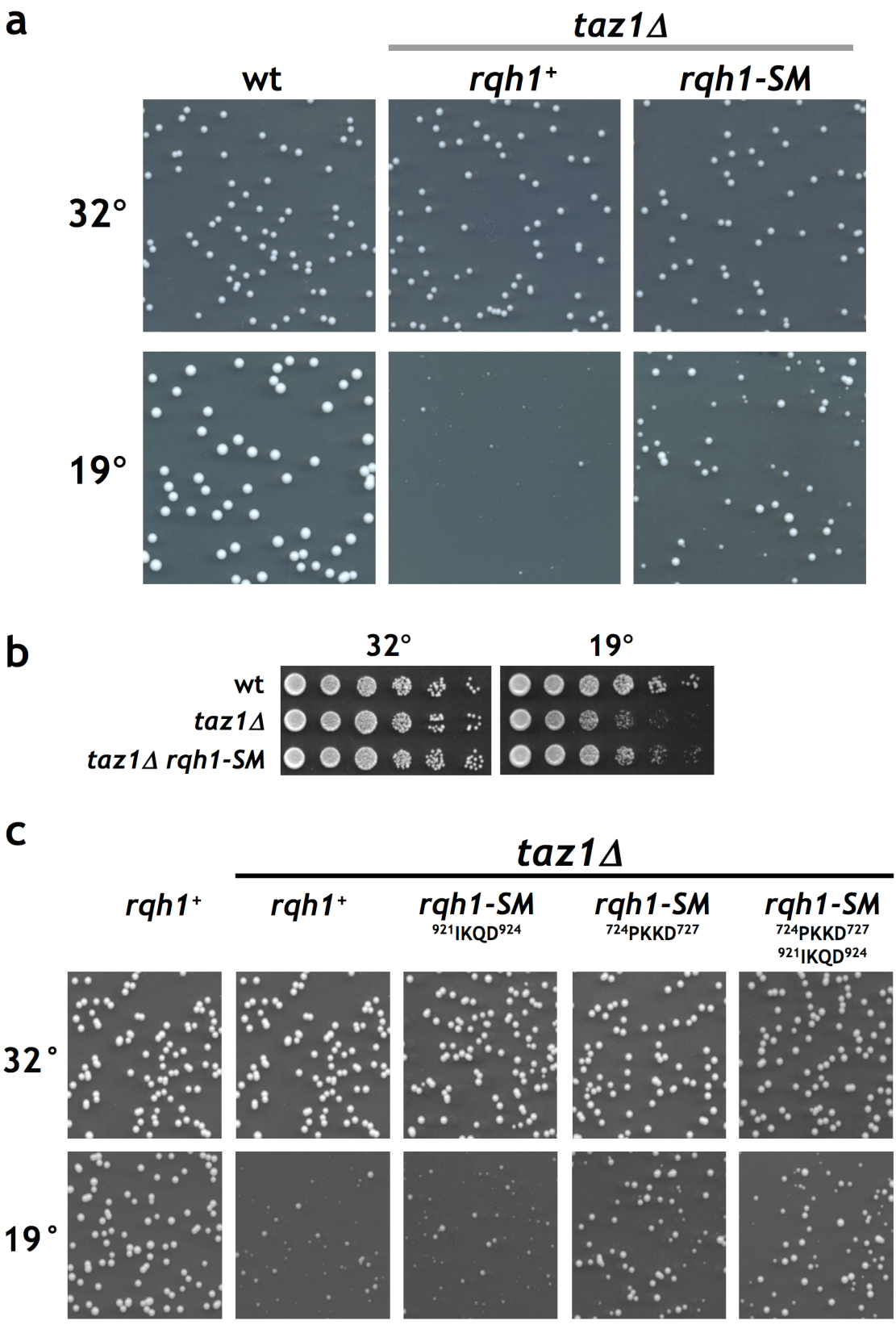
a
taz1Δ
wt
rqh1+
rqh1-SM
32°
19°
b
32°
19°
wt
taz1Δ
taz1Δ rqh1-SM
c
taz1Δ
rqh1+
rqh1+
rqh1-SM 921IKQD924
rqh1-SM 724PKKD727
rqh1-SM 724PKKD727 921IKQD924
32°
19°

Figure 5.5 Rqh1-SM suppresses *taz1Δ* cold sensitivity

(previous page) (a) ~300 log-phase cells were plated onto rich medium and incubated at 32º or 19º. (b) Five-fold serial dilutions of log-phase cultures were spotted onto rich medium (YES) and incubated at 32º or 19º. (c) The predicted sumoylation site ^{724}PKKD^{727} is solely responsible for suppression of *taz1Δ* cold sensitivity. Mutants were constructed to harbor mutations in either of the predicted sumoylation sites mutated in *rqh1-SM*. ~300 log-phase cells were plated onto rich medium and incubated at 32º or 19º.

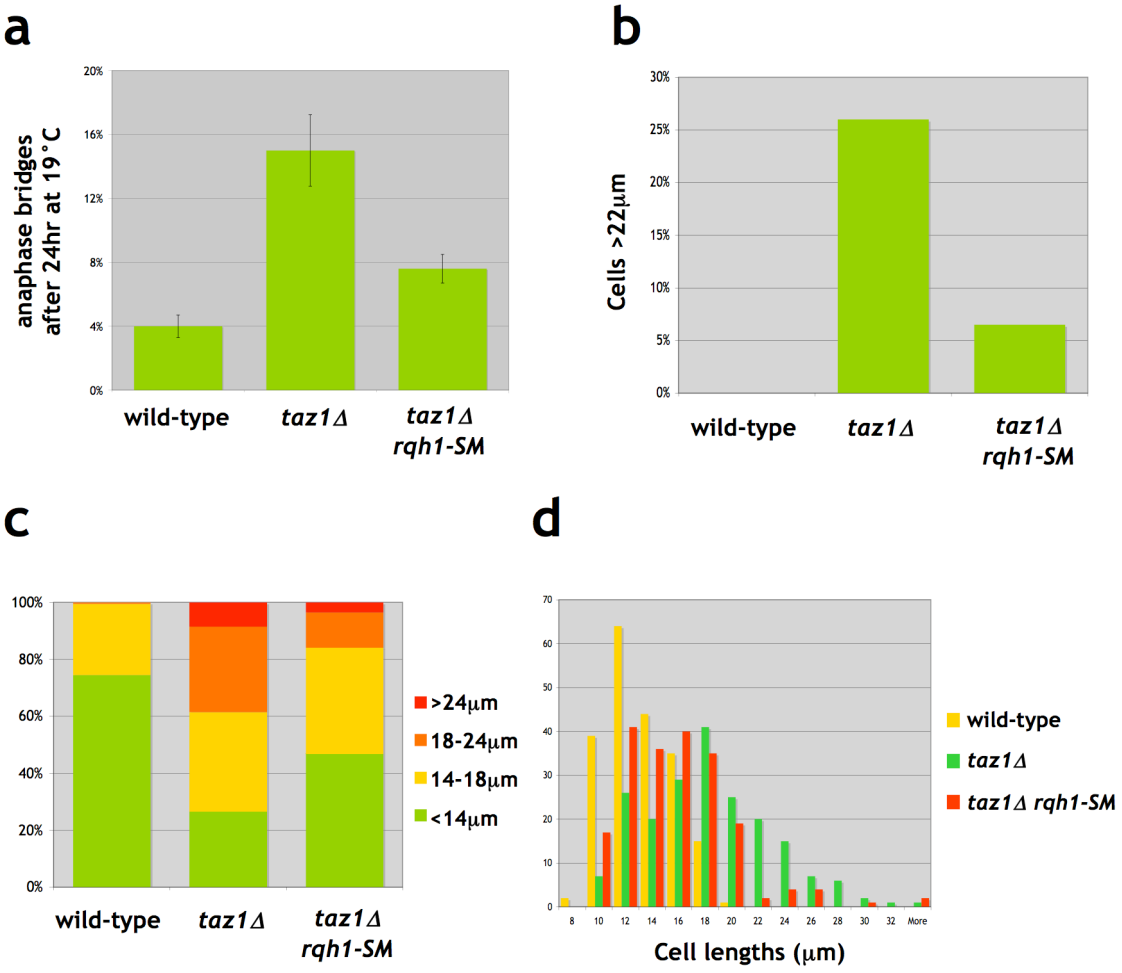

Figure 5.6 Characterization of *rqh1-SM*

(a-d) *rqh1-SM* suppresses cell elongation and anaphase bridges of *taz1Δ* cells at 19°. Cells for grown for 24hr at 19° in liquid rich media (YES), and then fixed with formaldehyde. Anaphase bridges were scored using DAPI staining. At least 200 cells of each genotype were measured.

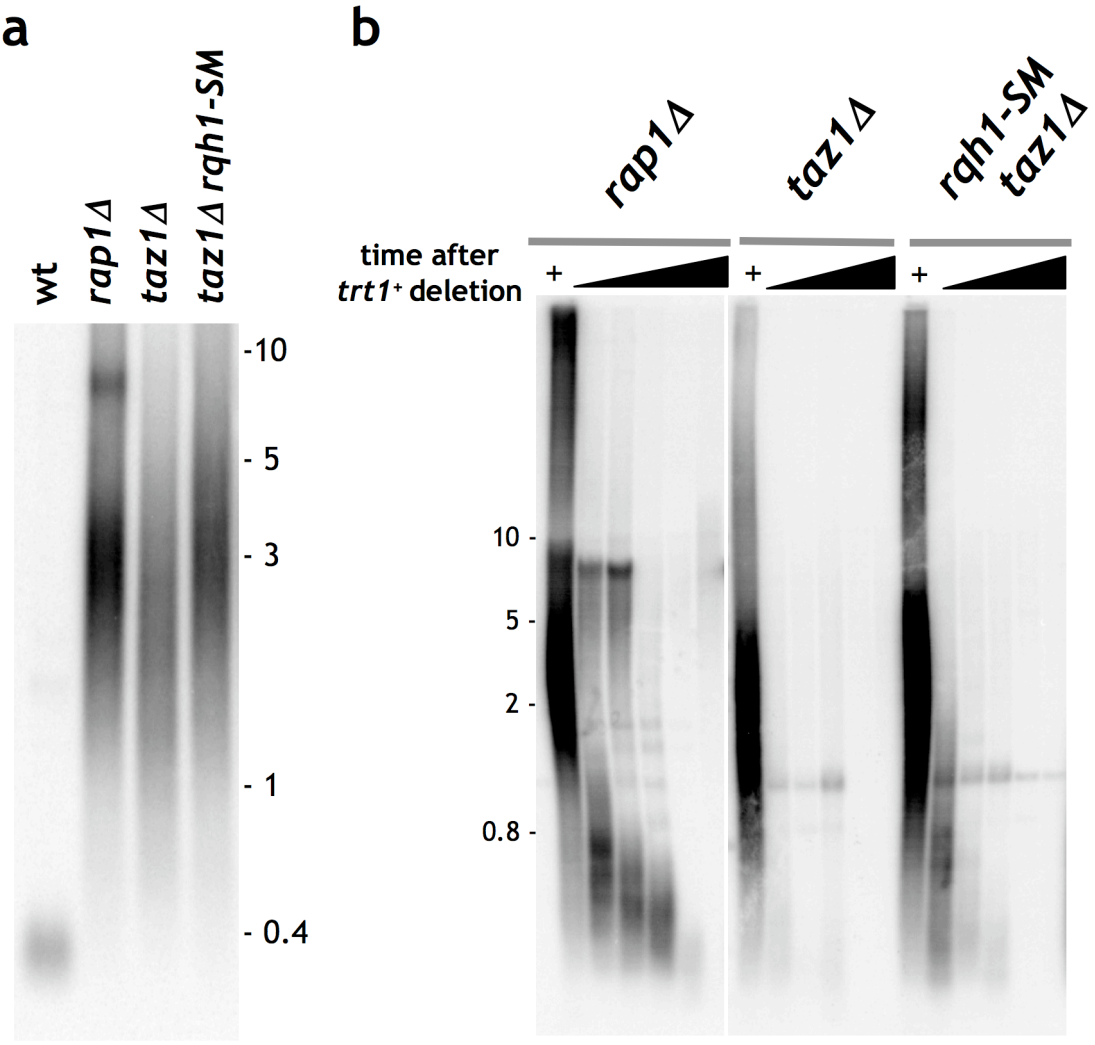

Figure 5.7 *rqh1-SM* suppresses rapid telomere loss in *taz1*Δ *trt1*Δ cells

(a) Telomere length was analyzed by ApaI digestion of genomic DNA, Southern blotting and hybridization to a telomere-repeat probe (Miller et al., 2006). (b) *trt1*$^{+}$ was deleted in *taz1Δ*, *rap1Δ* and *taz1Δ rqh1-SM* strains, and individual transformants were serially passaged on plates. Telomere length from each re-streak was analyzed by ApaI digestion and Southern blotting as in (a).

While telomere length in the *rqh1-SM* strain is indistinguishable from that of wild-type strains (data not shown), *rqh1-SM taz1Δ* telomeres are slightly longer than *taz1Δ* telomeres (Figure 5.7a). This telomere lengthening is reminiscent of *rap1Δ* telomeres (Kanoh and Ishikawa, 2001; Miller et al., 2005), which differ from *taz1Δ* telomeres in sustaining unimpeded semi-conservative DNA replication. Hence, the *rqh1-SM* allele exposes a role for Rqh1 in regulating telomere entanglement in *taz1Δ* cells.

An additional phenotype that correlates with the telomeric replication fork stalling and cold sensitivity of *taz1Δ* cells is rapid telomere loss upon deletion of telomerase *(trt1⁺*) (Miller et al., 2006). Unlike wt and *rap1Δ* telomeres, which are gradually lost upon loss of telomerase, *taz1Δ* telomeres are precipitously lost, as evidenced by the lack of appreciable telomere signal in cells taken from the first re-streak following *trt1⁺* deletion (Miller et al., 2006). This is reversed in *taz1Δ rqh1-SM* cells, in which telomeres are only gradually lost (Figure 5.7b). Thus, Rqh1 mediates the rapid loss of telomeres in *taz1Δ* strains lacking telomerase.

Telomerase loss is eventually followed by the emergence of telomerase-minus survivors, whose properties differ dramatically in *taz1⁺ versus taz1Δ* backgrounds. Fission yeast *trt1Δ* and *rap1*Δ *trt1*Δ cells grown on solid media generally survive by circularizing each of their three chromosomes, while *taz1Δ trt1*Δ cells maintain linear chromosomes and telomeres in a manner reminiscent of human ALT cells (see also Chapters 1, Chapter 3 and Miller et al., 2006; Nakamura et al., 1998). The specificity of fission yeast ALT to *taz1Δ trt1Δ* strains suggests it is a result of stalled telomeric replication forks (Miller et al., 2006). Remarkably, however, telomerase-minus survivors in a *taz1Δ rqh1-SM* background display a mixed pattern of survival, most frequently containing circular genomes (Figure 5.8a). Thus, sumoylation-competent Rqh1 stimulates the recombination events that maintain linear *taz1Δ trt1Δ* survivors.

Elevated subtelomeric recombination can also be seen in *taz1Δ* cells harboring telomerase, where it is again most likely a consequence of stalled replication forks. *taz1Δ* subtelomeres display an erratic restriction pattern of STE1 that changes from one re-streak to the next (see Chapter 3). However, *taz1Δ* subtelomeric hyper-recombination is abolished by the *rqh1-SM* mutation (Figure 5.8b). Thus, hyper-recombination at *taz1Δ* subtelomeres requires sumoylation-competent Rqh1.

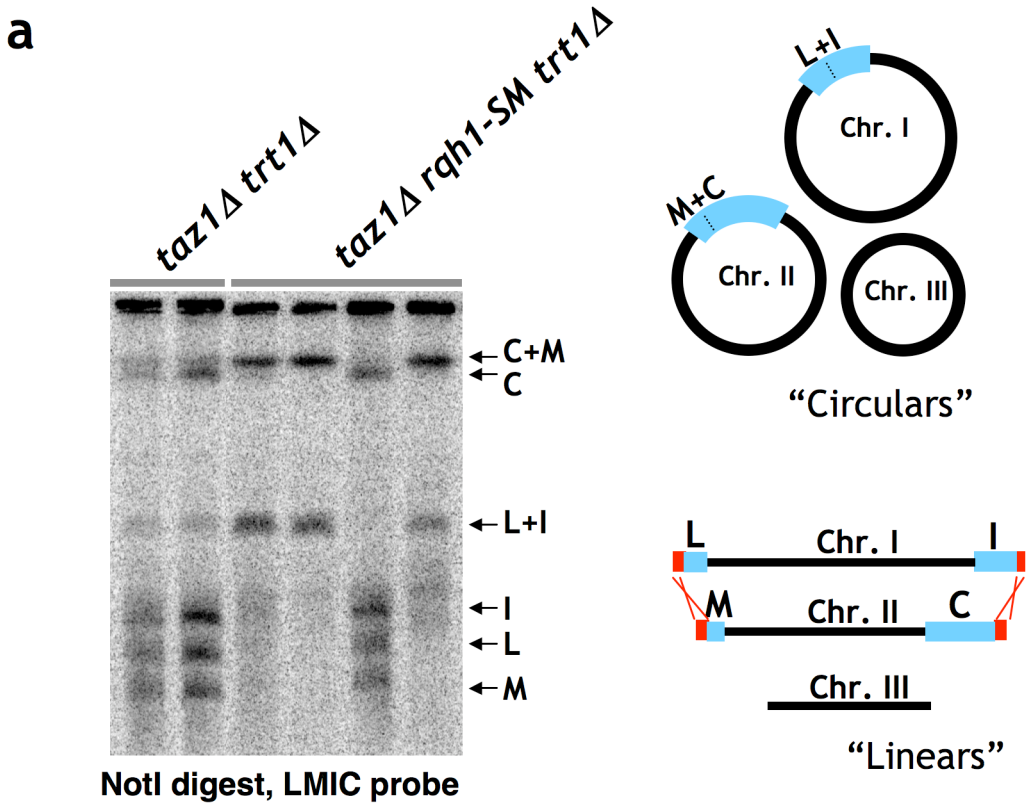
a
taz1Δ trt1Δ
taz1Δ rqh1-SM trt1Δ
C+M
C
L+I
I
L
M
NotI digest, LMIC probe
L+I
Chr. I
M+C
Chr. II
Chr. III
"Circulars"
L
Chr. I
I
M
Chr. II
C
Chr. III
"Linears"

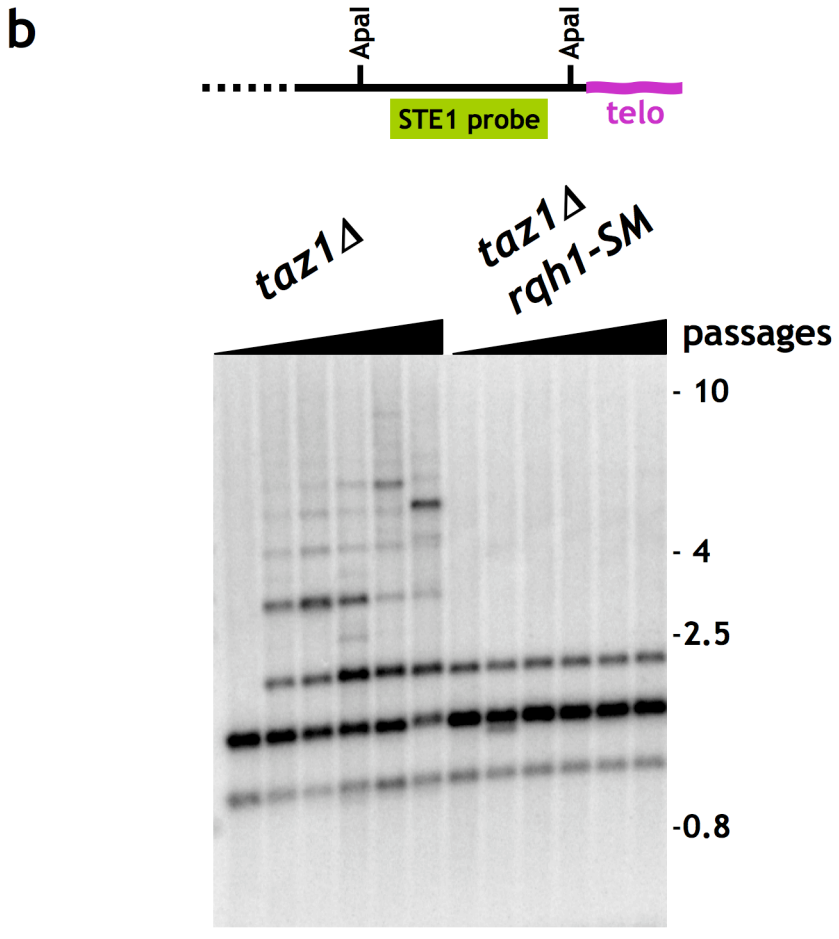
b
ApaI
ApaI
STE1 probe
telo
taz1Δ
taz1Δ rqh1-SM
passages
- 10
- 4
-2.5
-0.8

Figure 5.8 *rqh1-SM* suppresses *taz1Δ* telomeric hyper-recombination

(previous page) (a) *trt1*$^{+}$ was deleted in *taz1Δ* and *taz1Δ rqh1-SM* strains. Single colonies were propagated on plates until survivors arose (~3 re-streaks). *Not*I digested genomic DNA was analyzed by Pulsed-Field Gel Electrophoresis (PFGE), followed by Southern blotting for the terminal fragments of chromosomes I and II (LMIC bands). Right, a diagram of the two modes of survival of fission yeast lacking telomerase (see main text for details). (b) (top) Schematic diagram of fission yeast subtelomeres. Strains were re-streaked on rich medium plates (YES) every 2-3 days. A single colony from each re-streak was cultured, and sub-telomeres were analyzed by *Apa*I digestion of genomic DNA, followed by Southern blotting with a STE1 probe.

Figure 5.9 *rqh1-SM* does not affect *taz1Δ* replication-fork stalling at a telomeric sequence or excessive 3' overhang accumulation

(next page) (a) Genomic DNA from *taz1*$^{+}$, *taz1Δ* and *taz1Δ rqh1-SM* strains containing an internally placed telomeric sequence at the *ura4*$^{+}$ locus (Miller et al., 2006) was digested with *Nsi*I, and analyzed by 2DGE followed by Southern blotting. The interpretive diagram depicts the origin of replication (ori), *Nsi*I restriction sites (green bars), the inserted telomere sequence (purple swivel) and the probe used for Southern blotting (light blue bar; the *ScLEU2* gene inserted next to the telomere repeat sequence (Miller et al., 2006)). An accumulation of signal is apparent in the descending region of each Y-arc, indicating stalled replication forks at the telomeric sequence. (b) Genomic DNA was digested with *Hind*III and analyzed using native in-gel hybridization to end-labelled probes specific for the G-rich or the C-rich strands ('C-rich probe' and 'G-rich probe', respectively). ExoI (3'-5' ssDNA exonuclease) treatment reduced the signal observed with the C-rich probe, confirming that the majority of the signal in the untreated samples represents terminal over-hang. Following denaturing, gels were hybridized again to the same probes to confirm equal loading. A plasmid containing internal telomeric sequence ('telo-plasmid') was used as control for the native and denatured conditions. *rqh1-SM** includes mutations in a third sumoylation site in addition to the mutations in *rqh1-SM* (see section 5.2.3).

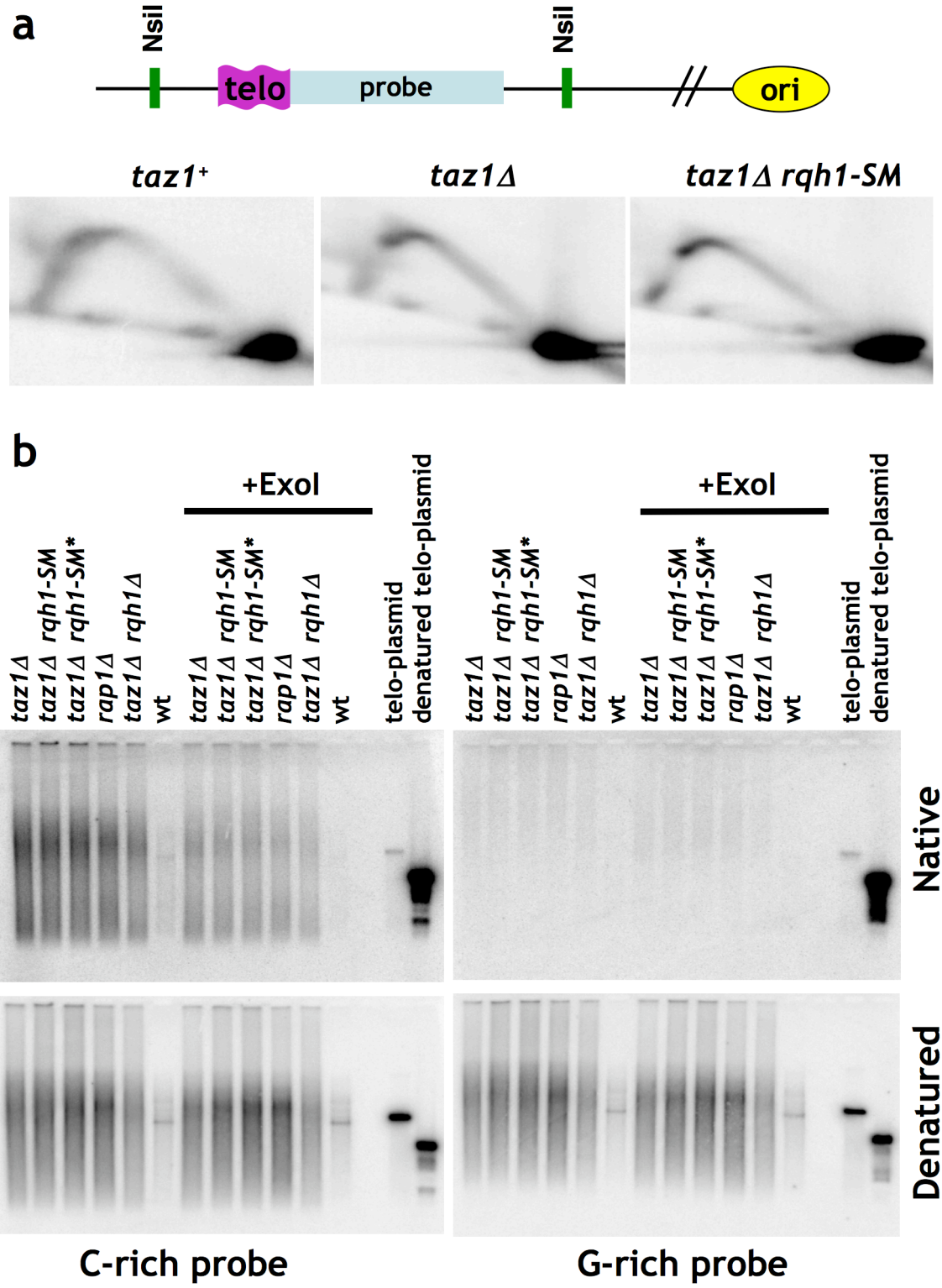
a
NsiI
NsiI
telo
probe
ori
taz1+
taz1Δ
taz1Δ rqh1-SM
b
+ExoI
+ExoI
taz1Δ
taz1Δ rqh1-SM
taz1Δ rqh1-SM*
rap1Δ
taz1Δ rqh1Δ
wt
telo-plasmid
denatured telo-plasmid
Native
Denatured
C-rich probe
G-rich probe

5.2.4 Rqh1-SM does not alleviate *taz1Δ* telomeric fork-stalling or excessive 3' overhang accumulation

The cold sensitivity, hyper-recombination and rapid *trt1Δ* telomere loss of *taz1Δ* cells are likely to stem from stalled telomeric replication forks. If *rqh1-SM* suppresses aberrant responses to telomeric fork stalling, does it do so by preventing fork-stalling or by modulating the events elicited by stalled telomeric forks? Neither *rqh1-SM* nor *rqh1Δ* affected replication fork-stalling at an internally-placed telomeric sequence in the absence of Taz1, as assessed by 2-dimensional gel-electrophoresis (2DGE) (Figure 5.9a and data not shown). In addition, Rqh1-SM had no appreciable effect on the replication patterns of endogenous *taz1Δ* telomeres (data not shown). Although we cannot rule out a minor effect on replication that is not detectable by 2DGE, our data suggest that Rqh1 does not directly modulate the progress of replication forks at telomeres. Thus, the suppression of the abovementioned *taz1Δ*-specific phenotypes by *rqh1-SM* suggests that sumoylated Rqh1 acts downstream of stalled telomeric replication forks to regulate their outcome.

RecQ helicases have been suggested to interact with proteins involved in the protection of the telomeric 3' overhang (Kibe et al., 2007; Opresko et al., 2005). Hence, we tested whether Rqh1 modulates the telomeric 3' overhangs in *taz1Δ* strains using native in-gel hybridization. In *taz1Δ* (and *rap1Δ*) strains, telomeric 3' overhang signals are abnormally high throughout the cell-cycle (Ferreira and Cooper, 2004; Miller et al., 2005; Tomita et al., 2003). We observe similar levels of 3' telomeric overhang signal in *taz1Δ*, *taz1Δ rqh1-SM* and *taz1Δ rqh1Δ* strains (Figure 5.9b). Thus, alteration of telomeric 3' overhang abundance is unlikely to explain the telomeric phenotypes of cells harboring Rqh1-SM.

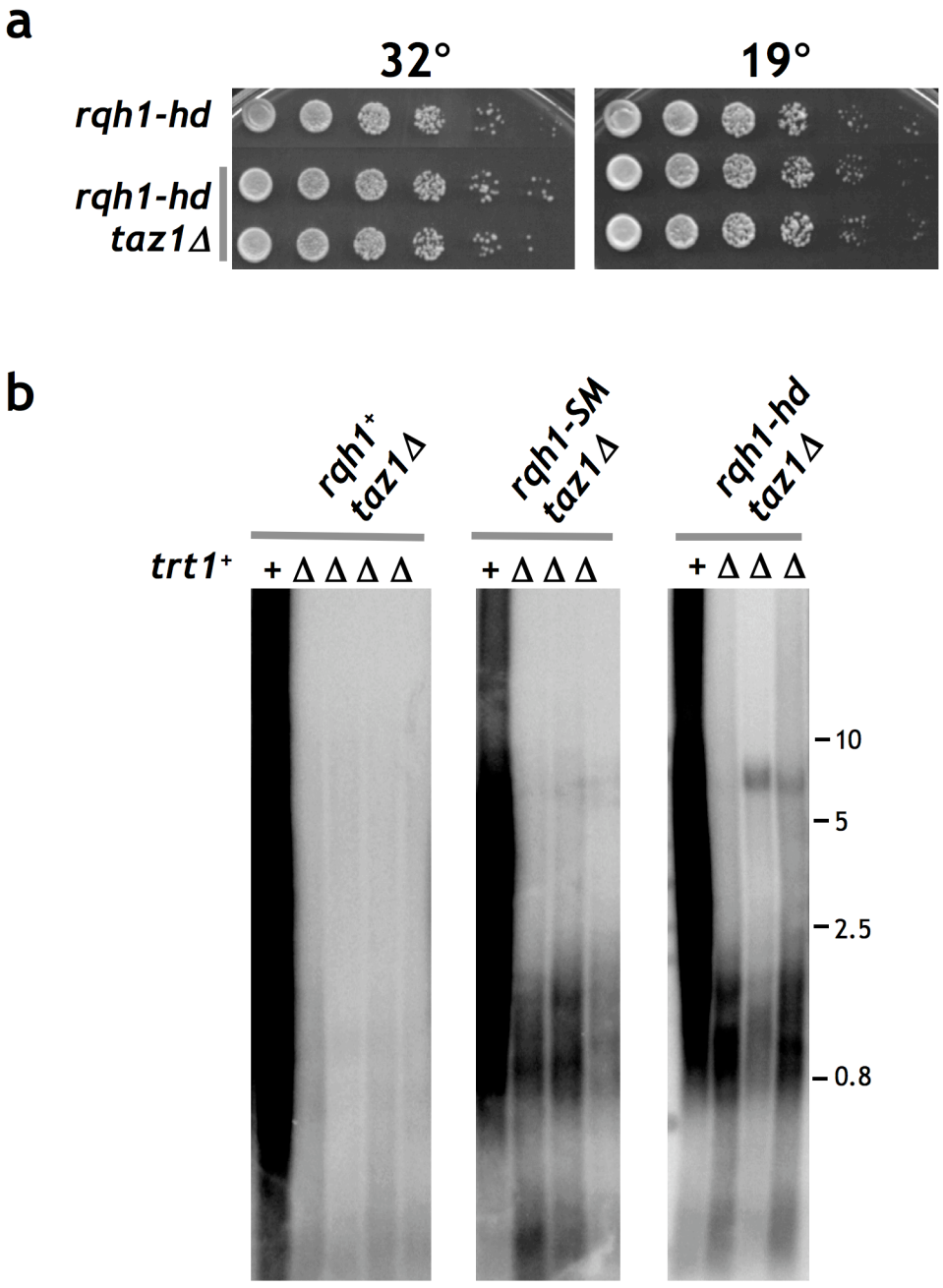

Figure 5.10 *rqh1-SM* acts as a loss-of-function allele

(a) Five-fold serial dilutions of log-phase cultures were spotted onto rich medium. (b) *trt1*$^{+}$ was deleted in *taz1Δ*, *taz1Δ rqh1-SM* and *taz1Δ rqh1-hd* strains, and telomere length of several individual transformants, all taken at a single time-point (3 days), were analyzed by Southern blotting as in Figure 5.7b.

5.2.5 *rqh1-SM* acts as a telomere-specific loss-of-function allele

The foregoing results suggest that sumoylation of Rqh1 modulates its activity at dysfunctional telomeres. To determine whether the *rqh1-SM* mutation inhibits, elevates or alters Rqh1 activity, we assessed the effects of Rqh1 inhibition on *taz1Δ* telomeres using the *rqh1-hd* allele (Figure 5.3a). *rqh1-hd* cells grow slowly at all temperatures (Figure 5.3b). Nonetheless, deletion of *taz1⁺* in an *rqh1-hd* background fails to elicit a further reduction in growth rate at cold temperatures (Figure 5.10a). Hence, the helicase activity of Rqh1 is required for *taz1⁺* deletion to confer cold sensitivity. Interestingly, *rqh1⁺* deletion failed to suppress *taz1Δ* cold sensitivity (Figure 5.3a), suggesting that Rqh1 has helicase-independent activities that promote survival of *taz1Δ* cells in the cold; however, the sickness conferred by *rqh1⁺* deletion confounds straightforward interpretation of this result. Overexpression of *rqh1-hd* in *rqh1⁺* cells also partially suppresses *taz1Δ* cold sensitivity (data not shown), presumably by displacing wild type Rqh1 in a 'dominant-negative' manner. Thus, impairing sumoylation of Rqh1 mimics inhibition of its helicase activity, as both lead to suppression of *taz1Δ* cold sensitivity. These data suggest that sumoylation stimulates Rqh1 activity at telomeres.

Loss-of-function alleles of *rqh1⁺* not only recapitulate the *taz1Δ* cold sensitivity suppression conferred by *rqh1-SM*, but also mimic its effects on several other *taz1Δ* phenotypes: First, both *rqh1Δ* and *rqh1-hd* alleviate the rapid telomere loss seen upon *trt1⁺* deletion (Figure 5.10b and data not shown). Second, like *rqh1-SM*, *rqh1Δ* and *rqh1-hd* confer lengthening of *taz1Δ* telomeres (Figure 5.11a). Finally, *taz1Δ* subtelomeric hyper-recombination is abolished by the *rqh1-hd* allele (Figure 5.11b). Taken together, these data indicate that Rqh1-SM acts in a loss-of-function manner at *taz1Δ* telomeres.

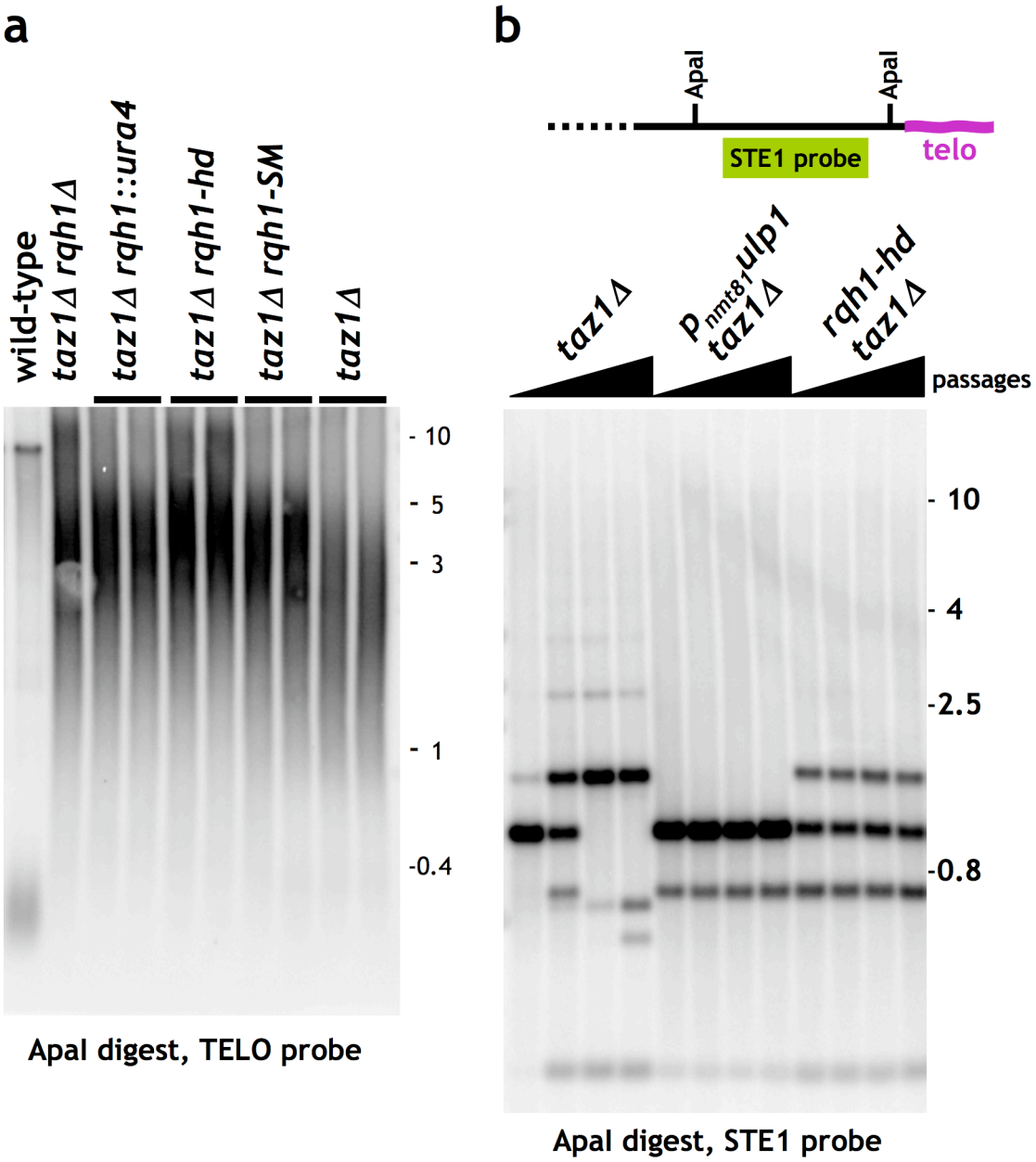

Figure 5.11 *rqh1*⁺ inactivation, like *rqh1-SM,* elongates *taz1Δ* telomeres and *rqh1-hd* and ectopic expression of *ulp1*⁺ or *cdc10*⁺ suppress *taz1Δ* telomeric hyper-recombination

(a) Telomere length was analyzed by *Apa*I digestion of genomic DNA, Southern blotting and hybridization to a telomere-repeat probe (Miller et al., 2006). (b) (top) Schematic diagram of fission yeast subtelomeres. Strains were re-streaked on rich medium plates (YES) every 2-3 days. A single colony from each re-streak was cultured, and sub-telomeres were analyzed by *Apa*I digestion of genomic DNA, followed by Southern blotting with a STE1 probe.

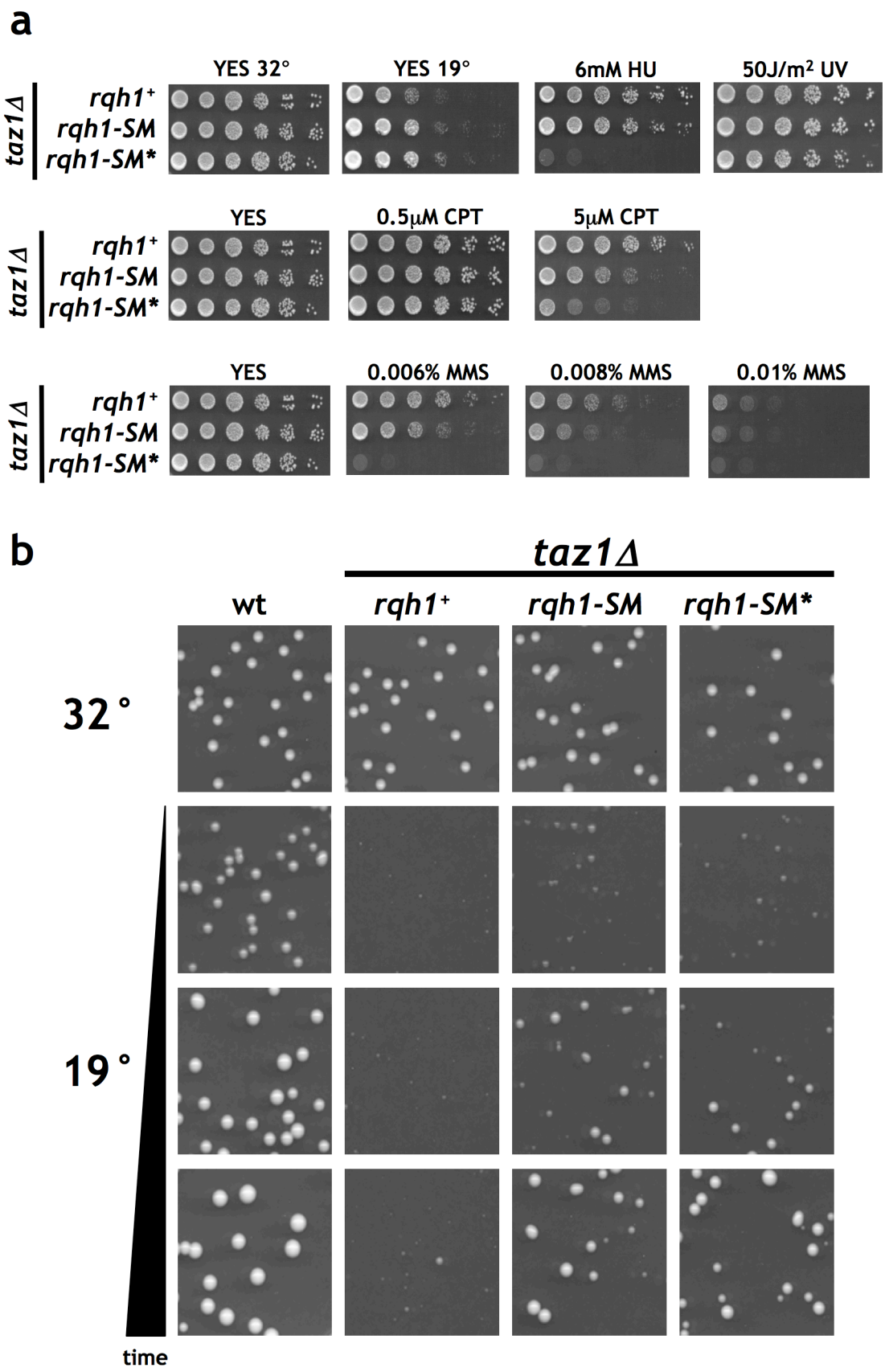
a
YES 32°
YES 19°
6mM HU
50J/m² UV
taz1Δ
rqh1⁺
rqh1-SM
rqh1-SM*
YES
0.5μM CPT
5μM CPT
YES
0.006% MMS
0.008% MMS
0.01% MMS
b
taz1Δ
wt
rqh1⁺
rqh1-SM
rqh1-SM*
32°
19°
time

Figure 5.12 *rqh1-SM is much more sensitive to genotoxins compared with *rqh1-SM*, but suppresses *taz1Δ* cold-sensitivity to similar extant**

(previous page) (a) Five-fold serial dilutions of log-phase cultures were spotted onto rich medium (YES), including the indicated genotoxins and incubated at 32º or 19°. UV-irradiation was performed immediately after spotting the cells onto the plates. (b) ~300 log-phase cells were plated onto rich medium and incubated at 32º or 19º. The 19° plates were scanned at different days to allow capturing of slight differences in growth. *rqh1-SM** allele includes mutations in ^{693}VKKD^{696} in addition to the mutations included in *rqh1-SM*.

Figure 5.13 *rqh1-SM* has only a slight effect on recombination between direct repeats

(next page) (a) Diagram of system used to measure recombination between direct repeats, using strains harbouring two direct repeats of the *ade6*$^{+}$ gene flanking an RTS site and a *his3*$^{+}$ reporter gene (Ahn et al., 2005). Only the active orientation of the RTS site blocks replication forks approaching from the origin of replication (ori). Asterisks mark data obtained from (Ahn et al., 2005). (b) Rate of obtaining Ade^{+} recombinants. Note the different scale for the two different orientations. (c) Rate of conversion types *versus* deletion types among the Ade^{+} recombinants (measured by the loss of the *his3*$^{+}$ gene located between the direct repeats). (d) Colonies grown on YE. On this media Ade^{-} colonies are red, while Ade^{+} colonies and sectors are white.

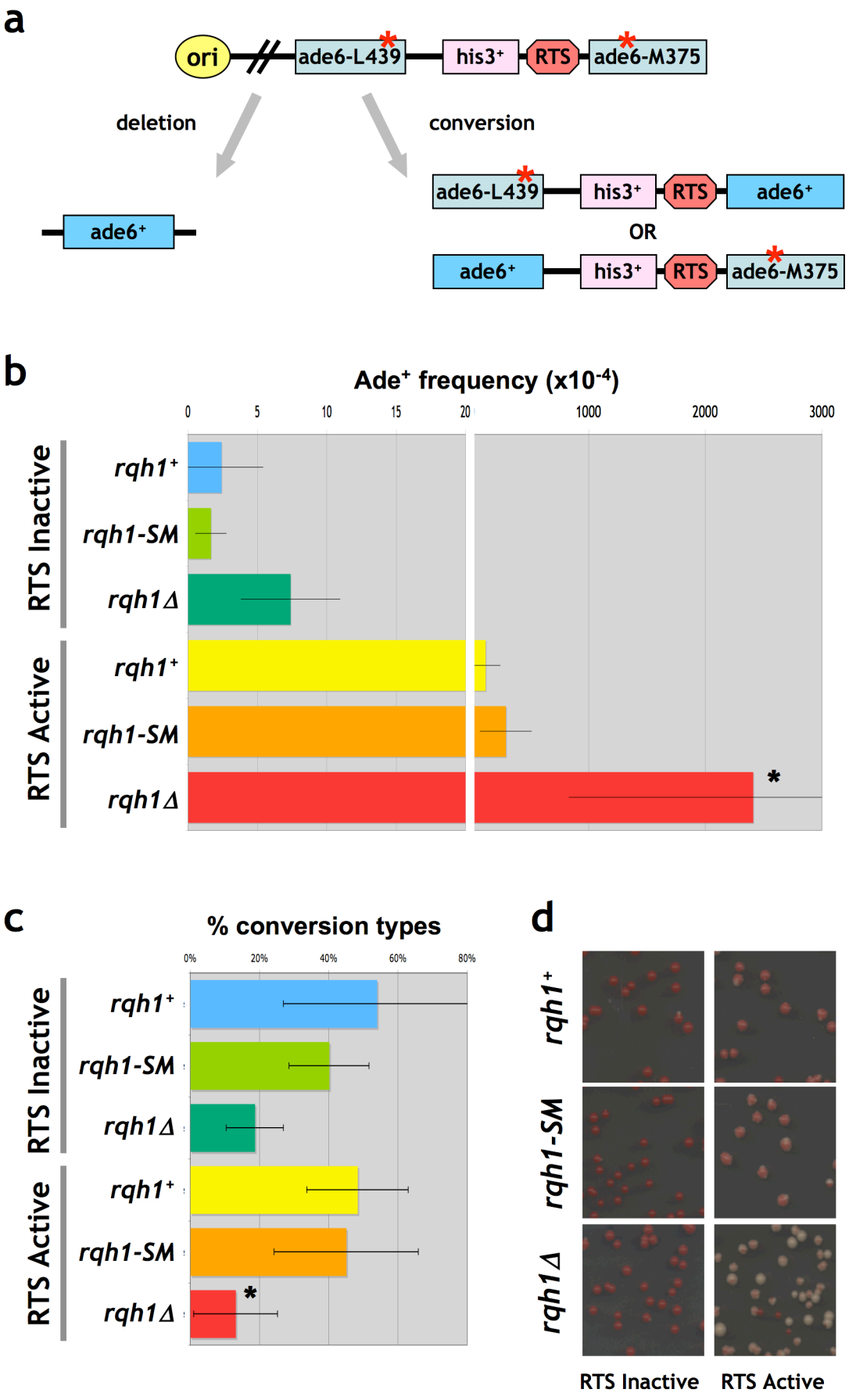
a
ori
ade6-L439
his3+
RTS
ade6-M375
deletion
conversion
ade6+
ade6-L439
his3+
RTS
ade6+
OR
ade6+
his3+
RTS
ade6-M375
b
Ade+ frequency (x10-4)
0
5
10
15
20
1000
2000
3000
RTS Inactive
RTS Active
rqh1+
rqh1-SM
rqh1Δ
rqh1+
rqh1-SM
rqh1Δ
*
c
% conversion types
0%
20%
40%
60%
80%
RTS Inactive
RTS Active
rqh1+
rqh1-SM
rqh1Δ
rqh1+
rqh1-SM
rqh1Δ
*
d
rqh1+
rqh1-SM
rqh1Δ
RTS Inactive
RTS Active

However, unlike the pleiotropic phenotypes resulting from loss of Rqh1 function, the effects of *rqh1-SM* appear to be specific to *taz1Δ* telomeres. First, in contrast with *rqh1Δ* cells, *rqh1-SM* cells exhibit no growth defect (Figure 5.4b and 5.5a) and only very mild sensitivity to HU and other genotoxins (Figure 5.4b-c), demonstrating that Rqh1-SM is not a generally non-functional protein. Second, an allele of *rqh1⁺* that includes, in addition to the previously mentioned sumoylation sites, a mutation in a third sumoylation site (*rqh1-SM**), confers a markedly increased sensitivity to various genotoxins compared with *rqh1-SM* (Figure 5.12a), but fails to further suppress *taz1Δ* cold sensitivity (Figure 5.12b). Thus, loss of genotoxic resistance does not correlate with suppression of *taz1Δ* cold sensitivity. Third, the SM mutations confer a slight growth advantage to *rqh1-hd* (data not shown) – an effect that is not expected from a generic hypomorph. Finally, we investigated the effect of *rqh1-SM* on recombination events between direct repeats in the presence and absence of an adjacent site-specific replication fork barrier (RTS1). In this system, *rqh1⁺* deletion not only greatly increases the frequency of HR between direct repeats (in both the presence and absence of RTS1 activity), but also elevates the ratio of excision *versus* conservative gene conversion between these repeats (Ahn et al., 2005). However, *rqh1-SM* failed to dramatically affect either HR frequency or type in this system (Figure 5.13). Thus, the effects of Rqh1-SM on recombination are clearly distinct from those expected for a generic hypomorph of *rqh1⁺*. Rather, *rqh1-SM* affects recombination at dysfunctional telomeres without affecting events at all repeated regions or all stalled replication forks. Taken together, *rqh1-SM* appears to alter the activity of Rqh1 at telomeres without abolishing its genome-wide functions.

5.2.6 Rqh1 is a SUMO target

The foregoing results demonstrate that *rqh1-SM*, which harbors mutations in two predicted sumoylation sites, reduces Rqh1 function at telomeres, thus suppressing several phenotypes that stem from stalled forks in *taz1*Δ cells: telomeric entanglements, telomeric hyper-recombination, and telomere loss and survival mode in the absence of telomerase. These data suggest that Rqh1 is the sumoylation target responsible for the suppression of *taz1Δ* cold sensitivity

by Ulp1 overexpression. Consistent with this idea, Ulp1 overexpression, like *rqh1-SM*, suppresses *taz1Δ* telomeric hyper-recombination (Figure 5.11b).

To verify that Rqh1 is indeed a SUMO target, we asked whether we could detect sumoylated Rqh1 *in vivo* utilizing an anti-SUMO antibody (αSUMO, Xhemalce et al., 2004). In whole cell extracts, a ladder of bands representing sumoylated proteins is detected; the absence of this ladder in extracts of a *pmt3Δ* strain confirms the specificity of the αSumo antibody (Figure 5.14a). Using strains in which Rqh1 is C-terminally tagged with 13-Myc at its endogenous locus (Figure 5.14a), we immunoprecipitated (IP) Myc-tagged Rqh1 and probed the IPs with αSUMO. IPs were performed on denatured protein extracts (TCA-precipitated protein pellets were resuspended in Laemmli buffer prior to dilution into IP buffer; see Chapter 2 for more details) to avoid detection of non-covalent interactions and to prevent the addition or removal of SUMO from occurring *in vitro*.

When IP were performed in extract from *taz1Δ* cells grown at 19°, αSumo revealed a high-molecular weight smear above Rqh1, indicating its sumoylation (Figure 5.14b). Within the smear, weak bands can be discerned, which presumably represent multiple sumoylation forms (see also Figure 5.15); these forms may stem from multiple mono-sumoylation events, poly-sumoylation events, or a mixture of both. To determine whether the mutations present in *rqh1-SM* reduce sumoylation of Rqh1, we analyzed IPs of Myc-tagged Rqh1-SM for cross-reaction with αSUMO. Notably, sumoylation of Rqh1 was mildly but reproducibly reduced in *rqh1-SM* strains relative to wt (Figure 5.14b). Residual sumoylation of Rqh1 is expected to occur at other sites on Rqh1 (see section 5.2.3). In addition, as the Myc tag contain lysines, it is conceivable that it may be responsible for some of the residual sumoylation.

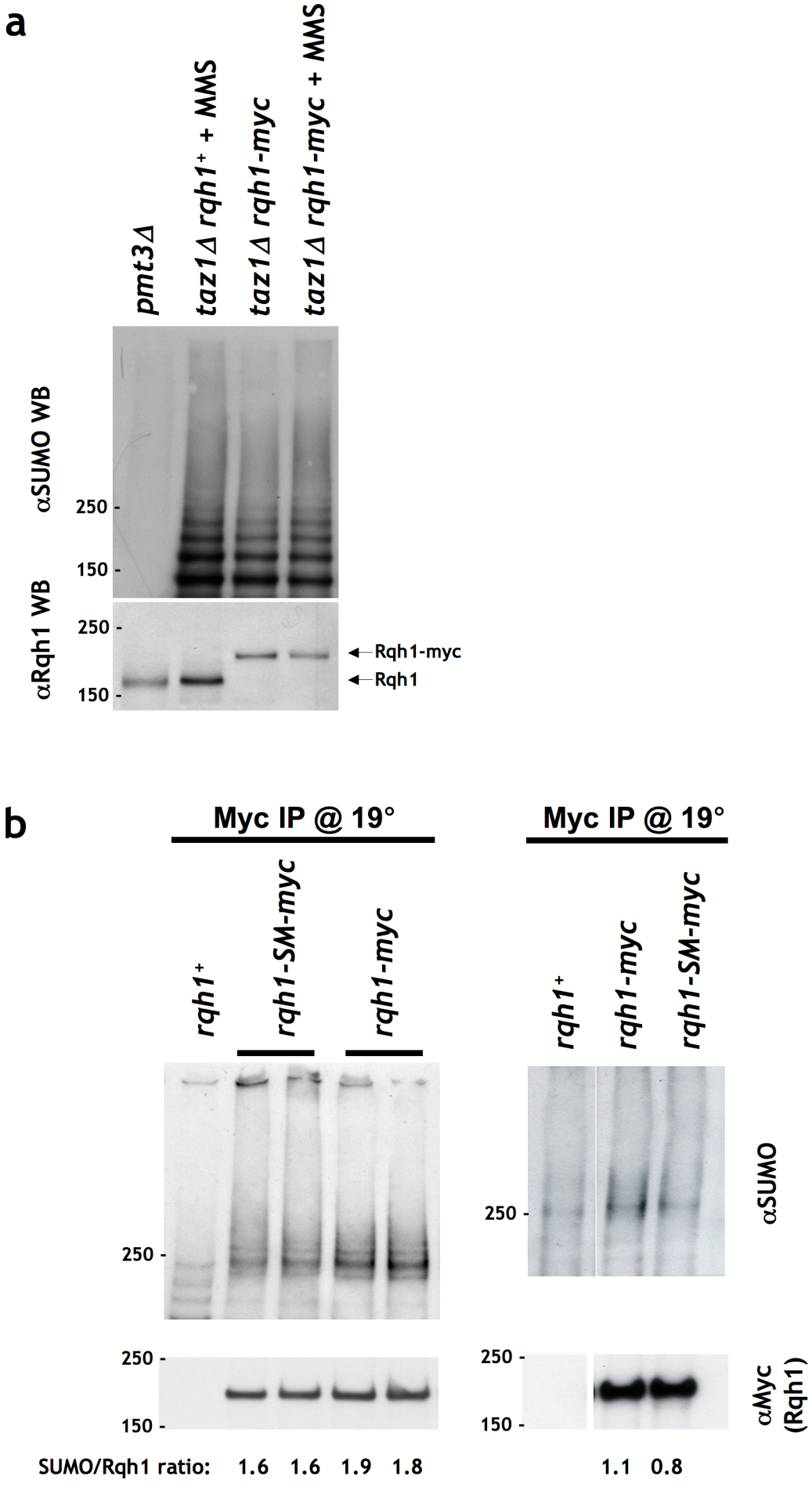
a
pmt3Δ
taz1Δ rqh1+ + MMS
taz1Δ rqh1-myc
taz1Δ rqh1-myc + MMS
αSUMO WB
250
150
αRqh1 WB
250
150
Rqh1-myc
Rqh1
b
Myc IP @ 19°
Myc IP @ 19°
rqh1+
rqh1-SM-myc
rqh1-myc
rqh1+
rqh1-myc
rqh1-SM-myc
250
250
αSUMO
250
150
250
150
αMyc (Rqh1)
SUMO/Rqh1 ratio: 1.6 1.6 1.9 1.8
1.1 0.8

Figure 5.14 Rqh1 is sumoylated

(previous page) (a) Western blots (WB) of whole-cell extracts (WCE) of *pmt3*Δ, wild type and myc-tagged Rqh1, with and without MMS treatment. (b) Rqh1-myc was immunoprecipitated (Myc IP) from *taz1Δ rqh1⁺*, *taz1Δ rqh1-myc* and *taz1Δ rqh1-SM-myc* cells grown in 19°. Rqh1-myc IPs were probed with αSUMO (top) or αMyc (bottom). Ratios of αSUMO to αMyc signal are indicated below. Examples of two independent experiments are shown.

Figure 5.15 Rqh1 is sumoylated after MMS treatment

(next page) (a) Rqh1-myc was immunoprecipitated from *taz1Δ rqh1⁺*, *taz1Δ rqh1-myc and taz1Δ rqh1-SM-myc* cells treated with MMS. Rqh1-myc IPs were probed with αSUMO (top) or αMyc (bottom). Ratios of αSUMO to αMyc signal are indicated below. (b) Rqh1-myc was immunoprecipitated as in (a) from *taz1Δ rqh1-myc* cells harboring the indicated plasmids and treated with MMS.

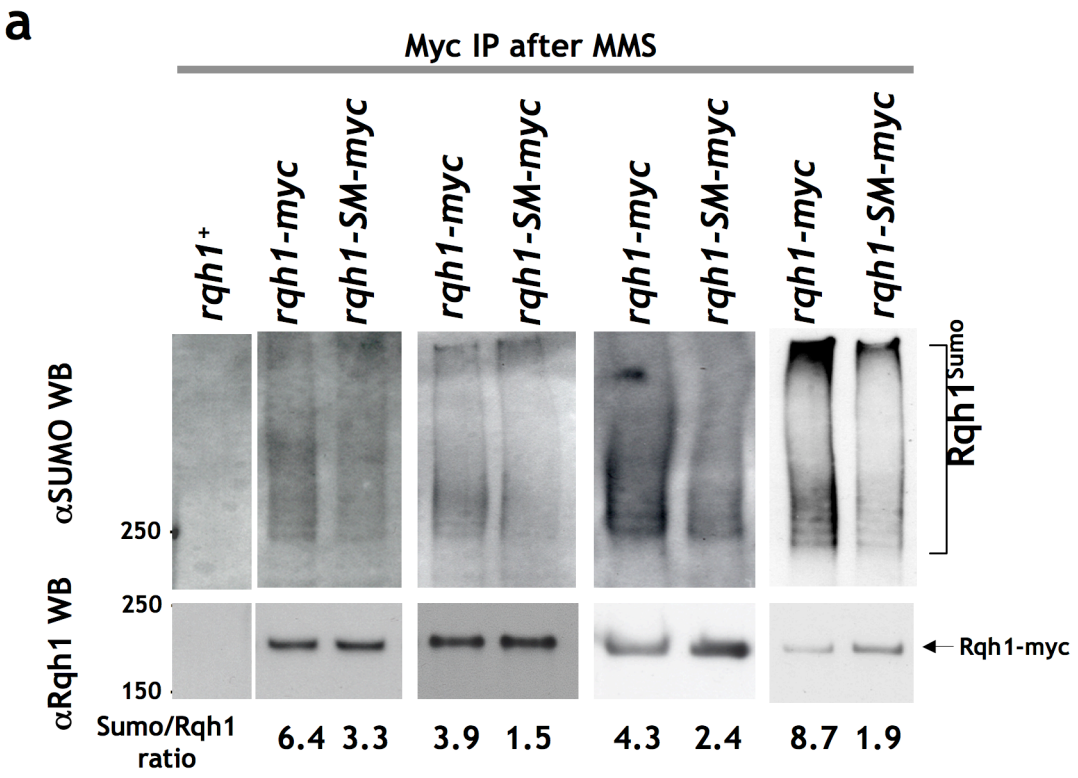
a
Myc IP after MMS
rqh1+
rqh1-myc
rqh1-SM-myc
rqh1-myc
rqh1-SM-myc
rqh1-myc
rqh1-SM-myc
rqh1-myc
rqh1-SM-myc
αSUMO WB
250
Rqh1Sumo
αRqh1 WB
250
150
Rqh1-myc
Sumo/Rqh1 ratio
6.4 3.3 3.9 1.5 4.3 2.4 8.7 1.9

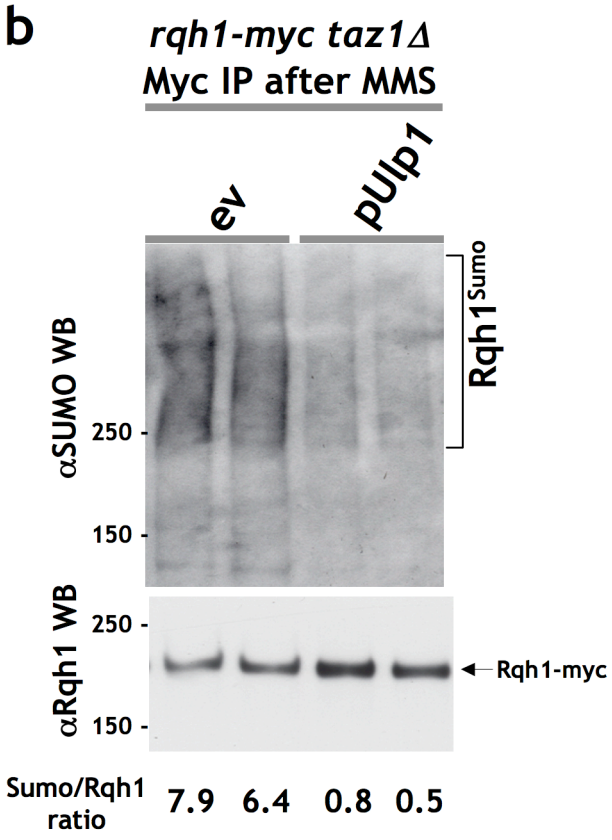
b
rqh1-myc taz1Δ
Myc IP after MMS
ev
pUlp1
αSUMO WB
250
150
Rqh1Sumo
αRqh1 WB
250
150
Rqh1-myc
Sumo/Rqh1 ratio
7.9 6.4 0.8 0.5

When IPs were performed in extracts of methylmethane sulfonate (MMS)-treated cells, αSumo revealed a high-molecular weight smear above Rqh1, which was significantly more abundant compared to undamaged cells (Figure 5.15a and data not shown). The induction of sumoylation upon MMS treatment was reported for Sgs1 in budding yeast (Branzei et al., 2006), and perhaps stems from the vast number of induced lesions. In this case as well, sumoylation was reduced ~2-fold or more in *rqh1-SM* strains (Figure 5.15a). Consistent with SUMO de-conjugation of Rqh1 being a relevant for *taz1Δ* cold sensitivity, overexpression of *ulp1*$^{+}$, to levels that did not modify overall sumoylation patterns (data not shown), reduced MMS-induced Rqh1 sumoylation by 6-10-fold (Figure 5.15b). Another situation where we observed elevated levels of sumoylation was in *rqh1-hd* cells. In this situation as well, sumoylation was significantly reduced upon introduction of the SM mutations into *rqh1-hd-myc* strains (data not shown). The reason for prevalence of sumoylation in an *rqh1-hd* background is currently unclear. However, it raises the possibility that SUMO de-conjugation may be coupled to the catalytic cycle of Rqh1.

The sumoylated forms, in all the abovementioned scenarios, are likely to constitute a small percentage of the total cellular pool of Rqh1, as αRqh1 and αMyc antibodies failed to detect higher molecular weight forms, even at longer exposures (Figure 5.14a and data not shown). A low abundance of the sumoylated form(s) is typical of many sumoylated proteins, and is probably due to the transient nature of sumoylation (Palancade et al., 2007). Nonetheless, the marked reduction of sumoylation suggests that the two predicted sites mutated in *rqh1-SM,* ^{724}PKKD^{727} and ^{921}IKQD^{924}, are indeed sumoylation sites *in vivo*.

Figure 5.16 Analysis of SUMO pathway mutants

(next page) (a) Five-fold serial dilutions of log-phase cultures were spotted onto rich medium (YES), and incubated at 32º or 19°. The *nse2.SA* allele includes mutations that inactivate the SUMO E3-ligase Nse2; *nse2.CH* is included as isogenic wt control. As reported, *nse2.SA* renders the cells sensitive to HU (Andrews et al., 2005). (b*)* Cells harboring the indicated *nse2*$^{+}$ alleles were treated with MMS, and Rqh1-myc was immunoprecipitated. Rqh1 sumoylation in response to MMS was largely dependent on Nse2 SUMO E3-ligase activity.

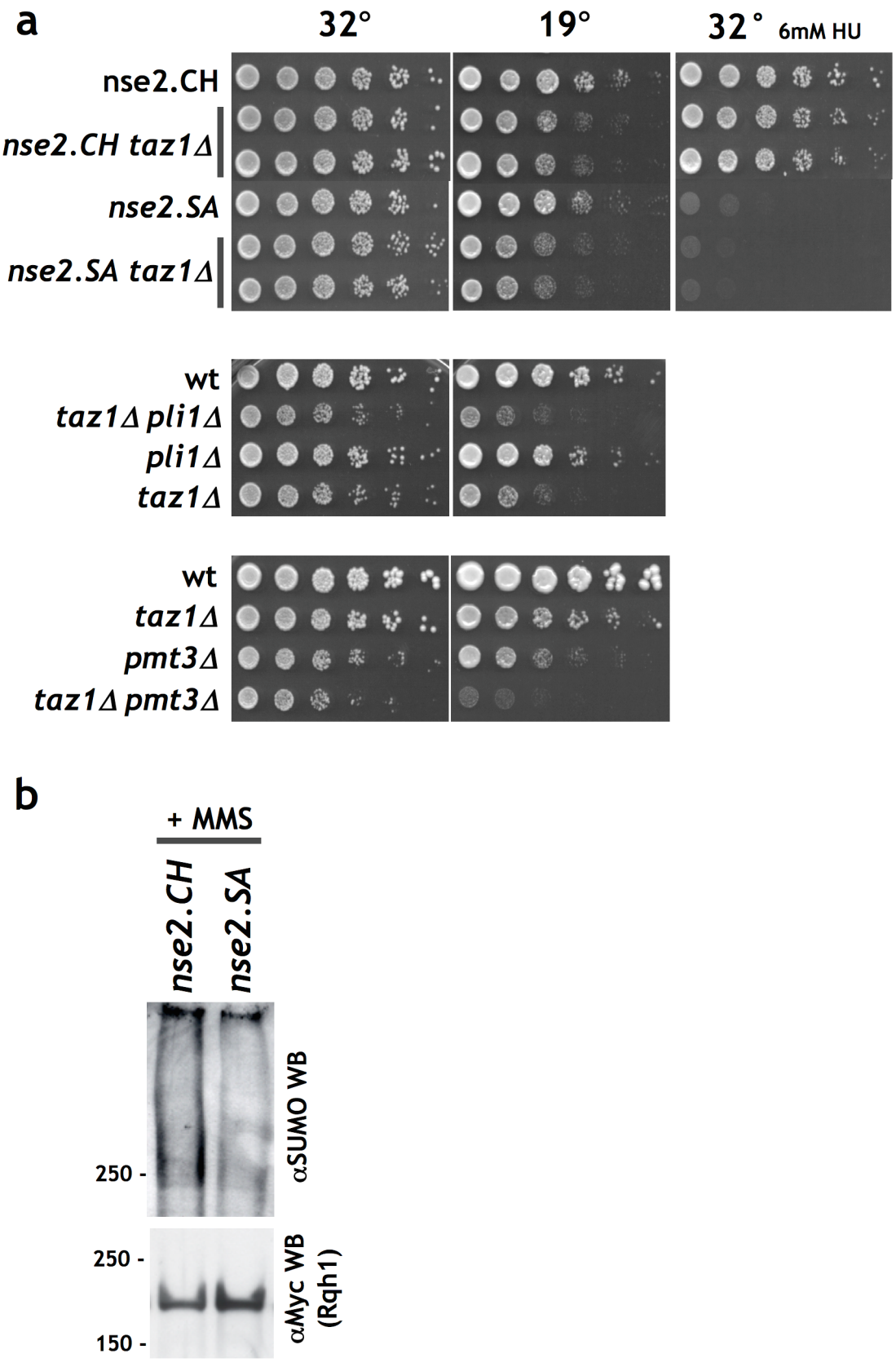
a
32°
19°
32° 6mM HU
nse2.CH
nse2.CH taz1Δ
nse2.SA
nse2.SA taz1Δ
wt
taz1Δ pli1Δ
pli1Δ
taz1Δ
wt
taz1Δ
pmt3Δ
taz1Δ pmt3Δ
b
+ MMS
nse2.CH
nse2.SA
250 -
αSUMO WB
250 -
150 -
αMyc WB
(Rqh1)

5.2.7 Possible regulators of Rqh1 sumoylation

5.2.7.1 SUMO E3-ligases Pli1$^{Siz1/2}$ and Nse2^{Mms21}

What might be the actors regulating Rqh1 sumoylation? An attractive candidate is the SUMO E3-ligase Nse2 (*ScMMS21*), a component of the SMC5/6 complex (Andrews et al., 2005; Potts and Yu, 2005; Zhao and Blobel, 2005). Inactivating the E3-ligase activity of Nse2 (using the 'ligase-dead' *nse2.SA* allele (Andrews et al., 2005)) failed to suppress *taz1Δ* cold sensitivity (Figure 5.16a). As mentioned above, deletion of the other E3-ligase-encoding gene *pli1*$^{+}$ also failed to suppress *taz1Δ* cold sensitivity (Figure 5.16a and Xhemalce et al., 2007). Thus, Pli1 and Nse2 may carry out sumoylation of Rqh1 redundantly, consistent with the observation the both can stimulate Rqh1 sumoylation *in vitro* (Watts et al., 2007). Testing this hypothesis may prove difficult, as strains mutated for both *pli1*$^{+}$ and *nse2*$^{+}$ are very sick, mimicking cells lacking SUMO altogether (*pmt3Δ*) (data not shown and Xhemalce et al., 2007). Genetic analysis is further complicated by the fact that *pmt3Δ* cells lose viability in the cold upon *taz1*$^{+}$ deletion (Figure 5.16a), hinting SUMO may play both a positive and a negative role in *taz1Δ* cold sensitivity. Inactivating the E3-ligase activity of Nse2 reduced the MMS-dependent sumoylation of Rqh1 (Figure 5.16b) without affecting bulk protein sumoylation (data not shown), suggesting Rqh1 sumoylation in response to MMS is largely dependent on Nse2 ligase activity. However, *nse2.SA* failed to suppress *taz1Δ* cold sensitivity, suggesting that either Nse2 has both negative and positive roles in *taz1Δ* cold-sensitivity, or that Rqh1 sumoylation in *taz1Δ* cells is carried out by a different E3-ligase.

5.2.7.2 Slx8

ScSLX5 & 8 were originally isolated as genes whose mutation confers synthetic lethality with *ScSGS1* mutation in budding yeast (Mullen et al., 2001). Later, they were shown to be involved, like Sgs1, in survival following loss of telomerase (Azam et al., 2006; Zhang et al., 2006). In addition, genetic data implicated them in SUMO metabolism, and their deletion resulted in accumulation of sumoylated species (Wang et al., 2006); as they harboured

SUMO interaction motifs (SIMs) and an E3-ligase RING motif, they were postulated to be SUMO-E3 ligases. However, recent data demonstrated that Slx5/8 is in fact a conserved SUMO-targeted ubiquitin E3-ligase (STUbL) (Prudden et al., 2007; Sun et al., 2007; Uzunova et al., 2007).

The connection of Slx5/8 to both RecQ helicases and SUMO prompted us to address its involvement in *taz1*Δ telomere dysfunction. Deletion of *slx8*$^{+}$ confers a severe growth defect (Sun et al., 2007). Thus, we constructed diploids heterozygous for deletions in *taz1*$^{+}$ and *slx8*$^{+}$, sporulated them, and germinated the spores on selective media. We found that selection for *taz1*Δ *slx8*Δ yields much slower growth compared with selection for *slx8*Δ alone (Figure 5.17a); relative sickness persisted when the small *slx8*Δ and *taz1*Δ *slx8*Δ colonies were restreaked onto non-selective media, resulting in a virtually synthetically lethal combination (Figure 5.17b). This result implicates Slx5/8 in *taz1*Δ telomere dysfunction. Taken together with our result showing Rqh1 sumoylation is deleterious to *taz1*Δ cells at cold temperatures, it is possible that Slx5/8 acts to ubiquitinate sumoylated Rqh1, possibly leading to its degradation. In the absence of Slx5/8, accumulation of sumoylated Rqh1 may bear disastrous consequences for *taz1*Δ telomeres, even at 32°.

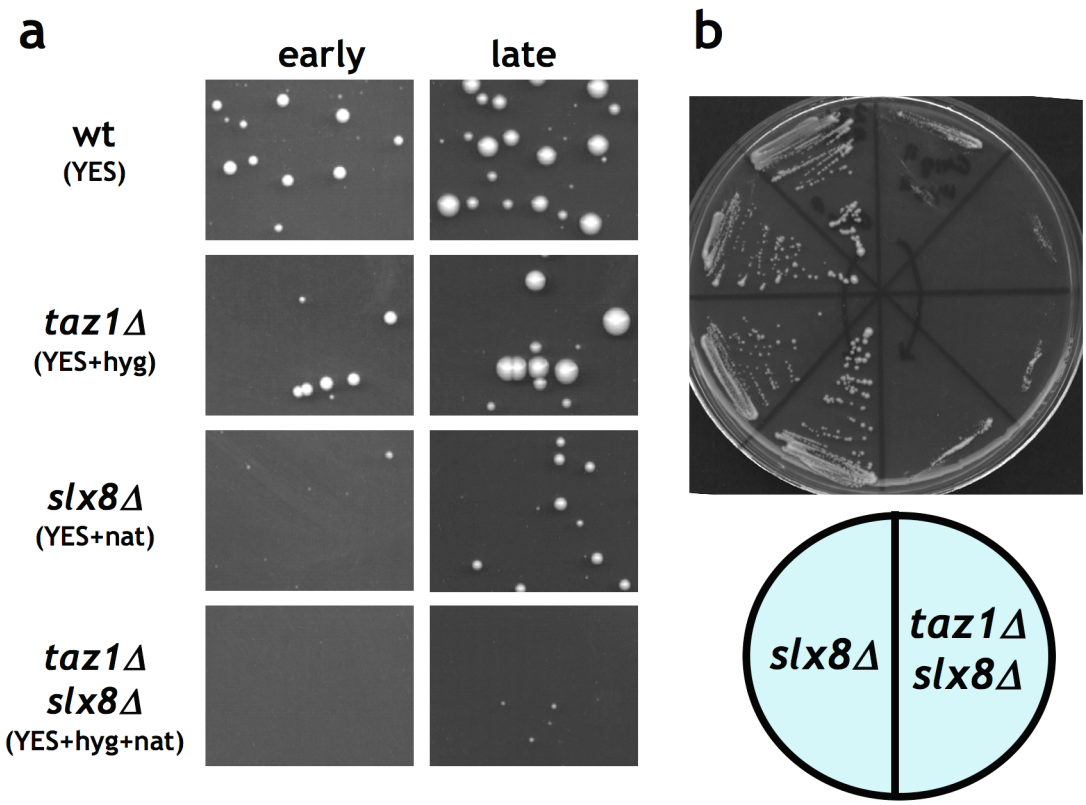

Figure 5.17 *slx8*⁺ deletion is synthetically sick with *taz1*⁺ deletion

(a) *slx8*$^{+/\Delta}$ *taz1*$^{+/\Delta}$ heterozygous diploids were sporulated, and the spores were plated on YES media including appropriate antibiotics to select for single and double mutants. *slx8*⁺ is deleted with a nourseothricin (nat) cassette, and *taz1*⁺ is deleted with a hygromycin B (hyg) cassette. Plates were incubated at 32°, and were scanned after 3 and 5 days ('early' and 'late', respectively). (b) *slx8*Δ and *slx8*Δ *taz1*Δ colonies were re-streaked from the selective plates onto YES media.

5.3 Discussion

In this work we have uncovered a surprisingly central role for Rqh1 in dictating the fate of dysfunctional telomeres. Furthermore, we find that the SUMO pathway controls the activity of Rqh1 at telomeres. Through a genetic screen, we linked the SUMO pathway to the entanglement of *taz1Δ* telomeres that occurs at cold temperatures. We mutated predicted sumoylation sites on Rqh1 and found that its sumoylation is likely to be responsible for several *taz1Δ* phenotypes. Rqh1-SM loses function specifically at the telomere, while retaining many, if not all, of the non-telomere-related functions of Rqh1. Hence, we suggest that sumoylation serves as a key regulator of the different activities attributed to RecQ helicases.

5.3.1 Telomere loss and entanglement

The phenotypes conferred by *rqh1-SM* further strengthen the correlation between the following *taz1Δ*-specific phenomena: telomeric entanglement at cold temperatures, rapid telomere loss in the absence of telomerase, and telomeric hyper-recombination. Indeed, the involvement of sumoylated Rqh1 in this specific array of phenotypes provides a tool for dissecting the precise nature of telomeric entanglement. Cells lacking Rap1, despite phenocopying *taz1Δ* cells in many aspects of telomere dysfunction, are cold-resistant, lose telomeres gradually in the absence of telomerase, and fail to exhibit hyper-recombination (Miller et al., 2006). In addition, *rap1Δ* telomeres are longer than *taz1Δ* telomeres (Kanoh and Ishikawa, 2001), consistent with the notion that impeded replication limits *taz1Δ* telomere length despite the hyperactivity of telomerase at *taz1Δ* telomeres. Introduction of the *rqh1-SM* allele reverses the *taz1Δ*-specific phenotypes such that *taz1Δ rqh1-SM* strains mimic *rap1Δ* strains, exhibiting telomerase hyperactivity and excessive 3' overhang generation without suffering the consequences of stalled telomeric replication forks. As the *rqh1-SM* allele does not suppress the *taz1Δ* fork progression defect, we surmise that sumoylated Rqh1 acts downstream of stalled replication forks, most likely processing them in a manner that prevents fork re-start.

Our results may be related to an intriguing set of observations made in cells harboring a point mutation (*rad11-D223Y*) in the large subunit of RPA that putatively increases its affinity for ssDNA. This mutation causes rapid and complete loss of telomeres when combined with *taz1*$^{+}$ deletion, but not when combined with *rap1*$^{+}$ deletion. However, *rqh1*$^{+}$ inactivation suppresses the rapid telomere loss observed in *taz1Δ rad11-D223Y* cells (Kibe et al., 2007). The *taz1Δ*-specificity of this rapid telomere loss suggests the involvement of stalled telomeric replication forks, and would be consistent with a role for Rqh1 in unwinding DNA at replication forks to allow RPA binding.

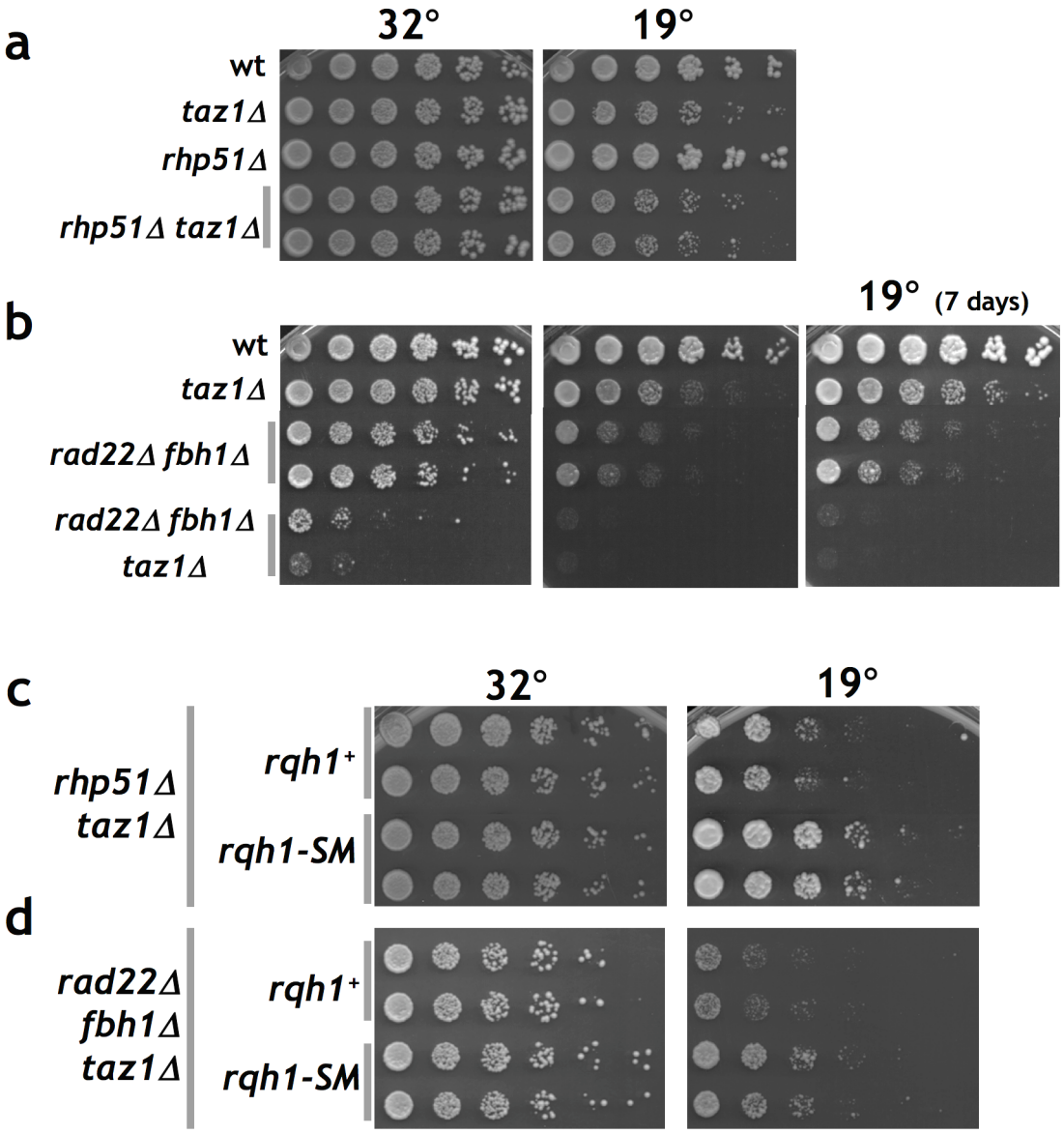

Figure 5.18 Recombination mutants affect *taz1Δ* cold sensitivity

(a) In the slightly sick recombination-deficient *rhp51Δ* strain, *taz1*$^{+}$ deletion conferred further viability loss in the cold. (b) *taz1*$^{+}$ deletion reduces *rad22Δ* viability at cold temperatures in strains lacking *fbh1*$^{+}$, a gene whose mutation commonly arises as a suppressor of the sickness caused by *rad22*$^{+}$ deletion (Osman et al., 2005). The 19° plate was scanned at different days as the *rad22Δ fbh1Δ* cells were considerably slower growing compared to *rad22*$^{+}$ *fbh1*$^{+}$ cells. (c-d) The *rqh1-SM* mutation improved growth of *taz1Δ rhp51Δ* and *taz1Δ rad22Δ fbh1Δ* in the cold. (a-d) Five-fold serial dilutions of log-phase cultures were spotted onto rich medium (YES) and incubated at 32º or 19º.

As the *rqh1-SM* allele prevents both hyper-recombination of *taz1Δ* telomeres and their propensity to confer cold sensitivity, we considered the possibility that *taz1Δ* cold sensitivity could be rescued by blocking recombination. However, in the recombination-deficient *rad22*^{rad52}*Δ* background, *taz1*$^{+}$ deletion caused a general loss of viability at all temperatures and an additional viability loss at cold temperatures (Miller and Cooper, 2003). *rhp51*$^{rad51+}$ deletion also failed to suppress *taz1Δ* cold-sensitivity. Furthermore, neither *rad22*$^{rad52+}$ nor *rhp51*$^{rad51+}$ deletion abolished the suppression conferred by *rqh1-SM* (Figure 5.18). These observations suggest that recombination plays a positive role in disentangling *taz1Δ* telomeres, and that the relevant Rqh1 activity does not directly process Rad22^{Rad52}/Rhp51^{Rad51}-dependent recombination intermediates. However, these results do not rule out the involvement of telomere strand invasion reactions that are independent of Rhp51^{Rad51} and Rad22^{Rad52}.

Analysis of the double mutant *taz1*Δ *rap1*Δ provides additional evidence for the positive role that recombination plays at *taz1*Δ telomeres. Surprisingly, while the absence of Rap1 exacerbates the cold sensitivity of *taz1*Δ cells (Miller and Cooper, 2003; Miller et al., 2005), it also prevents linear survival mode of *taz1*Δ *trt1*Δ cells (Subramanian et al., 2008) – thus resembling absence of Rad22^{Rad52}. As Rap1 is likely to be absent at most *taz1*Δ telomeres (Chikashige and Hiraoka, 2001; Kanoh and Ishikawa, 2001; Subramanian et al., 2008), these observations hint that Rap1 may be modulating recombination *in trans*.

A pertinent unanswered question is whether Rqh1 participates in telomere metabolism in cells with functional telomeres. Fission yeast lacking Rqh1 exhibit neither an obvious telomere length deficit, telomeric end-to-end fusions, nor replication fork stalling at telomeric sequences (data not shown). In human cells lacking both functional WRN and telomerase, telomeres are lost from the sister chromatids that serve as template for lagging strand replication; this defect is suppressed by telomerase expression (Crabbe et al., 2004). Hence, WRN promotes semi-conservative telomere replication, in apparent contrast with our observation that Rqh1 has deleterious effects on *taz1Δ* telomere replication. This contrast may be explained in several ways. First, RecQ helicases may

promote proper telomere maintenance in a manner that depends on Taz1/TRF2. Indeed, the WRN helicase promotes deleterious telomeric HR reactions when TRF2 function is compromised by expressing a dominant negative form ($TRF2^{\Delta B}$) (Li et al., 2008). Alternatively, RecQ sumoylation, which appears to be required for its deleterious effects, might occur specifically in a setting of telomere dysfunction. In these scenarios, Taz1 would be required to control, or to prevent, Rqh1 activity at telomeres, respectively. Finally, not only are human Werner Syndrome (WS) phenotypes alleviated by telomerase expression, but also the phenotypes typical of human WS appear in *WRN*$^{-/-}$ mice only when telomeres are short (i.e. in a late-generation telomerase-minus setting) (Chang et al., 2004). Hence, WRN may be active at telomeres only when the telomeric complex is imbalanced by shortened telomeres.

5.4 Sumoylation regulates Rqh1

An intriguing mystery is how sumoylation affects Rqh1 activity. First, sumoylation may affect its localization to telomeres. Similarly, SUMO may act as 'glue', bringing together telomeric Rqh1 molecules at telomeres, thereby bringing telomeres together and facilitating their entanglement. This type of role has been proposed for SUMO in the assembly of ALT-associated PML bodies (see below) (Eladad et al., 2005; Potts and Yu, 2007). However, the differential effects of distinct K->R mutations in *rqh1*$^{+}$ argue that specific conformational changes are required for its activities at *taz1Δ* telomeres. SUMO may instead affect a specific regulatory interaction between Rqh1 and telomeric proteins or DNA processing factors, e.g. Top2, Top3 or Mus81/Eme1, all of which have been reported to interact with RecQ helicases (Sharma et al., 2006; Watt et al., 1995).

Alternatively, sumoylation of Rqh1 may allow it to process DNA structures that are unique to telomeres. Telomere-specific structures may arise from topological constraints affecting replication forks approaching a chromosome terminus, or from extrusion of G-rich secondary structures. SUMO modification may also alter a specific facet of the many biochemical activities reported for RecQ helicases. *E. coli* RecQ unwinds stalled replication forks prior to RecA loading (Hishida et al., 2004). By analogy, sumoylated Rqh1 may unwind stalled

replication forks at telomeres, preventing fork re-start and channeling the telomeres to a perilous fate. Other biochemical activities of Rqh1 that would be consistent with our observations is promotion of strand annealing (Garcia et al., 2004) or promotion of 5'-end resection together with Exo1 or Dna2 (Mimitou and Symington, 2008; Zhu et al., 2008). In addition, RecQ helicases have been implicated in resolution of branched DNA structures associated with perturbed DNA replication (Branzei et al., 2006). However, we do not observe such X-structures by 2D gel analysis of *taz1Δ* telomere replication (Miller et al., 2006).

5.5 Mechanisms of ALT

RecQ helicases and sumoylation have been separately implicated in promoting recombination at telomeres in budding yeast and mammalian cells lacking telomerase. Budding yeast can survive without telomerase by amplifying either sub-telomeres (Type I) or telomeric repeats (Type II) (Lundblad and Blackburn, 1993)(see also section 1.3.2.1). Type II survival requires Sgs1 (Cohen and Sinclair, 2001; Huang et al., 2001; Johnson et al., 2001); however, a role for sumoylation in this process has not been reported. In mammalian cells proliferating without telomerase through activation of the ALT pathway, telomeres localize to PML bodies in the nucleus, where their elongation presumably occurs *via* recombination (Bryan et al., 1997). Interestingly, these ALT-associated PML bodies contain not only the SUMO-binding protein PML, but also the SMC5/6 complex (which contains the Mms21/Nse2 SUMO E3-ligase) and sumoylated TRF1, TRF2 and BLM; sumoylation-deficient mutants of these proteins hamper their localization to PML bodies (Eladad et al., 2005; Potts and Yu, 2007). Furthermore, upon inhibition of the SMC5/6 complex in ALT cells, telomeres fail to localize to PML bodies and telomere length declines (Potts and Yu, 2007). Hence, the theme of local sumoylation may be common to both human ALT survivors and the ALT-like recombination seen in *taz1Δ trt1Δ* survivors.

Our work provides a plausible scenario for the molecular role of sumoylation in ALT cells: stalled telomeric replication forks (analogous to those seen in *taz1Δ* cells) may accompany the chronic telomere shortening and concomitant imbalance of telomere binding proteins that occurs in these cells.

These stalled forks may be processed by sumoylated RecQ helicases (WRN and/or BLM) to provide substrates for the recombination events that result in the amplification of telomeres. It remains to be determined whether sumoylation of human RecQ helicases is required for ALT, but given the many instances of conserved function between the human and fission yeast telomere complexes, such a requirement is not unlikely.

This study identified Rqh1 and sumoylation as key players in the genesis of entangled telomeres. The *rqh1-SM* allele specifically hampers Rqh1 activity at telomeres, alleviating the telomere breakage, hyper-recombination and entanglement that occur at *taz1Δ* telomeres. These observations prompt the notion that Rqh1 activity transforms stalled telomeric replication forks into highly volatile structures. Elucidating the precise biochemical activities that are regulated by sumoylation will illuminate not only the nature of telomeric entanglements, but also the regulation of the diverse activities attributed to RecQ helicases.

5.5.1 Future Directions

The main mystery stemming from this work is the molecular function(s) of Rqh1 that confers its effects on telomeres. The SUMO requirement for this effect is both a useful tool and a hint for how the myriad roles of RecQ helicases are regulated. Such regulation is likely, as many RecQ helicases were reported to have diverse, and in some cases opposing, activities. For example, BLM can unwind and destabilize D-loops, but is also capable of promoting extension of the invading strand in a D-loop by polymerase η (Bugreev et al., 2007). In another example, the assembly state (oligomerization) of the RecQ homologues RECQ1 and WRN was proposed to regulate their helicase *versus* strand annealing activities (Muftuoglu et al., 2008; Muzzolini et al., 2007).

Sumoylation may regulate the cellular localization of Rqh1. Using immunofluorescence (IF) we have confirmed the previous findings that Rqh1 is present mainly in the nucleolus, and noticed changes in its localization upon DNA replication or damage (Caspari et al., 2002; Laursen et al., 2003) (Figure 5.19 and data not shown). Rqh1 localization was not significantly altered in *rqh1-SM* or *taz1Δ* cells, arguing that localization is unaffected by sumoylation

(Figure 5.19). In our preliminary attempts to assess co-localization of Rqh1 with telomeres using a 6xPK tagged Pot1 (V. Kuznetsov), we did not observe significant changes upon introduction of *rqh1-SM* or *taz1*$^{+}$ deletion (data not shown).

However, due to the very low abundance of Rqh1-SUMO, changes in its localization may be masked by unmodified Rqh1. Several strategies may allow us to overcome this difficulty: first, we can analyze Rqh1-SUMO localization through consecutive chromatin immunoprecipitations (ChIP) against Rqh1 and SUMO, followed by detection of telomeric sequences. Second, we can try to mimic constitutive sumoylation by fusing SUMO in-frame with Rqh1, and examine the localization of this chimera protein.

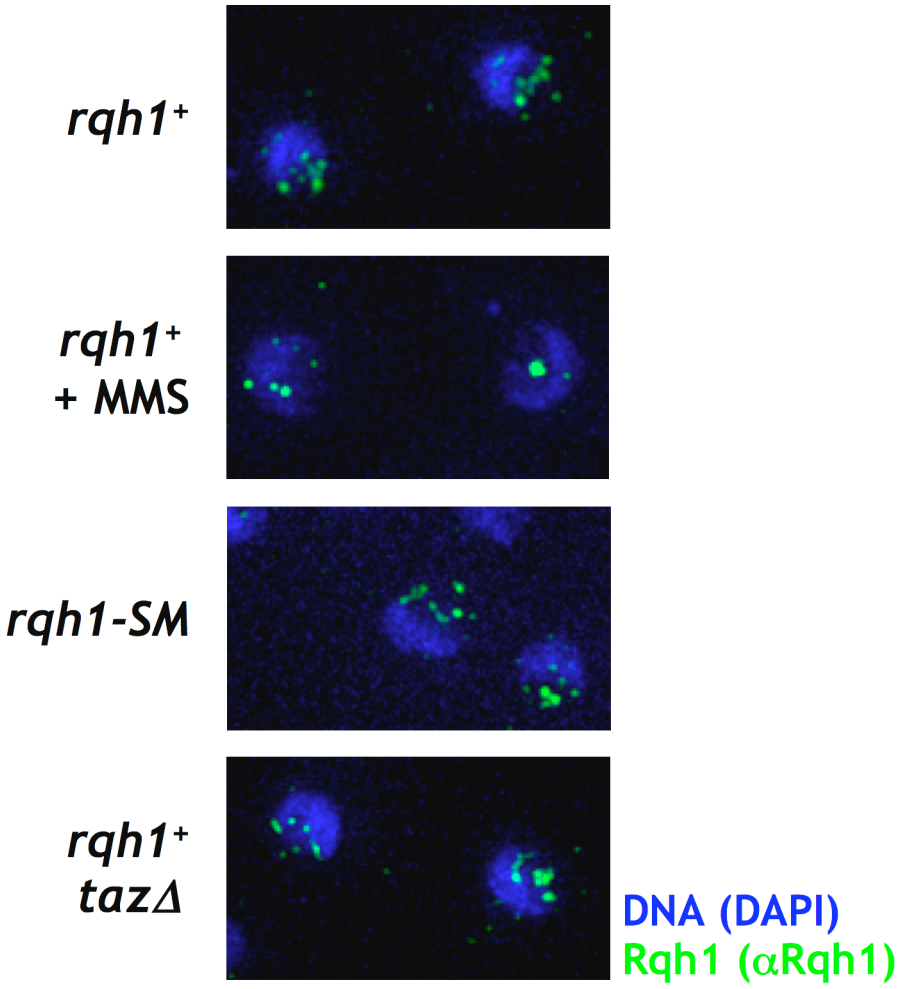

Figure 5.19 Localization of Rqh1

Rqh1 (green) was detected using and αRqh1 antibody (Caspari et al., 2002). DNA (blue) is detected with DAPI. Cells were treated with 0.1% MMS for 3hr, when indicated.

Another attractive hypothesis is that sumoylation changes Rqh1's biochemical activity, the structural specificity for its substrates, or its interaction with regulatory factors. Due to the low abundance of Rqh1-SUMO in the cell (Figures 5.14 and 5.15), it would be impractical to directly purify it. Therefore, we plan to purify bacterially expressed Rqh1, Rqh1-SM and Rqh1-hd, and use previously characterized *in vitro* sumoylation systems (Ho et al., 2001) to obtain large quantities of Rqh1-SUMO. With this reagent in hand, it would be possible to determine the effects of sumoylation on Rqh1 activity in well-established helicase assays on various substrates, and to assess whether sumoylation modulates *in vitro* protein-protein interactions.

6 References

Adams Martin, A., Dionne, I., Wellinger, R.J., and Holm, C. (2000). The function of DNA polymerase alpha at telomeric G tails is important for telomere homeostasis. Mol Cell Biol *20*, 786-796.

Ahn, J.S., Osman, F., and Whitby, M.C. (2005). Replication fork blockage by RTS1 at an ectopic site promotes recombination in fission yeast. Embo J *24*, 2011-2023.

Allshire, R.C., Nimmo, E.R., Ekwall, K., Javerzat, J.P., and Cranston, G. (1995). Mutations derepressing silent centromeric domains in fission yeast disrupt chromosome segregation. Genes Dev *9*, 218-233.

Amiard, S., Doudeau, M., Pinte, S., Poulet, A., Lenain, C., Faivre-Moskalenko, C., Angelov, D., Hug, N., Vindigni, A., Bouvet, P*., et al.* (2007). A topological mechanism for TRF2-enhanced strand invasion. Nat Struct Mol Biol *14*, 147-154.

Ampatzidou, E., Irmisch, A., O'Connell, M.J., and Murray, J.M. (2006). Smc5/6 is required for repair at collapsed replication forks. Mol Cell Biol *26*, 9387-9401.

Andrews, E.A., Palecek, J., Sergeant, J., Taylor, E., Lehmann, A.R., and Watts, F.Z. (2005). Nse2, a component of the Smc5-6 complex, is a SUMO ligase required for the response to DNA damage. Mol Cell Biol *25*, 185-196.

Aparicio, O.M., Billington, B.L., and Gottschling, D.E. (1991). Modifiers of position effect are shared between telomeric and silent mating-type loci in S. cerevisiae. Cell *66*, 1279-1287.

Armanios, M., Chen, J.L., Chang, Y.P., Brodsky, R.A., Hawkins, A., Griffin, C.A., Eshleman, J.R., Cohen, A.R., Chakravarti, A., Hamosh, A*., et al.* (2005). Haploinsufficiency of telomerase reverse transcriptase leads to anticipation in autosomal dominant dyskeratosis congenita. Proc Natl Acad Sci U S A *102*, 15960-15964.

Arneric, M., and Lingner, J. (2007). Tel1 kinase and subtelomere-bound Tbf1 mediate preferential elongation of short telomeres by telomerase in yeast. EMBO Rep *8*, 1080-1085.

Askree, S.H., Yehuda, T., Smolikov, S., Gurevich, R., Hawk, J., Coker, C., Krauskopf, A., Kupiec, M., and McEachern, M.J. (2004). A genome-wide screen for Saccharomyces cerevisiae deletion mutants that affect telomere length. Proc Natl Acad Sci U S A *101*, 8658-8663.

Azam, M., Lee, J.Y., Abraham, V., Chanoux, R., Schoenly, K.A., and Johnson, F.B. (2006). Evidence that the S.cerevisiae Sgs1 protein facilitates recombinational repair of telomeres during senescence. Nucleic Acids Res *34*, 506-516.

Azzalin, C.M., Reichenbach, P., Khoriauli, L., Giulotto, E., and Lingner, J. (2007). Telomeric repeat containing RNA and RNA surveillance factors at mammalian chromosome ends. Science *318*, 798-801.

Bae, N.S., and Baumann, P. (2007). A RAP1/TRF2 complex inhibits nonhomologous end-joining at human telomeric DNA ends. Mol Cell *26*, 323-334.

Bahler, J., Wu, J.Q., Longtine, M.S., Shah, N.G., McKenzie, A., 3rd, Steever, A.B., Wach, A., Philippsen, P., and Pringle, J.R. (1998). Heterologous modules for efficient and versatile PCR-based gene targeting in Schizosaccharomyces pombe. Yeast *14*, 943-951.

Bailey, S.M., Brenneman, M.A., and Goodwin, E.H. (2004). Frequent recombination in telomeric DNA may extend the proliferative life of telomerase-negative cells. Nucleic Acids Res *32*, 3743-3751.

Bailey, S.M., Cornforth, M.N., Kurimasa, A., Chen, D.J., and Goodwin, E.H. (2001). Strand-specific postreplicative processing of mammalian telomeres. Science *293*, 2462-2465.

Baumann, P., and Cech, T.R. (2000). Protection of telomeres by the Ku protein in fission yeast. Mol Biol Cell *11*, 3265-3275.

Baumann, P., and Cech, T.R. (2001). Pot1, the putative telomere end-binding protein in fission yeast and humans. Science *292*, 1171-1175.

Baur, J.A., Zou, Y., Shay, J.W., and Wright, W.E. (2001). Telomere position effect in human cells. Science *292*, 2075-2077.

Beernink, H.T., Miller, K., Deshpande, A., Bucher, P., and Cooper, J.P. (2003). Telomere maintenance in fission yeast requires an Est1 ortholog. Curr Biol *13*, 575-580.

Bennett, C.B., Lewis, A.L., Baldwin, K.K., and Resnick, M.A. (1993). Lethality induced by a single site-specific double-strand break in a dispensable yeast plasmid. Proc Natl Acad Sci U S A *90*, 5613-5617.

Bianchi, A., and Shore, D. (2007a). Early replication of short telomeres in budding yeast. Cell *128*, 1051-1062.

Bianchi, A., and Shore, D. (2007b). Increased association of telomerase with short telomeres in yeast. Genes Dev *21*, 1726-1730.

Bjergbaek, L., Cobb, J.A., Tsai-Pflugfelder, M., and Gasser, S.M. (2005). Mechanistically distinct roles for Sgs1p in checkpoint activation and replication fork maintenance. Embo J *24*, 405-417.

Blasco, M.A. (2007). The epigenetic regulation of mammalian telomeres. Nat Rev Genet *8*, 299-309.

Boulton, S.J., and Jackson, S.P. (1998). Components of the Ku-dependent non-homologous end-joining pathway are involved in telomeric length maintenance and telomeric silencing. Embo J *17*, 1819-1828.

Branzei, D., Sollier, J., Liberi, G., Zhao, X., Maeda, D., Seki, M., Enomoto, T., Ohta, K., and Foiani, M. (2006). Ubc9- and mms21-mediated sumoylation counteracts recombinogenic events at damaged replication forks. Cell *127*, 509-522.

Brewer, B.J., and Fangman, W.L. (1987). The localization of replication origins on ARS plasmids in S. cerevisiae. Cell *51*, 463-471.

Brosh, R.M., Jr., Majumdar, A., Desai, S., Hickson, I.D., Bohr, V.A., and Seidman, M.M. (2001). Unwinding of a DNA triple helix by the Werner and Bloom syndrome helicases. J Biol Chem *276*, 3024-3030.

Brosh, R.M., Jr., Waheed, J., and Sommers, J.A. (2002). Biochemical characterization of the DNA substrate specificity of Werner syndrome helicase. J Biol Chem *277*, 23236-23245.

Bryan, T.M., Englezou, A., Dalla-Pozza, L., Dunham, M.A., and Reddel, R.R. (1997). Evidence for an alternative mechanism for maintaining telomere length in human tumors and tumor-derived cell lines. Nat Med *3*, 1271-1274.

Bugreev, D.V., Yu, X., Egelman, E.H., and Mazin, A.V. (2007). Novel pro- and anti-recombination activities of the Bloom's syndrome helicase. Genes Dev *21*, 3085-3094.

Cam, H.P., Sugiyama, T., Chen, E.S., Chen, X., FitzGerald, P.C., and Grewal, S.I. (2005). Comprehensive analysis of heterochromatin- and RNAi-mediated epigenetic control of the fission yeast genome. Nat Genet *37*, 809-819.

Carson, M.J., and Hartwell, L. (1985). CDC17: an essential gene that prevents telomere elongation in yeast. Cell *42*, 249-257.

Caspari, T., Murray, J.M., and Carr, A.M. (2002). Cdc2-cyclin B kinase activity links Crb2 and Rqh1-topoisomerase III. Genes Dev *16*, 1195-1208.

Celli, G.B., and de Lange, T. (2005). DNA processing is not required for ATM-mediated telomere damage response after TRF2 deletion. Nat Cell Biol *7*, 712-718.

Celli, G.B., Denchi, E.L., and de Lange, T. (2006). Ku70 stimulates fusion of dysfunctional telomeres yet protects chromosome ends from homologous recombination. Nat Cell Biol *8*, 885-890.

Cesare, A.J., and Reddel, R.R. (2008). Telomere uncapping and alternative lengthening of telomeres. Mech Ageing Dev *129*, 99-108.

Chai, W., Du, Q., Shay, J.W., and Wright, W.E. (2006). Human telomeres have different overhang sizes at leading versus lagging strands. Mol Cell *21*, 427-435.

Chang, M., Arneric, M., and Lingner, J. (2007). Telomerase repeat addition processivity is increased at critically short telomeres in a Tel1-dependent manner in Saccharomyces cerevisiae. Genes Dev *21*, 2485-2494.

Chang, S., Multani, A.S., Cabrera, N.G., Naylor, M.L., Laud, P., Lombard, D., Pathak, S., Guarente, L., and DePinho, R.A. (2004). Essential role of limiting telomeres in the pathogenesis of Werner syndrome. Nat Genet *36*, 877-882.

Chen, Q., Ijpma, A., and Greider, C.W. (2001). Two survivor pathways that allow growth in the absence of telomerase are generated by distinct telomere recombination events. Mol Cell Biol *21*, 1819-1827.

Chikashige, Y., Ding, D.Q., Funabiki, H., Haraguchi, T., Mashiko, S., Yanagida, M., and Hiraoka, Y. (1994). Telomere-led premeiotic chromosome movement in fission yeast. Science *264*, 270-273.

Chikashige, Y., Ding, D.Q., Imai, Y., Yamamoto, M., Haraguchi, T., and Hiraoka, Y. (1997). Meiotic nuclear reorganization: switching the position of centromeres and telomeres in the fission yeast Schizosaccharomyces pombe. EMBO J *16*, 193-202.

Chikashige, Y., and Hiraoka, Y. (2001). Telomere binding of the Rap1 protein is required for meiosis in fission yeast. Curr Biol *11*, 1618-1623.

Chikashige, Y., Tsutsumi, C., Yamane, M., Okamasa, K., Haraguchi, T., and Hiraoka, Y. (2006). Meiotic proteins bqt1 and bqt2 tether telomeres to form the bouquet arrangement of chromosomes. Cell *125*, 59-69.

Chiolo, I., Saponaro, M., Baryshnikova, A., Kim, J.H., Seo, Y.S., and Liberi, G. (2007). The human F-Box DNA helicase FBH1 faces Saccharomyces cerevisiae Srs2 and postreplication repair pathway roles. Mol Cell Biol *27*, 7439-7450.

Cohen, H., and Sinclair, D.A. (2001). Recombination-mediated lengthening of terminal telomeric repeats requires the Sgs1 DNA helicase. Proc Natl Acad Sci U S A *98*, 3174-3179.

Cohen, S., and Mechali, M. (2002). Formation of extrachromosomal circles from telomeric DNA in Xenopus laevis. EMBO Rep *3*, 1168-1174.

Constantinou, A., Tarsounas, M., Karow, J.K., Brosh, R.M., Bohr, V.A., Hickson, I.D., and West, S.C. (2000). Werner's syndrome protein (WRN) migrates Holliday junctions and co-localizes with RPA upon replication arrest. EMBO Rep *1*, 80-84.

Cooper, J.P., Nimmo, E.R., Allshire, R.C., and Cech, T.R. (1997). Regulation of telomere length and function by a Myb-domain protein in fission yeast. Nature *385*, 744-747.

Cornforth, M.N., and Eberle, R.L. (2001). Termini of human chromosomes display elevated rates of mitotic recombination. Mutagenesis *16*, 85-89.

Cotta-Ramusino, C., Fachinetti, D., Lucca, C., Doksani, Y., Lopes, M., Sogo, J., and Foiani, M. (2005). Exo1 processes stalled replication forks and counteracts fork reversal in checkpoint-defective cells. Mol Cell *17*, 153-159.

Crabbe, L., Jauch, A., Naeger, C.M., Holtgreve-Grez, H., and Karlseder, J. (2007). Telomere dysfunction as a cause of genomic instability in Werner syndrome. Proc Natl Acad Sci U S A *104*, 2205-2210.

Crabbe, L., Verdun, R.E., Haggblom, C.I., and Karlseder, J. (2004). Defective telomere lagging strand synthesis in cells lacking WRN helicase activity. Science *306*, 1951-1953.

Cristofari, G., and Lingner, J. (2006). Telomere length homeostasis requires that telomerase levels are limiting. EMBO J *25*, 565-574.

d'Adda di Fagagna, F., Reaper, P.M., Clay-Farrace, L., Fiegler, H., Carr, P., Von Zglinicki, T., Saretzki, G., Carter, N.P., and Jackson, S.P. (2003). A DNA damage checkpoint response in telomere-initiated senescence. Nature *426*, 194-198.

Dahlen, M., Olsson, T., Kanter-Smoler, G., Ramne, A., and Sunnerhagen, P. (1998). Regulation of telomere length by checkpoint genes in Schizosaccharomyces pombe. Mol Biol Cell *9*, 611-621.

de Lange, T. (2005). Shelterin: the protein complex that shapes and safeguards human telomeres. Genes Dev *19*, 2100-2110.

Denchi, E.L., and de Lange, T. (2007). Protection of telomeres through independent control of ATM and ATR by TRF2 and POT1. Nature *448*, 1068-1071.

Deng, Z., Dheekollu, J., Broccoli, D., Dutta, A., and Lieberman, P.M. (2007). The origin recognition complex localizes to telomere repeats and prevents telomere-circle formation. Curr Biol *17*, 1989-1995.

Diede, S.J., and Gottschling, D.E. (1999). Telomerase-mediated telomere addition in vivo requires DNA primase and DNA polymerases alpha and delta. Cell *99*, 723-733.

Ding, H., Schertzer, M., Wu, X., Gertsenstein, M., Selig, S., Kammori, M., Pourvali, R., Poon, S., Vulto, I., Chavez, E.*, et al.* (2004). Regulation of murine telomere length by Rtel: an essential gene encoding a helicase-like protein. Cell *117*, 873-886.

Dionne, I., and Wellinger, R.J. (1998). Processing of telomeric DNA ends requires the passage of a replication fork. Nucleic Acids Res *26*, 5365-5371.

Downey, M., Houlsworth, R., Maringele, L., Rollie, A., Brehme, M., Galicia, S., Guillard, S., Partington, M., Zubko, M.K., Krogan, N.J.*, et al.* (2006). A genome-wide screen identifies the evolutionarily conserved KEOPS complex as a telomere regulator. Cell *124*, 1155-1168.

Dubey, D.D., Zhu, J., Carlson, D.L., Sharma, K., and Huberman, J.A. (1994). Three ARS elements contribute to the ura4 replication origin region in the fission yeast, Schizosaccharomyces pombe. EMBO J *13*, 3638-3647.

Ekwall, K., Javerzat, J.P., Lorentz, A., Schmidt, H., Cranston, G., and Allshire, R. (1995). The chromodomain protein Swi6: a key component at fission yeast centromeres. Science *269*, 1429-1431.

Ekwall, K., and Ruusala, T. (1994). Mutations in rik1, clr2, clr3 and clr4 genes asymmetrically derepress the silent mating-type loci in fission yeast. Genetics *136*, 53-64.

Eladad, S., Ye, T.Z., Hu, P., Leversha, M., Beresten, S., Matunis, M.J., and Ellis, N.A. (2005). Intra-nuclear trafficking of the BLM helicase to DNA damage-induced foci is regulated by SUMO modification. Hum Mol Genet *14*, 1351-1365.

Evans, S.K., and Lundblad, V. (1999). Est1 and Cdc13 as comediators of telomerase access. Science *286*, 117-120.

Ferguson, B.M., and Fangman, W.L. (1992). A position effect on the time of replication origin activation in yeast. Cell *68*, 333-339.

Ferreira, M.G., and Cooper, J.P. (2001). The fission yeast Taz1 protein protects chromosomes from Ku-dependent end-to-end fusions. Mol Cell *7*, 55-63.

Ferreira, M.G., and Cooper, J.P. (2004). Two modes of DNA double-strand break repair are reciprocally regulated through the fission yeast cell cycle. Genes Dev *18*, 2249-2254.

Fersht, N., Hermand, D., Hayles, J., and Nurse, P. (2007). Cdc18/CDC6 activates the Rad3-dependent checkpoint in the fission yeast. Nucleic Acids Res *35*, 5323-5337.

Forstemann, K., Hoss, M., and Lingner, J. (2000). Telomerase-dependent repeat divergence at the 3' ends of yeast telomeres. Nucleic Acids Res *28*, 2690-2694.

Frampton, J., Irmisch, A., Green, C.M., Neiss, A., Trickey, M., Ulrich, H.D., Furuya, K., Watts, F.Z., Carr, A.M., and Lehmann, A.R. (2006). Postreplication repair and PCNA modification in Schizosaccharomyces pombe. Mol Biol Cell *17*, 2976-2985.

Frank, C.J., Hyde, M., and Greider, C.W. (2006). Regulation of telomere elongation by the cyclin-dependent kinase CDK1. Mol Cell *24*, 423-432.

Frei, C., and Gasser, S.M. (2000). The yeast Sgs1p helicase acts upstream of Rad53p in the DNA replication checkpoint and colocalizes with Rad53p in S-phase-specific foci. Genes Dev *14*, 81-96.

Gao, H., Cervantes, R.B., Mandell, E.K., Otero, J.H., and Lundblad, V. (2007). RPA-like proteins mediate yeast telomere function. Nat Struct Mol Biol *14*, 208-214.

Garcia, P.L., Liu, Y., Jiricny, J., West, S.C., and Janscak, P. (2004). Human RECQ5beta, a protein with DNA helicase and strand-annealing activities in a single polypeptide. Embo J *23*, 2882-2891.

Garvik, B., Carson, M., and Hartwell, L. (1995). Single-stranded DNA arising at telomeres in cdc13 mutants may constitute a specific signal for the RAD9 checkpoint. Mol Cell Biol *15*, 6128-6138.

Gasser, R., Koller, T., and Sogo, J.M. (1996). The stability of nucleosomes at the replication fork. J Mol Biol *258*, 224-239.

Geiss-Friedlander, R., and Melchior, F. (2007). Concepts in sumoylation: a decade on. Nat Rev Mol Cell Biol.

Gottschling, D.E., Aparicio, O.M., Billington, B.L., and Zakian, V.A. (1990). Position effect at S. cerevisiae telomeres: reversible repression of Pol II transcription. Cell *63*, 751-762.

Gravel, S., Larrivee, M., Labrecque, P., and Wellinger, R.J. (1998). Yeast Ku as a regulator of chromosomal DNA end structure. Science *280*, 741-744.

Gravel, S., and Wellinger, R.J. (2002). Maintenance of double-stranded telomeric repeats as the critical determinant for cell viability in yeast cells lacking Ku. Mol Cell Biol *22*, 2182-2193.

Greenwell, P.W., Kronmal, S.L., Porter, S.E., Gassenhuber, J., Obermaier, B., and Petes, T.D. (1995). TEL1, a gene involved in controlling telomere length in S. cerevisiae, is homologous to the human ataxia telangiectasia gene. Cell *82*, 823-829.

Greider, C.W., and Blackburn, E.H. (1985). Identification of a specific telomere terminal transferase activity in Tetrahymena extracts. Cell *43*, 405-413.

Greider, C.W., and Blackburn, E.H. (1987). The telomere terminal transferase of Tetrahymena is a ribonucleoprotein enzyme with two kinds of primer specificity. Cell *51*, 887-898.

Griffith, J.D., Comeau, L., Rosenfield, S., Stansel, R.M., Bianchi, A., Moss, H., and de Lange, T. (1999). Mammalian telomeres end in a large duplex loop. Cell *97*, 503-514.

Groff-Vindman, C., Cesare, A.J., Natarajan, S., Griffith, J.D., and McEachern, M.J. (2005). Recombination at long mutant telomeres produces tiny single- and double-stranded telomeric circles. Mol Cell Biol *25*, 4406-4412.

Hall, I.M., Noma, K., and Grewal, S.I. (2003). RNA interference machinery regulates chromosome dynamics during mitosis and meiosis in fission yeast. Proc Natl Acad Sci U S A *100*, 193-198.

Hardy, C.F., Sussel, L., and Shore, D. (1992). A RAP1-interacting protein involved in transcriptional silencing and telomere length regulation. Genes Dev *6*, 801-814.

Harley, C.B. (2008). Telomerase and cancer therapeutics. Nat Rev Cancer *8*, 167-179.

Hartwell, L.H., and Smith, D. (1985). Altered fidelity of mitotic chromosome transmission in cell cycle mutants of S. cerevisiae. Genetics *110*, 381-395.

Hathcock, K.S., Hemann, M.T., Opperman, K.K., Strong, M.A., Greider, C.W., and Hodes, R.J. (2002). Haploinsufficiency of mTR results in defects in telomere elongation. Proc Natl Acad Sci U S A *99*, 3591-3596.

Hector, R.E., Shtofman, R.L., Ray, A., Chen, B.R., Nyun, T., Berkner, K.L., and Runge, K.W. (2007). Tel1p preferentially associates with short telomeres to stimulate their elongation. Mol Cell *27*, 851-858.

Hemann, M.T., Strong, M.A., Hao, L.Y., and Greider, C.W. (2001). The shortest telomere, not average telomere length, is critical for cell viability and chromosome stability. Cell *107*, 67-77.

Henikoff, S. (1992). Position effect and related phenomena. Curr Opin Genet Dev *2*, 907-912.

Hishida, T., Han, Y.W., Shibata, T., Kubota, Y., Ishino, Y., Iwasaki, H., and Shinagawa, H. (2004). Role of the Escherichia coli RecQ DNA helicase in SOS signaling and genome stabilization at stalled replication forks. Genes Dev *18*, 1886-1897.

Ho, J.C., Warr, N.J., Shimizu, H., and Watts, F.Z. (2001). SUMO modification of Rad22, the Schizosaccharomyces pombe homologue of the recombination protein Rad52. Nucleic Acids Res *29*, 4179-4186.

Hockemeyer, D., Daniels, J.P., Takai, H., and de Lange, T. (2006). Recent expansion of the telomeric complex in rodents: Two distinct POT1 proteins protect mouse telomeres. Cell *126*, 63-77.

Hu, Y., Raynard, S., Sehorn, M.G., Lu, X., Bussen, W., Zheng, L., Stark, J.M., Barnes, E.L., Chi, P., Janscak, P.*, et al.* (2007). RECQL5/Recql5 helicase regulates homologous recombination and suppresses tumor formation via disruption of Rad51 presynaptic filaments. Genes Dev *21*, 3073-3084.

Huang, P., Pryde, F.E., Lester, D., Maddison, R.L., Borts, R.H., Hickson, I.D., and Louis, E.J. (2001). SGS1 is required for telomere elongation in the absence of telomerase. Curr Biol *11*, 125-129.

Huber, M.D., Duquette, M.L., Shiels, J.C., and Maizels, N. (2006). A conserved G4 DNA binding domain in RecQ family helicases. J Mol Biol *358*, 1071-1080.

Ira, G., Malkova, A., Liberi, G., Foiani, M., and Haber, J.E. (2003). Srs2 and Sgs1-Top3 Suppress Crossovers during Double-Strand Break Repair in Yeast. Cell *115*, 401-411.

Ivessa, A.S., Lenzmeier, B.A., Bessler, J.B., Goudsouzian, L.K., Schnakenberg, S.L., and Zakian, V.A. (2003). The Saccharomyces cerevisiae helicase Rrm3p facilitates replication past nonhistone protein-DNA complexes. Mol Cell *12*, 1525-1536.

Ivessa, A.S., Zhou, J.Q., Schulz, V.P., Monson, E.K., and Zakian, V.A. (2002). Saccharomyces Rrm3p, a 5' to 3' DNA helicase that promotes replication fork progression through telomeric and subtelomeric DNA. Genes Dev *16*, 1383-1396.

Johnson, E.S., and Blobel, G. (1999). Cell cycle-regulated attachment of the ubiquitin-related protein SUMO to the yeast septins. J Cell Biol *147*, 981-994.

Johnson, F.B., Marciniak, R.A., McVey, M., Stewart, S.A., Hahn, W.C., and Guarente, L. (2001). The Saccharomyces cerevisiae WRN homolog Sgs1p participates in telomere maintenance in cells lacking telomerase. Embo J *20*, 905-913.

Kanoh, J., and Ishikawa, F. (2001). spRap1 and spRif1, recruited to telomeres by Taz1, are essential for telomere function in fission yeast. Curr Biol *11*, 1624-1630.

Kanoh, J., Sadaie, M., Urano, T., and Ishikawa, F. (2005). Telomere binding protein Taz1 establishes Swi6 heterochromatin independently of RNAi at telomeres. Curr Biol *15*, 1808-1819.

Karlseder, J., Broccoli, D., Dai, Y., Hardy, S., and de Lange, T. (1999). p53- and ATM-dependent apoptosis induced by telomeres lacking TRF2. Science *283*, 1321-1325.

Karlseder, J., Hoke, K., Mirzoeva, O.K., Bakkenist, C., Kastan, M.B., Petrini, J.H., and de Lange, T. (2004). The telomeric protein TRF2 binds the ATM kinase and can inhibit the ATM-dependent DNA damage response. PLoS Biol *2*, E240.

Karow, J.K., Chakraverty, R.K., and Hickson, I.D. (1997). The Bloom's syndrome gene product is a 3'-5' DNA helicase. J Biol Chem *272*, 30611-30614.

Karow, J.K., Constantinou, A., Li, J.L., West, S.C., and Hickson, I.D. (2000). The Bloom's syndrome gene product promotes branch migration of holliday junctions. Proc Natl Acad Sci U S A *97*, 6504-6508.

Kibe, T., Ono, Y., Sato, K., and Ueno, M. (2007). Fission yeast Taz1 and RPA are synergistically required to prevent rapid telomere loss. Mol Biol Cell *18*, 2378-2387.

Kibe, T., Tomita, K., Matsuura, A., Izawa, D., Kodaira, T., Ushimaru, T., Uritani, M., and Ueno, M. (2003). Fission yeast Rhp51 is required for the maintenance of telomere structure in the absence of the Ku heterodimer. Nucleic Acids Res *31*, 5054-5063.

Klobutcher, L.A., Swanton, M.T., Donini, P., and Prescott, D.M. (1981). All gene-sized DNA molecules in four species of hypotrichs have the same terminal sequence and an unusual 3' terminus. Proc Natl Acad Sci U S A *78*, 3015-3019.

Kosoy, A., Calonge, T.M., Outwin, E.A., and O'Connell, M.J. (2007). Fission yeast Rnf4 homologs are required for DNA repair. J Biol Chem *282*, 20388-20394.

Krauskopf, A., and Blackburn, E.H. (1996). Control of telomere growth by interactions of RAP1 with the most distal telomeric repeats. Nature *383*, 354-357.

Kyrion, G., Liu, K., Liu, C., and Lustig, A.J. (1993). RAP1 and telomere structure regulate telomere position effects in Saccharomyces cerevisiae. Genes Dev *7*, 1146-1159.

Lambert, S., Watson, A., Sheedy, D.M., Martin, B., and Carr, A.M. (2005). Gross chromosomal rearrangements and elevated recombination at an inducible site-specific replication fork barrier. Cell *121*, 689-702.

Larrivee, M., LeBel, C., and Wellinger, R.J. (2004). The generation of proper constitutive G-tails on yeast telomeres is dependent on the MRX complex. Genes Dev *18*, 1391-1396.

Laud, P.R., Multani, A.S., Bailey, S.M., Wu, L., Ma, J., Kingsley, C., Lebel, M., Pathak, S., DePinho, R.A., and Chang, S. (2005). Elevated telomere-telomere recombination in WRN-deficient, telomere dysfunctional cells promotes escape from senescence and engagement of the ALT pathway. Genes Dev *19*, 2560-2570.

Laursen, L.V., Ampatzidou, E., Andersen, A.H., and Murray, J.M. (2003). Role for the fission yeast RecQ helicase in DNA repair in G2. Mol Cell Biol *23*, 3692-3705.

Leonardi, J., Box, J.A., Bunch, J.T., and Baumann, P. (2008). TER1, the RNA subunit of fission yeast telomerase. Nat Struct Mol Biol *15*, 26-33.

Levy, D.L., and Blackburn, E.H. (2004). Counting of Rif1p and Rif2p on Saccharomyces cerevisiae telomeres regulates telomere length. Mol Cell Biol *24*, 10857-10867.

Li, B., Jog, S.P., Reddy, S., and Comai, L. (2008). WRN controls formation of extrachromosomal telomeric circles and is required for TRF2DeltaB-mediated telomere shortening. Mol Cell Biol *28*, 1892-1904.

Li, B., and Lustig, A.J. (1996). A novel mechanism for telomere size control in Saccharomyces cerevisiae. Genes Dev *10*, 1310-1326.

Li, S.J., and Hochstrasser, M. (1999). A new protease required for cell-cycle progression in yeast. Nature *398*, 246-251.

Lingner, J., Cooper, J.P., and Cech, T.R. (1995). Telomerase and DNA end replication: no longer a lagging strand problem? Science *269*, 1533-1534.

Loayza, D., and De Lange, T. (2003). POT1 as a terminal transducer of TRF1 telomere length control. Nature *423*, 1013-1018.

Londono-Vallejo, J.A., Der-Sarkissian, H., Cazes, L., Bacchetti, S., and Reddel, R.R. (2004). Alternative lengthening of telomeres is characterized by high rates of telomeric exchange. Cancer Res *64*, 2324-2327.

Lorentz, A., Heim, L., and Schmidt, H. (1992). The switching gene swi6 affects recombination and gene expression in the mating-type region of Schizosaccharomyces pombe. Mol Gen Genet *233*, 436-442.

Louis, E.J., and Haber, J.E. (1990). Mitotic recombination among subtelomeric Y' repeats in Saccharomyces cerevisiae. Genetics *124*, 547-559.

Lundblad, V., and Blackburn, E.H. (1993). An alternative pathway for yeast telomere maintenance rescues est1- senescence. Cell *73*, 347-360.

Lustig, A.J. (2003). Clues to catastrophic telomere loss in mammals from yeast telomere rapid deletion. Nat Rev Genet *4*, 916-923.

Lustig, A.J., and Petes, T.D. (1986). Identification of yeast mutants with altered telomere structure. Proc Natl Acad Sci U S A *83*, 1398-1402.

Lydeard, J.R., Jain, S., Yamaguchi, M., and Haber, J.E. (2007). Break-induced replication and telomerase-independent telomere maintenance require Pol32. Nature *448*, 820-823.

Machwe, A., Xiao, L., Groden, J., Matson, S.W., and Orren, D.K. (2005). RecQ family members combine strand pairing and unwinding activities to catalyze strand exchange. J Biol Chem *280*, 23397-23407.

Makovets, S., Herskowitz, I., and Blackburn, E.H. (2004). Anatomy and dynamics of DNA replication fork movement in yeast telomeric regions. Mol Cell Biol *24*, 4019-4031.

Mandell, J.G., Goodrich, K.J., Bahler, J., and Cech, T.R. (2005). Expression of a RecQ helicase homolog affects progression through crisis in fission yeast lacking telomerase. J Biol Chem *280*, 5249-5257.

Mankouri, H.W., and Hickson, I.D. (2004). Understanding the roles of RecQ helicases in the maintenance of genome integrity and suppression of tumorigenesis. Biochem Soc Trans *32*, 957-958.

Manolis, K.G., Nimmo, E.R., Hartsuiker, E., Carr, A.M., Jeggo, P.A., and Allshire, R.C. (2001). Novel functional requirements for non-homologous DNA end joining in Schizosaccharomyces pombe. EMBO J *20*, 210-221.

Marcand, S., Brevet, V., and Gilson, E. (1999). Progressive cis-inhibition of telomerase upon telomere elongation. Embo J *18*, 3509-3519.

Marcand, S., Brevet, V., Mann, C., and Gilson, E. (2000). Cell cycle restriction of telomere elongation. Curr Biol *10*, 487-490.

Marcand, S., Gilson, E., and Shore, D. (1997). A protein-counting mechanism for telomere length regulation in yeast. Science *275*, 986-990.

Maringele, L., and Lydall, D. (2002). EXO1-dependent single-stranded DNA at telomeres activates subsets of DNA damage and spindle checkpoint pathways in budding yeast yku70Delta mutants. Genes Dev *16*, 1919-1933.

Martin, V., Du, L.L., Rozenzhak, S., and Russell, P. (2007). Protection of telomeres by a conserved Stn1-Ten1 complex. Proc Natl Acad Sci U S A *104*, 14038-14043.

McClintock, B. (1939). The Behavior in Successive Nuclear Divisions of a Chromosome Broken at Meiosis. Proc Natl Acad Sci U S A *25*, 405-416.

Michelson, R.J., Rosenstein, S., and Weinert, T. (2005). A telomeric repeat sequence adjacent to a DNA double-stranded break produces an anticheckpoint. Genes Dev *19*, 2546-2559.

Miller, K.M., and Cooper, J.P. (2003). The telomere protein Taz1 is required to prevent and repair genomic DNA breaks. Mol Cell *11*, 303-313.

Miller, K.M., Ferreira, M.G., and Cooper, J.P. (2005). Taz1, Rap1 and Rif1 act both interdependently and independently to maintain telomeres. Embo J *24*, 3128-3135.

Miller, K.M., Rog, O., and Cooper, J.P. (2006). Semi-conservative DNA replication through telomeres requires Taz1. Nature *440*, 824-828.

Mimitou, E.P., and Symington, L.S. (2008). Sae2, Exo1 and Sgs1 collaborate in DNA double-strand break processing. Nature.

Miyoshi, T., Kanoh, J., Saito, M., and Ishikawa, F. (2008). Fission yeast Pot1-Tpp1 protects telomeres and regulates telomere length. Science *320*, 1341-1344.

Mohaghegh, P., Karow, J.K., Brosh Jr, R.M., Jr., Bohr, V.A., and Hickson, I.D. (2001). The Bloom's and Werner's syndrome proteins are DNA structure-specific helicases. Nucleic Acids Res *29*, 2843-2849.

Moretti, P., Freeman, K., Coodly, L., and Shore, D. (1994). Evidence that a complex of SIR proteins interacts with the silencer and telomere-binding protein RAP1. Genes Dev *8*, 2257-2269.

Morishita, T., Furukawa, F., Sakaguchi, C., Toda, T., Carr, A.M., Iwasaki, H., and Shinagawa, H. (2005). Role of the Schizosaccharomyces pombe F-Box DNA helicase in processing recombination intermediates. Mol Cell Biol *25*, 8074-8083.

Mozdy, A.D., and Cech, T.R. (2006). Low abundance of telomerase in yeast: implications for telomerase haploinsufficiency. RNA *12*, 1721-1737.

Muftuoglu, M., Kulikowicz, T., Beck, G., Lee, J.W., Piotrowski, J., and Bohr, V.A. (2008). Intrinsic ssDNA Annealing Activity in the C-Terminal Region of WRN. Biochemistry.

Mullen, J.R., Kaliraman, V., Ibrahim, S.S., and Brill, S.J. (2001). Requirement for three novel protein complexes in the absence of the Sgs1 DNA helicase in Saccharomyces cerevisiae. Genetics *157*, 103-118.

Muller, H.J. (1938). The remaking of chromosomes. Collecting Net *13*, 181-185.

Murray, J.M., and Carr, A.M. (2008). Smc5/6: a link between DNA repair and unidirectional replication? Nat Rev Mol Cell Biol *9*, 177-182.

Murray, J.M., Lindsay, H.D., Munday, C.A., and Carr, A.M. (1997). Role of Schizosaccharomyces pombe RecQ homolog, recombination, and checkpoint genes in UV damage tolerance. Mol Cell Biol *17*, 6868-6875.

Muzzolini, L., Beuron, F., Patwardhan, A., Popuri, V., Cui, S., Niccolini, B., Rappas, M., Freemont, P.S., and Vindigni, A. (2007). Different quaternary structures of human RECQ1 are associated with its dual enzymatic activity. PLoS Biol *5*, e20.

Naito, T., Matsuura, A., and Ishikawa, F. (1998). Circular chromosome formation in a fission yeast mutant defective in two ATM homologues. Nat Genet *20*, 203-206.

Nakamura, T.M., Cooper, J.P., and Cech, T.R. (1998). Two modes of survival of fission yeast without telomerase. Science *282*, 493-496.

Natarajan, S., and McEachern, M.J. (2002). Recombinational telomere elongation promoted by DNA circles. Mol Cell Biol *22*, 4512-4521.

Nimmo, E.R., Pidoux, A.L., Perry, P.E., and Allshire, R.C. (1998). Defective meiosis in telomere-silencing mutants of Schizosaccharomyces pombe. Nature *392*, 825-828.

Ohki, R., and Ishikawa, F. (2004). Telomere-bound TRF1 and TRF2 stall the replication fork at telomeric repeats. Nucleic Acids Res *32*, 1627-1637.

Olovnikov, A.M. (1973). A theory of marginotomy. The incomplete copying of template margin in enzymic synthesis of polynucleotides and biological significance of the phenomenon. J Theor Biol *41*, 181-190.

Opresko, P.L., Mason, P.A., Podell, E.R., Lei, M., Hickson, I.D., Cech, T.R., and Bohr, V.A. (2005). POT1 stimulates RecQ helicases WRN and BLM to unwind telomeric DNA substrates. J Biol Chem *280*, 32069-32080.

Opresko, P.L., von Kobbe, C., Laine, J.P., Harrigan, J., Hickson, I.D., and Bohr, V.A. (2002). Telomere-binding protein TRF2 binds to and stimulates the Werner and Bloom syndrome helicases. J Biol Chem *277*, 41110-41119.

Osman, F., Dixon, J., Barr, A.R., and Whitby, M.C. (2005). The F-Box DNA helicase Fbh1 prevents Rhp51-dependent recombination without mediator proteins. Mol Cell Biol *25*, 8084-8096.

Palancade, B., Liu, X., Garcia-Rubio, M., Aguilera, A., Zhao, X., and Doye, V. (2007). Nucleoporins prevent DNA damage accumulation by modulating Ulp1-dependent sumoylation processes. Mol Biol Cell *18*, 2912-2923.

Papouli, E., Chen, S., Davies, A.A., Huttner, D., Krejci, L., Sung, P., and Ulrich, H.D. (2005). Crosstalk between SUMO and ubiquitin on PCNA is mediated by recruitment of the helicase Srs2p. Mol Cell *19*, 123-133.

Pearson, C.E., Nichol Edamura, K., and Cleary, J.D. (2005). Repeat instability: mechanisms of dynamic mutations. Nat Rev Genet *6*, 729-742.

Pfander, B., Moldovan, G.L., Sacher, M., Hoege, C., and Jentsch, S. (2005). SUMO-modified PCNA recruits Srs2 to prevent recombination during S phase. Nature *436*, 428-433.

Potts, P.R., and Yu, H. (2005). Human MMS21/NSE2 is a SUMO ligase required for DNA repair. Mol Cell Biol *25*, 7021-7032.

Potts, P.R., and Yu, H. (2007). The SMC5/6 complex maintains telomere length in ALT cancer cells through SUMOylation of telomere-binding proteins. Nat Struct Mol Biol *14*, 581-590.

Prudden, J., Pebernard, S., Raffa, G., Slavin, D.A., Perry, J.J., Tainer, J.A., McGowan, C.H., and Boddy, M.N. (2007). SUMO-targeted ubiquitin ligases in genome stability. Embo J *26*, 4089-4101.

Qi, H., and Zakian, V.A. (2000). The Saccharomyces telomere-binding protein Cdc13p interacts with both the catalytic subunit of DNA polymerase alpha and the telomerase-associated est1 protein. Genes Dev *14*, 1777-1788.

Raices, M., Verdun, R.E., Compton, S.A., Haggblom, C.I., Griffith, J.D., Dillin, A., and Karlseder, J. (2008). C. elegans telomeres contain G-strand and C-strand overhangs that are bound by distinct proteins. Cell *132*, 745-757.

Rajaraman, S., Choi, J., Cheung, P., Beaudry, V., Moore, H., and Artandi, S.E. (2007). Telomere uncapping in progenitor cells with critical telomere shortening is coupled to S-phase progression in vivo. Proc Natl Acad Sci U S A *104*, 17747-17752.

Ritchie, K.B., Mallory, J.C., and Petes, T.D. (1999). Interactions of TLC1 (which encodes the RNA subunit of telomerase), TEL1, and MEC1 in regulating telomere length in the yeast Saccharomyces cerevisiae. Mol Cell Biol *19*, 6065-6075.

Rog, O., and Cooper, J.P. (2008). Telomeres in Drag: dressing as DNA damage to engage telomerase. Curr Opin Genet Dev *18*, 212-220.

Rustici, G., Mata, J., Kivinen, K., Lio, P., Penkett, C.J., Burns, G., Hayles, J., Brazma, A., Nurse, P., and Bahler, J. (2004). Periodic gene expression program of the fission yeast cell cycle. Nat Genet *36*, 809-817.

Sabourin, M., Tuzon, C.T., and Zakian, V.A. (2007). Telomerase and Tel1p preferentially associate with short telomeres in S. cerevisiae. Mol Cell *27*, 550-561.

Saharia, A., Guittat, L., Crocker, S., Lim, A., Steffen, M., Kulkarni, S., and Stewart, S.A. (2008). Flap endonuclease 1 contributes to telomere stability. Curr Biol *18*, 496-500.

Sato, M., Dhut, S., and Toda, T. (2005). New drug-resistant cassettes for gene disruption and epitope tagging in Schizosaccharomyces pombe. Yeast *22*, 583-591.

Schoeftner, S., and Blasco, M.A. (2008). Developmentally regulated transcription of mammalian telomeres by DNA-dependent RNA polymerase II. Nat Cell Biol *10*, 228-236.

Segurado, M., de Luis, A., and Antequera, F. (2003). Genome-wide distribution of DNA replication origins at A+T-rich islands in Schizosaccharomyces pombe. EMBO Rep *4*, 1048-1053.

Sfeir, A.J., Chai, W., Shay, J.W., and Wright, W.E. (2005). Telomere-end processing the terminal nucleotides of human chromosomes. Mol Cell *18*, 131-138.

Shampay, J., Szostak, J.W., and Blackburn, E.H. (1984). DNA sequences of telomeres maintained in yeast. Nature *310*, 154-157.

Sharma, S., Doherty, K.M., and Brosh, R.M., Jr. (2006). Mechanisms of RecQ helicases in pathways of DNA metabolism and maintenance of genomic stability. Biochem J *398*, 319-337.

Shay, J.W., and Wright, W.E. (2006). Telomerase and Human Cancer. In Telomeres, 2nd Edition, T. de Lange, V. Lundblad, and E.H. Blackburn, eds. (Cold Spring Harbor Laboratory Press).

Shen, J.C., Gray, M.D., Oshima, J., and Loeb, L.A. (1998). Characterization of Werner syndrome protein DNA helicase activity: directionality, substrate dependence and stimulation by replication protein A. Nucleic Acids Res *26*, 2879-2885.

Smogorzewska, A., Karlseder, J., Holtgreve-Grez, H., Jauch, A., and de Lange, T. (2002). DNA ligase IV-dependent NHEJ of deprotected mammalian telomeres in G1 and G2. Curr Biol *12*, 1635-1644.

Smolikov, S., Mazor, Y., and Krauskopf, A. (2004). ELG1, a regulator of genome stability, has a role in telomere length regulation and in silencing. Proc Natl Acad Sci U S A *101*, 1656-1661.

Sogo, J.M., Lopes, M., and Foiani, M. (2002). Fork reversal and ssDNA accumulation at stalled replication forks owing to checkpoint defects. Science *297*, 599-602.

Stewart, E., Chapman, C.R., Al-Khodairy, F., Carr, A.M., and Enoch, T. (1997). rqh1+, a fission yeast gene related to the Bloom's and Werner's syndrome genes, is required for reversible S phase arrest. Embo J *16*, 2682-2692.

Subramanian, L., Moser, B.A., and Nakamura, T.M. (2008). Recombination-based telomere maintenance is dependent on Tel1-MRN and Rap1 and inhibited by telomerase, Taz1, and Ku in fission yeast. Mol Cell Biol *28*, 1443-1455.

Sugawara, N.F. (1988). DNA Sequences at the Telomeres of the Fission Yeast S. pombe (Cambridge, MA, Harvard University).

Sun, H., Karow, J.K., Hickson, I.D., and Maizels, N. (1998). The Bloom's syndrome helicase unwinds G4 DNA. J Biol Chem *273*, 27587-27592.

Sun, H., Leverson, J.D., and Hunter, T. (2007). Conserved function of RNF4 family proteins in eukaryotes: targeting a ubiquitin ligase to SUMOylated proteins. Embo J *26*, 4102-4112.

Taggart, A.K., Teng, S.C., and Zakian, V.A. (2002). Est1p as a cell cycle-regulated activator of telomere-bound telomerase. Science *297*, 1023-1026.

Takai, H., Smogorzewska, A., and de Lange, T. (2003). DNA damage foci at dysfunctional telomeres. Curr Biol *13*, 1549-1556.

Tanaka, K., Nishide, J., Okazaki, K., Kato, H., Niwa, O., Nakagawa, T., Matsuda, H., Kawamukai, M., and Murakami, Y. (1999). Characterization of a fission yeast SUMO-1 homologue, pmt3p, required for multiple nuclear events, including the control of telomere length and chromosome segregation. Mol Cell Biol *19*, 8660-8672.

Taylor, D.L., Ho, J.C., Oliver, A., and Watts, F.Z. (2002). Cell-cycle-dependent localisation of Ulp1, a Schizosaccharomyces pombe Pmt3 (SUMO)-specific protease. J Cell Sci *115*, 1113-1122.

Teixeira, M.T., Arneric, M., Sperisen, P., and Lingner, J. (2004). Telomere length homeostasis is achieved via a switch between telomerase- extendible and -nonextendible states. Cell *117*, 323-335.

Teo, S.H., and Jackson, S.P. (2001). Telomerase subunit overexpression suppresses telomere-specific checkpoint activation in the yeast yku80 mutant. EMBO Rep *2*, 197-202.

Thon, G., Cohen, A., and Klar, A.J. (1994). Three additional linkage groups that repress transcription and meiotic recombination in the mating-type region of Schizosaccharomyces pombe. Genetics *138*, 29-38.

Thon, G., and Klar, A.J. (1992). The clr1 locus regulates the expression of the cryptic mating-type loci of fission yeast. Genetics *131*, 287-296.

Tomita, K., and Cooper, J.P. (2007). The telomere bouquet controls the meiotic spindle. Cell *130*, 113-126.

Tomita, K., Kibe, T., Kang, H.Y., Seo, Y.S., Uritani, M., Ushimaru, T., and Ueno, M. (2004). Fission yeast Dna2 is required for generation of the telomeric single-strand overhang. Mol Cell Biol *24*, 9557-9567.

Tomita, K., Matsuura, A., Caspari, T., Carr, A.M., Akamatsu, Y., Iwasaki, H., Mizuno, K., Ohta, K., Uritani, M., Ushimaru, T.*, et al.* (2003). Competition between the Rad50 complex and the Ku heterodimer reveals a role for Exo1 in processing double-strand breaks but not telomeres. Mol Cell Biol *23*, 5186-5197.

Torres-Rosell, J., De Piccoli, G., Cordon-Preciado, V., Farmer, S., Jarmuz, A., Machin, F., Pasero, P., Lisby, M., Haber, J.E., and Aragon, L. (2007). Anaphase onset before complete DNA replication with intact checkpoint responses. Science *315*, 1411-1415.

Torres-Rosell, J., Machin, F., Farmer, S., Jarmuz, A., Eydmann, T., Dalgaard, J.Z., and Aragon, L. (2005). SMC5 and SMC6 genes are required for the segregation of repetitive chromosome regions. Nat Cell Biol *7*, 412-419.

Uzunova, K., Gottsche, K., Miteva, M., Weisshaar, S.R., Glanemann, C., Schnellhardt, M., Niessen, M., Scheel, H., Hofmann, K., Johnson, E.S.*, et al.* (2007). Ubiquitin-dependent proteolytic control of SUMO conjugates. J Biol Chem.

Varley, H., Pickett, H.A., Foxon, J.L., Reddel, R.R., and Royle, N.J. (2002). Molecular characterization of inter-telomere and intra-telomere mutations in human ALT cells. Nat Genet *30*, 301-305.

Verdun, R.E., Crabbe, L., Haggblom, C., and Karlseder, J. (2005). Functional human telomeres are recognized as DNA damage in G2 of the cell cycle. Mol Cell *20*, 551-561.

Verdun, R.E., and Karlseder, J. (2006). The DNA damage machinery and homologous recombination pathway act consecutively to protect human telomeres. Cell *127*, 709-720.

Vodenicharov, M.D., and Wellinger, R.J. (2006). DNA degradation at unprotected telomeres in yeast is regulated by the CDK1 (Cdc28/Clb) cell-cycle kinase. Mol Cell *24*, 127-137.

Wang, F., Podell, E.R., Zaug, A.J., Yang, Y., Baciu, P., Cech, T.R., and Lei, M. (2007). The POT1-TPP1 telomere complex is a telomerase processivity factor. Nature *445*, 506-510.

Wang, R.C., Smogorzewska, A., and de Lange, T. (2004). Homologous recombination generates T-loop-sized deletions at human telomeres. Cell *119*, 355-368.

Wang, Z., Jones, G.M., and Prelich, G. (2006). Genetic analysis connects SLX5 and SLX8 to the SUMO pathway in Saccharomyces cerevisiae. Genetics *172*, 1499-1509.

Watson, J.D. (1972). Origin of concatemeric T7 DNA. Nat New Biol *239*, 197-201.

Watt, P.M., Louis, E.J., Borts, R.H., and Hickson, I.D. (1995). Sgs1: a eukaryotic homolog of E. coli RecQ that interacts with topoisomerase II in vivo and is required for faithful chromosome segregation. Cell *81*, 253-260.

Watts, F.Z. (2006). Sumoylation of PCNA: Wrestling with recombination at stalled replication forks. DNA Repair (Amst) *5*, 399-403.

Watts, F.Z., Skilton, A., Ho, J.C., Boyd, L.K., Trickey, M.A., Gardner, L., Ogi, F.X., and Outwin, E.A. (2007). The role of Schizosaccharomyces pombe SUMO ligases in genome stability. Biochem Soc Trans *35*, 1379-1384.

Webb, C.J., and Zakian, V.A. (2008). Identification and characterization of the Schizosaccharomyces pombe TER1 telomerase RNA. Nat Struct Mol Biol *15*, 34-42.

Weinrich, S.L., Pruzan, R., Ma, L., Ouellette, M., Tesmer, V.M., Holt, S.E., Bodnar, A.G., Lichtsteiner, S., Kim, N.W., Trager, J.B.*, et al.* (1997). Reconstitution of human telomerase with the template RNA component hTR and the catalytic protein subunit hTRT. Nat Genet *17*, 498-502.

Wellinger, R.J., Ethier, K., Labrecque, P., and Zakian, V.A. (1996). Evidence for a new step in telomere maintenance. Cell *85*, 423-433.

Wellinger, R.J., Wolf, A.J., and Zakian, V.A. (1993). Saccharomyces telomeres acquire single-strand TG1-3 tails late in S phase. Cell *72*, 51-60.

Wu, L., Bachrati, C.Z., Ou, J., Xu, C., Yin, J., Chang, M., Wang, W., Li, L., Brown, G.W., and Hickson, I.D. (2006a). BLAP75/RMI1 promotes the BLM-dependent dissolution of homologous recombination intermediates. Proc Natl Acad Sci U S A *103*, 4068-4073.

Wu, L., and Hickson, I.D. (2003). The Bloom's syndrome helicase suppresses crossing over during homologous recombination. Nature *426*, 870-874.

Wu, L., Multani, A.S., He, H., Cosme-Blanco, W., Deng, Y., Deng, J.M., Bachilo, O., Pathak, S., Tahara, H., Bailey, S.M.*, et al.* (2006b). Pot1 deficiency initiates DNA damage checkpoint activation and aberrant homologous recombination at telomeres. Cell *126*, 49-62.

Wyllie, F.S., Jones, C.J., Skinner, J.W., Haughton, M.F., Wallis, C., Wynford-Thomas, D., Faragher, R.G., and Kipling, D. (2000). Telomerase prevents the accelerated cell ageing of Werner syndrome fibroblasts. Nat Genet *24*, 16-17.

Xhemalce, B., Riising, E.M., Baumann, P., Dejean, A., Arcangioli, B., and Seeler, J.S. (2007). Role of SUMO in the dynamics of telomere maintenance in fission yeast. Proc Natl Acad Sci U S A *104*, 893-898.

Xhemalce, B., Seeler, J.S., Thon, G., Dejean, A., and Arcangioli, B. (2004). Role of the fission yeast SUMO E3 ligase Pli1p in centromere and telomere maintenance. Embo J *23*, 3844-3853.

Xin, H., Liu, D., Wan, M., Safari, A., Kim, H., Sun, W., O'Connor, M.S., and Songyang, Z. (2007). TPP1 is a homologue of ciliate TEBP-beta and interacts with POT1 to recruit telomerase. Nature *445*, 559-562.

Zhang, C., Roberts, T.M., Yang, J., Desai, R., and Brown, G.W. (2006). Suppression of genomic instability by SLX5 and SLX8 in Saccharomyces cerevisiae. DNA Repair (Amst) *5*, 336-346.

Zhao, X., and Blobel, G. (2005). A SUMO ligase is part of a nuclear multiprotein complex that affects DNA repair and chromosomal organization. Proc Natl Acad Sci U S A *102*, 4777-4782.

Zhu, X.D., Kuster, B., Mann, M., Petrini, J.H., and de Lange, T. (2000). Cell-cycle-regulated association of RAD50/MRE11/NBS1 with TRF2 and human telomeres. Nat Genet *25*, 347-352.

Zhu, X.D., Niedernhofer, L., Kuster, B., Mann, M., Hoeijmakers, J.H., and de Lange, T. (2003). ERCC1/XPF removes the 3' overhang from uncapped telomeres and represses formation of telomeric DNA-containing double minute chromosomes. Mol Cell *12*, 1489-1498.

Zhu, Z., Chung, W.H., Shim, E.Y., Lee, S.E., and Ira, G. (2008). Sgs1 helicase and two nucleases dna2 and exo1 resect DNA double-strand break ends. Cell *134*, 981-994.